THE UNIVERSITY OF HULL

MUSCULOSKELETAL MODELING AND FINITE ELEMENT ANALYSIS OF THE PROXIMAL JUVENILE FEMUR

being a Thesis submitted for the Degree of

in the University of Hull

by

David Edmund Lunn, BSc (Hons), MSc

October 2013

ABSTRACT

The influence of mechanical loading on bone modelling and remodelling has been, and still is the subject of many studies. It is widely accepted that the internal structure of long bones is orientated to the strains experienced throughout activities, and the morphometry of the bones are as a result of the loading. Although other influences play a role in bone development including, hormonal, nutritional and genetic. The internal structure is orientated in such a way that it transfers the loads experienced without being excessive in weight, providing an efficient weight bearing structure. Many researchers have analysed the adult femur but little work has been undertaken to understand femoral development in juveniles. Therefore the aim this work was to develop an understanding of the mechanical stresses and strains that the femur experiences during growth.

The juvenile femur changes dramatically throughout growth. These changes occur from prenatal through to full maturity. The most notable include the ossification from a highly cartilaginous structure in the early years of development, to bone at ~18 years old, an increase in the length and angle of the neck, a change in the shaft torsion and a change in the bicondylar angle. Similarly, the development of movement patterns and locomotion in humans changes significantly throughout growth. Movement is restricted *in utero*, in neonates the movement begins to engage muscular activity, at 6 months a baby is usually able to sit upright; 9 months crawling begins; by 1 year old there is the ability to walk without support and at 4 years old an adult like gait pattern has developed. Full adult gait pattern has been documented to be achieved between 8-11 years old.

In this work through gait analysis and musculoskeletal modelling the loads which the femur experiences at specific stages/ages of bipedal locomotion are analysed. Finite element analyses were then performed to develop an understanding of the stresses and strains of the proximal juvenile femur in relation to the attainment and development of bipedal gait. This was achieved by evaluating changes in these mechanical stresses and strains throughout different ages, relating them to the variations discovered in the gait patterns.

Digitisation of the femora was performed on four specimens; prenatal, 3 years old, 7 years old and an adult. Following the scanning of the specimens in a micro CT scanner,

some restoration to the damaged samples was required. Furthermore the dry samples were incomplete, and the models were needed to be modelled to accurately resemble fully intact femurs. The CT scans contained the full shaft however were missing the fully articulated proximal femur, due to the dry nature of the specimens the cartilages were absent. MRI scans which contained the femoral head data but were missing the full shaft were merged with the CT data to create a fully articulated femur for use in subsequent modelling.

Gait analysis was performed on five children aged from 3-7 years old, with an average of five adults gait data used for comparison. The analysis showed that kinematic data was similar between all ages, however kinetic results revealed some differences. Ground reaction force in the 3 year old showed a higher heel strike compared to a higher toe off observed in adult during the gait cycle, indicating a lack of control in the 3 year old. Furthermore the 3 year old, compared to the other ages, had different values in joint moments. These joint moment results in particular played a role in the muscle forces produced from the musculoskeletal modelling.

To obtain the muscle force data required for the FEA, musculoskeletal models were built. Testing the reliability of the musculoskeletal model was performed comparing the kinematic and kinetic data from the musculoskeletal modelling against the data obtained from the motion capture system. A good agreement was found between these data sets with the kinematics having the largest difference in the ankle plantar flexion of 8.6°. The kinetic results revealed almost exact matches. Further testing was attempted between the muscle force data and collected EMG. The collected EMG matched reported EMG in the literature and the onset and offset times of muscle activity corresponded well to muscle force peaks produced in the musculoskeletal model. Comparisons between the EMG and force through calculating the EMG as a force were inconclusive, although a degree of accuracy was shown but a more comprehensive method is required. It was concluded that with the accuracy of the kinematic and kinetic results the musculoskeletal modelling was accurate enough to give a true representation of physiological muscle forces to be modelled during FEA.

Analysis of the musculoskeletal modelling results in the children revealed that the 3 year old had the highest significance between all the age groups. With the greatest significance in the hip flexors and abductors throughout the gait cycle. Joint reaction

forces as a percentage of bodyweight were found to be much higher in the juvenile models. The adult model had a value of 265% bodyweight whereas the 3 year old showed a reaction force of 537% bodyweight. These differences observed in the musculoskeletal modelling had a direct effect on the FEA because the loads calculated here were applied to the finite element models to evaluate the effects that these would have on the stresses and strains during growth and development of the femur.

FE models were built to represent a 3 year old, 7 year old and adult femur. Age specific loads calculated over 100% of a gait cycle, were applied to the models. The stress/strain analysis revealed some differences between the models but in general the areas exposed to high and low strain levels were similar. The similarities could suggest that each model was structurally adapted to the loads the femur regularly experiences.
The thesis was successful in evaluating the stress and strain distribution apparent in the developing femur. However the work would be advanced by evaluating models from age ranges with a much more varied movement pattern i.e. crawling. This would increase an understanding of the structural optimisation of the femur.

Keywords: Femur, Juvenile, Musculoskeletal Modelling, Children's Gait, Finite Element Analysis, Ontogeny.

ACKNOWLEDGEMENTS

I would like to express my gratitude to Dr Catherine Dobson and Professor Michael Fagan for their continuous supervision and advice throughout this project. I also would like to thank past and present colleagues from CMET who have been a pleasure to work with and be around. Thanks is also needed to be given to Professor Sue Black for access to the femur specimens at the Scheuer Collection at the University of Dundee, additionally to Guillaume Gorincour from Laboratoire d'Anatomie Comparée of the Muséum National d'Histoire Naturelle of Paris for MRI data and prenatal bone sampled without which would have made this project a difficult task to complete. Finally a thank you to Caroline Stewart who provided part of the gait data used in this project. A special mention to Professor Ulrich Witzel who, with his knowledge and experience, guided me through the mechanobiological work of the thesis.

On a personal note I would like to say a special thank you to my family, friends and my wife Sarah for the continued support throughout this research, and without whom this would have been a much less enjoyable process.

TABLE OF CONTENTS

LIST OF FIGURES

LIST OF TABLES

GLOSSARY

°	Degree (angle)
%	Percentage
µCT	Computer Tomography
µE	Microstrain
2D	Two-dimensional
3D	Three-dimensional
4D	Four dimensional
A	Anterior
AgAgCl	Silver Chloride
AL	Anterior lateral
AM	Anterior medial
AP	Anterior-posterior
Apophysis	A natural protuberance from a bone
Apoptosis	The process of programmed cell death
BMC	Bone mineral content
BMD	Bone mineral density
BW	Bodyweight
Cartilage anlagen	The initial clustering of embryonic cells from which a part or an organ develops
Chondrogenesis	The formation of cartilage
Coalesced	Come together and form one mass
CS	Cumulative stress
Cursorial Species	An organism adapted specifically to run
Diaphysis	The shaft or central part of a long bone.
DOF	Degrees of freedom
Erythropoiesis	Production of red blood cells

EMG	Electromyography
Epiphyses	The end part of a long bone
FD	Femur Depth
FE	Finite-element
FEA	Finite element analysis
FEM	Finite element model
FL	Femur Length
FW	Femur Width
Gait Cycle	The gait cycle begins when one foot contacts the ground and ends when that foot contacts the ground again.
GRF	Ground reaction force
HH	Helen Hayes
iMVC	Isometric Maximal Voluntary Contraction
L	Lateral
M	Medial
ML	Medial-lateral
MuscleSF	Muscle standardised femur
MVC	Maximal Voluntary Contraction
Kg	Kilogram
LED	Light emitting diode
MPa	Megapascals
m/s	metres per second
N	Newton
P	Posterior
PD	Proximal-distal
Phylogenetics	The study of evolutionary relationships among groups of organisms
PL	Posterior lateral
PM	Posterior medial

1 INTRODUCTION

The skeletal system of the human body has a number of functions, including protection, movement and support. The structure of the bone directly relates to its function, for example, when the role is to protect the bone is flat whereas for locomotion the bone is long. The shape and what tissue the skeletal system consists of changes dramatically during growth. Initially the skeletal system is made up of cartilage anlagen this is then gradually ossified into bone throughout growth. For the femur, ossification is not complete until about the age of 20. During this time a number of changes in the shape of the femur occur such as a change in the angle between the neck and the shaft (neck shaft angle), torsion of the shaft and the bicondylar angle (BA). The structure of the femur has been a focal point for much research. Over a century ago it was first observed that the trabecular orientation of the adult femur was likened to that of the strain trajectories of a buttress (Culmann, 1866; Pauwels, 1980). Following this observation, the theory that bone remodels in response to the loading was developed. This is known as Wolff's Law (1892) however it is still not understood in its entirety. The loads that bone is influenced by include joint contact forces, muscles, ligaments and other soft tissue structures. Ruff (2003b) added evidence to this theory through analysing the different rate of development in the humerus and the femur of chimpanzees. Prior to bipedal locomotion the humerus and femur shows a similar rate of development, once bipedal locomotion was attained the femur increased in development relating this to the increased loading. Although there is still evidence that does not support this theory, Morimoto *et al* (2010) reported that *in vivo* functional bone modifications only account for a minor part in morphological changes and much is accountable to taxon-specific development.

The human femur has been subject to much of this work due to the initial findings regarding bone adaptation to mechanical strain. Thus the femur is an ideal bone to perform analysis on so that comparisons can be made to previous literature and knowledge of the structure is widely available to be utilised. Pauwels (1980) performed an in depth study of the biomechanics of the locomotor system to understand how the joint contacts, muscles and surrounding tissues affect the structure of the femur from a mechanical aspect. The

trajectorial theory is one proposal which relates the trabecular orientation to the strains observed during loading of the femur (Wolff, 1892; Culmann, 1866).

The use of finite element analysis (FEA) to evaluate the strain found in bone under physiological loading is used in many areas including orthopaedic, biological and anatomical studies. Early finite element models (FEM) used simple loading techniques i.e. only using joint contact forces. Progressing from this, mathematical models were created to estimate muscle forces (Duda, 1997). The reliability of musculoskeletal models has been greatly improved through work which was able to measure the *in vivo* hip contact force during varied locomotor activities including fast walking, walking, and stair climbing (Heller *et al* 2001a). To produce more accurate FEA, musculoskeletal models of human movement have been created through the utilisation of motion capture and modelling software's. More recent work has used subject specific musculoskeletal modelling through the use of magnetic resonance imaging (MRI) to get specific and accurate muscle and joint contact placements. Consideration of these FEA models in the literature is needed to inform the work to be undertaken in the current thesis of the most accurate and up to date techniques being used in research.

One area that has received a lot less attention is bone development throughout growth. Human locomotion changes dramatically from birth through to adulthood, and these changes have been well documented in the literature. The key stages of development have been grouped as at 6 months a baby is able to sit upright; 9 months crawling begins; by 1 year old there is the ability to walk without support and finally at 4 years old an adult like gait pattern has developed (Sutherland, 1997), although a number of other developments occur in gait beyond 4 years of age (Chester *et al*, 2006). Thus it would seem that although a mature gait pattern in terms of kinematics is achieved by 4 years old, developments which would directly affect the loading of the femur may not be fully mature until 8 years (Kirtley, 2006). These changes may affect the stress and strain patterns observed in the bone at the relevant ages. More specifically the muscle patterns and joint reaction forces may also change during gait development. Therefore it is necessary to understand these changes and if Wolffs law is assumed to be correct then this would play a large role in influencing bone development until a mature gait pattern is achieved.

Despite vast interest in the femur, an investigation into what stresses and strains the proximal femur experiences during growth has never been performed in great depth. In an attempt to fill this gap in the literature a number of methods will be employed. These include modelling the geometry of juvenile femora, capturing kinematic and kinetic data associated with activities of daily living in the appropriate age of the femora models. Then applying the information provided from this data collection to FEM for analysis.

1.1 AIMS AND THESIS STRUCTURE

The aim of this research is therefore to develop an understanding of the growth of the proximal juvenile femur in relation to the attainment and development of bipedal gait. Evaluating changes in mechanical stresses and strains within the proximal femur throughout different ages, and relating them to the changes of loads in the development of gait, will give an insight into the mechanical forces that the femur undergoes throughout growth and an idea of how bone development may occur because of these stresses and strains.

The next chapter will present a rationale for this thesis through a comprehensive review of the literature. This review will discuss past and current literature that is related to the ontogeny of the femur, gait maturity, musculoskeletal modelling and finite element analysis of the femur.

Presented in Chapter 3 are the methods used in the segmentation and digitisation of the micro-computer tomography (μCT) scans into three dimensional (3D) models. This chapter details the specimens and the scanning process, as well as the methods required for reconstruction of the damaged or incomplete specimens. This is a necessary step to create 3-D models for subsequent FEA to be performed.

Chapter 4 reports the results of the children's and adult's gait analysis. This chapter aims not only to discover any variations that may occur between the kinematics and kinetics of the different ages but also to provide data to be used in musculoskeletal modelling.

Chapters 5 and 6 form the musculoskeletal modelling section of the thesis. Specifically Chapter 5 discusses the reliability of the musculoskeletal models using a number of

different methods. With the results informing how accurate the muscle force data is, that is to be applied to FE models; Chapter 6 details the results of the musculoskeletal modelling of the children and adults during one gait cycle presenting the results for the muscles active in femoral articulation. The results of the musculoskeletal modelling will be a novel finding. Because these differences will play a role in the FEA it is important that these are analysed and differences between the ages identified.

Chapter 7 brings together the results from previous chapters and aims to evaluate the strains and stresses of the proximal femur. It discusses the results of the finite element analysis with reference to how the applied loads of a 3 year old, a 7 year old and adult musculoskeletal models played a role in the stresses and strains observed in the femur.

Finally Chapter 8 offers a conclusion of the overall findings of this investigation, limitations are highlighted and recommendations are made for future work that could progress this work.

2 LITERATURE REVIEW

To gain a greater understanding of the area of research that is to be undertaken in this thesis a review of the literature is needed. This thesis covers a number of subject areas and therefore the literature review will be organised as follows. Initially bone form and function will be discussed, followed by bone development and growth, gait analysis, musculoskeletal modelling and finally finite element analysis. The review will also help to realise the interaction of all these areas.

2.1 BONE FORM AND FUNCTION

To evaluate the changes in stresses and strains observed in the femur during growth an important aspect of the work is to understand the structure of bone. This includes how bone develops, what the function of bone is, and what specific developments are seen in the femur.

2.1.1 SKELETAL ANATOMY

The skeleton is the main supporting structure of an animal's body, the main functions of which are locomotion, support, protection, mineral storage and erythropoiesis (the production of red blood cells). The skeleton can be classified into two groups, the axial and the appendicular. The axial skeleton consists of the skull, vertebral column and rib cage. This section of the skeleton is in general used for the protection of organs and the support of other body parts. Whereas the appendicular skeleton consists of the upper and lower body limbs, and the pelvic and shoulder girdle, with the main function being locomotion and movement. The skeleton can be further divided into four bone types, these are: flat, short, irregular and long bones. The bone's shape often reflects its function, flat bones for example are used for protection, examples of which include the skull and the sternum. Long bones have a primary function of enabling movement and locomotion, and therefore need to accommodate large muscle groups, (e.g. the femur and humerus).

The developing skeleton is initially made up of cartilage and fibrous membranes that are replaced with bone at a relatively rapid rate during growth and development. In the adult, bone tissue is the main constituent of the skeleton and is a highly dynamic material undergoing a constant renewal process. Bone is a rigid organ that forms the skeletal system comprising of two structures, namely cortical and trabecular bone. Cortical bone forms the surface of bones and is characterised by the compact shell

appearance that is often associated with bone. It has the function of being an attachment site for muscles and ligaments and is often found in the shaft of long bones. Trabecular bone is found, amongst other areas, inside the cortical shell in all long bones, and within the vertebrae. Trabecular bone has a porous, mesh like structure comprising of a complex arrangement of struts and plates (Figure 2.1).

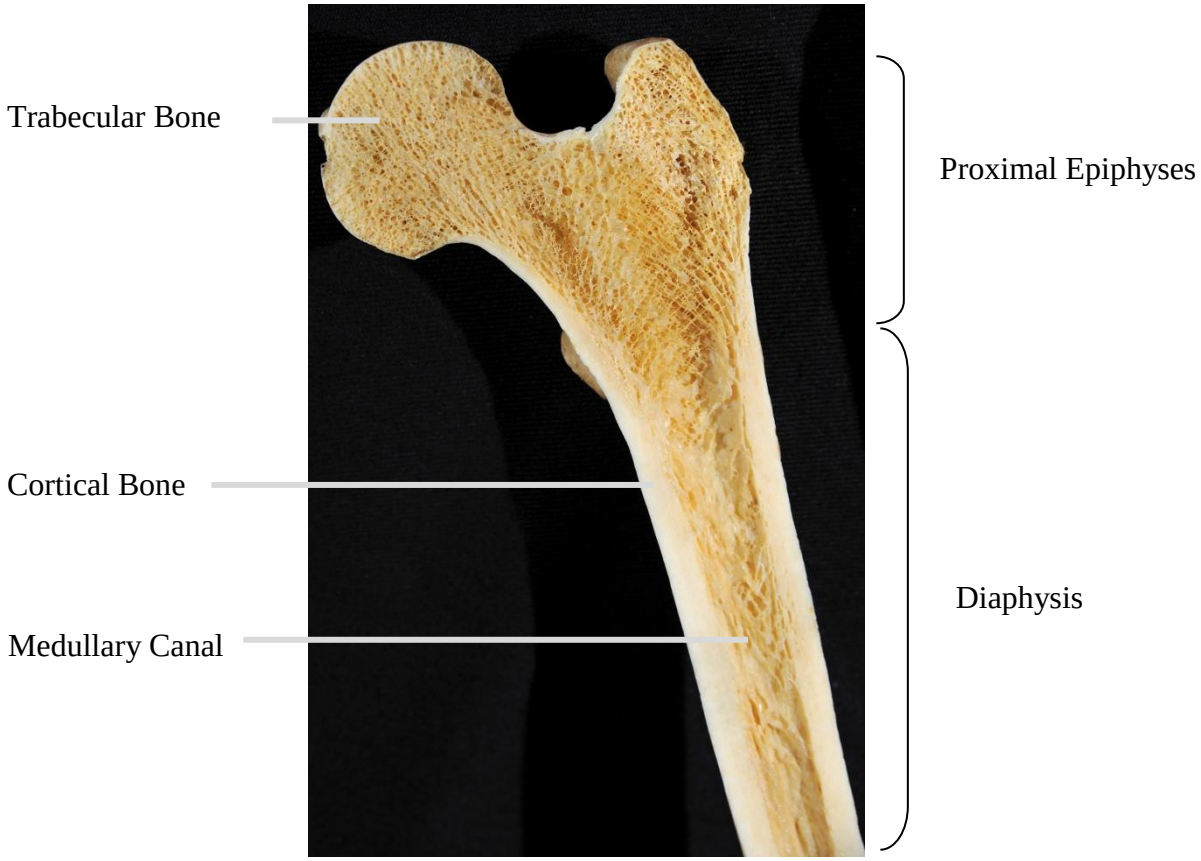

Figure 2.1 A longitudinal cross section of the proximal femur illustrates the difference between trabecular bone and cortical bone.

Bone research has received a vast amount of attention for over a century (Wolff, 1892; Culmann, 1866). The interest in bone ranges from the cellular level up to the structure and shape of whole bones. At the cellular level, the way that the stimuli produced by loading are detected by osteocytes is of interest as this then elicits a response from the osteoblasts and osteoclasts to lay down more bone or remove it (Carter *et al*, 1996). Understanding the behaviour under loading at the cellular level helps to inform of the morphological changes at a structural level, which may be as a result of changes in

muscle loading. This has relevance for studies examining ontogeny, evolution, and changes in locomotion to name but a few. Therefore to gain a complete understanding of the mechanisms of bone growth and adaptation, both cellular and structural level information needs to be considered.

2.1.2 BONE GROWTH

The geometric shape of bones results from embryonic development, modelling and evolution more of which will be explored in the next section of this review. The initial position, size and shape of the cartilage in the embryo are determined directly by the genome during embryonic development and this determines a template for the shape of the bone (Scheuer and Black, 2005). Although genes are the units of inheritance and play a large role in the initial development of bone, they do not directly encode bone shape beyond patterning of the embryo (Doube *et al* 2009), and therefore are not the only influence on bone development. Mechanical influence has been well documented in the literature as a significant contributor to the development of bone (Carter and Wong., 1996; Ruff *et al,* 2003a), with forces imposed by muscles, ligaments, tendons, and joint reaction forces all having an effect. This is particularly obvious in bones undergoing high levels of loading such as the femur. Foetal muscle contraction is necessary for the normal development of bone size and shape, indicating that bone shape is influenced by the mechanical environment from an early developmental stage (Rodriguez *et al,* 1988). Further evidence of this mechanical influence can be seen when considering the crests at muscle attachment sites (greater trochanter) and hollows that accommodate muscle bellies. These relate directly to the loading exerted by the muscle attachments, which also influences the geometry and mechanics of the underlying bone (Doube *et al,* 2009). These morphological features are a result of the continuous dynamic activity of bone, a process known as modelling and remodelling.

2.1.2.1 Modelling and Remodelling

Modelling and remodelling refer to two means of bone structure alteration. Bone modelling has the ability to make large changes in a bone structure and is the process of the initial shaping of bone due to function. Whereas remodelling is the process where bone turnover is modulated. It refers to when bone resorption and formation do not act independently of each, and can only make small changes in bone structure.

Remodelling of bone is a continuous process and acts to influence bone shape and repair damaged bone (Huiskes, 2000). Cortical bone is replaced continuously with 5-7% of its volume replaced weekly and trabecular bone volume is completely replaced every 3-4 years (Marieb, 2004). This remodelling rate is high during growth (Tanck *et al*, 2001), but reduces when skeletal maturity is reached (Frost, 1990). The rate is not exclusively due to mechanical influences but also has others such as chemical substances i.e. calcium availability, hormones, and nutrition. Remodelling of bone has been suggested to occur within a strain value range of 50-3500 microstrain (μE) (Martin, 2000). As remodelling occurs at bone surfaces trabecular bone is believed to remodel up to 10 times quicker than cortical bone due to its much larger surface to volume ratio (Lee and Einhorn, 2001). The strain value where remodelling occurs is no larger than 3500 $\mu\varepsilon$ the yield strain of bone where damage can occur is 7000 $\mu\varepsilon$ (Sommerfeldt and Rubin, 2001). These values are especially useful when using FEA to observe areas where bone may be more disposed to remodelling. Bone mass is retained in a healthy young individual when the loading is consistent, although to maintain this homeostatic state an equal rate of apposition and resorption is required. However, when the loading regime alters, the rate at which apposition and resorption occurs changes accordingly. It is said that this apposition and resorption is performed through a bone 'drift' which moves the bone through space in response to load (Frost 1980). For example an increased loading will activate the formation of bone in adults and a reduction in the loading would increase the resorption rate (Tanck *et al*, 2001). This remodelling has been explored extensively in the literature. Frost (1987) proposed the Mechanostat theory that states that local strain regulates bone mass. The model distinguishes between modelling and remodelling, on the premise of disuse and overload of bone, as dictated by the strain. Disuse activates remodelling and inhibits bone formation modelling leading to net bone loss, whereas (above a threshold of 1500 $\mu\varepsilon$) overload inhibits remodelling but activates bone formation resulting in bone gain. Figure 2.2 illustrates that excessive overload increases formation of bone, although Frost's Mechanostat model does consider that excessive loading could cause damage. Furthermore it can be seen that there is a point at which homeostasis is achieved and therefore bone structure and mass is preserved. Beyond this point when pathological overload occurs osteoblasts begin to lay bone rapidly and would not be idealised for minimum weight and optimum strength as is often necessary in the skeleton.

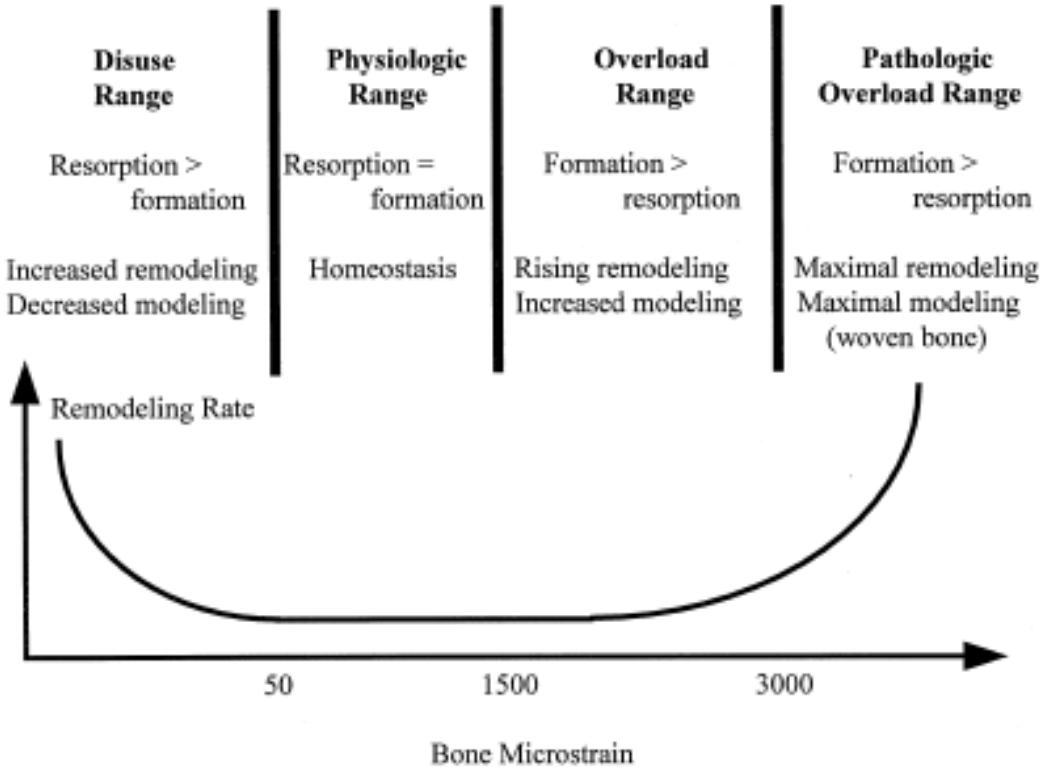

Figure 2.2. Resorption formation balance based on bone remodelling rate (Martin, 2000)

Martin (2000) described a new theory in addition to previously accepted concepts of resorption when the bone is in disuse, and formation when under loading. Martin suggested another mechanism, which hypothesised that the remodelling is at a continuous rate unless there is an inhibitory signal which restrains it. The inhibitory signal could be in response to excessive loading or reduced loading. This would imply that remodelling is maintained at the physiologic rate by the inhibitory signal which either lessens or is increased depending on the load response, rather than the bone signal determining directly the activity of osteoblasts and osteoclasts. There is much more detail available in the literature (e.g. Boyle *et al*, 2003) on the signalling process of the sensory cells which would be beyond the scope of the current study, although it is important to recognise that it plays an important role in understanding the growth of bone.

2.1.2.2 Cortical Bone

Cortical bone responds differently to mechanical loading when compared to trabecular bone, with it remodelling at a much slower rate. Cortical bone is therefore more reactive to habitual loading regimes rather than adapting to infrequent and random loads. Recent work has shown loading provided by external stimulation of the muscles can elicit the same remodelling effect on bone as normal muscle function. Gargiulo *et al,* (2011) used functional electrical simulation (FES) to repair muscle and tendon function which helped to increase bone mass of the patella. This study largely agrees with Garcés and Santandreu (1988) where denervation in rats was performed to remove the load on the bone resulting from the muscle function, where bone mass and shape were shown to develop abnormally. Similarly Gross *et al* (2010) performed a review discussing three methods which have shown the effect of poor muscle function on the mass and morphology of bone. The methods reviewed were spinal cord injury models, transgenic mice with altered muscle function and experimental models affecting one hind limb or specific muscle groups. All three of these methods showed that muscle function affects bone growth and development. Also when habitual forces i.e. muscle contractions, are not present a reduced bone mass is observed. Although the mechanism of how these methods affected bone development, beyond reduced loading, was not explored.

The normal cortical bone growth in long bones is similar across different mammals. Tardieu (1998) studied the difference in development of the femur in primates and humans, examining the rates at which they develop. The development of the bicondylar angle was found to occur during the infantile growth spurt but the reshaping of the distal epiphysis does not occur until adolescence. This is different to that observed in primates where a much quicker growth spurt and bone development is present. Similarly Tardieu and Damsin (1997) discussed the uniqueness of the adolescent growth period to be characteristic of modern humans. Although this study aims to enhance the knowledge of phylogenetics it can help to explain the role of the activity and its effect on bone growth. In primates the need for quicker development is required due to the reduced dependency time compared to that of modern humans. However in terms of the mechanical influence on the skeleton, it is quite probable that the increased activity from an earlier age in primates is related to bone growth. Serrat *et al* (2007) compared the ossification pattern between different mammals. There were two distinct differences, chimpanzees and humans have separate epiphyses and trochanters, whereas cursorial species (adapted to running) i.e. horses, have coalesced femora. Other notable

differences between these groups are the hip mobility and the femoral neck length. It was suggested that this, as previously suggested in the distal epiphyses and for the shaft, is a result of the functional demands of loading. The specific loading which causes the ossification centre has been looked at using computer modelling techniques and these will be explored in a later section of the literature review. Other comparative research has been performed by Morimoto *et al* (2011), who compared the cortical thickness and other variables of the femora from both captive and wild chimpanzees using morphometrics. No statistical significance in the cortical thickness was found between the captive and wild chimpanzees, although movement patterns were shown to differ. It was concluded on this basis that Wolff's law as a hypothesis could be rejected. However to dismiss Wolff's law in circumstances of constrained and restricted movements of zoo chimpanzees would be premature. The unrestricted movements were said to reduce the peak volumes of muscle activation not the accumulative stresses. As previously discussed, it has found that low stress intensities rather than peak strains can satisfy loading of bone enough for remodelling to be achieved (Rubin *et al,* 2002).

2.1.2.3 Trabecular Bone

The function of trabecular bone is to optimise bone strength whilst limiting bone weight. There are many articles that discuss trabecular adaptation with respect to mechanical loading (Scott, 1940; Hammer 2002; Lu *et al,* 1997; Fox and Keaveny, 2001). It has been documented in adult specimens that the trabeculae are orientated along the trajectories of high strain in the femur (Duda, 1997; Stokes, 2002; Cristofolini *et al,* 2009) and furthermore, when there is a lack of 'normal' femoral loading the trabecular network is underdeveloped (Modlesky *et al,* 2008) or unorganised (Osborne *et al,* 1980). Modlesky *et al* (2008) observed the different trabecular structure when comparing a control group and children with Cerebral Palsy (CP). It was found that children with CP who were unable to walk exhibited markedly underdeveloped trabecular bone. This was the first study produced on children with limited loading on limbs although previous work has been done on adults (Edwards *et al,* 2008). The results suggest that children with CP who are unable to walk have a significantly increased risk of fracture because of the poor trabecular structure and low bone mineral density (BMD) (Ko *et al,* 2006). Previous studies suggest similar theories but using a causative method, rather than a non-causative one. Rubin *et al* (2002) induced a mechanical stimulus on the hind legs of sheep, with the results showing that even low

levels of stimulus can improve trabecular quantity and quality. This suggests that it is possible in children with CP that a small mechanical stimulus could be induced to help decrease fracture risk. Miller *et al* (2003) found that in babies of very low birth weight (VLBW) where bone disease was present, it could be attributed to the lack of intrauterine movements, failing to drive normal movement development. Similarly in a kinematic analysis of pre-term and full term infants (Jeng *et al*, 2002) there were age related differences which may suggest that the movement patterns are also affected by early developmental problems. These studies help to emphasise the importance of loading on the trabecular structure. However, what is still not clear is how the loading helps to develop the trabecular architecture and the development path during growth. Further to the study by Rubin *et al* (2002), it was also illustrated that not only do large loads (>2000 microstrain) improve trabecular quantity and quality but low level high frequency strains can also improve the trabecular network. Although this is useful when considering diseases such as osteoporosis which predominantly affects the trabecular structure (Parfitt, 2008), it was not clear however whether these low level and high frequency strains change or help to develop the direction that is often observed in the trabeculae.

Panattoni *et al* (2000) measured the bone mineral content (BMC) in the femoral ossification centres in patients aged from 11.5 conceptual weeks to 1 year. The study, using an ultra-high resolution densitometer, indicated that there was a general increase in BMC from conception through to 1 year in the greater and lesser trochanter regions. However as the ossified trochanters do not appear until 3-4 years (greater trochanter) and 7-9 years (lesser trochanter) the regions which were measured as the trochanters can be somewhat questionable. Despite this the information on the BMD regardless of the named areas can show the effects of varying environmental conditions. During the measurement of the BMC and BMD after approximately 80 weeks both show a significant drop at 90 weeks which was not explained in the study. A possible cause could be the fact that just after birth there is a decrease in the mechanical load as there is no resistance from the uterus wall (Land and Schoenau, 2008) and furthermore resistance from the fluid in the womb would be greater than the air resistance. Tanck *et al,* (2001) suggested that the production of bone mass is a priority during early stages of growth and that alignment of trabecular bone does not appear until later in maturity. This finding does not correlate with findings of that observed in recent studies by Ryan

and Krovitz (2006) in which orientation of trabecular bone in prenatal femurs showed organisation, which was also suggested by Osborne, (1980).

2.1.2.4 Bone Development

The remodelling rate of bone and its structure has been discussed, however an important aspect of the current research is to understand how the skeleton grows and develops. Bone ontogeny begins at approximately 8 weeks when the human embryo consists of fibrous membranes and cartilaginous material. In early stages of development involuntary embryonic muscular contractions encourage bone formation at the site of muscle attachment (Carter and Beaupre, 2001). In the femur, according to Carter and Beaupre's research, bending stresses set up by proximal and distal contractions result in intermittent bending moments in the cartilaginous shaft template, that focus in the mid-shaft region thus initiating perichondral ossification. They also suggest that mild axial tension and hydrostatic tensile stresses in pluripotential tissue enhance bone formation, and chondrogenesis can be promoted by hydrostatic and axial compression. The ossification of bone can occur either as a result of intramembranous (dermal or perichondral) or endochondral ossification. Perichondral intramembranous centres of ossification develop in response to the *in utero* stretching of the surrounding soft tissue structures. Endochondral ossification is more complex than intramembranous ossification; with cartilage being replaced by bone rather than bone being formed without the presence of cartilage. This process can be seen in a model developed by Kummer (2005), showing that intramembranous and endochondral ossifications have different pathways. Endochondral ossification is responsible for the growth of long bones such as the femur and it is therefore necessary to discuss this process in more detail.

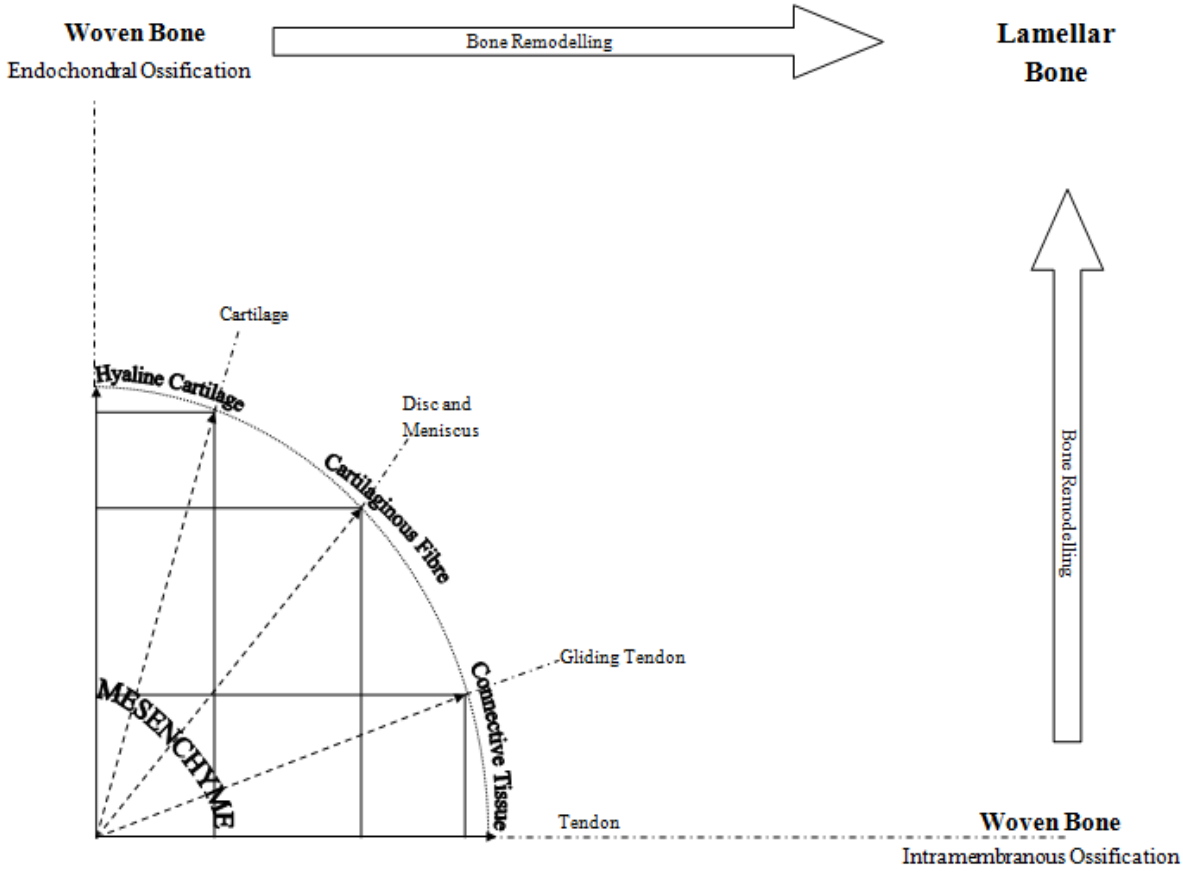

Figure 2.3. Causal histogram for bone development adapted from Kummer, (2005)

2.1.2.5 Endochondral Ossification

The process of endochondral ossification primarily begins with the proliferation of chondrocytes and deposition of a cartilage matrix which grows the initial cartilage anlagen. The chondrocytes mature to hypertrophic chondrocytes, blood vessels then infiltrate the anlagen accompanied by osteoblasts and osteoclasts which can then form the primary centre of ossification. The process which follows can be described in five stages, as shown in Figure 2.4

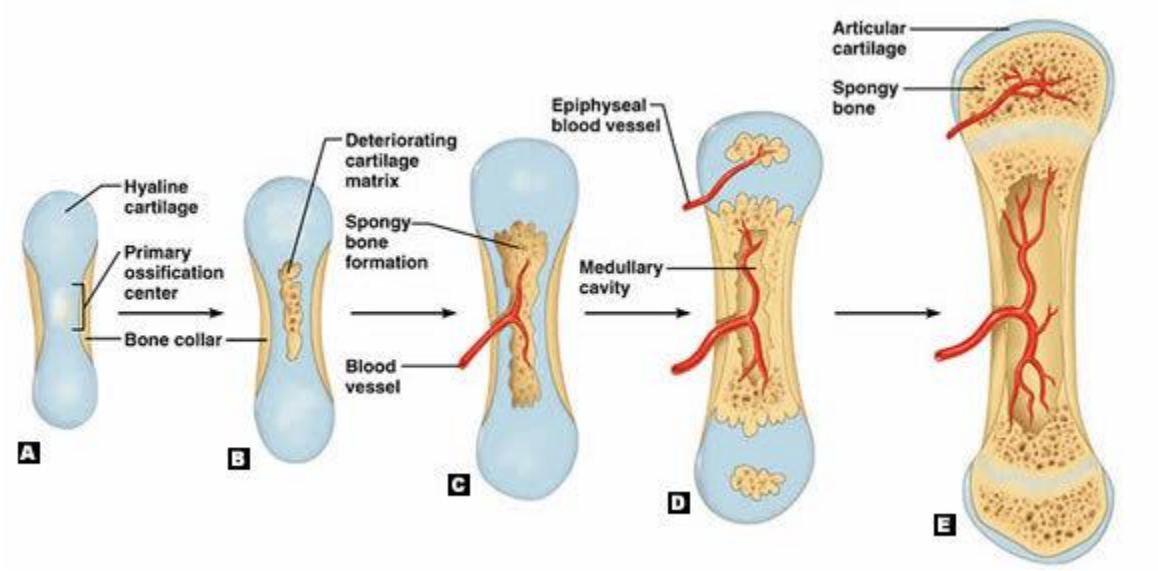

Figure 2.4. Five stages (A-E) used to describe endochondral ossification (Marieb, 2004)

- During the initial stage (A) of ossification the hypertrophic chondrocytes undergo apoptosis and osteoblasts begin to replace the cartilage with trabecular bone. Also the osteoblasts secrete osteoid against the hyaline cartilage which encases the centre of ossification in a bony collar.
- The secondary stage (B), cartilage calcifies in the centre of the diaphysis and the remaining chondrocytes in this region die leaving cavities to allow nutrient infiltration.
- The third stage of endochondral ossification (C) is where nutrient arteries, amongst other vessels, can provide osteoblasts and osteoclasts with the necessary environment for bone modelling. At this stage bone also begins to form and the calcified cartilage matrix is eroded.
- The fourth stage (D) is the elongation of the diaphysis and the formation of the medullary canal. This process follows chondrocyte proliferation, maturation, degeneration and ossification, whereby the bone growth ‘chases’ the cartilage formation of the shaft to ossify. The medullary canal is formed by the removal of the newly formed spongy bone where the primary centre of ossification began, as it enlarges.
- The final stage (E) is the ossification of the epiphyses, which are formed as secondary ossification centres and produced in the same manner as the primary ossifications.

Primary and secondary centres are separated by an organised cartilaginous region of rapid growth. When the rate of cartilage proliferation is exceeded by the rate of osseous deposition, then the growth plate will start to narrow and eventually fusion will take place between primary and secondary centres, marking the end of longitudinal bone growth.

Remodelling of this bone continues throughout growth and maturity and these stages are followed for all bones undergoing endochondral ossification, however the timeline at which they occur may differ. Javaid *et al*, (2006) studied the effect of infancy growth on the bone mass and femoral geometry of adults. Femoral geometry and bone mass was measured for 333 women and men aged 60-75 years whose birth weight and weight at 1 year old was known. In this study, variations in proximal femur geometry were influenced by low weight gain from birth to 1 year. These geometric variations included a reduced femoral neck width, which is known to give predisposition to fractures. Although only weight gain was used to assess the influence on the adult geometry, there may be greater influences such as activity. However this has shown that although juvenile growth plays a large role in the health of the adult skeleton, understanding other influences on the femur during growth is important.

2.1.3 ANATOMY OF THE FEMUR

In humans the femur is the most proximal bone in the lower extremity and the largest in the human body. It spans two joints and forms part of the hip and the knee, with a highly complex arrangement of muscle and ligament attachments to develop movement and stability in both joints (Marieb, 2004). The femur is characterised by a number of distinct structures, namely; the femoral head and neck, the shaft of the femur, the greater trochanter, the lesser trochanter and the epicondyles. These sites are either joint contact points or muscle attachment sites, however these are not the only attachment sites. Other important landmarks on the femur include the fovea, intertrochanteric crest, quadrate tubercle, gluteal ridge, pectineal line, linea aspera and the intercondylar notch (Figure 2.5).

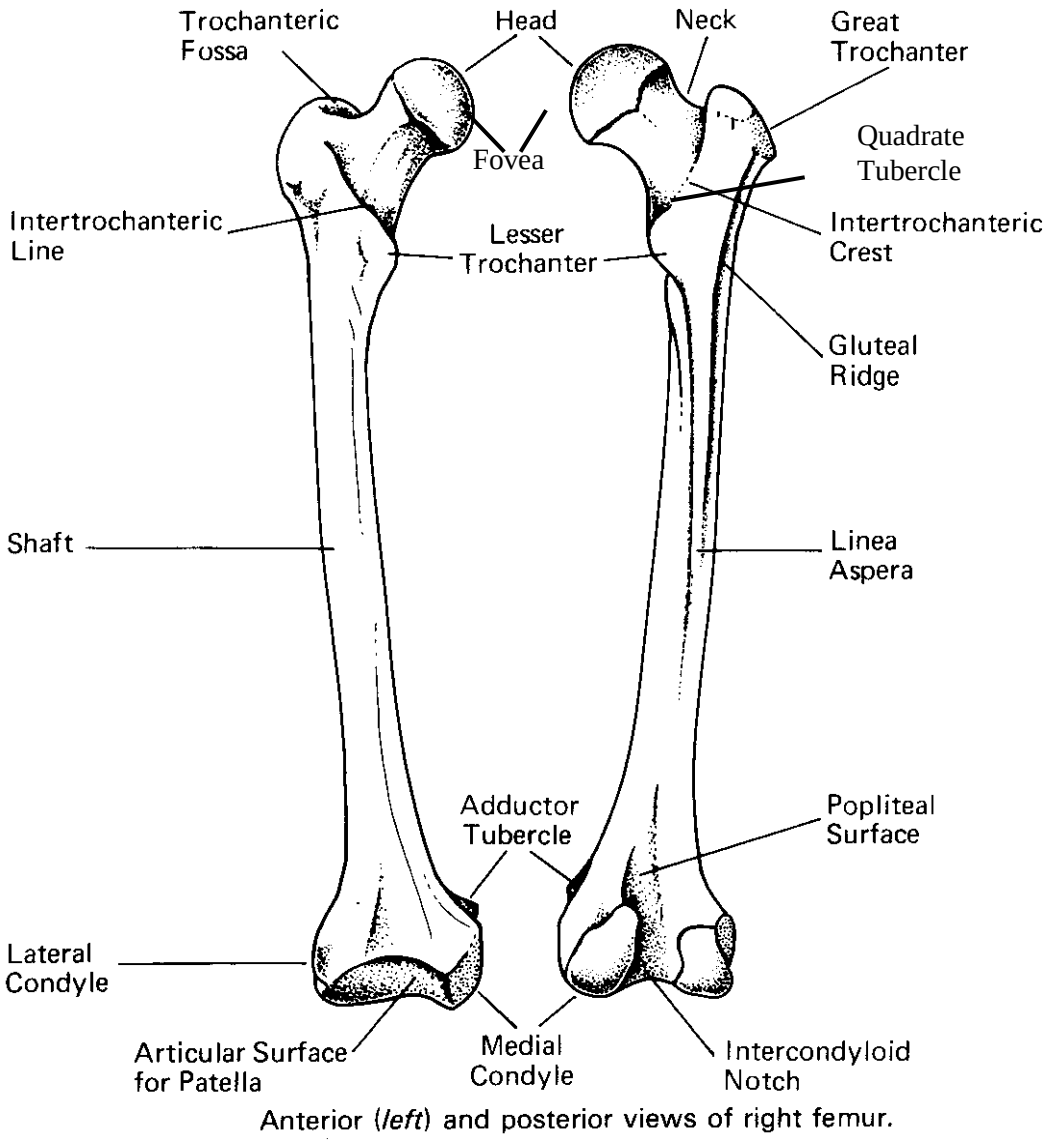

Figure 2.5. The adult femur showing important structural landmarks (http://www.arthursclipart.org/medical/skeletal/femur%20right.gif)

Bony prominences and landmarks of the femur include the lesser and greater trochanters which are separated by the intertrochanteric crest. The greater trochanter extends superiorly from the lateral part of the shaft and it continues posteriorly. The medial part of the greater trochanter is deeply grooved and forms the trochanteric fossa, which acts as an attachment site for the obturator externus muscle. Muscle attachment sites on the lateral side of the greater trochanter include the gluteus minimus and gluteus medius. On the medial side the obturator internus, gemelli, and piriformis muscles attach. The lesser trochanter projects posteriorly and medially from the shaft and acts as an

attachment site for psoas major and the iliacus muscles. The intertrochanteric line from which the trochanters extend descends distally and medially and joins the pectineal line (Figure 2.5), which then merges with the gluteal tuberosity, which in turn descends into the linea aspera and continues down the shaft of the femur. These lines are muscle attachment points, the intertrochanteric line is as an insertion point for the iliacus and the pectineal line an insertion for the pectineus. The linea aspera descends down a large portion of the shaft and is an attachment point for a number of muscles. These include the vastus lateralis, vastus medialis, short head of the bicep femoris, adductor magnus, adductor brevis, adductor longus, gluteus maximus, iliacus and pectineus. Appendix I shows details of all muscle that have an insertion and origin on the femur.

The femoral head is spherical in shape and articulates with the acetabulum of the pelvis forming a ball and socket joint. The femoral neck is cylindrical in shape and extends from the shaft of the femur to the femoral head at an angle of 120°-135° in adults, this is known as the neck shaft angle (NSA) (Figure 2.6a) and varies during growth. Bulandra et al, (2003) said that the NSA should cause the longitudinal axes of the femoral necks to cross at the point of bodyweight. The NSA can be defined as the angle between the centre axis of the neck and centre axis of the shaft (Isaac et al, 1997). The femoral shaft in the frontal plane has a lateral to medial direction and, known as bicondylar angle, is on average between 8° and 11° in adults (Tardieu et al, 2006) (Figure 2.6b). The shaft also has a change in the angle in the transverse plane, known as femoral torsion. As with other changes observed in the femur this varies with age, but in an adult the torsion angle is approximately 12°. Although torsion angle is also known as femoral anteversion, where the torsion angle refers to the orientation of the femoral head and neck in references to the frontal plane of the body, the term anteversion refers to the orientation in reference to the condylar plane (Figure 2.6c).

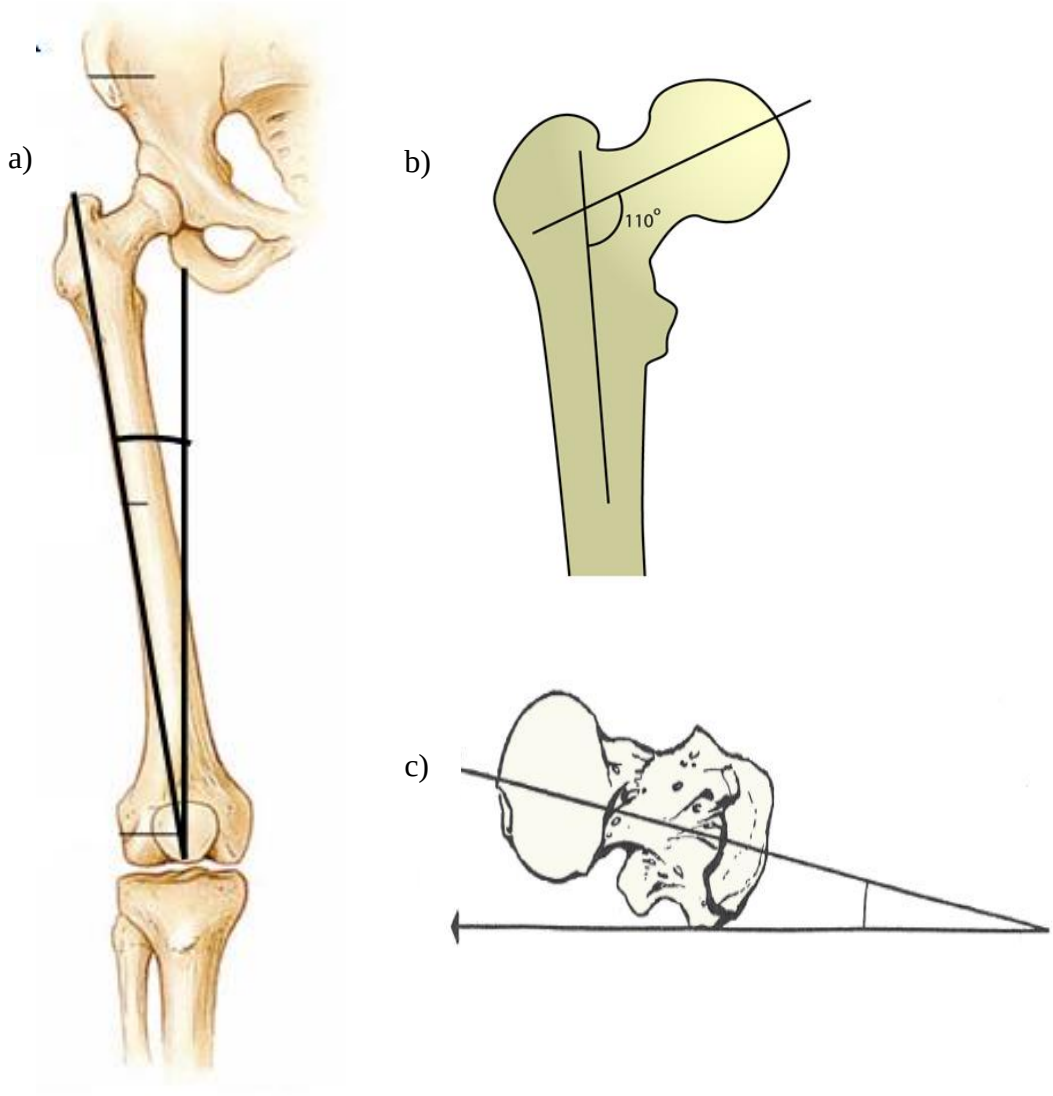

Figure 2.6. The bicondylar angle (a) and neck shaft angle (http://www.healthhype.com/femoral-neck.html) (b) can be seen in the frontal plane, whereas femoral torsion (c) is best observed in the superior direction of the transverse plane (www.dartmouth.edu/humananatomy/figures/chapter_12/12-16)

2.1.4 FUNCTION OF THE FEMUR

As the largest and strongest bone in the body, the femur is able to withstand loads of up to 280kg/cm² during vigorous jumping (Marieb, 2004) and its function as a supporting and locomotory bone is well established. The femur is part of two joints, the hip and the knee, therefore there are a large number of possible movements involving the femur. The hip joint is a conventional ball and socket joint which is has capability for a range of movement, stability and weight bearing. Because of the significant weight bearing aspect of the hip joint, the range of movement is not as large as other ball and socket

joints in the skeleton such as the shoulder. The movements that can be performed by the hip include flexion, extension, abduction, adduction, medial and lateral rotation and circumduction. The ligamentous structures surrounding the hip joint help to overcome the challenge of containment of the femoral head within the acetabulum throughout these varied movements. Three ligaments encompass the femoral head, these being the iliofemoral ligament, pubofemoral ligament and the ischiofemoral ligament (Figure 2.7).

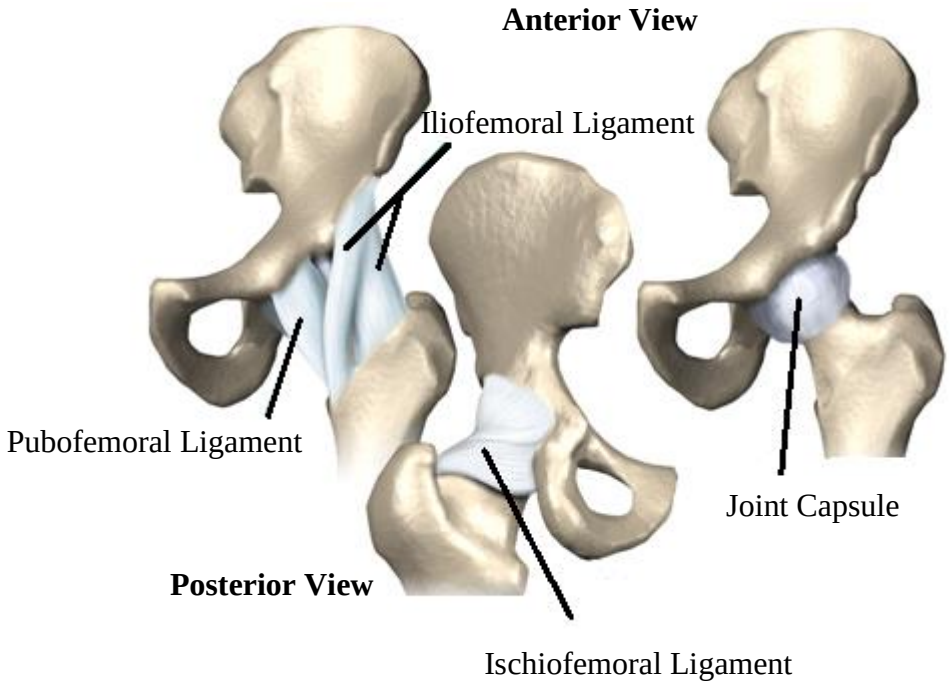

Figure 2.7 Ligaments of the hip joint (eorthopod.com)

The ligaments not only play a large role in maintaining the stability of the hip joint, but they also reduce the amount of muscle energy needed to maintain a standing position. The knee joint is the weight bearing articulation between the tibia and the femur and also between the patella and the femur. As a hinge joint it allows basic flexion and extension of the knee. Complex ligament structures of the knee maintain stability, which is necessary due to the weight bearing nature of the joint.

2.1.5 FEMUR BONE STRUCTURE

The structure of the adult proximal femur can be seen in Figure 2.1, where the trabecular bone, cortical bone and medullary canal can be clearly seen and the proximal

epiphyses and diaphysis are identified. The internal architecture of the femur has created much speculation debating possible causes for its highly optimised structure. The development of the long bones has been attributed to a number of factors including genetics, hormones, mechanical influence and vascularisation. The order and amount of influence that these factors affect the development of the skeleton is however unclear.

One aspect of the internal structure of the femur that has been studied is the vascularisation. The infiltration of the blood vessels, specifically in the femoral head, has been suggested to have a large influence on the trabecular structure (Trueta, 1954). Having a holistic view on the development of bone, the vascularisation of the femur that occurs before the ossification has been said to suggest that the nutrient supply to the femoral head plays an important role in the orientation of the trabecular network. The femoral head's main supply of blood is from the vessels of the ligamentum teres (Trueta, 1957), although this is varied through growth (Figure 2.8).

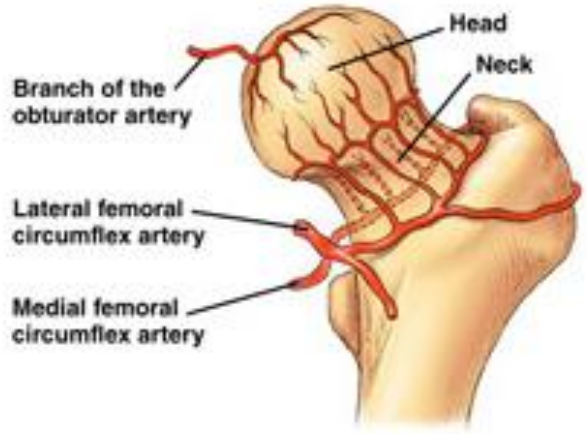

Figure 2.8. Nutrient supply to the adult femur from blood vessels (http://www.mypacs.net/cases/3173677.html)

The epiphyses and the metaphysis receive blood supply from different sources, with the epiphyseal arteries named medial and lateral, and the metaphysial arteries named superior and inferior. Trueta (1957) described the key events in the vascularisation of the femur during development. From birth to four years the main supply in the adult, ligamentum teres, does not contribute to the nourishment of the head. From four years to eight years old the metaphysial importance is reduced and then they disappear, leaving only the lateral epiphysial vessels as blood supply. From eight years to puberty the associated blood vessel of the ligamentum teres becomes active. Beyond puberty the

vessel supply has adult characteristics with epiphyseal fusion occurring bringing the three blood supplies together. Recent work has shown that disruption of the epiphyseal vascularisation does not massively damage the femoral growth plate (Kim *et al,* 2009), as this blood supply may not be the only way that nutrients can be supplied to the growth plate. However, it has been said that the metaphysial arteries become less important from four years old, but on this basis may still play a large part in supplying nutrients to the growth plate, if not the metaphysis. Therefore the importance of the blood supply to the femur may have a higher reliance in certain areas of the femur to produce normal development than others. This change in the vascular orientation could be seen as a key factor influencing the ability of the trabeculae to orientate to the stress distribution by infiltrating the areas with vessels to supply nutrients for the remodelling of trabecular, which is seen as the case in the adult femur.

The femoral trabecular structure in adults can be categorised into five groups as described by Osborne *et al,* (1980) (Figure 2.9).

1. The principal medial trabeculae, which arise from the medial aspect of the proximal end of the shaft and fan out in a broad band in the femoral head.

2. A secondary medial group that arises from the medial aspect of the proximal end of the shaft and extends superiorly and laterally toward the greater trochanter.

3. A principal lateral group that arises from the lateral aspect of the proximal end of the femur and curves across the superior aspect of the femoral neck, ending in the femoral head.

4. A secondary lateral group that arises from the lateral aspect of the proximal end of the femur and is directed superiorly and medially across the lower femoral neck.

5. A final group of trabeculae that curves upward from the lateral trochanter.

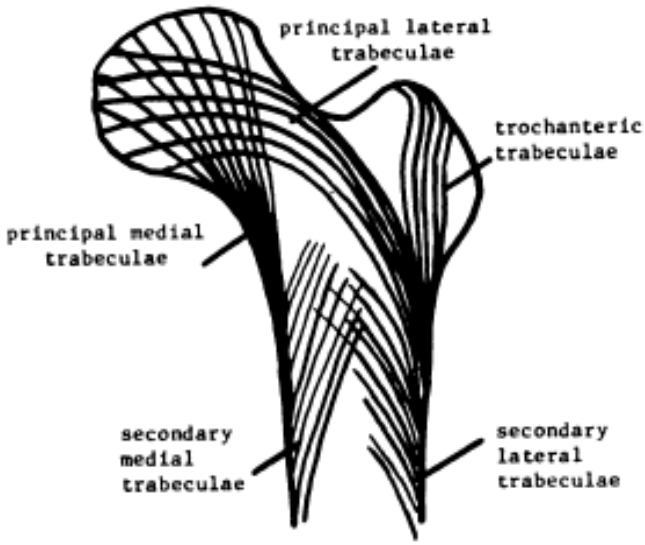

Figure 2.9. Grouping of trabeculae in the adult femur. Reproduced from Osborne et al, (1980)

The function of this well established internal architecture of the adult femur has been discussed extensively in the literature, with the groups of trabeculae being attributed to mechanically driven functions. Figure 2.10 shows these groups as the principal compressive group, principal tensile group, greater trochanter group, secondary compressive group and secondary tensile group.

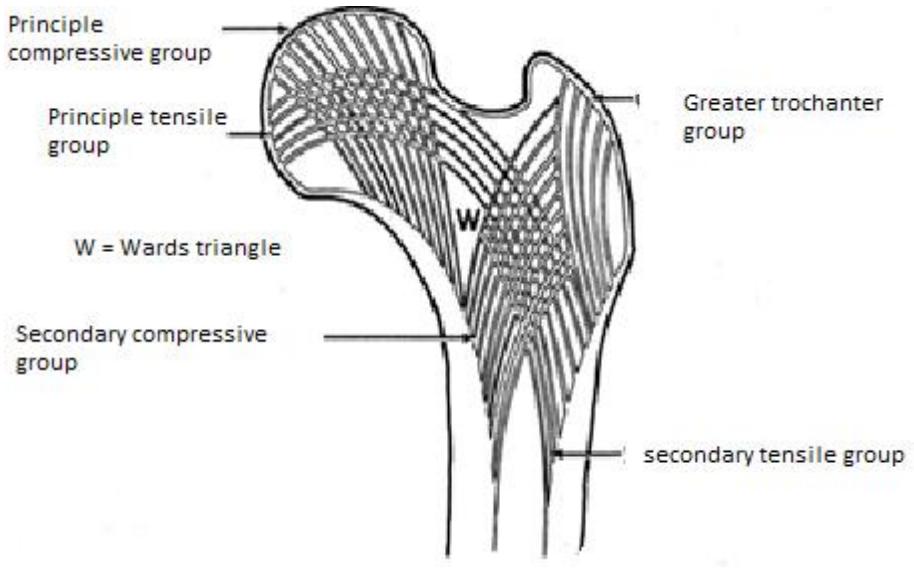

Figure 2.10. Functional orientations of trabeculae in the adult femur, showing Ward's triangle (W) (http://orthopedicsurgeons.blogspot.co.uk)

The proximal femur is often used to show Wolffs' Trajectorial Theory, which can be described as "the trabeculae of cancellous bone follow the lines of trajectories in the homogenous body of the same form as the bone and stressed in the same way.'' (Murray 1936, *in* Skedros and Baucom, 2007). The vertical lines in the femur's trabecular structure absorb the compressive forces which pass vertically through the acetabulum during locomotion and standing (Pauwels, 1980). The horizontal lines of the femur are said to transmit the tension stresses which oppose the compressive forces during standing. Hammer (2010) discussed the theory, and during the investigation it was theorised that both directional lines of trabeculae deal with compression under different everyday activities i.e. vertical trabecular for standing activities and horizontal trabecular for squatting positions. This theory would adhere to Wolff's Law but conflict the accepted Trajectorial Theory. Although, as suggested in the study more in depth work such as FEA would be needed to strengthen this concept. Further to this, in Hammer *et al*, (2010) two areas of interest within the proximal femur were identified during dissection, Ward's Triangle and the calcar femorale. Ward's triangle is created by three of the trabecular directional lines (Figure 2.10). This area has a low BMD and is an area of interest for osteoporosis researchers. Yoshihashi *et al*, (1998) found that measurement of the Ward's triangles, which has a low BMD, can be classed as a good indicator of osteoporosis whereas other areas, including the spine and trochanters, did not display as strong indicators of osteoporosis. The calcar femorale has been described as "a bony spur projecting into the cancellous tissue of the base of the femoral neck" (Newell, 1997). The role of the calcar femorale has been suggested to bear compressive load, redistribute stress or load from the femoral head to the proximal femur, and can reduce bending moment and torsional moment (Zhang *et al*, 2009). Hammer (2010) showed that the calcar femorale is not only an external spur but is an extension of the internal trabecular structure although it does not appear until the later stages of growth, the reasons for which are unknown. It does however appear to play an important role in the stress distribution of the proximal femur. The influence of muscle forces on the reduction of bending moments in the femur and thus an increase in the compressive force has been an area of research interest and these are influences need to be discussed.

2.1.6 COMPRESSIVE LOADING OF BONE

The idea that bone is predominantly in a compressive state of stress rather than a state of bending, which is often thought, is not a new theory but rather an underdeveloped one. The earliest work in this theory is from Roux (1912), where it was said that bone is formed under compressive stress, whereas connective tissue is formed under tensile stress. Taylor *et al* (1996) questioned the amount of bending stress in the femur by producing a FEA of a fully intact muscle and joint loaded femur and measuring the deflections. One criticism of the model was said to be the lack of *in vivo* loads applied as the muscles were idealised into groups, and the high forces used to represent the muscles may not be completely accurate. However, this would more than likely increase the compressive state than increase in tensile stress, as shown when load cases were increasingly more physiological (Hammer *et al*, 2010). Further evidence can be observed in trabecular bone which transmits the compressive stress to the bone, and ligaments or tendons transfer the tension away from the bone (Rudman *et al*, 2006). Further in this study, the inclusion of ligament and muscle forces on the femur were shown to increase the compressive stresses in the proximal femur and reduce the tensile stresses on the medial side of the femur. This reduction in bending stresses was addressed by Pauwels (1980) in an extensive study looking at the biomechanics of the locomotor apparatus and in particular looking at the engineering aspect of the lower extremities and its apparent ability to reduce the bending moments in the bone through the use of ligament and muscular structures. The application of the ligaments moved the vector of the stress in the vertical axis to the centre of the diaphysis resulting in a compressive stress in the shaft of the femur. Tanck *et al* (2001) also found that in the rapid increase of weight in pigs bone is formed away from the bone axis so that the bending moments are withstood. Likewise in humans where a tension band (tendon) is seen at the centre of the bone axis to help cope with the bending load which lies outside of the bone.

More recent work includes the work produced by Sverdlova and Witzel (2010) in which a number of ideas and results promoting this theory have been published. This work postulates about the control mechanisms involved with bending minimisation in bone. A number of limitations do occur within this work. The authors have the same criticism that Taylor *et al* (1996) had of the model, suggesting that the muscles in the model have a larger, over compensating influence, much greater than *in vivo*. This however could be due to the lack of a fully designed *in vivo* model, as the model lacks ligamentous

structures and has non-physiological origin and insertion points for the muscles. A more sophisticated musculoskeletal model is required to adequately represent the lower extremity of an adult human. This model should include the response of the agonist and antagonist muscle action in a supporting role rather than creating movement. However the true interaction between muscles working as agonist and antagonist 'pairs' is not truly understood because of the complexity of the pairing. As suggested by Sverdlova and Witzel (2010) an opposing active muscle would act as a tension band to resist the bending moment caused by the agonist muscle as was previously suggested by Pauwels; (Munih *et al*, 1992). Through the use of EMG Munih *et al* (1992) found that co-activation of muscles caused less bending irrespective of posture, similar to the behaviour observed in the aforementioned work (Sverdlova and Witzel, 2010) from a sit to standing movement. In further work by Munih *et al*, (1997) modelling the muscle activity, it was shown that rather than there being contraction of a single muscle there was a specific interaction between a number of muscles. One suggestion by both researchers is that the neurocontrol system may have corresponding sensors that may control the effect of these co-activated muscles so as to reduce the bending stresses. However no work has been produced to evaluate this theory, but what can be said is that there is certainly the proprioceptors in place that would be able to create a feedback loop for the control of this minimisation of bending in bone. The theory of predominant compressive forces in bone extends further than just the femur and is evident in number of other structures. The zygomatic arch in skulls has a fascia attached to it but this is not always modelled, and the absence of this can increase the bending stresses (Curtis *et al*, 2011). This same occurrence is evident in the femoral structure, with the iliotibial tract reducing the bending stresses in the shaft of the femur (Pauwells 1980).

The anatomy of the adult femur has been explored but the growth of the femur does not occur linearly and the femur is ever changing in terms of structure and shape. Hence, these changes during growth need to be examined in more detail.

2.1.7 JUVENILE OSTEOLOGY

During the development of the femur, a number of geometric changes occur and the ages at which these occur are well documented in the literature (Scheuer and Black, 2001). These changes include ossification, femoral anteversion, femoral torsion, bicondylar angle and NSA.

2.1.7.1 Ossification

The growth and ossification of bone have been discussed previously, in the thesis, however during this section the literature review will be specifically related to the femur. The femoral ossification occurs via perichondral intramembranous ossification in the region of the mid-shaft around prenatal week 7. Although by definition there should only be one primary centre, per bone in reality there is sometimes numerous primary centres i.e. the pelvis, ischium, ilium and pubis and many develop as late as pre-adolescent years. It can also be said that primary ossification is the template of the skeletal element and can even go on to form the entirety of the adult bone. In addition to this, it can fuse with smaller centres of ossification which is the case in the femur.

The primary ossification site is in the diaphysis of the long bone, this being the initial ossification in the shaft of the femur. Although this is the main site for the ossification of the shaft, the process may also occur at a number of other sites (known as secondary ossifications). These may extend to include 3-4 ossification sites at both the proximal and distal epiphyses. The diaphysis and epiphysis are separated by a growth plate and a cartilaginous area. The growth plates at both the proximal and distal ends facilitate growth of the limbs, which is why they fuse late in development, hence this late fusion should not be considered as a result of lack of mechanical loading. The stages of development and the ages at which these occur can be seen in Table 2.1and Figure 2.11.

AGE	DESCRIPTION
Pre-natal	
7-8 wks	Primary ossification centre appears in shaft
36-40 wks	Secondary centre for distal epiphysis appears
Birth	
By 1 yr	Secondary centre for head appears
2-5 yrs	Secondary centre for greater trochanter appears, neck separates into trochanter and head
3-4 yrs	Epiphysis of head hemispherical and recognizable
3-5 yrs	Distal epiphysis recognisable by characteristic shape
3-6 yrs	Ossification appears in the patella
6-8 yrs	Greater trochanter becomes recognisable
7-12 yrs	Secondary centre for lesser trochanter appears
12-16 yrs	Head fuses in females
16-18 yrs	Head fuses in males
16-17 yrs	Lesser trochanter fuses
14-18yrs	Distal epiphysis fuses in females
16-20yrs	Distal epiphysis fuses in males

Table 2.1. Summary of stages of femoral growth (Scheuer and Black 2001)

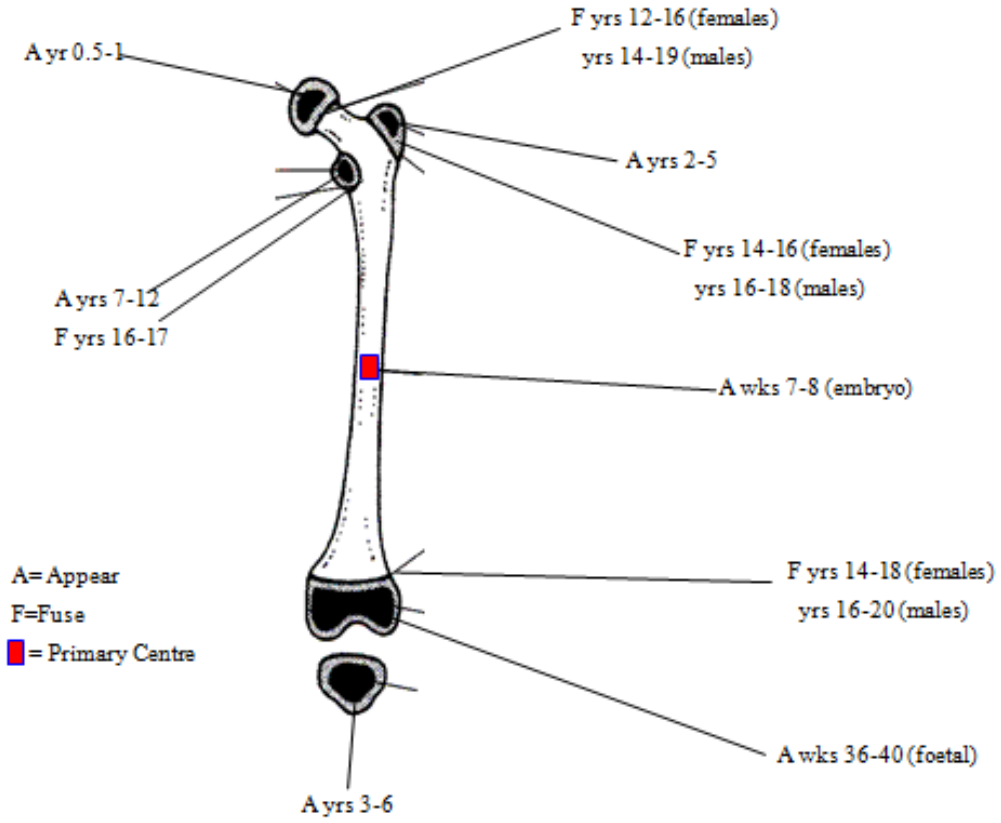

Figure 2.11 Appearance and fusion of ossification centres in the femur (Scheuer and Black, 2005).

Prenatally, the initial ossification of the diaphysis appears at 7-8 weeks. At 12-13 weeks the ossification of the diaphysis reaches the neck and the gluteal tuberosity and linea aspera develop and increase in bone thickness. By 28 weeks, the end of the shaft rather than being a dome shape has two angulations towards the cartilaginous head and the other directed towards the cartilaginous greater trochanter. At the distal end a secondary centre of ossification appears and torsion of the shaft occurs. At birth 75-80% of the femur is ossified and a secondary centre of ossification of the femoral head is formed at approximately 6 months. Between 1 and 3 years there is a rapid decrease in the normal shaft torsion and the neck divides into two separate growth plates for the head and the greater trochanter. Principal and lateral trabeculae become visible, and there is a curvature in the shaft at approximately 18 months. A secondary centre of ossification in the greater trochanter is seen at 2-5 years and the epiphysis grows rapidly in width as ossification spreads into the condylar areas of the cartilage. From 3- 4 years there is a large change in the neck shaft angle, and from 4 to 5 years the secondary trabeculae are observed, and the condylar and trochlear areas can be seen on the metaphyseal surface. By 7 years the linea aspera becomes more defined and a lateral lip can be seen as can

the gluteal tuberosity. From 7-13 years the condyles and intercondylar fossa are visible and the adductor tubercle is observed. Between 14-16 years there is another change in shaft torsion and finally a complete fusion of the femur at the comparatively late age of approximately 20 years old.

As ossification occurs during development at a number of sites, Panattoni *et al* (2000) studied the ossification in the femoral head from 11.5 weeks to 1 year of age. The work revealed that ossification centres of the femoral head appear synonymous with increased stresses. Carter and Beaupre (2001) showed that in cartilage exposed to intermittent octahedral shear stresses an acceleration in ossification was evident, thus encouraging the development of additional centres of ossification within a cartilage mass. This has been shown to inhibit ossification in the region of articular cartilage and in the growth plate, which separates the primary from the secondary centre. The greater trochanter however does not follow this limitation, with the reason suggested for this being that it originally develops as part of a continuous cap with the head before it becomes separated by the development of the neck in the second year. Anderson *et al,* (1964) assessed the length of the femur and tibia in normal boys and girls from 1-18 years, measuring from the most proximal articulating surface of the capital epiphyses to the most distal point on the lateral condyle, including the proximal and distal epiphyses. The results from this study indicate a linear increase in growth is observed until the age of 16. This may be in response to hormonal influences on the skeletal development, suggesting that mechanical influence is not solely responsible for growth. However, Ruff *et al* (2003a) compared the humeral strength and length proportions to the growth of the femur and found that, results until the age of 1 year were comparable, but at the onset of weight bearing and locomotion, a shift in growth trajectories of the femur was identified, accelerating as the onset of a mature gait pattern emerged. This suggests that there is also a high degree of mechanical influence on the development of the femur during growth.

2.1.7.2 Femoral Torsion

Femoral torsion in adults is the angle between the condyles and the angle of the head and neck of the femur (Figure 2.6). This angle changes during growth and has been documented in a number of studies. The normal torsion angle changes from 33° at 0-2 years old to 10° in 14 to 16 year olds (Upadhyay *et al,* 1990) although standard

deviations are relatively large and variations between gender and limbs are apparent. Abnormal variations of femoral torsion can lead to disabilities and an in-toeing during gait. Bonneau *et al*, (2011) studied the change in femoral torsion during prenatal growth and associated the changes observed with relation to intrauterine pressure. There was an observed increase of 6° between 28 weeks of gestation and 40 weeks which, although not a large change, correlated well with previous literature and therefore can be perceived as an accepted finding. The results were hypothesized to be as a result of the femur acting as a lever arm with the force being applied to the condyles and the femoral head acting as a resisting force causing the torsion of the femoral shaft. Rather than suggesting that this torsion is a genetically determined development, this hypothesis seems to fit well with the observed decrease in the femoral torsion from birth to adulthood, due to the changes in the uterus forces and forces acting on the femur compared to the forces after birth.

2.1.7.3 Bicondylar Angle

As previously mentioned, the bicondylar angle in adults is approximately 8-11° but 0° in newborns (Tardieu and Trinkaus, 1994). This angle changes until about 8 years of age at which point it stabilises Tardieu and Damsin (1997) observed through the use of X rays and osteological measurements that the bicondylar angle starts at 0° at birth, and then increases with growth to 6°-8° between 4 and 8 years, before stabilising to the observed adult values of 8-11°. The role of mechanical influence in the development of this angle has been studied in the literature. Tardieu and Trinkaus, (1994) found that in paraplegic children who do not develop bipedal locomotion there is a lack of bicondylar angle. Further to this, during mechanobiological simulations using FEA Shefelbine *et al*,(2002) found that with a more medially directed load (20%) a bicondylar angle would be formed similar to the observed *in vivo* value of 10° over 8 years. Therefore it was determined that a more medially directed load from a change in locomotion would cause this bicondylar angle. However further FEA would be needed to assess the changes during gait and its effect on ontogeny.

2.1.7.4 Femoral Neck Shaft Angle

In early infancy the neck-shaft angle or angle of inclination is about 150°, in childhood about 140°, in the adult about 125°, and in the elderly about 120° (Norkin and Levangie,

1983 as reported by Isaac *et al,* 1997). Bulandra *et al,* (2003) suggested a predetermined change in NSA in preparation for bipedal locomotion from changes in the foetal femur. A decrease in NSA was seen in the foetus from 142.01° in the youngest to a mean of 137.58° in the oldest group of foetuses. However changes in *in utero* loading were not considered and therefore these variations from growth in the womb may alter the loading. Changes from birth to adulthood have been documented. Jenkins *et al,* (2003) found that the neck shaft angle stabilises at 10 years old and from 4- 8 years old an angle from 114° to 110° was observed. During growth these changes have been suggested to cause the load axis to intersect the axis of the femoral shaft and bring the knee closer to midline relative to the hip (Scheuer and Black, 2005).

2.1.7.5 Internal Structure of the Juvenile Femur

Many clinical and experimental studies have assessed the structure of the adult and juvenile femur, but analysis of the stresses and strains appear to have been limited to those of the adult femur (Edwards *et al* 2008; Duda *et al*, 1998; Glitsch and Baumann, 1997). As discussed in section 2.1.5 the internal architecture of the adult femur has been well documented, whereas juvenile studies make very limited reference to the internal architecture of the proximal femur. Townsley (1948) detailed the orientation of trabeculae in the juvenile femur during development. As well as the change in structure orientation of the femur the trabecular bone orientation changes at an equal magnitude. It was identified that from the prenatal where the trabecular struts in the diaphysis are vertical and almost parallel to each other, at 12 months the orientation of the trabecular bone begins to change to what was described as a cross braced system. This was associated with the onset of increased muscular activity and standing. The remodelling of the trabecular bone conforms to the changes of the cortical bone shape such as an increase in the neck length. Although the trabecular direction becomes more defined and thicker struts are developed from 12 months onwards the orientation of the trabeculae remains constant through to adulthood (Figure 2.12).

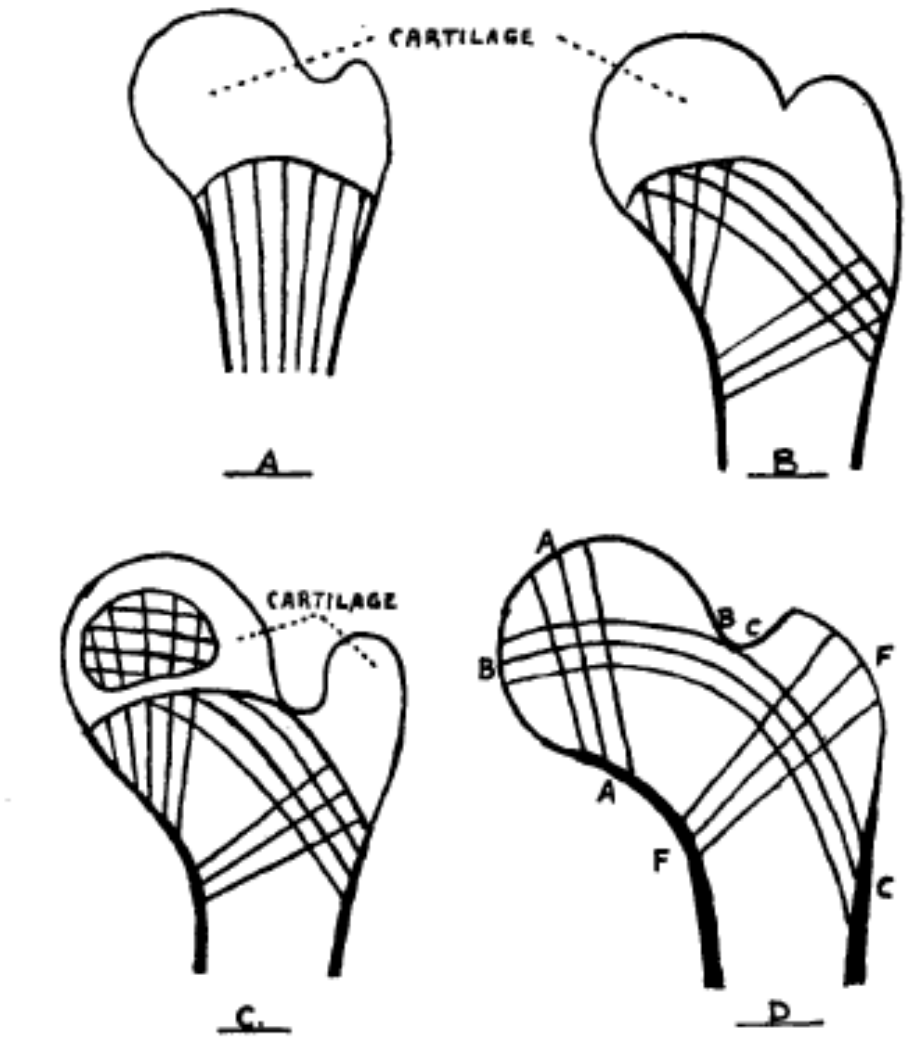

Figure 2.12. Reproduced from Townsley (1948) showing the cross braced system of the trabeculae bone developing from 12 months onwards. A) 8 months fetal life, B) 1 Year, C) 2.5 years, and D) adult life.

When the epiphyses are formed at the age of 2 years, the trabecular structure showed a higher density in the vertical orientation rather than horizontal. This is the case until the age of 4 when horizontally orientated trabeculae become more prominent than in the younger ages and an adult-like structure is formed. This again was attributed to the weight distribution and activity changes during growth and development. Similarly Osborne *et al* (1980) described distinct patterns of orientation of the trabecular bone during growth, which can be divided into five groups. However unlike the observations made by Townsley (1948), Osborne did not observe an adult like trabecular orientation until 10 years of age, at which stage the secondary lateral group of trabeculae became

apparent. Further to this the trabecular network was said to be randomly orientated until 18 months, however this may only be true when relating the early orientation to the five groups. Whereas the orientation of the early trabeculae may in fact be aligned to the stresses that they are being exposed to (Ryan and Krovitz, 2006). However this study can help to inform researchers of normal development within the juvenile femur. Also it allows a comparison to be made between adult trabecular structures so that variations can be made in reference to the loading that may affect the orientation. Ryan and Krovitz (2006) detailed trabecular bone ontogeny in the femur. Specimens ranged from prenatal to nine years of age, and specified volumes of interest were tested for bone volume, trabecular thickness, trabecular number and fabric anisotropy. All of these variables were seen to decrease from the age of 6 to 12 months, concurrent with decreased BMD observed by Panattoni *et al,* (2000). By the age of 2-3 years these increase and the cortical bone surrounding the neck increases. These were attributed to the increased weight bearing activities such as the onset of independent walking. It was concluded that the structure of the trabeculae within the femoral head and neck closely matches the onset and continuation of bipedal walking. The volumes of interest chosen for analysis were primarily in the shaft as this is the only area that consistently has a trabecular structure because of the cartilaginous nature of the rest of the femur. However although the loading is not documented by any structure within the cartilage there must still be some loading present. Other differences observed in the juvenile trabecular bone orientation which are apparent in the adult femur include the lack of Ward's triangle and calcar femorale. These are not present until the age of 8 years which coincides with when gait maturity being reached (Sutherland, 1997), and therefore these may be developed in response to mature gait.

The development and growth of the skeleton and with specific reference to the femur has been documented here. As has been discussed mechanical forces are thought to have an influence on the shape of the bones. These mechanical influences are produced mainly from muscle and joint reaction forces. One activity that produces these forces and is seen throughout growth is locomotion. An understanding of this locomotion and the femoral structure can be combined and used to explain bone growth and development.

2.2 GAIT ANALYSIS AND DEVELOPMENT

As there is thought to be a direct relationship between bone growth and development, and mechanical influence (Ruff *et al*, 2003a; Carter and Beaupre, 2001), it is important to understand the changes in mechanical loading that occur throughout growth. Therefore an imperative area of this research is the analysis of gait development leading up to mature bipedal locomotion. Key stages of development are known to occur at the following stages: prenatal, neonatal, neonatal to three years, three years to eight years and adulthood (Sutherland, 1980). Therefore the movements associated with these development stages will be discussed. A large change in movement patterns and locomotive capabilities is seen between birth and 3 years, however a gait pattern similar to that of an adult is achieved from 3 years onwards with only minor changes being observed until maturity is reached. It is these minor changes that are to be discussed.

2.2.1 ADULT GAIT

Human gait is a highly organised movement, and although variations between subjects do occur, a standard gait pattern is usually observed within a reasonable degree of deviation. The importance of these standardised gait parameters are realised during clinical trials (Sutherland, 1980), as when abnormal gait is observed the abnormalities can be compared to the standard gait. Retraining through various methods can then be undertaken, where possible with the aim of achieving a more standardised gait for the individual.

To identify variations in gait throughout maturation it is important to understand the characteristics of adult gait which is the goal of developing gait. One gait cycle is defined as heel strike to heel strike on the same leg, whilst toe off divides the gait cycle into a swing and stance phase. Toe off occurs at approximately 60% of the gait cycle and stance phase makes up 60% and swing phase 40% of the gait cycle. The stance and swing phase have three main targets these are weight acceptance, single limb support and limb advancement. These variables can be further subdivided into subphases. Initial contact and loading response create the weight acceptance goal, and form the initial 10% of the gait cycle. Single limb support has a mid-stance phase and a terminal stance phase from 10 to 50%, the goal of these phases are to support the body whilst the opposing leg advances. The final stage of limb advancement is comprised of a pre swing, initial swing, mid swing and terminal swing phase. There are also two periods at

which both feet are in contact with the floor, called the double support phase. The initial double support phase occurs at initial contact and the first heel strike and lasts from 0-10% of the gait cycle and the terminal support phase occurs at 50-60% of the gait cycle until toe off (Figure 2.13).

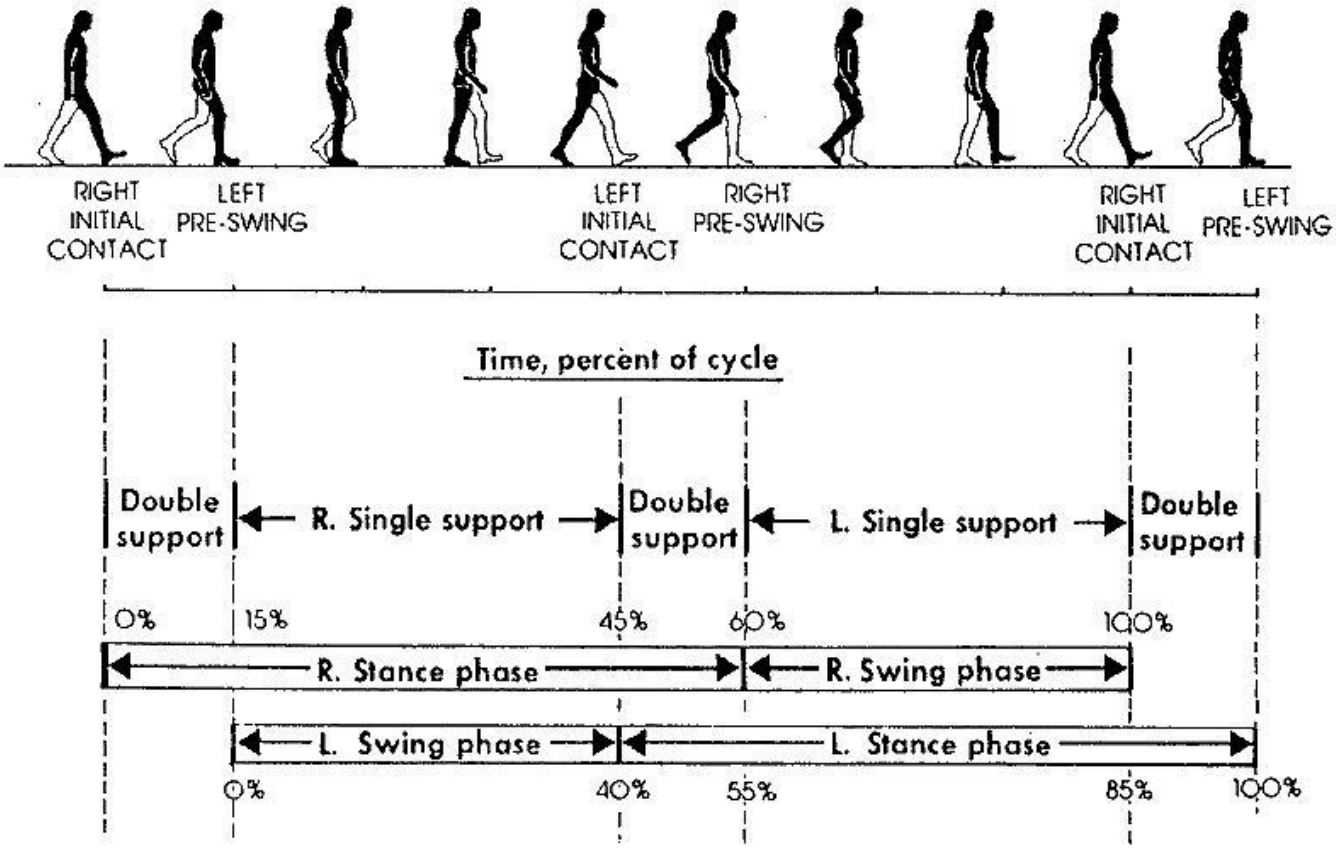

Figure 2.13. 100% of the gait cycle with the key stages identified (Kirtley, 2006)

2.2.2 TEMPORAL SPATIAL PARAMETERS

Temporal spatial parameters describe the time and distance variables, including cadence which refers to the number of steps per minute and stride length. Although there are variations in the temporal spatial parameters and relationships between them, normative ranges can be seen in Table 2.2.

	Speed (m/s)	Cadence (steps/min)	Stride length (m)
Male	1.3-1.6	110-115	1.4-1.6
Female	1.2/1.5	115-120	1.3-1.5

Table 2.2 Normative ranges for temporal spatial parameters (Kirtley, 2006)

The relationship between the increase in speed and the increase in cadence is linear, whereas speed and stride length have a logarithmic relationship. Speed, cadence, and stride length can be normalised so that changes between subjects can be considered without the influence of inter-subject variability's such as stride length (Stansfield *et al*, 2003).

It is important to explore the tools and methods that are necessary to assess gait to gain a full understanding in the process and reliability of the collected data. The most common methods and those that are most relevant to this research are motion capture and ground reaction force measured through the use of force plates. Following discussion of each of these methods normal gait data for adults will be examined in the context of the current study.

2.2.3 MOTION CAPTURE

Motion capture is the process of recording and analysing movement. Early motion capture was performed using 2D video analysis (Hennessy *et al*, 1984), however this only allowed for single plane motions or a maximum of two planes of motion to be analysed simultaneously (Sutherland, 1980). Although these early methods produced accurate and informative data, technological developments allowed improved movement analysis through the use of 3D motion capture systems, and this is now commonly seen as the gold standard method in motion analysis. 3D motion capture can give vast amounts of data including joint angles, velocities and acceleration of joints. Movement is quantified by describing how a local Cartesian coordinate system, a frame fixed to the body, is located and orientated with respect to global coordinate frame (Zatsiorsky, 2000; Fisk, 2004). Motion capture can either be passive or active, depending on the type of skin markers used. Passive markers are most commonly used, utilising reflective properties, to reflect light omitted by the cameras back in the direction from which it comes (Fisk, 2004). The advantages of these markers are that they can be seen simultaneously by the sensors, they are easily attached and do not hinder the subject's movements. Figure 2.14 represents how motion capture retrieves

marker location in 3-D object space in a 2-D image plane. Where a ray of light follows a straight line from marker (M) through the plane of the camera to lens of the camera (P). As long as each marker is seen by two cameras then it can be given 3D coordinates and therefore can be used to create measurable data.

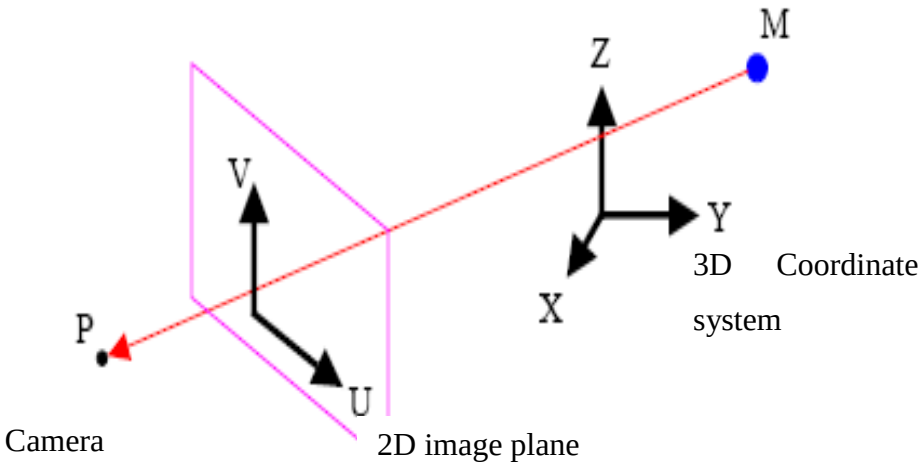

Figure 2.14. Marker locations (M) in 3D object space and the 2D image plane

Motion capture software such as Visual3D (C-Motion, Inc, USA) and Vicon bodybuilder (Vicon, UK), create body segments between the markers to visualise and calculate the required kinematic data. To do this, markers need to be placed on identifiable anatomical landmarks, and a number of marker set up models are frequently used throughout the literature. The Helen Hayes marker set in the lower extremities requires markers to be bilaterally attached to the following landmarks: anterior superior iliac spine (ASI), posterior superior iliac spine (PSI), proximal third of the thigh (THI), lateral condyle of the knee(KNEE), distal third of shank (TIB), lateral malleolus (ANK), calcaneus (HEE), first and fifth metatarsals (Figure 2.15).

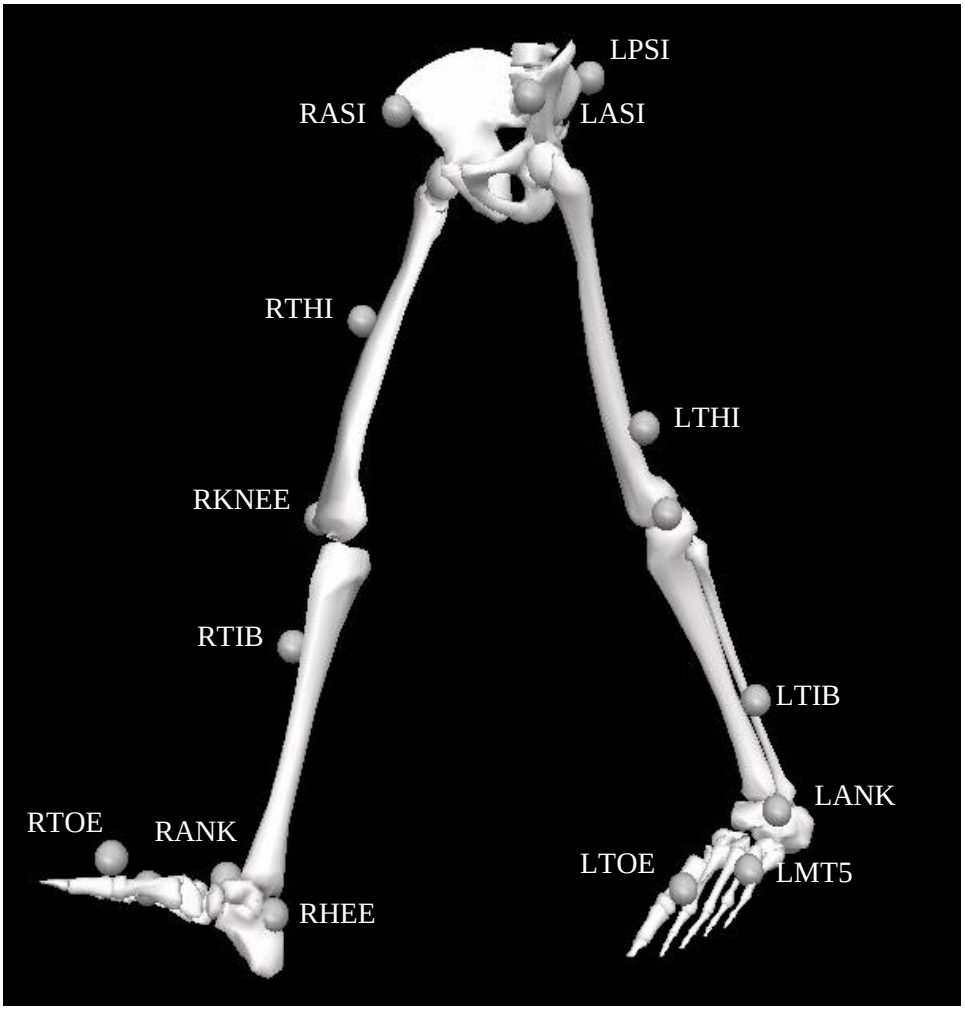

Figure 2.15. Marker positions in the Helen Hayes (HH) formation and segments formed through 3D motion analysis in Visual 3D.

These marker positions allow for segments to be built in relation to the landmarks and kinematic results can be calculated including joint angles and angular velocities. In the lower extremities there are three main variables in three directional axes that are regularly reported in the literature. These variables are as follows hip flexion/extension, abduction/adduction and rotation; knee flexion, varus/valgus angle and knee rotation; and ankle dorsi/plantar flexion, foot progression and foot rotation. The normative data can be seen in Figure 2.16, with these normative values being representative of adult gait which are generally accepted as the standardised gait pattern although variations do occur.

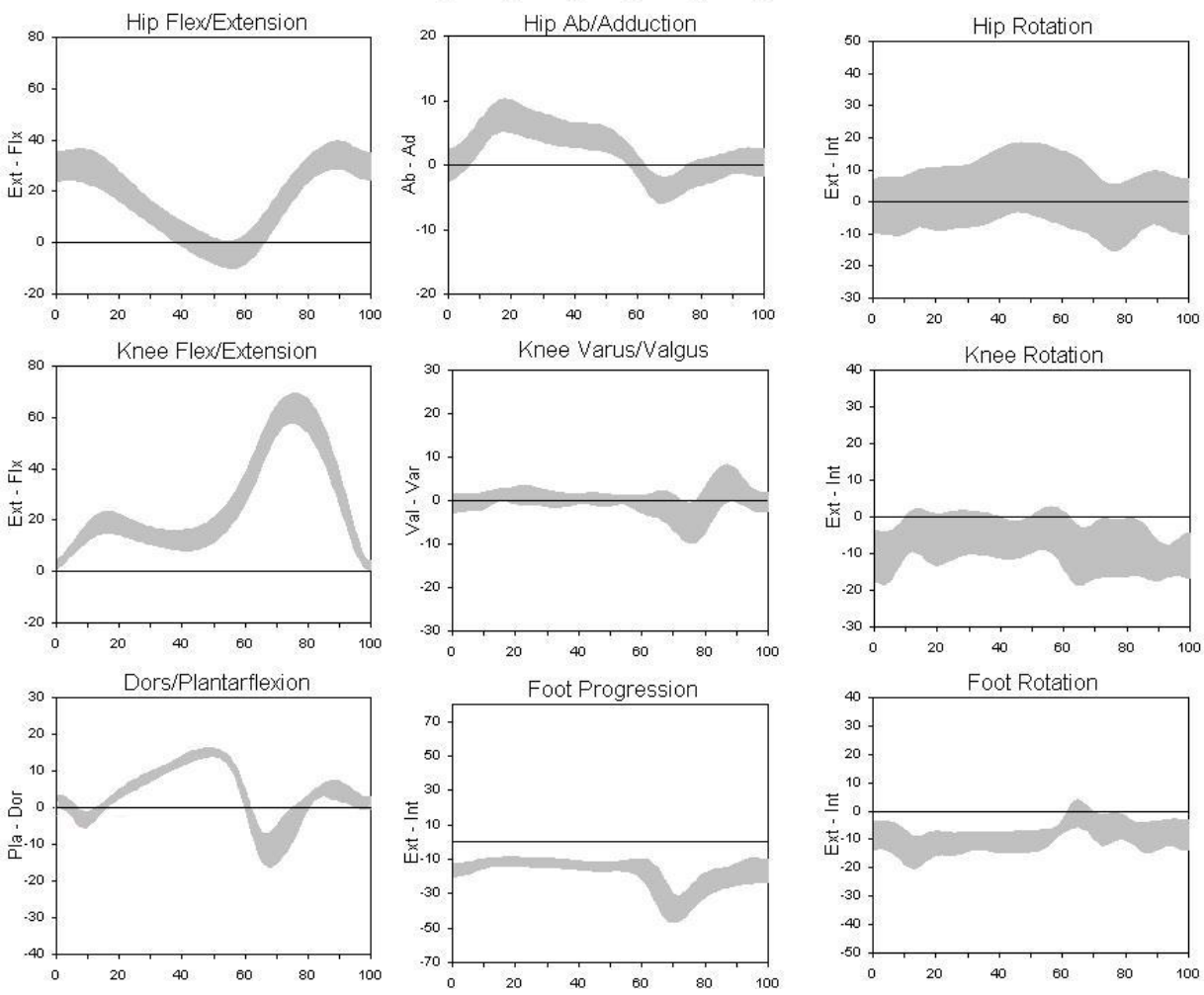

Figure 2.16. Normative values of lower extremity kinematics over 100% gait cycle. Normative range is shown as mean ±1 SD (Kirtley, 2006)

During the gait cycle the hip is flexed at initial contact then it begins to extend until the end of the stance of phase where flexion begins. This is coupled with a hip abduction during mid-stance phase when the hip begins to abduct until the end of stance phase where adduction begins until the end of the gait cycle. Flexion /extension are the main kinematic movement analysed for the knee. A 0° flexion angle is observed initially which is increased to approximately 20°, the knee then extends before another phase of flexion which continues until reaching the highest peak at mid swing phase at approximately 70°. The knee then begins to extend until the end of the gait cycle. The ankle joint movement in the sagittal plane is seen with an almost neutral ankle before a dorsiflexion is produced until the start of terminal stance where the foot changes rapidly into a plantar flexed angle corresponding with toe off. The ankle then begins to dorsiflex ready for ground clearance during swing phase. These patterns of gait are

fairly consistent between adults however these can change according to pathological disorders or during the developing gait.

2.2.4 FORCE DATA

Kinematic data can be explored through the use of 3D motion capture as described above, however for kinetic analysis measurements of force data is required. This can be collected through the use of force plates. During gait analysis force plates are sited on the ground in a suitable configuration for the subjects to walk over them. The force plates measure the forces applied on them using Newton's second '*the acceleration of a body is parallel and directly proportional to the net force and inversely proportional to the mass'* and third laws *'the mutual forces of action and reaction between two bodies are equal, opposite and collinear'*. In the case of gait analysis the force applied by the subject to the floor is measured as illustrated in Figure 2.17.

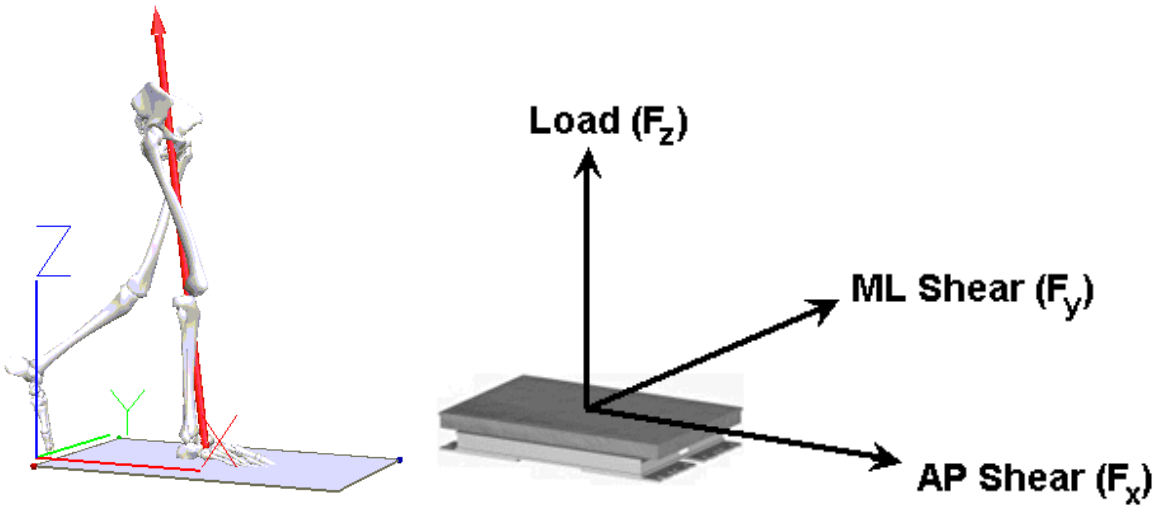

Figure 2.17. Force plate reaction and directions of the axis. Fz shows the vertical reaction force, Fy shows medio lateral force, and Fx shows force in the anterior posterior direction.

The direction of the force can be measured in three directions proximal-distal (PD) (Fz), medio-lateral (ML) (Fy) or anterior-posterior (AP) (Fx) (Figure 2.17). These can give indications of the direction of the force. For example, during a vertical jump the Fz direction would be the most significant force, but if a jump with a more forward direction was performed a greater emphasis would be on the reaction in the Fx axis as there would be a greater posterior force required to propel the body forward. During

standing the ground reaction is constant, however during walking the ground reaction force changes, these are to be discussed.

During gait the stance phase of the cycle is the only point when the foot is in contact with the floor and this is when the ground reaction force is measured. Therefore, when reporting GRF it is reported in one of two ways, either as a full gait cycle where data is only shown in 60% of the gait cycle (the stance phase) or it can be represented on a graph only showing the stance phase and disregarding the swing phase of the gait cycle. GRF is measured in 3 directions, the vertical force (proximal-distal), horizontal force (medial-lateral) and frontal force (anterior-posterior). The force is measured in Newton's (N) but is often normalised to bodyweight to allow easy comparison between subjects and is expressed as Newton's per kilogram (N/Kg). A typical graph of the ground reaction components can be seen in Figure 2.18 where the largest value is the vertical component (Fz), which is consistently the case for normal gait.

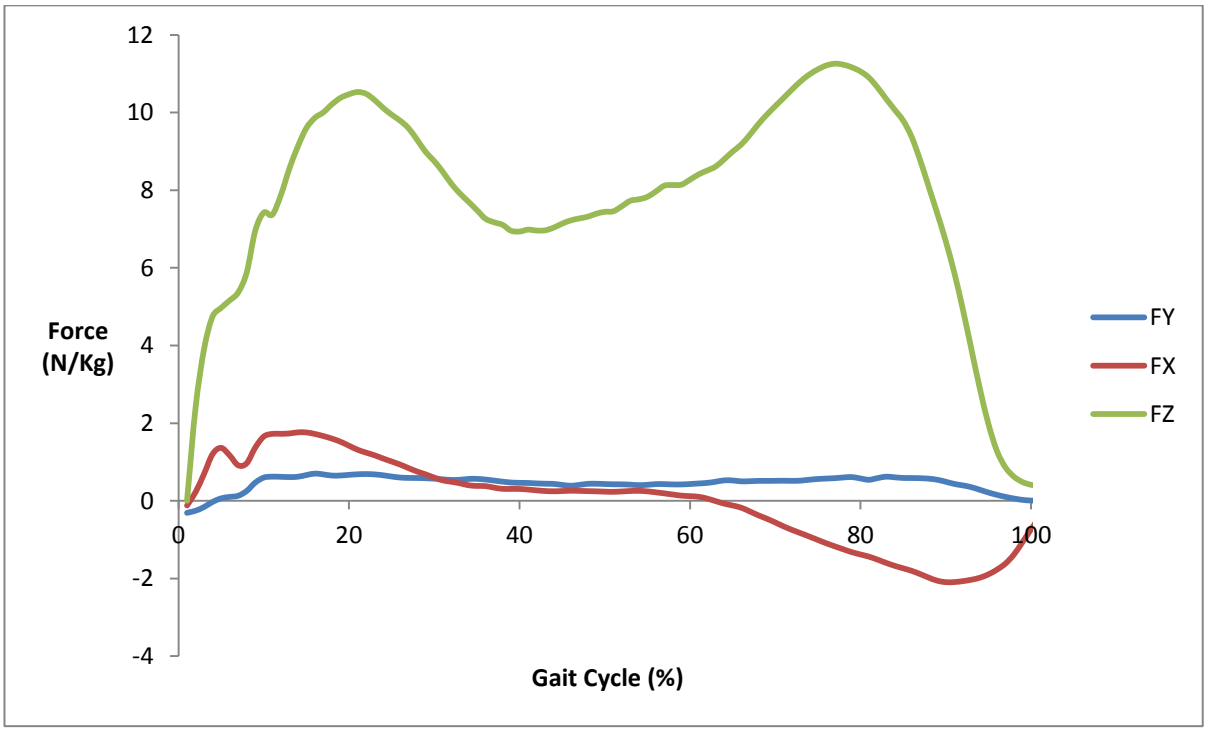

Figure 2.18. A typical GRF of all three force components, the Y axis shows N/Kg to normalise the data shown against gait cycle between subjects.

The GRF in all axes have very distinct patterns. In the Z direction a twin peaked 'butterfly' shape is portrayed, where initially the force quickly rises with the initial

contact to the first peak (which is above resting bodyweight values) and then falls below resting bodyweight during mid-stance, rising again for the second peak at terminal stance. At this point the bodyweight is transferred to the opposite leg causing the force to rapidly decrease, resulting in a zero GRF for the observed leg during swing phase. In the X direction, the anterio-posterior force initially is negative indicating a posterior force during early stance phase and this develops into an anterior force at terminal stance phase. These indicate an initial propulsion forward by the posterior force and then a controlling force directed anteriorly during late stance. The Y direction which is the always the smallest value in normal gait, where initially there is a lateral force and then this shifts to the medial direction reaching a peak during early stance, then remaining in a medial direction before peaking again during late stance. As seen in the kinematic data speed of walking and when a run is performed the GRF is seen to increase substantially (Keller *et al,* 1996). In all cases, the force data collected can be used to calculate the joint moments produced during gait.

2.2.5 JOINT MOMENTS

Moments of force are produced by muscles across joints during gait cycles. These parameters are calculated using inverse dynamics which calculate the net turning effect of muscles and ligaments across a joint, which are responsible for the motion of that joint, these are joint moments. The computation of joint moments facilitates the identification of muscle group activities throughout the gait cycle and the quantification of torque values produced by the muscle group. A moment which increases speed or height of the body is a positive moment (extension), and a negative moment is one which decreases speed or height of the body (flexion)(Winter, 1991). Normal joint moments in an adult during gait are reported in Figure 2.19. Normative joint moment data of the hip (Figure 2.19a) shows the moment to be predominantly an extensor force as would be expected, although just after toe off there is hip flexor moment, indicating the initiation of ground clearance. The knee moment (Figure 2.19b) shows an extensor moment changing into a flexor moment during terminal stance phase, indicating hamstring activity. Ankle moment (Figure 2.19c) starts with an initial dorsiflexion moment at initial contact producing a heel strike. A rapid and constant increase into a plantar flexor moment is then seen until toe off where a zero moment is seen during swing phase. Joint moments are affected by speed, as would be expected because of the greater forces produced by the movement as observed in GRF. Stansfield *et al,* (2003)

showed that with an increase of 0.5m/s in gait, a 33% increase in extensor and flexor moments in the knee are observed. Other influences on the joint moments include ascending and descending slopes (Kirtley, 2006). Joint moments define which muscle group is active, either flexor or extensor.

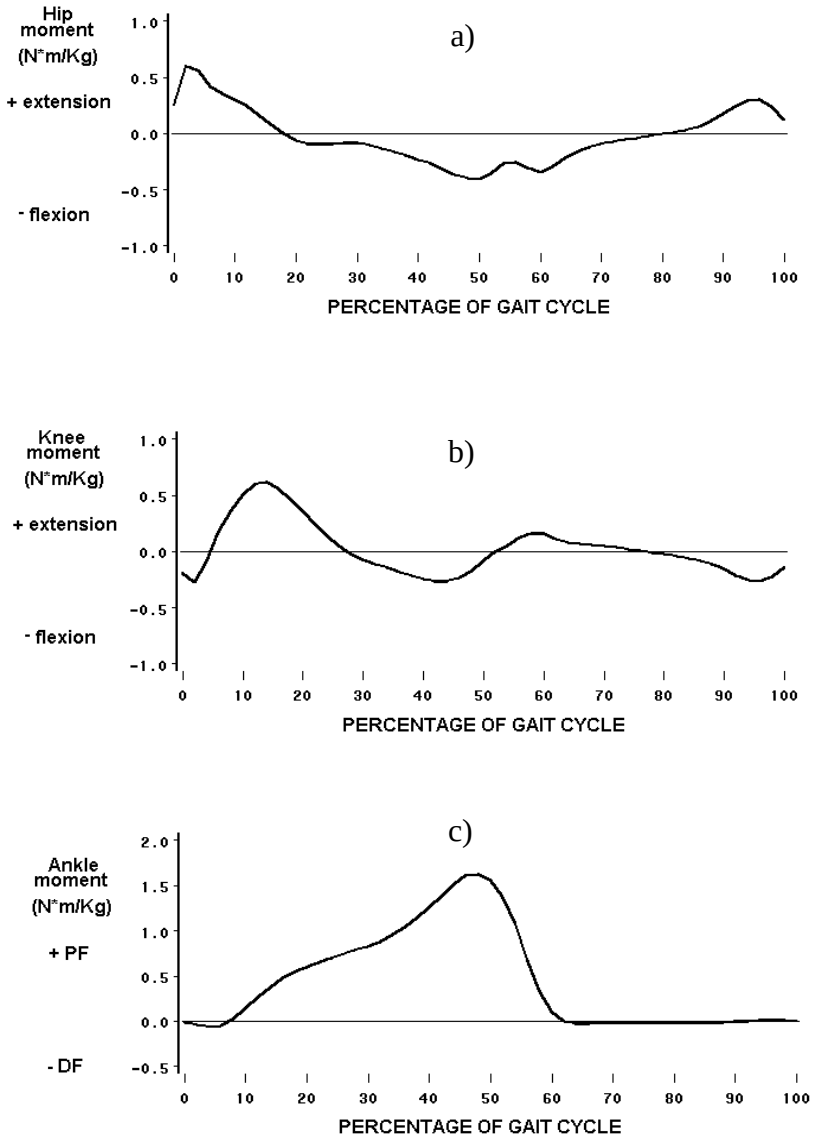

Figure 2.19. Normative joint moments of an adult during gait; a) Hip, b) Knee and c) Ankle. (Winter, 2005)

Joint moments allow for a certain amount of insight into what forces are acting across the joint but for a greater insight a technique called electromyography (EMG) can be used to explore muscle activity.

2.2.6 ELECTROMYOGRAPHY

A muscle contracts when an electrical signal is sent through a neural pathway which stimulates the muscle fibres to contract. EMG is a technique which measures this signal through surface electrodes placed on the skin over an identified muscle or fine wire electrodes placed directly into the muscle. EMG provides detailed information concerning the timing of muscle activity (onset and offset), and also the magnitude of muscular activity when normalised relative to the strength of individual muscles. The onset and offset activity can provide useful information to assess the activities of muscles during different movements and to ascertain which muscles are utilised. Accurate modelling of muscle signals during dynamic movement offers potential applications in many scientific fields; orthopaedics, physiotherapy and rehabilitation, and ergonomics.

When using surface EMG it is difficult to record data from all muscles, specifically ones which are deep or overlapped by other muscles. This is because the electrical signal can be interrupted by other muscle signals and therefore a clear reading cannot be recorded. However, as is the case with other variables considered during gait i.e. ground reaction force, EMG profiles have a standard normative gait pattern. For example, Figure 2.20 shows the EMG pattern during gait for the gastrocnemius and the bicep femoris. The activity is measured in millivolts (mV) or as a percentage of the maximal muscle activity, which is collected during a maximal test.

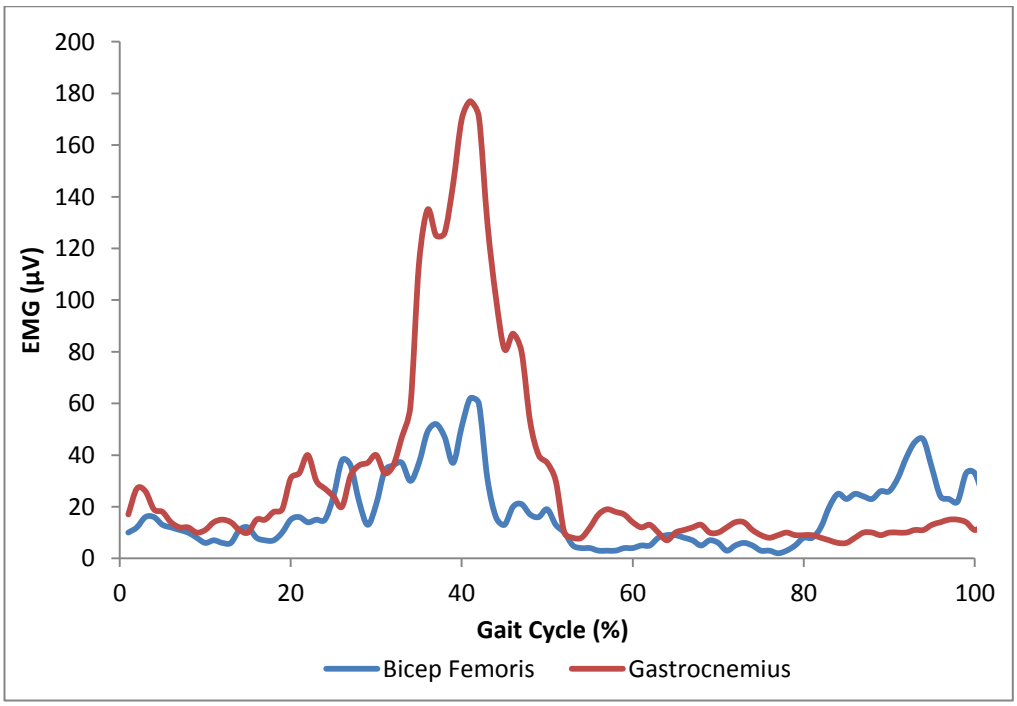

Figure 2.20 EMG activity of the gastrocnemius (red) and the bicep femoris (blue) during 100% of the gait cycle

The EMG profile can be explained when analysing limb movements during gait. In Figure 2.20 there is a large peak in gastrocnemius activity at ~40% of the gait cycle. This results in plantar flexion of the foot in preparation for the toe off phase of the gait cycle. Depending on the demand of the muscle EMG profiles can change. During increased walking speeds Hof *et al* (2002) found that the increase in muscle activity is directly proportional to the increase in speed. Onset and offset variability between subjects may be explained by speed variability and slight variances in adult gait pattern. Further still it said that there is much more variability between children, even in ages when a mature gait pattern has already developed (Agostini *et al*, 2009). Beyond analysis of muscular activity during movements, EMG has been used to inform musculoskeletal models aiding the prediction of muscle behaviour. Amarantini *et al* (2010) proposed a method to calculate accurate muscle force estimation during dynamic movements. The researchers used EMG to constrain min/max optimisation techniques, resulting specifically in the antagonist muscles producing a higher muscle force. Suggesting this method accounted more for agonist/antagonist co-contractions than previous methods used. Further to this, neuro-musculoskeletal models driven by EMG have been developed for level gait (Heintz & Gutierrez-Farewik, 2007). EMG data provided a guide for maximal muscle activity for the model. The model showed that

through this method accurate muscle force could be calculated, however only a small number of muscles can be driven this way and therefore the method would not allow for a fully validated model.

Exploring the normative data of adult gait develops an understanding of what developing locomotion aims to achieve. The following sub chapters will explore the movements prior to attaining this mature gait.

2.2.7 PRENATAL MOVEMENT

The first instance of limb movement is seen prenatally, in the womb, however the quantification this movement is difficult and kinetic information has never, to this researcher's knowledge, been collected. Kinematic positioning data has been studied, although it is difficult to quantify the movements accurately and very little has been reported. The foetal position (Figure 2.21) that the baby adopts during pregnancy has been modelled in previous research. Although correct movements are difficult to model and therefore only simple modelling has ever been performed. (Spoor *et al,* 1989).

Figure 2.21. The position adopted by the foetus within the womb (www.ladyspeak.com).

It has been reported that as the gestational age advances, the incidence of general movements occurring during observation is seen to reduce (Soddenburg *et al,* 1991). This is due to greater restriction caused by the decreasing space in the womb. Some research has suggested that this imparts mechanical loading on the bone, driving in some part the bone development (Jouve *et al,* 2005, Bonneau, *et al,* 2011). Whilst others suggest that the forces applied do not significantly influence the growth (Henderson and Carter, 2002). Recent work observing the movements *in utero* has utilised new technological developments, where Kurjak *et al* (2005) used four dimensional (4D) ultrasonography to capture the movements of *in utero* foetal life. Movements such as eye flicker and hand to face movement amongst others were recorded and it was found that the movements from prenatal to neonatal were not dissimilar. This may help to explain the reason why BMD is reduced after birth (Panattoni *et al,* 2000). This would be because the viscosity of the fluid in the womb gives a greater resistance to that of gravity and would create a higher magnitude of loading on the bones another reason could be due to the reduced resistance on the limbs with the absence of the womb wall. These methods could be used to quantify kinematic movements of the lower limbs and be used to help explain foetal development in relation to mechanical influence utilising this more detailed information than was previously available.

2.2.8 NEONATAL MOVEMENT PATTERNS

The term neonatal classifies the age from newborn to 6 months old. During this time movements appear erratic and unorganised, Thelen (1979) observed this behaviour in 2-12 month olds and described 47 recurring movement patterns, 18 of which were primarily lower limb movements. Since this research contradictory evidence has found that there is in fact a large amount of coordination in movements of the neonate. Heriza (1988) performed a 2D video analysis on neonatal babies and quantified the movement patterns observed in children with a gestational age of 34 to 36 weeks. This study was longitudinal and the babies were tested 3 days after birth and again 40 weeks post gestational age. The informative nature of this study showed a high degree of movement organisation. A high level of coordination between the hip, knee and ankle angle during a kick was observed. The organisation of the joints remained constant although there was a variation in velocities. The 34-36 weeks group had a higher velocity than the more mature group(40 weeks), and this could indicate a greater sense of control over the limbs. Piek et al (1996) performed a similar study to Heriza (1988) but using 7-8 weeks

olds and found similar findings. However it was found that synchronous activity between legs is not present in the younger age group but is found from ages 3-4 months until more complex movements are performed. This could be early evidence of the coordination that is required to develop gait. Although this has been seen in younger age groups, Barbu-Roth *et al*, (2009) used terrestrial optical flow to test whether near newborn babies (3 days old) had the coordination to simulate walking. Terrestrial optical flow simulates the movement that is seen by the eye during gait. Whilst being suspended in the air the newborns elicited bipedal gait like movements when subjected to terrestrial optical flow. This not only shows a high level of visual information and understanding but also shows that there is ability for coordination of limbs at a very young age. This may also suggest that because of this coordination the observed movement has a specific role in the development of bipedal locomotion and could be inherent in all normal infants. However this has never been explored and would require a longitudinal study.

2.2.9 NEONATAL TO THREE YEARS OLD MOVEMENT PATTERNS

The neonatal to 3 years age range is often referred to as toddler (Halleman *et al*, 2005; Cowgill *et al*, 2010) or infant (Thelen *et al*, 1979; Forssberg, 1985; Kimura *et al*, 2005). Motion capture can be challenging when studying children's gait because of the large variability between individuals. However it is probably still the most useful tool in helping to clarify the differences between older children's gait patterns and infant movement patterns. As was the case for prenatal and neonatal stages, kinetic data has not been published on children under the age of 2 years, this is partly due to the difficulties associated with collecting the data. Kinematic studies have used a number of methods to quantify movement patterns in the early stages of walking. The reason for the lack of a consistent method being utilised for quantifying the movements during these stages, is the diversity of movements observed causing difficulties in quantification. The methods that have been used previously include observational (Thelen, 1979), 2D motion analysis (Cioni *et al*, 1993) and 3D motion analysis (Halleman, 2005).

Cioni *et al* (1993) studied the changes in early development of independent walking between fullterm births and preterm births. The movements of the subjects were recorded using 2D video analysis and then two investigators quantified the movements

and a high agreement was found between the investigators, although 10% of the movements needed reassessing due to the lack of agreement. The study was novel due to its longitudinal type observation at 3-4 weeks after the onset of independent walking and then again 4 months later, which had not been performed in previous studies. Cioni *et al* (1993) grouped the movements into a number of different areas, these being trunk movements, balance reaction, posture and movement of the upper limbs, width of the base of support, predominant joint movement in the leg during walking, foot strike and asymmetry. The main findings suggest that there is very little difference between the two groups in terms of locomotive development. When compared to previous data the subjects in this study showed a lack of heel strike, whereas Grimshaw *et al* (1997) has suggested children initially walk flat footed or just heel strike. This illustrates the differences between subjects but it was also suggested that the definition of heel strike, toe strike and flat foot strikes can vary between studies, as a heel strike may be defined as a foot contact that is not toe walking. Irrespective of the definition, there appears to be a large variation in the way children learn bipedal locomotion in the early stages of development. This can not only vary because of development factors between subjects such as early crawling or standing, but also variations in how individuals develop. Hallemans *et al,* (2005) overcame the limitation of the varied age development by including subjects classified by length of time that gait had been acquired rather than age. This has also been used by a number of other studies (Grimshaw *et al,* 1997), however it does not take into account the changes in height of the subjects which may affect the kinematics and add to the varied inter-subject differences. The variability in the early movement patterns does not appear to suggest that there is a direct pathway of gait development. For example, if a child lacks heel strike at an early age there is no clarification in the literature that this then affects the way in which a mature gait pattern is developed. Although Jeng *et al,* (2002) observed kinematic differences between preterm infants and full term infants, suggesting that there may be consequences due to poor early development which manifest themselves at later stages.

Grimshaw *et al* (1997) performed 3D kinematic analyses on children aged between 10 and 24 months, where a single gait cycle was analysed for each subject. The kinematic results showed that children at this age restrain from full knee flexion and hip extension, resulting in a shorter step length. Further still, the time spent in double support phase was on average 15% longer than that observed in adults. These changes were attributed to the centre of gravity being further forward as a result of the lack of knee and hip

extension, and therefore more control was needed during a more stable position like the double support phase to avoid falling. What is also possible is that there are adaptations in the frontal or transverse plane to cope with changes in the centre of gravity (Sutherland, 1980), unfortunately the researchers did not assess any other plane of motion other than in the sagittal and therefore this was unable to be discussed.

Hallemans *et al*, (2005) were the first researchers to attempt to quantify any kinetic information from 'toddlers'. Toddler's age range was from 13.5 months to 18 months, kinematic data reported was similar to previous literature, however the kinetic data was compared to adult data to assess any differences. The net joint moments in the subjects were reportedly significantly lower than those seen in adult data, which were attributed to slower walking speeds. Slower dimensionless walking speeds have been shown to exist up until 1.5 years old when compared to adults (Kimura *et al,* 2005). Further results showed a lack of gastrocnemius activity at toe off which occurs in adults, although previous work has suggested this is not observed until a much more mature gait pattern of 7 years old (Sutherland *et al,* 1980). What maybe likely to compensate for this is an increased hip moment to aid in the toe off. Kimura *et al*, (2005) as well as identifying slowing walking speeds in children up to the age of 1.5 years, found that under the age of 2 years stance phase was longer than that seen in adults, which agrees with previous work (Grimshaw *et al,* 1998). This has been attributed as a response to a lack of balance and changed centre of gravity which again is seen up to the age of two years. Also associated with this is a change in the braking period of forward momentum following each gait cycle. This occurs on the leading leg during double support phase and can be referred to as loading response (Kharb *et al,* 2011). It has been shown that children up to 3 years have a larger braking period and a shorter recovery time (Kimura *et al,* 2005). This indicates a lack of control and ability when compared to that required to maintain a smooth gait cycle, highlighting another form of gait maturation which is not attained until 3 years old. Although it is possible that this does not increase until 7 years old which has been the benchmark of gait maturity, but this age range was beyond the scope of the study.

One criticism of the recent work that has used 3D motion capture is the increased likelihood of marker movement in children wearing suits and the inherent reduced ability to correctly identify the landmarks needed for gait analysis. These are unavoidable limitations that are unresolved at this time.

2.2.10 THREE TO EIGHT YEARS OLD

Sutherland *et al,* (1980) provided the first large scale comparison of gait between the ages of 1-8 years and adult. The development of gait from 1-3 years shows the largest changes in gait. From the ages of 3-8 years Sutherland *et al* (1980) showed that a linear relationship between a number of variables is apparent with regards to the temporal-spatial parameters. These parameters included step length vs. leg length, age vs. velocity and step length vs. age. The latter may be a consequence of growth increase as age increases and therefore this increase in step length is attributed to leg length. All other gait variables other than those related to growth and aging that were observed by Sutherland *et al* were comparable, when normalised, to adult gait. Research that had been produced since this work has largely agreed with the findings of this study. Discrepancies in gait variables however have been seen between the ages of 3-8 years and the adult in kinetic changes. The main variations seem to be reported between 3-4 years (Chester *et al,* 2006).

Since the landmark study of Sutherland *et al,* (1980) a number of other studies have assessed the temporal spatial parameters of the developing mature gait pattern. Most have agreed with the initial findings of Sutherland *et al,* however more in depth and complex variables have been analysed. Hillman et al (2009) performed a longitudinal study on 33 children from the age of 7-11 years, the main aim of the study was to assess the maturity in idiosyncratic features of gait. The ratio of speed and cadence or step length was used to assess any changes. If, as suggested by previous work, a mature pattern in temporal spatial parameters is reached at the age of 8 (Beck *et al,* 1981), then the ratio would not be expected to change with age as a mature gait pattern would be achieved by this age. A lack of trend in the results between any age range suggested that gait, even up until the age of 11 years, is still maturing and obtaining a consistent relationship between speed and cadence.

Chester *et al* (2006) performed kinetic analysis of gait for 3-13 year olds. The kinematic findings of the study matched well with previous work and demonstrated typical changes in the temporal spatial parameters. Significant differences in mean peak moment values were observed between the group of 3-4 year olds and the 9-13 year olds for the hip and knee in the sagittal plane, and moments were seen to increase throughout age. The results of the 9-13 year olds were comparable to those of adult joint moment values, so based on the findings it was stated that mature gait kinetics are not reached until 9 years and above. This is in contrast with a number of studies which

suggest a younger age for the attainment of mature gait (Sutherland *et al,* 1980; Beck *et al,* 1981). Although work assessing 7 year old gait data compared to adults (Ganley and Powers, 2005), showed similar findings to those seen by Chester *et al,* (2006). These findings of a reduction in ankle moment in both of these studies have been attributed to neuromuscular immaturity. Moreover, with children this immaturity may rely on the increased hip power to initiate the swing phase of the gait cycle (Sutherland, 1997). The conflict between these findings might be related to the maturity level of the subjects. In Chester *et al's* (2006) work the gender of the subjects was not stated, so as females mature quicker than males this could have had an effect on the maturity of the kinetics during gait (Kerrigan *et al,* 1998). Subjects as young as neonates have been found to have differences between genders in movement patterns (Almi *et al,* 2000). Therefore careful consideration in gender differences and also subject maturity levels irrelevant of age may need to be taken into account when studying children's gait. To produce more accurate data, a method may need to be devised to assess subject maturity rather than age especially when grouping ages. It is possible that longitudinal studies of the same subjects can gain a greater sense of maturation of gait, such as the study by Hillman *et al* (2009). An interesting finding in the GRF ratio between the three directions showed that the direction of force changes with age (Cowgill *et al,* 2010). The different ages were grouped into 3 categories representing different stages of gait development. The findings showed that the ML-PD force ratio was significantly higher in the youngest age category, where the other two ratios (ML-AP and AP-PD) were highest in the adult. The reasoning behind the changes may have been as a result of the lack of control of walking in the youngest age group. However, the findings may have profound influence on the femur development and it was suggested that the medial lateral force may the cause of the differences in the cross sectional areas of the mid shaft in femur which are observed between children and adults.

Although the development of bipedalism is often referred to in terms of the propulsion forward, there are other important mechanisms and cognition that is required to perform bipedal gait. Changes in the activation levels of muscles may play an important role in the control aspect of gait. Berger *et al* (1987) included stance as an important factor to analyse during their study on the control of muscles during gait. EMG responses from cerebral signals were measured during different phases of walking in children aged from 1-10 years. It was found that adult-like signals were reached by the age of 6 years, concurring with some suggestions that mature gait pattern is obtained between the ages

of 6-8 years (Chester *et al,* 2006). Assaiante *et al,* (1998) also considered the effects of postural control during ontogenetic changes. Pelvic control appears to be stable from the onset of independent walking although the head postural control is still developing until 6 years old.

The discussed literature has been collected whilst the subjects have been performing at self-selected 'normal' paced gait, one variation of this is to assess gait at different speeds. In the adult gait speeds have been shown to affect all aspects of gait (Kirtley, 2006). Assessing this change in speed in children can help to identify the how GRF might change due to the self-selected speeds of walking. Speed may also need to be a normalised parameter during gait analysis to examine the changes in full without it influencing other variables such as joint moments and GRF's.

2.3 MUSCULOSKELETAL MODELLING

Musculoskeletal modelling can be used to evaluate loading of tissue by the muscle and the muscle function during movement. Extensive reviews of these areas can be found in the papers produced by Erdemir, *et al,* (2007) and Zajac *et al,* (2002; 2003). The goal of any musculoskeletal modelling of a biological system is to produce a model that accurately represents the *in vivo* physiology and processes. A number of areas need to be considered for such modelling. Firstly, how the muscle forces are calculated through either inverse or forward dynamics, how the muscles are modelled to replicate the contractile properties, and finally how the optimisation of the muscle forces are calculated whether this should be linear or non-linear.

Through the use of the motion capture technology and Newton-Euler equations, kinetic aspects of gait can be determined (Winter, 2005). Inverse dynamics is the process of deriving forces and moments through mathematical modelling from the body's kinematics, inertial properties (mass and moment of inertia) and ground reaction forces. The lower body of a human can be broken into three segments to create a link segment model, representing the thigh, shank and foot. The variables that are required to calculate moments using inverse dynamics are linear and angular accelerations of each segment; vertical and horizontal distances between the joints and the centre of mass; and the mass and moment of inertia of each segment. For further reading on inverse dynamics and how the joint moments are calculated the reader is referred to Winter (1990). The computation of inverse dynamics can provide the necessary steps for a

musculoskeletal model to be computed. However, this calculation is based on a number of assumptions which must be addressed as part of the limitations inherent to any musculoskeletal modelling system that uses inverse dynamics. The assumptions are that the segments are rigid, and that their mass is concentrated at their centre of mass, the joints are frictionless and that there is no co-contraction of the muscles. Further to the limitations of inverse dynamics in adults, there are a number of considerations in the inverse dynamics of children. Jensen *et al,* (1989) showed that children under the age of 14 years have a non-proportional mass segment to that of adults, this can be due to the increase in bone mass which is not always correlated with growth. Therefore when the accepted segment masses, which are taken from Winter (1991) in most studies, are used and just scaled to height the assumptions of the body mass could be inaccurate. Because the segment masses are an important part of inverse dynamics this would lead to inaccurate calculations.

2.3.1 MUSCLE MODELLING

In order for musculoskeletal models to calculate muscle forces, a number of methods need to be employed so that accurate calculations can be introduced. It is important to understand how the body selects which muscles to activate to produce a required movement. Maximal movements have been suggested to be less complicated in terms of muscle recruitment, although, Zajac *et al*, (2002) suggested that sub maximal tasks are difficult because the objective function is multi-factorial rather than just supplying maximal force. Other considerations include minimisation of energy expenditure, joint loading and muscle fatigue. Although it was also suggested that during sub maximal walking minimisation of the energy expenditure is a reasonable criteria by which the muscles adhere to. Dynamic models try to replicate this through the process of muscle recruitment solvers and optimisation techniques. The muscle recruitment solver is the process of determining which muscles need to be activated to balance an external load. A number of techniques are available to use, but it is dependent on whether the equations for the solver are linear or non-linear, or in some instances the non-linear models can be further split into different models. If a linear function is imposed on the model, then if it is possible for two muscles to share the work then they will do so (Zajac *et al,* 2003). The problem with this linear optimisation is that it only ever recruits the minimum number of muscles to balance the system and furthermore the model bases the recruitment on which muscle would provide the greatest force, neither of which

reflect physiological function. Heller *et al* (2001a) identified limitations that are inherent in linear modelling, one is the dependency on the physiological cross sectional area (PCSA) values, and another is the dependence on the object function employed for the muscle calculations which can lead to high muscle forces. To avoid these limitations in Heller's study, the muscle forces were not allowed to exceed a critical limit. It was determined that these limitations allow for accurate modelling for non-complex recruitment of muscles such as gait simulations. However muscle recruitment solvers with a greater complexity are available, these are non-linear models. Comparisons between linear and non-linear models have been made in the literature although firstly it is worth gaining a brief understanding of what differences non-linear modelling produces compared to linear modelling. Non-linear modelling has the ability to distribute the load over the muscles and considers other characteristics of the muscles including length, contraction velocity and pennation angle. These can all increase the accuracy of the modelling which is not able to be modelled through the linear technique. Phillips *et al,* (2009) found that during a free boundary condition modelling good agreement was found with *in vivo* data when solving the model using a non-linear approach as compared to a linear one. The model was taken from a single time step of the gait cycle, and therefore this seems contrary to the previously reported accuracy of linear modelling during non-complicated loading. Although the results do agree with previously reported data of work performed by Pedersen *et al,* (1987), and Crowninshield and Brand (1978; 1981). This brief review of muscle recruitment solver problems has been sufficient for the scope of this research. However, to gain a greater understanding of the models it may be useful to be directed towards further reading in references of Brand et al (1982) and Pedersen *et al,* (1987). As well as the optimisation of the muscles, the muscular properties also play an important role in force production. The Hill type model is used vastly in the literature (Phillips 2009; Speirs *et al,* 2007; Duda *et al,* 1997) as it has been seen to reproduce the properties of muscle behaviour well. The model does this through accurately describing the physiological relationship between muscle force and the kinetics of the muscle such as length velocity and activation. The Hill type model is commonly used because of this, however other models are available to define the muscle model properties (Zajac, 1989). Once the mathematical modelling of the muscles has been determined the next stage is to define the way in which the muscles are applied to a model.

It would be difficult to model the full gait cycle and therefore previous studies have analysed key stages of gait. One stage is the single stance phase which is at an average 20% of the gait cycle (Bergmann *et al*, 2001; Phillips, 2009). The potential limitation to the studies used for comparison is that they only look at one phase of the gait cycle. This is often the phase which shows the highest hip contact force, but nonetheless it is evident that a more comprehensive approach is needed. Duda (1997) looked at 10%, 30%, 45%, and 70% of the gait cycle to coincide with key events during the gait cycle. Dalstra and Huiskes (1995) employed a more comprehensive approach using 8 phases of gait cycle. These were 2% (double support: beginning), 13% (single support: beginning), 35% (single support: halfway), 48% (single support: end), 52% (double support: end), 63% (swing phase: beginning), 85% (swing phase: halfway). 98% (swing phase: end).

With more technological advancements and greater accessibility the next stage has been subject specific modelling. Increased availability of CT and MRI scans and software which is able to segment out different materials with increased speed has made subject specific modelling more common place (Jonkers *et al* 2008, Scheys *et al*, 2006;2008; 2011, Lenaerts, *et al* 2008), using subject specific modelling maps, geometrical position and size of bones muscles and tendons (Scheys *et al*, 2006). This type of modelling is especially useful in total hip replacement (THR) studies to understand the stress and strain resulting from the hip joint loading in the femur and the implant (Lenaerts *et al*, 2008). The necessity of subject specific musculoskeletal modelling has been well explored. Delp (1994) was one of the first authors to address the change in the neck length and neck shaft angle due to THR's on the muscles moment arm. The findings indicated that it is important for subject specific modelling due to these changes and that a generalised model was not satisfactory when taking into consideration the changes in loads that would be resulted from these changes in geometry. Further to this Lenaerts *et al* (2008) studied the effect of altered hip geometries on muscle activity levels, instead of just moment arm changes (Delp, 1994) to determine how subject specific modelling can inform surgical procedures. The muscle model was a generic model scaled from Delp *et al*, (1990) and contained 43 muscles and had 5 degrees of freedom (DOF). The activation of the muscles was computed over one gait cycle using a static optimisation algorithm which minimises the sum of the muscle activations. Both the neck shaft angle and the neck length of the femur were changed and the effect on the hip contact force and the muscle activities were measured. Due to an increase in neck shaft angle

there was an increase in the activity of the abductor muscles but no change in the hip contact force was observed. The increase in neck length showed the opposite where any changes in the muscle activity was negligible but the hip contact force was affected considerably. One limitation, which was addressed by the authors, was the lack of subject specific gait analysis. The changes in the kinematics because of the THR (Bergmann *et al*, 2001) may have compensated for this change and the muscle moment arm during gait may have been adjusted accordingly to create a similar muscular pattern to what it was before the change in NSA to maintain bone remodelling caused from muscular loading (Bitsakos *et al*, 2005). Lenaerts *et al* (2008) incorporated these findings and furthered them by implementing a new variable which was subject specific joint centre location. Significant changes in the joint contact forces and muscle forces were observed when all variables of subject specific modelling were taken into consideration. These variables were: neck length, neck shaft angle, femoral anteversion and hip joint centre, although the associated change in hip joint centre location did not directly affect the forces the changes in muscle moment arms because of this joint centre geometry change were significantly affected. Subject specific modelling of these variables was suggested to be necessary so that forces would not be underestimated. Although comparisons to previous work in which *in vivo* measurements were taken were made to test the validity of the results, it is not possible to know whether the changes observed in this study were more physiologically correct for the subject specific models.

As mentioned earlier, musculoskeletal models can be computed by forward dynamics where the muscle forces are computed from predicted forces and moments (Duda, 1997; Brand *et al*, 1982; Delp 1990) or inverse dynamics where the muscles forces are computed from known forces and moments and can be incorporated into musculoskeletal modelling software's such as AnyBody or Open SIMM. Both models have shown that they can accurately produce in vivo results. The research by Brand *et al*, (1982) and Delp (1990) is predominantly used by other work to build the geometrical positioning of the muscles. Where Brand determined the optimisation techniques of the muscle modelling, Delp's work included modelling insertion and origin points as well as via points which are used to wrap the muscles around other muscles or bony landmarks which would replicate true in vivo lines of actions. Delp's model consists of seven segments 43 muscles, and 8 degrees of freedom (DOF), and the use of this model can help to normalise results from different studies. This model has

been a bases of many musculoskeletal models and helps to uphold the consistency of modelling human movement.

A contemporary issue within human simulation is creating a consistent and accurate model which can be used in all studies. These issues will be further discussed in section 2.5, however within musculoskeletal modelling an attempt has been made to do this. Horsman *et al,* (2007) produced a paper to complete a consistent anatomical data set of the lower extremity including orientations of joints muscle parameters (optimum length, physiological cross sectional area), and geometrical parameters (attachment sites, 'via' points). This data set could prove to be invaluable in modelling of the human body as previous datasets have done for motion capture and inverse dynamics (Winter, 1990).

2.3.2 CHILDREN'S MUSCULOSKELETAL MODELS

There has been very little musculoskeletal modelling of children reported in the literature, Scheys *et al* (2011) modelled children from age 8-11 years old who were diagnosed as having CP, this work being one of the most recent studies modelling children. The earliest work performed on the juvenile femur was produced by Heimkes (1993). A mathematical model was produced and applied to a 2D femur model. Although a simplistic model, by the present modelling standards, the understanding of the resultant forces with in the femur created by the trochanteric and hip forces provides invaluable information. By producing this work the importance of the great trochanteric apophysis in weight bearing was highlighted which was perhaps understated previously. Other models produced to represent children have used the same muscle models as in adults but have scaled the models to the correct height (Carriero *et al,* 2011). The muscle loading of the femur was created from an isotropically scaled generic adult mode and forces from a musculoskeletal model which had 43 muscles and 8 DOF. The kinematics and kinetics were applied from collected motion capture data and then these loads were applied to a second isotropically scaled adult generic model. The model was loaded with muscle data and JRF from four stages during the gait cycle as described by Duda et al (1997). As suggested previously, changes in bone geometry can affect the forces applied by the muscles on the bone, and therefore these models may well be represented poorly. *In vivo* work identifying differences in moment arms between children and adults can be useful for assessing changes in muscle forces. O'Brien *et al,* (2009) investigated changes in the patella tendon moment arm of the knee extensor in

children and adults. The ages of the children were approximately 9 years old and were grouped as pre-pubertal. The patella tendon moment arm was found to be greater by 20% in adults than in children irrespective of the force changing capacity therefore it was suggested that it is not a true representative when muscle lengths are just scaled to the correct size.

There are a number of considerations that will need to be addressed when considering further musculoskeletal modelling of children, in order to achieve accurate results. One consideration which is often overlooked is that human locomotion and movement extends beyond just walking and standing, which are often the only motion modelled during FEA (Speirs *et al*,2007; Carriero *et al*,2010). Greater focus needs to be placed on modelling other activities such as running and stair walking. When considering modern day human activities, a seated position is more common and therefore this form of muscle activity and loading on bones need to be assessed. Other considerations are also needed when combining musculoskeletal modelling and FEA which will be considered in the next section.

2.4 FINITE ELEMENT ANALYSIS

When a structure is loaded stresses are produced within the material of these structures. One method that is used to predict these stresses is FEA, which is particularly useful for complex structures. Computational methods of stress analysis were initially only used for engineering projects and were then introduced applied to bone in 1972 (Heimkes, 1993). A FEA models accuracy and validity will depend on a number of factors, including the geometry, loading and constraints. Primarily the geometric position of the structure including shape and size, orientation and interaction to other structures including muscles and other segments (Viceconti *et al,* 1996) should be considered. Secondly the loading conditions applied to the femur need to be as physiological as possible including line of action of forces, angle of muscle attachment, and wrapping of the muscle to take account of adjacent structures (Speirs *et al,* 2009; Polgar *et al,* 2003a). Finally the last concern is constraint of the model (Speirs *et al* 2009; Phillips, 2009). FEA of the femur has been performed by many researchers for the purpose of assessing hip replacements (Jonkers *et al,* 2008). For this reason much of the work discussed here will be orientated around orthopaedic work in the elderly as limited work has been performed on juvenile femora.

2.4.1 GEOMETRY

Accurate geometry is an important factor in FEA modelling. 3D geometrical modelling of the femur has improved in accuracy throughout the history of FEA. Early models were either produced from a radiograph in 2D (Heimkes, 1993) or 3D models were developed in computer aided design software's (Taylor, 1996; Huiskes, 1990). At this point there was no geometric standardised femur and this led to a large variation in results. Viceconti *et al* (1996) addressed this issue and developed a standardised composite femur which also led onto the development of the muscle standardised femur (MuscleSF), (Viceconti *et al*, 2003). The composite model was a result of the work by Cristofolini *et al* (1996), in which an extensive validation of a composite model against two human models, one frozen and one dried-rehydrated, was conducted. This validation was performed using strain gauges and the models were put under axial, torsion and a bending load, then strain and stiffness measurements taken. It was found that not only did the composite femur have similar results to the cadaveric specimens but also that the composite model elicited a much larger inter femur reliability. From this it was suggested that the future projects in this research group would be using a single standardised femur and it was further suggested that this work could be used as a standardised model for laboratories worldwide (Viceconti, 1996). Subsequently, a large volume of FE work has been produced using this model (Figure 2.22). The next stage in standardising a model was to create a model with standardised muscle locations. This model comprised of anatomical references which were obtained from a number of anatomical atlases and were mapped onto a CT scanned model. This mapped data was then compared to other reported data in which there were discrepancies, however these were deemed unavoidable due to original measurement errors between studies and differences in the specimens.

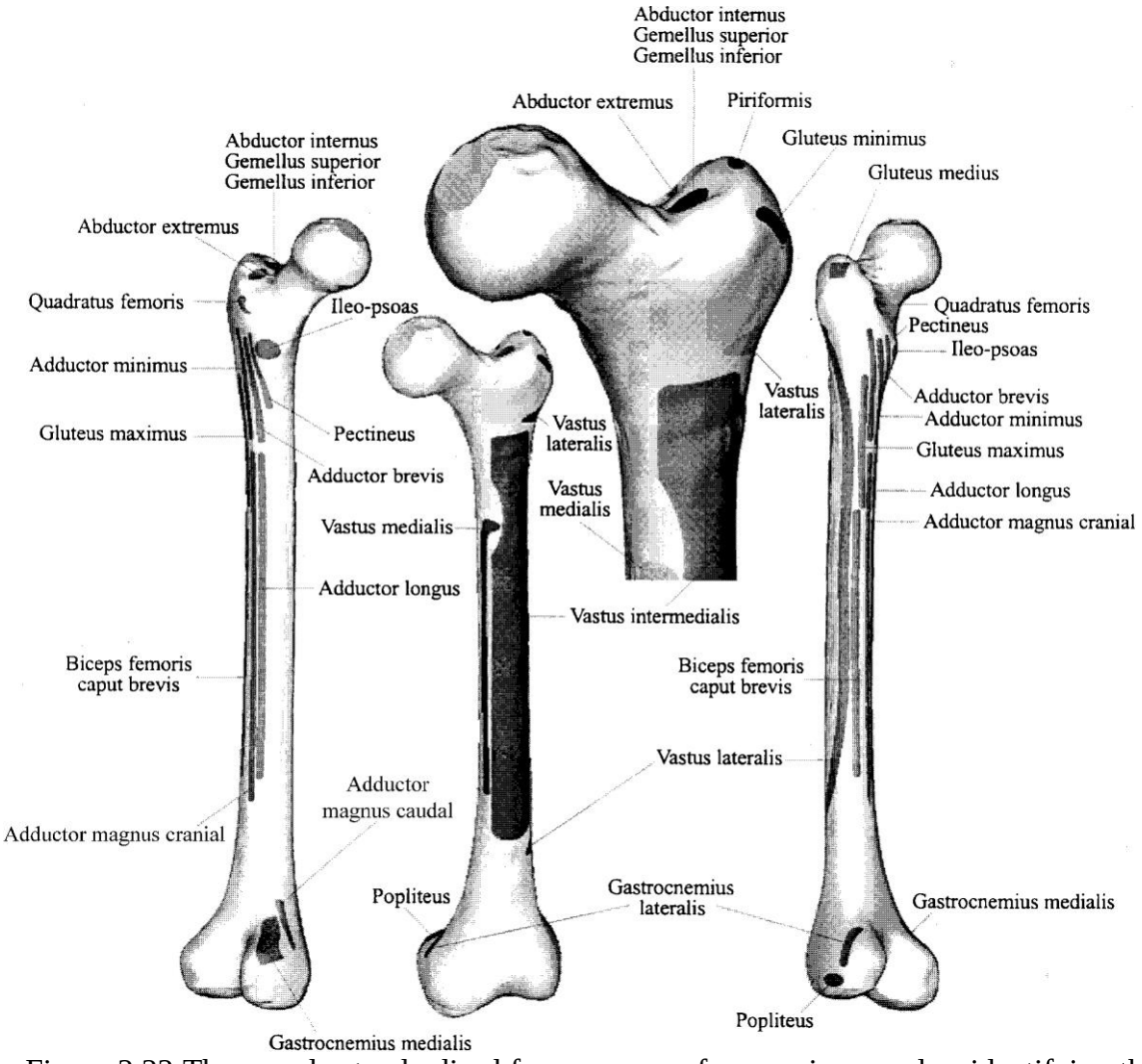

Figure 2.22 The muscle standardised femur as seen from various angles, identifying the muscle insertion and origin points.

Polgar *et al* (2003a) validated the separate meshing of the muscle attachment sites for the MuscleSF model for use in FE under simple loadings which were a bending load and under a torsion load, it found that the MuscleSF FE model produced similar results to previous studies when using the same mesh. The next step in the validation for this model was to use physiological loading. Polgar *et al*, (2003b) produced a number of musculoskeletal models with 9 different load conditions on the same model to investigate the effect of simplified load cases against grouped loads according to different muscle groups, although this will be discussed further in the loading section. One critique of this work is that the model was loaded at 10% of the gait cycle which would result in sub-maximal hip contact force and a reduced muscle force (Heller *et al*, 2001). Despite this the maximal strain within the cortical bone was found to exceed the

physiological range (Carter *et al*, 1988a). It would be possible to suggest that at a higher contact force the strains would be higher. Although this has still since become the *de facto* of the adult femur modelling. FEA of the femur has been significantly improved since the introduction of this model (Speirs *et al*, 2007; Phillips, 2009; Jonkers *et al*, 2008) Further still the model has also been isotropically scaled to that of a younger age (Carriero *et al*, 2010), although this has a number of limitations such as the lack of ability to model the age specific geometrical changes observed during growth (as discussed in Chapter 2.1). In addition to improving the geometric aspect of the modelling through the standardisation of the femur model, this also provided a base to address the other areas of FEA such as the loads and constraints that can vary between studies.

Recent work has used subject specific geometries created through the use of MRI scans (Lenaerts *et al*, 2008). The effects of subject specific musculoskeletal modelling on the muscle forces have been discussed in the previous section (Chapter 2.4). The effect of subject specific geometries on FEA has also been analysed. Lenaerts *et al*, (2008) studied the effect of 3 different models' specific detail: (1) a generic scaled musculoskeletal model, (2) a generic scaled musculoskeletal model with subject-specific hip geometry (femoral anteversion, neck-length and neck-shaft angle) and (3) a generic scaled musculoskeletal model with subject-specific hip geometry including HJC location. The study found that hip joint contact inaccuracies caused the resultant hip force to also be erroneous, thus where possible it was said that subject specific geometries should be used to avoid inaccurate results.

Although the geometry of the adult femur has been addressed, the juvenile femur can be seen as a completely different concept. The changes during growth make this task very difficult (Gardener and Gray, 1970), and geometry used during the analysis of the juvenile or prenatal femur is obviously age dependant, hence it is often idealised and the loading is often simplified (Carter and Wong, 1988; Shefelbine *et al*, 2002; 2004, Tardieu, 1997). Ribble *et al* (2001) created two 2D models, representing a 2 year old and an 8 year old. The models were changed in accordance with x-ray data obtained, with the aim of determining how the stresses at the growth plate affect the development of valgus deformity at the hip during spasticity. Further discussion of these results will be covered later in this section, however the modelling is relevant to this section. Because of the 2D aspect and the main focus on hip load, the geometry of the femur may not be as important as it is when using 3D models. This is due to the lack of

importance in having correct muscle attachment locations because of the limited availability of muscle attachment sites. Which is arguably why there is a greater importance of having the correct geometry (Viceconti *et al,* 1996). During 3D modelling of the juvenile femur, the model is often simplified (Shefelbine *et al,* 2002) or just an incorrectly scaled down adult femur (Heimkes *et al,* 1993). These simplifications of the model may lead to varied results as shown in the adult femur (Cristofolini *et al,* 1996). Therefore although a difficult prospect when creating a model of the juvenile femur with the aim to assess the full stress distribution, the same precautionary measures in attaining a correct geometry is needed.

2.4.2 LOADING

The femur undergoes loading from muscles, ligaments and joint contact forces. Stress and strain distribution in the femur has been measured in the literature extensively with vastly varied results being produced. A variety of methods are available for the application of loads and the way in which the muscle force data is calculated.

Duda *et al,* (1998) studied the effect on the strain distribution in the femur during different loading conditions. The muscle forces applied were calculated for four different stages of the gait cycle and were derived from mathematically models as discussed previously (Pederson and Brand, 1987). Five different loading regimes were used, during simplified loading regimes principal strains were shown to be up to 1000με larger than when all muscle forces were included. Furthermore when major muscle groups were neglected the bending moments in the shaft of the femur were overestimated, when compared to *in vivo* measurements. Although when looking at the strains in different regions of the femoral shaft there was only a major influence on the bone when muscle attachment sites associated with that region were neglected.

Initial studies (Taylor *et al,* 1996) opted to study just the stance phase of a walking action to study whether the femur is primarily under a bending or compressive state (Figure 2.23). It was found that the femur was primarily under a compressive stress. The results challenged the findings of other studies (Huiskes, 1990) which found that loads create dominant bending stress distribution, which may not be a true representative of the loads applied *in vivo*.

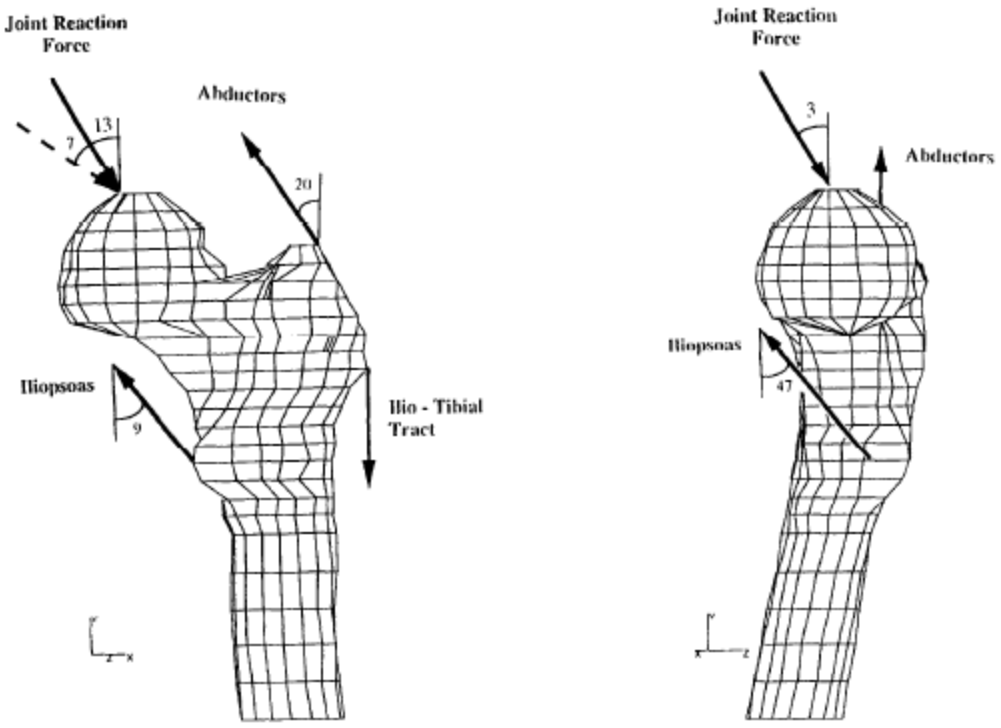

Figure 2.23 Simplified loading regime applied by Taylor *et al,* (1996).

More recent studies also agree that the femur is under compression. The differences in these results may be due to different loading conditions utilised by many studies. Although in some cases the different methods are necessary to enable researchers to acquire answers to their questions, however there was deliberation about a standard method to produce the true results. The first attempt to create a generic muscular loaded model was by Polgar *et al* (2003a). As previously stated this was part of the standardised femur program. The loading regimes used by Polgar *et al* (2003b) can be categorised into two main sections, the initial models used physiological load cases. The difference was how the loads were distributed across the nodes, one used point loading the other distributed evenly throughout the attachment site as reported in Viceconti (1996). The other load cases were chosen to represent the loading from previous work in the literature, which systematically excluded certain muscles although all muscle groups i.e. adductors, flexors etc; were represented. Finally, in the last load cases only the proximal femur muscles were applied. Although the muscles were fully applied in two cases the model was still constrained non-physiologically and this therefore would, according to more recent work (Phillips, 2009), have affected the results. Nonetheless, these results can still be informative regarding the accuracy required when applying loading to obtain more accurate and realistic results. In this work the muscles were

modelled using non-linear optimisation techniques. This study not only helped to validate the MuscleSF model, by having comparative results to previous work when using similar loading conditions, but the study also allowed an elaborate comparison between different methods of muscular loading applied to FE models. One important consideration of the study was to indicate the effect of point loading against distributed loads, where the point loading was shown to give unrealistic strains within the femur and indicating that where possible, distributed loads should be applied. Further findings showed that simplified load sets generated an unrealistic stress distribution compared to physiologically correct loads. Bitsakos *et al* (2005) further enhanced these findings and discovered the importance of specific loading conditions in the simulation of bone remodelling. Although the simplified muscle loading compared to the *in vivo* representative loading produced similar remodelling patterns, the simplified loading did not conserve the bone as well as the more complex muscle loading. Subsequently these findings have big implications for areas of research in the area of osteoporosis which is an imbalance in the remodelling of bone causing an increased fracture rate. This is because there is a necessity in modelling *in vivo* events on bone and not just a representation. Furthermore, this indicates the importance of correct loading in a wide number of applications when using computer modelling to study bone.

Whereas the aforementioned studies used computer simulations and FEA, other methods that are utilised to test strain levels on a model and to validate a computer simulation are strain gauges. Simoes *et al* (2000) used strain gauge testing to measure the strain distribution in the femur under three different loading conditions; joint reaction force (JRF) ; JRF and abductors; JRF, abductors, iliopsoas and vastus lateralis with respective forces of 700N, 300N, 188N and 292N. The minimal muscle attachments were justified by the authors using substantial evidence in the literature suggesting that adding more muscles has little effect on the strain (Cristofolini *et al*, 1995). However this was only evident in the stance phase of gait and therefore cannot be when validating model that is trying to truly represent the full loading of the femur during human bipedal gait. Far from this being irrelevant though, interestingly Polgar *et al* (2003a) showed that muscles are able to be grouped rather than modelled as a number of muscles i.e. abductors. The study indicated that although each individual muscle produces a significant level of strain on the femur, when certain muscles are grouped together the effect on the overall results is nominal when compared to using individual muscles. The result of this study gives a great understanding of the intricacy required

for a musculoskeletal model in order for it to be accurately produced and to achieve an optimal musculoskeletal loading. Polgar et al (2003a) tested the sensitivity of complex loading on the MuscleSF with 10 different load cases. When all muscle forces were included physiological strain values were observed. A large difference in peak strain was found when the nodes that the when the applied loads were averaged over a number of nodes rather than single point loading. Although this was localised where the loads were applied. The overall strain showed little difference between these two loads cases. In the simplified load cases much larger displacements of the femoral head and larger maximum and minimum principal strains were observed.

More recent studies have taken advantage of technological developments and used subject specific bone geometries. Jonkers *et al* (2008) quantified the effect of subject specific geometry and subject specific loading on the stress distribution in the femur. Two FE models were produced pre and post-operative THR's, the difference between the models being in the geometry and muscle locations. It was shown that the stress distribution within the proximal femur was significantly changed when subject specific hip loading and geometry was used. The effect of the geometry change was said to be dominated by the effect of the subject specific loading. The stress distribution was measured over seven areas and a difference between the models was found to be between 10-15Mpa in all the measured zones. The stress distribution change between the subject specific loading and the generic model, was related to the ratio change between the ML force and the PD force. When the PD force was coupled with bending action of the abductors a medial bending was seen. Whereas when the ML force was of an equal magnitude the bending was neutralised.

Subject specific loading, as was the case in the subject specific geometry, is now more common practice. Scheys *et al,* (2011) used MRI based models to identify the muscle line of actions in 8 year olds with CP. The study had a specific function to identify the effects of the variability in muscle moment arm lengths in CP patients due to abnormal bone shapes. To do this three models were developed, one model was a scaled generic model from Delp *et al,* (1990) which has previously been discussed. Another model was produced directly from the MRI scan, The MRI model showed large percentage variations in moment arm lengths when compared to the scaled models and the changes were associated with the geometric positioning of the muscle insertion and origin points. Further to this, the results also showed variations between subjects to be significantly different. Inverse kinematics was used to calculate the muscle activity

necessary to create the movements and although this approach is useful in identifying the positioning of the muscles, forces from the muscles could not be produced. Therefore the muscle activity, and the moment arm length, may be influenced by optimization of the movement when performing musculoskeletal modelling through the use of the inverse dynamics. Nonetheless this study has helped to emphasise where possible subject specific muscle modelling is necessary to provide greater accuracy in musculoskeletal modelling.

2.4.3 CONSTRAINTS

As previously mentioned, the lack of a generic musculoskeletal model in the literature has resulted in a large variation in the techniques used to load and constrain models of the femur. Speirs *et al* (2007) stated that although constraining a model is essential for any analysis the choice of the constraints has a direct consequence on the results. This is evident throughout many studies using different constraints. Speirs *et al* (2007) showed this by comparing varying constraints (Figure 2.24) and loading emphasising the different deflections in the femoral head due to the different constraints.

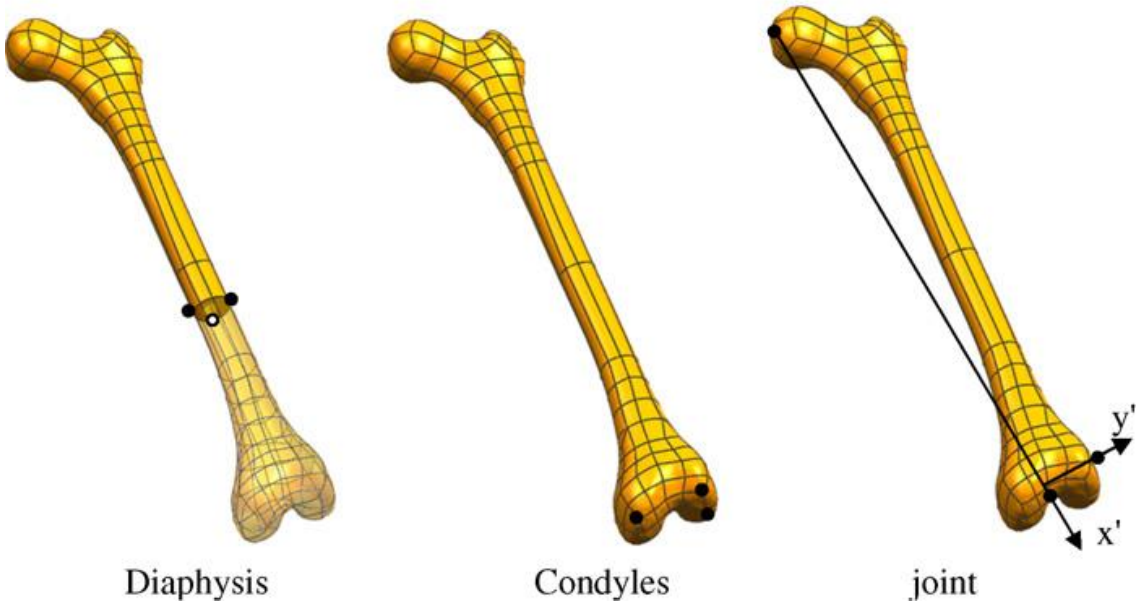

Figure 2.24 The femur model used by Speirs *et al,* (2007) showing the location of node constraints used in the study.

The two main constraints that are apparent in the literature are constraint of the mid-diaphysis (Kuiper and Huiskes, 1996), which is not physiologically correct, and constraint of nodes on the distal condyles (Taylor *et al*, 1996; Duda *et al*, 1998) which, whilst simulating the constraint of the condyles at the knee, means the head remains unconstrained. A further constraint is also used on the femoral head, replicating the acetabulum, in addition three different load cases were used (Heller *et al*, 2001). Unsurprisingly due to the nature of the constraints the largest deflection of the hip was when the femur was constrained at the condyles and the least overall deflection at the hip was observed when the femur was constrained at the hip joint. This study has shown that non physiological deflections of the femur during FEA are observed when the femur is unrealistically constrained, reinforcing the need for physiologically based modelling. This was also suggested in an earlier study (Simoes *et al* 2000) although there was no comparison of different constraints in this study. Simoes *et al*, (2000) considered the effects of constraining the femoral head during strain gauging experiments when a simple set up is required. The strain distribution observed in the femur, when constraining the femoral head, did not produce a predominantly compressive state within the femur although bending was reduced. However when muscle forces were also added a compressive strain state was induced in the femur as is seen *in vivo*. Using only three loading conditions it was determined that in the absence of a complex experimental set up the femoral head can be constrained to produce physiologically representative strain distributions.

Phillips (2009) used a free boundary condition modelling approach which was a technique that accounted for the movement at the knee and hip joint instead of having a fully constrained model. Previous work by Speirs et al (2007) was a basis for this physiologically based model, in which a number of constraint and loading methods were considered. Five different load cases were applied, two models had a simplified hip joint load and one included the vasti muscles and the other had vasti muscles and the glutei muscles, both were constrained at the diaphysis. The remaining three models had a complex JCF and a full body of muscles which were calculated from a validated musculoskeletal model (Heller *et al*, 2001). They differed in the constraints, where one was constrained at the diaphysis, one at the condyles and final model at the knee and hip joint. Large reaction forces were found in all load cases except the joint constrained model, likewise a much larger deflection in the femoral head was found in the simplified loading cases. Further still the non-physiologically loaded models showed

high strain levels, above 3000με which would cause fatigue damage to the bone. In the Phillips model, a linear free boundary condition was compared to non-linear free boundary condition model. The linearity of the models referred to the force-displacement relationship, in which in this study were considered to be the two extremes of muscle optimisation in modelling. The constraints modelled in this study were unique as it was not fully constrained but allowed equilibrium within the model. The validity of the model was determined by comparing it to *in vivo* results (Bergmann *et al*, 2001). Reduced strains were seen in the non-linear model on the medial side of the femur. These were attributed to the increased forces in the ITB, creating a more balanced model. The structural effect of the ITB has been documented in previous work (Pauwels, 1980). The results indicated that the free boundary condition model showed the most representative *in vivo* forces indicating that when true boundary type conditions are adopted more valid results can be attained.

2.4.4 FEA OF JUVENILE FEMORA

Carriero *et al,* (2009) compared the strain levels at the growth plate in normal children and children with CP at 7 years old, was further to the work produced by Shefelbine *et al* (2002). The work used subject specific modelling through the use of motion capture, however the bone specimen used was a scaled down model of an adult, and therefore may have lacked the accurate geometry of the juvenile femur which is known to change throughout growth (Scheuer and Black, 2005). The results showed that abnormal normal loading caused by CP load cases caused an increase in NSA and femoral anteversion over time by changing the stress in the growth plate. Although this model can help to show the mechanical influence on bone remodelling one criticism could be on the lack of subject specific bone modelling, as changes in bone geometry can affect the forces applied by the muscles on the bone. *In vivo* work identifying differences in moment arms between children and adults can be useful for assessing changes in muscle forces. O'Brien *et al,* (2009) investigated changes in the patella tendon moment arm of the knee extensor in children and adults. The ages of the children were approximately 9 years old and were grouped as pre-pubertal. The patella tendon moment arm was found to be greater by 20% in adults than in children irrespective of the force changing capacity therefore it was suggested that it is not a true representative when muscle lengths are merely scaled to the correct size.

2.4.5 MATERIAL PROPERTIES

As has been discussed the major influences on FEA are the geometry of the model, the loading including boundary conditions, and finally the material properties of the model. When the structure being analysed is part of the skeleton a number of material properties need to be assigned. The material properties of bone obviously need to be assigned namely Young's modulus which describes the elasticity of the material and Poisson's ratio is the negative ratio of transverse to axial strain of a material. Two main materials are often modelled in FEA of the femur these are cortical and trabecular bone. There is a large amount of agreement on the material property of cortical bone which is usually given a Young's modulus of 17GPa (Polgar *et al*, 2003a). Trabecular bone however has a much larger variation in the literature, due to its highly anisotropic nature, ranging from 100MPa to 1.5GPa (Appendix II). The value assigned to the material can be dependent on what is being modelled. Van Rietbergen *et al* (2003) used high resolution scans to enable very accurate modelling capabilities. It was possible at this resolution to model individual trabecular struts, therefore a Young's modulus of 15GPa was assign to represent the material property of that. However in many cases trabecular bone is modelled as bulk modulus and a reduced value is specified. These variations may however be site specific trabecular values as the trabecular is dependent upon volume fraction and architecture (Bayraktar *et al*, 2004). BMD studies on the femur can help to inform researchers of areas of dense trabecular bone so that models may be built more accurately (Lai *et al*, 2005).

Even if the values of the material property are correctly assigned the location of the material properties also needs to be correct. One variation that is considered in the literature is the variation of the cortical thickness. Cortical bone is often applied as shell elements, over a trabecular core, this thickness however is not uniform. Silvestri and Ray (2009) validated a FE model with varied thickness of cortical shell against cadaveric specimens. Figure 2.25 shows the varied cortical thickness from one specimen.

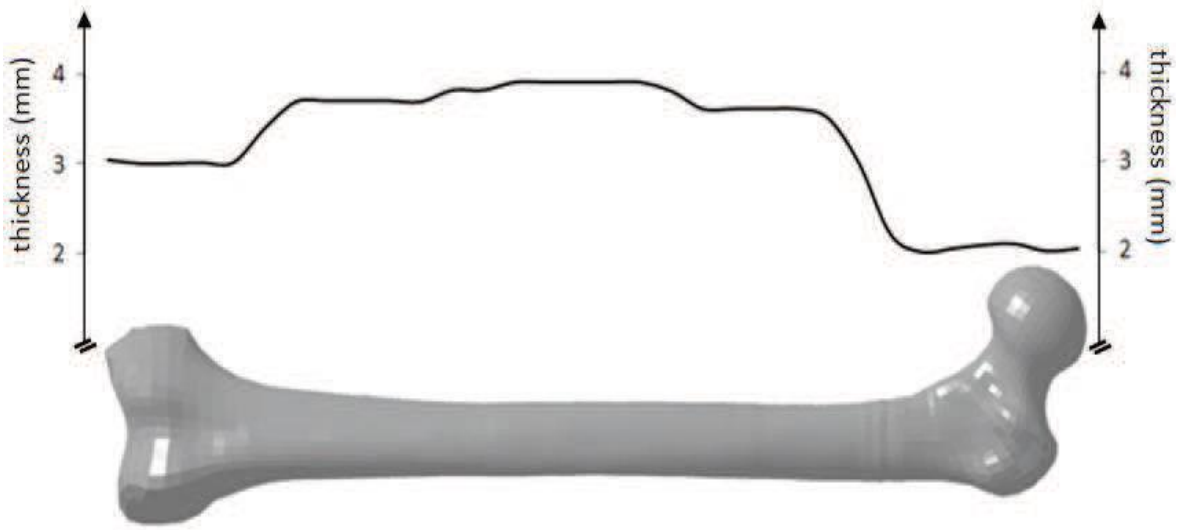

Figure 2.25 Reproduced from Silvestri and Ray (2009). Showing the cortical thickness variations in the FE model, based on cadaveric studies, for each element.

Taddei *et al,* (2006) used material properties calculated from CT scan data to compare the accuracy of inhomogeneity of material properties against a density based method for assigning material properties. Young's modulus for each element was computed on the basis of the density information derived from the CT dataset. The resulting values of the Young's modulus for cortical bone were up to 19.8GPa, with an average value of 12.9GPa. The study showed that material mapping positively influenced the accuracy of mechanical property prediction and suggested that if the stress distribution inside the bone is of importance then this method should be utilised. Wagner *et al* (2010) also used information obtained from the CT scan data to assign over 400 unique Young's Modulus to a FEM of a femur using an automated procedure. For trabecular these ranged between 77 - 1,835MPa and cortical bone 1,850 - 16,737MPa. A good agreement between the results of this automated procedure and previous FEA results were found.

The juvenile femur differs from the adult femur in terms of its material property in both the cortical and trabecular bone. Juvenile cortical bone has been modelled with a material property range of 11500-20000 MPa and trabecular 345-600 MPa (Ribble *et al,* 2001; Carriero *et al,* 2011). These variations from adults would have a varied effect on the behaviour, Ohman *et al,* (2011) confirmed this when studying the compressive behaviours of cortical bone in children and adults. It was found that the child cortical

bone tissue had significant lower compressive Young's modulus (−34%) compared to that of an adult. There are also other materials that need to be considered, these materials include the epiphyseal cartilage and growth plate. The epiphyseal cartilage is the cartilage were the ossification of the femoral head and trochanter is occurring, the material property of this has been seen to be from 5-600MPa. The growth plate is the areas that are between the epiphyses and the diaphysis, also known as a transition zone (Ribble *et al*, 2001). This material has a reported Young's modulus of 5-108MPa. These two material properties are in between bone and cartilage and the transition from cartilage to bone is represented as such.

2.5 CONCLUSION

The literature review has explored in great detail relevant areas to the proposed research. It has provided knowledge of bone growth and development in particular the femur. Identifying the morphometric changes associated with development e.g. change in neck shaft angle, and gaining an understanding of the modelling and remodelling of bone throughout growth. This has given knowledge of structural changes that could be used for to explain stresses and strains which are measured during FEA.

Bipedal locomotion is attained following a number of stages where movement is varied dramatically. The examination of these movement patterns and locomotion changes reveal what different loads and forces that the femur experiences throughout growth. Musculoskeletal modelling has been revealed to be an accurate method to calculate muscle forces, which has great implications for future work in human simulation, although research is lacking in children's musculoskeletal modelling. Finite element analysis research on the femur has spanned four decades and the complexity of recent analyses' are evidence of such. Recent work has been able to simulate the femur with great accuracy and therefore true *in vivo* analysis can be produced. However as in the musculoskeletal modelling much of the work has only extended to adults models and very little has been produced on juvenile femora.

Finally the review of the literature has provided a base of knowledge which will allow the proposed work to be at the forefront of research, and made areas of research that are lacking evidence. It is hypothesised that due to the structural organisation of the femur from an early age, as discovered in the literature, the evaluation of the stress/strain distribution will show similarities in all models. This hypothesis is based on the

knowledge that the femora, irrelevant of age, will all be structurally adapted to the loading that they experience. However this will be dependant up on the loads that are applied and therefore dependant on any differences in bipedal locomotion calculated during the musculoskeletal modelling.

3 DIGITISATION OF THE FEMUR SPECIMENS

To build a 3D volumetric model of the juvenile femur, digitisation of the models must be performed. These are produced by initially performing MRI and/or μCT scans and then using 3D modelling software to create a computer model. The digitisation of the samples would not create complete models without merging the CT and MRI scan data. This merging was necessary because neither data set contained information of a fully intact femur. The CT data contained full details of the shaft (diaphysis) of the specimens (Figure 3.1) however there was no cartilaginous growth plate or complete set of epiphyses. The MRI scans did however contain this data but the full shaft was not available, therefore merging these two scans would provide a full model. The aim of the work reported in this chapter was to construct computer models which represented different ages of development in the juveniles femur, allowing for finite element models to be produced at later stages of the work.

3.1 DIGITISATION OF THE DRY SPECIMENS

Scan data from CT scans and MRI scans can be used to create 3D models in computer simulations such as FEA and musculoskeletal modelling. In the present study five human juvenile femora were used, provided by Scheuer Collection at the University of Dundee. All of the specimens were dry with no cartilage attached, and so the epiphyses in the older femora were disarticulated. The femora studied consisted of a 4.6 months (*in utero)*, 3 year old and a 7 year old specimen (Figure 3.1). The 6month and 1 year old models in the figure were not digitised due to the lack of gait data for full analysis in future chapters. All ages were identified by the curators of the Scheuer collection. These ages were least damaged samples that were available to study and a range of locomotion development could be analysed through these specified ages

Figure 3.1. Juvenile femora provided by the Scheuer collection. Ages of the femora left to right: 4.6 months (*in utero)*, 6 months, 1 year old, 3 year old and a 7 year old. Only the 4.6month old, 3 year old and 7 year old models were used in this study.

Preparation of the femora for the CT scanning was identical for all of the specimens including the epiphyses. The models were scanned in a µCT (X-Tek, HMX160 micro CT system) (X-tek, Tring, UK) at different resolutions depending on the sample, details of which will be provided later in this chapter. The data provided by the µCT scanner was exported as stacked .tiff files which were then imported into Amira Software (Amira Visage Imaging, USA) for segmentation and 3D model generation. Due to the condition of the specimens the models were not in their true physiological entirety and some manual segmentation had to be performed in an attempt to repair the damaged areas of the bone. The damage that was present in the specimens was in areas where trabecular bone was on an exterior surface due to the lack of cartilage i.e. the end of the diaphysis.

3.1.1 PRENATAL MODEL

The prenatal model (SB) was aged 4.6 months *in utero* as classified by the Scheuer Collection curators, Dundee University and had a total length of 73mm. At this age the femur is not fully ossified as described in section 2.1 and therefore the only area available for scanning was the diaphysis. The femur comprises of an estimated 50% of cartilage at this prenatal age and therefore a large proportion of the full femur was not able to be directly modelled (Figure 3.2).

Figure 3.2. The prenatal femur specimen scanned (left) and a cross section through an intact femur of a similar age (Osborne, 1980) (right) showing bony shaft and cartilaginous epiphyses.

The specimen was scanned at a resolution of 0.0574mm x 0.0574mm x 0.0574mm. Although the femur could not be modelled in full because of the missing cartilage, reconstruction of the damaged bone was carried out. As the sample scanned was entirely bone with no cartilage present, the bone areas were clearly identifiable for the segmentation process. To repair the damaged areas of the bone slice by slice segmentation had to be performed in all three axes. The reconstructed model was smoothed to create an accurate

representation of the bone and to reduce irregular shapes on the surfaces thus enabling subsequent modelling work, FEA, to be performed (Figure 3.3). The smoothing process is an automated procedure in the Avizo software, it has the capability to create realistic models despite any difficulties with low resolution or noise artefacts created from scanning. This removed any blemishes to ensure a continuous surface was modelled.

Figure 3.3. Original scanned prenatal model (left) and rebuilt prenatal model with damage rectified (right).

Further reconstruction to include the cartilage was subsequently carried out to enable FEA of the prenatal femur. This work, which can be seen in Appendix III, was a sensitivity study which used computer simulation to replicate ossification of the juvenile femur, to test the

importance of the cartilaginous head in the prenatal femur when performing FEA. Due to the lack of muscle force data and a fully reconstructed model the prenatal model was not analysed beyond what is in Appendix III.

3.1.2 3 YEAR OLD MODEL

The specimen STH-SS1 was identified as from a 3 year old, and comprised of the femoral shaft which had a length of 190mm, the distal condyles and the femoral head (Figure 3.4). This was scanned at a resolution of 0.1211mm x 0.1211mm x 0.1211mm, although the 3D model again required reconstruction of damaged areas and the incomplete structure due to non-fusion of the epiphyseal cartilage .

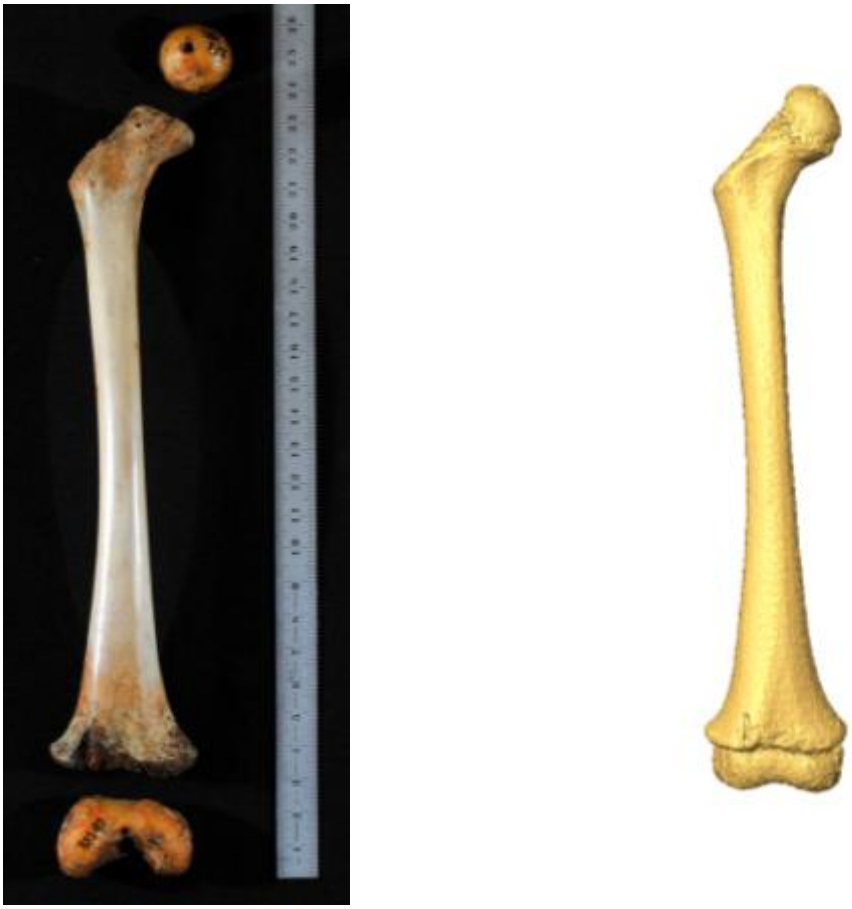

Figure 3.4 Components of the 3 year old specimen provided by the Scheuer collection (left) and the reconstructed 3D computer model (right).

3.2 DIGITISATION OF THE FULLY INTACT SPECIMENS

The models from Scheuer collection provided information of diaphysis/shaft of the femora, the following models contain information of the cartilaginous areas, but lack the information of the femora shafts. Together a whole model of the femur can be produced as will be presented in the following sections.

3.2.1 MRI SCAN DATA

MRI scans data provided by Guillaume Gorincour from Laboratoire d'Anatomie Comparée of the Muséum National d'Histoire Naturelle of Paris, was also available to be used for digitised modelling. The samples were of various ages and genders from 3 years – 18 years, the scan was from upper thorax to the distal diaphysis of the femur, a full list of the samples available can be seen in Appendix IV. Data was supplied in DICOM (Digital Imaging and Communication in Medicine) format which was able to be processed in AMIRA. The anatomical location of this MRI scan data was dependent on the patient and hence often only the femoral head and neck was included in the scan with little of the shaft present on the scan (Figure 3.5).

Figure 3.5. Typical MRI scan from a 7 year old child showing femoral head, trochanter, neck and little of the shaft.

However, the required epiphyseal information for the FEA and musculoskeletal modelling could be seen and hence modelled. Although the resolution was insufficient to differentiate between the cartilage and surrounding soft tissue, the area between the epiphyses and diaphysis was defined as cartilage and modelled as such.

3.2.2 3 YEAR OLD MODEL

The specimen for the three year old was identified as having an age of 3 years and 10 months. The scan information provided was distal to the lesser trochanter and proximal to the pelvis (Figure 3.6). The right femur was selected for modelling, to match the same limb as the disarticulated models, and the same procedure described previously was used to build the model and identify the different materials from the scan data.

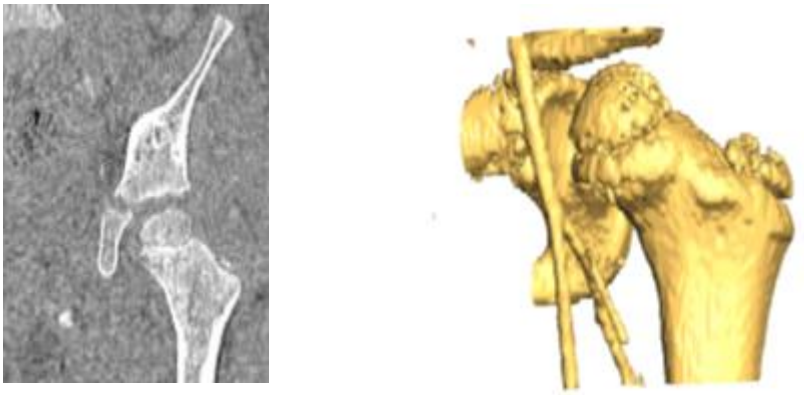

Figure 3.6. MRI slice showing data available to be used (left) and model built from scan data (right).

As previously discussed, the cartilage could not be differentiated by changing the threshold and therefore manual segmentation of the cartilage was required (Figure 3.7).

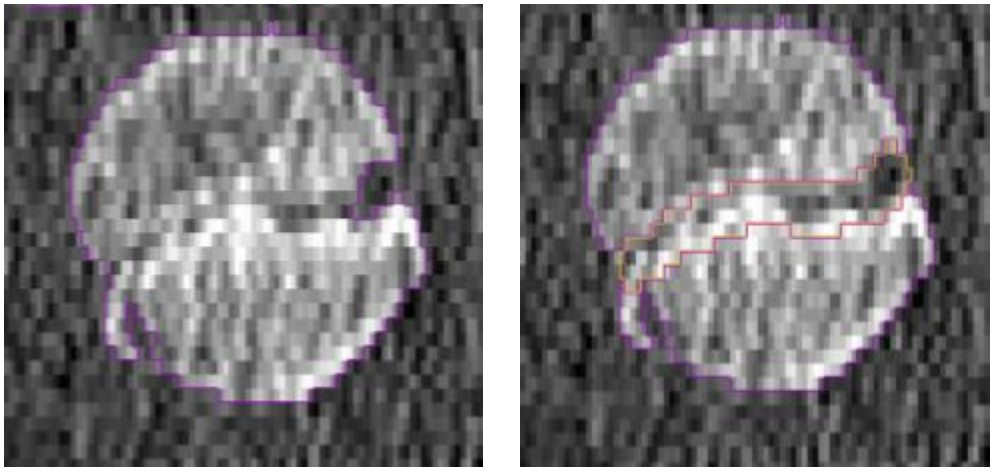

Figure 3.7. Showing epiphyses of the femur (left) and showing cartilage manual identified on the same slice (right).

Manual segmentation of the model was required for both the femoral head and the greater trochanter. Once completed a continuous bone and cartilage model was constructed as shown in Figure 3.8.

Figure 3.8. Complete 3 year old model. Purple identifying bone and yellow showing manually segmented cartilage.

3.2.3 7 YEAR OLD MODEL

The same procedure was followed for the 7 year old although less cartilage segmentation was required. The segmentation and final model can be seen in Figure 3.9.

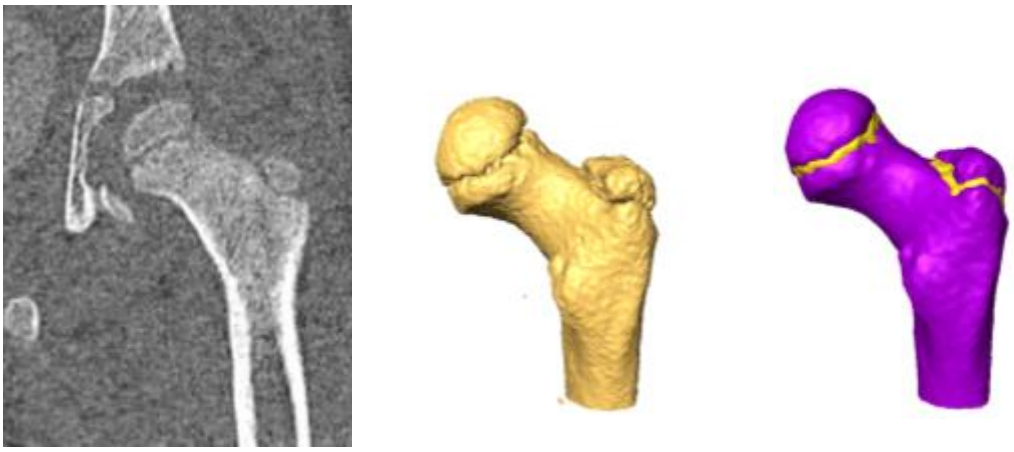

a) b) c)

Figure 3.9. MRI slice of a 7 year old model (a); original 7 year old model (b) and completed 7 year old model (c). Purple identifying bone and yellow showing manual segmented cartilage

For musculoskeletal modelling and FEA the proximal femur needed to include a greater length of shaft to enable muscle attachment. The rebuilt model of the proximal femur was then used to merge the shaft of the femur of the corresponding age which is included in the models provided by the Scheuer Collection.

3.3 MERGING MODELS

From the two sets of data, MRI data supplied by Laboratoire d'Anatomie Comparée of the Muséum National d'Histoire Naturelle of Paris and specimens provided by Scheuer Collection at the University of Dundee, it is possible to create a full length proximal femur. The CT data could provide the full shaft length and the MRI data could provide the information required to create the epiphysis.

To merge the models it was important to ensure the orientation of the fully intact femoral head, created from the MRI scans, was the same as that of the disarticulated models generated from the CT scans. In both models eight identical locations were landmarked chosen through visual inspection of the CT and MRI scanned specimens. The identified locations were on the anterior, posterior, lateral and medial aspects of the femoral heads

growth plate; the most prominent distal part of the lesser trochanter; the most anterior and posterior aspect of the greater trochanter growth plate and the midpoint between these two landmarks. Landmarked models can be seen in Figure 3.10.

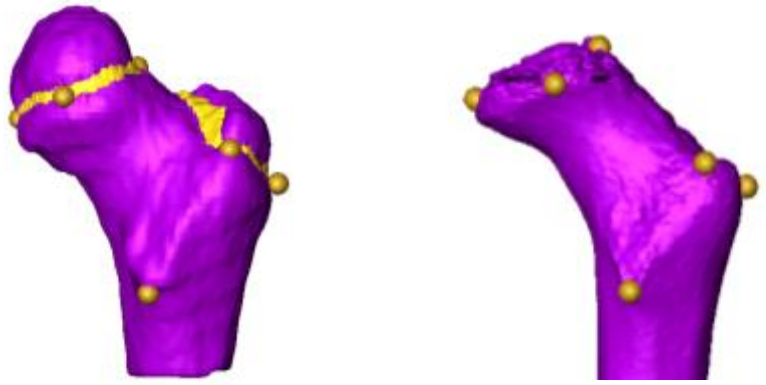

Figure 3.10. Landmarked models of the 3 year old models, MRI model of intact femoral head (left) and CT model of disarticulated femur (right).

To ensure correct orientation the fully intact femoral head was translated and rotated in the global coordinate system so that the landmarks matched those of the disarticulated model. The fully intact model could then be merged to the shaft of the disarticulated model to create a fully intact proximal femur (Figure 3.11)

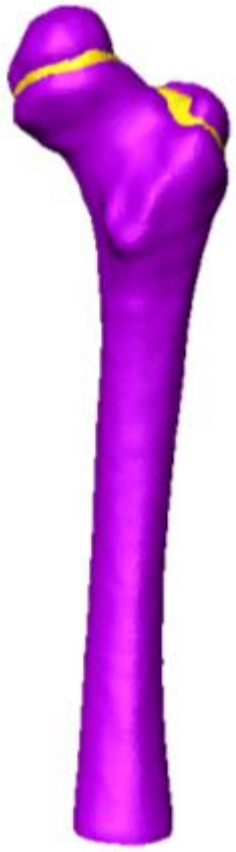

Figure 3.11. Fully articulated femur of the 3 year old model.

Once fully articulated the 3 year old and 7 year old model were able to be used for FEA and musculoskeletal modelling. A fully articulated prenatal femur was also digitised but due to the lack of information on loading and muscle locations the prenatal model would not be used in this thesis, but may be used for subsequent research.

3.4 FINAL MODELS FOR FEA

The final models for the 3 year old and 7 year old can be seen in Figure 3.12 along with an adult femur obtained from the VAKHUM collection.

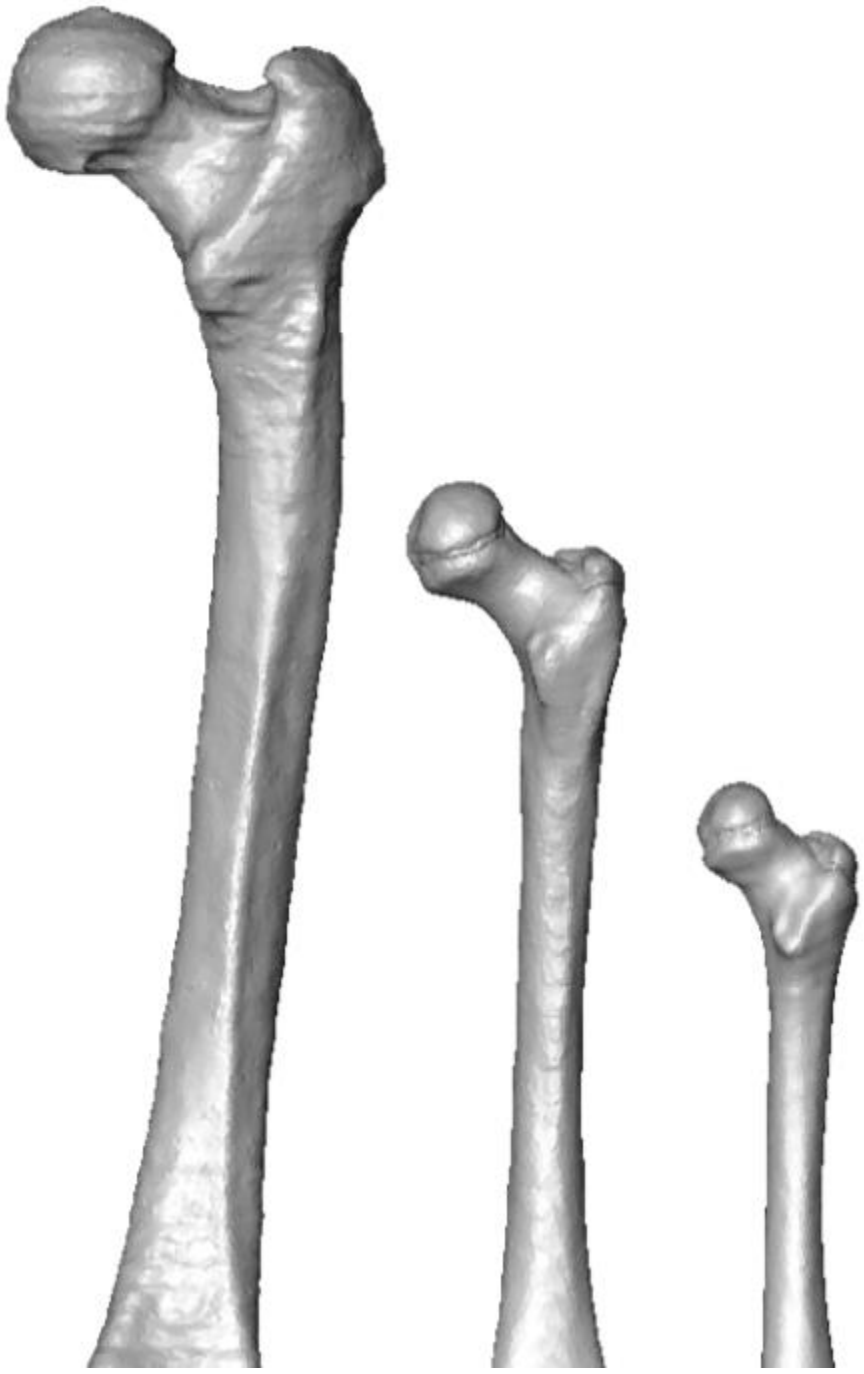

Figure 3.12. From left to right: comparative adult from VAKHUM, and the reconstructed 7 year old, and 3 year old to be used for musculoskeletal modelling and finite element modelling.

The digitisation of the femora was not as straightforward as it would have been if the appropriate equipment and subjects were available. The required MRI data to complete the most ideal femora models would have been expensive and beyond the means of this

research. However the construction and digitisation of the femora created models which are a representation of the desired age range for further analysis. Because of this it was then possible to begin to landmark the muscle insertion and origin points on the model for the loading of the finite element analysis (Chapter 7).

4 CHILDRENS GAIT ANALYSIS

4.1 INTRODUCTION

An important part of this work is to analyse the gait of children from different stages of development. The reasons are twofold; firstly the data collected during gait analysis is directly input to musculoskeletal software, enabling muscle force calculation. Secondly analysis of the gait will identify any differences in gait patterns due to gait development between the sampled subjects, which may help to explain any differences that are produced during FEA. The collection of standardised kinematic and kinetic gait data collection for children aged under 3 years is a difficult task (Kirtley, 2006) and therefore for this next stage of this work (musculoskeletal modelling) the results for the models would be difficult to validate due to the lack of data in the literature. Therefore gait analysis of only children aged 3 and above will be performed.

4.2 METHODS

4.2.1 SUBJECTS

Ten subjects were used for this study, one subject per age for the 3-7year olds and five adults (average age 24 years old). The adult data was captured to use as comparison against the children's gait pattern, the data presented for the adults gait pattern represents a mean score. Further details of the subjects can be seen in Table 4.1.

Age (years)	Height (cm)	Weight (kg)
3	93	13
4	105.5	17.6
5	117	25
6	111.5	18.5
7	130.5	32.9
	Adult	
24	179	76
25	185	86
23	189	92
24	173	81
22	174	73
Average	**180**	**82**

Table 4.1 Characteristics of the subjects' age, height and weight.

The collection of the gait data for the children and adults was performed at different laboratories, and therefore the set up was different, hence both protocols will be described. The information and process by which the data is collected is similar, using the same principals, information on this can be found in Chapter 2.3. The children's gait data was kindly supplied and collected by Dr Caroline Stewart and associates at the Orthotic Research and Locomotor Assessment Unit, Robert Jones and Agnes Hunt Orthopaedic Hospital, Oswestry. The adult's gait data was collected by the researcher at the Health and Human Performance Laboratory, University of Hull. The important differences between the two laboratories were camera number and the software used for capture. These factors would not have affected the results.

4.2.2 CHILDRENS PROTOCOL

The data was collected using a 12 camera Vicon MX system (Vicon Motion Systems Ltd., Oxford, UK) with one Kistler (Hampshire, UK)) force platform and a 10 m long walkway. A lower limb standard Helen Hayes marker set was used and the data was then processed in Visual 3d (C-motion, Sweden. Segments were defined using the landmarks and then a model could be produced so that kinematic data could be calculated. Although the raw data was collected by other researchers, the author of this thesis was responsible for all data processing and model building thereafter.

4.2.3 ADULT PROTOCOL

The data was collected using 10 ProReflex MCU (Qualisys, Sweden) 1000Hz cameras and with two Kistler force platforms. The walkway was 10m long and a lower limb Helen Hayes marker set up was used. The marker set up consisted of markers at the following landmarks bilaterally; lateral condyle of the knee (KNEE), anterior superior iliac spine (ASIS), posterior superior iliac spine (PSIS), heel (HEE), medial malleolus (ANK) first and fifth metatarsal (MT1, MT5).

The children and adult gait data was processed in the same way and carried out by the researcher. Left and right strikes were collected separately and events (initial contact and toe off) were identified automatically for the strike and manually for the following initial contact and the contralateral limb. Kinematic data were interpolated and filtered using a low-pass filter with a cut-off frequency of 6Hz. Kinetic data were filtered using a low-pass

filter with a cut-off frequency of 25Hz. The data points were then normalised to a gait cycle producing data points from 0% to 100% of the gait cycle.

4.2.4 DATA ANALYSIS

Data analysis was identical for both the adult and children. The data was exported to Microsoft Excel to be analysed for comparisons between ages. The results that are to be presented here include temporal spatial parameters, joint kinematics and kinetics.

4.3 RESULTS

4.3.1 TEMPORAL SPATIAL PARAMETERS

Table 4.2 shows that cadence decreased with age, and step length was seen to increase as a general trend. Although the stance and swing times are increased, this is as a result of the cycle time being increased, with the percentage of stance and swing time not significantly altering, ranging from 56%-60% and 40%- 44% respectively. Step length is increased as height is increased, which is normally associated with an increase in age.

Age	Speed (m/s)	Cadence (steps/minute)	Step Length (m)	Stance Phase (%)	Swing Time (%)
3	1.05	172	0.74	57	43
4	1.11	159	0.83	56	44
5	1.42	127	1.36	60	40
6	1.23	167	0.87	57	43
7	1.11	137	0.97	58	42
Adult	1.38	109	1.49	56	44

Table 4.2 Temporal spatial parameters for the different ages.

4.3.2 KINEMATICS

During gait analysis the knee angle for all ages were very similar when considering the shape of the graph (Figure 4.1). A peak flexion of the knee is at 10-20% of gait cycle representing the loading response phase of gait, the largest angle at this phase is seen in the 6 year old. The highest peak knee angle is seen at the ground clearance stage approximately 70% of the gait cycle, the highest was in the 4 year old where a peak of 82 ° was observed. Hip angle in the sagittal plane (Figure 4.2) shows the flexion and extension angles during the initial contact the hip is flexed at approximately 40° and then extends to -10° at 50% of

the gait cycle during toe off. During peak extension the largest angle is observed with a value of -15° in the adult and the lowest with a value of -1° in the 7 year old. Captured data for the hip adduction (Figure 4.3) shows quite a large variation between subjects. The data for the 7 year old showed the lowest hip abduction level at 20% of 2.4° and the highest was seen in the 4 year old at 12.2°. For all ages the highest hip adduction was produced around 70% of the gait cycle the highest being observed in the 7 year old and the lowest in the 4 year old. The ankle angle in the sagittal plane showed a similar pattern throughout the different ages with the ankle going in plantar flexion preparing for push off phase and then going into dorsi flexion at around 60% of the gait cycle for ground clearance. Maximum plantar flexion angles of 14° were seen in the 5 year old and maximum dorsi flexion angle of 22° in the 4 year old. The 5 year old shows the highest eversion angle of -18.5 ° and also showed the highest inversion angle of 14 °.

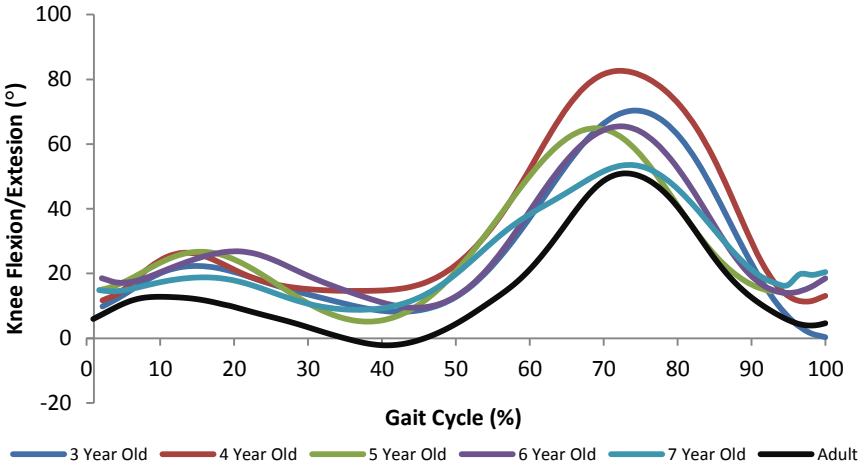

Figure 4.1 Knee flexion (+) and extension (-) angles during 100% gait cycle for all age groups including adult data.

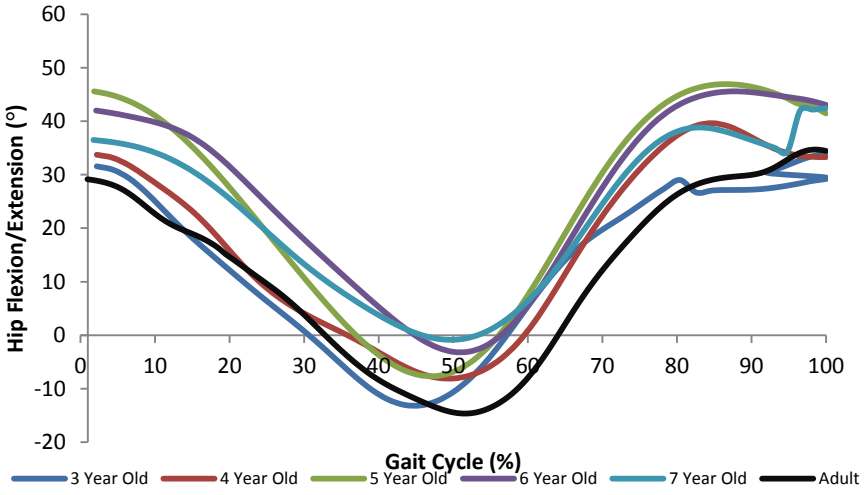

Figure 4.2 Shows hip flexion (+) and hip extension (-) through 100% of the gait cycle.

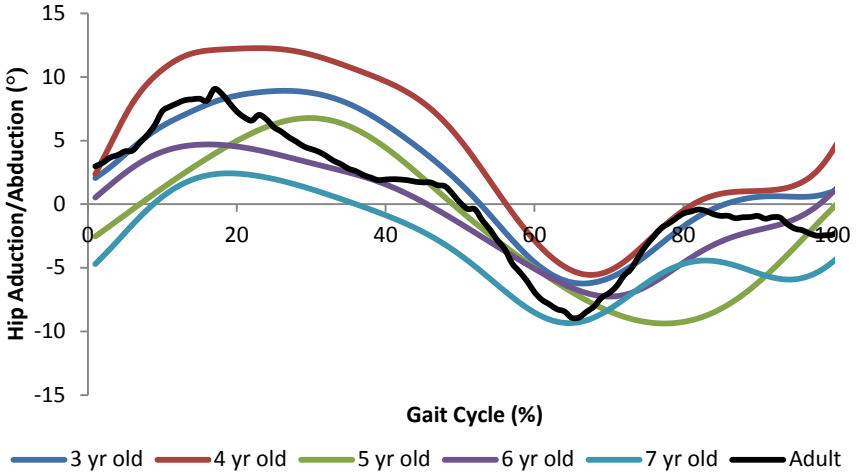

Figure 4.3 Hip abduction (+) and adduction (-) for all age groups

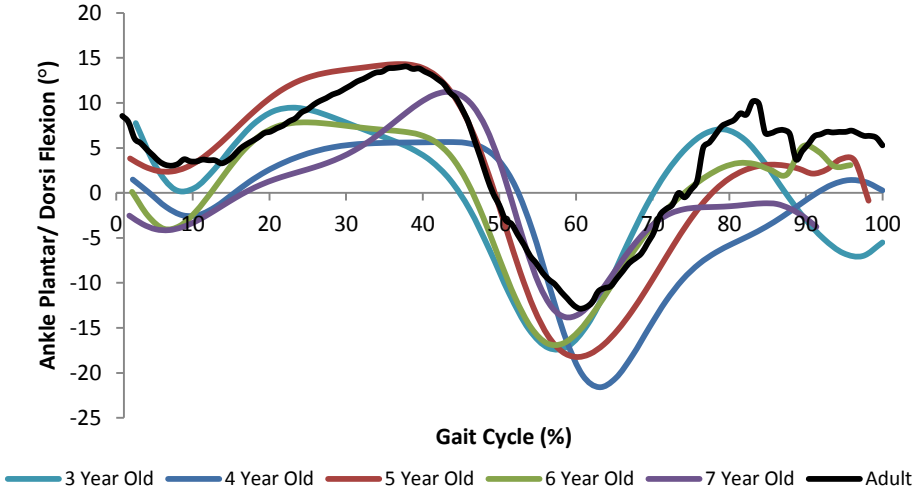

Figure 4.4 Ankle plantar flexion (-) and dorsi flexion (+) throughout the gait cycle

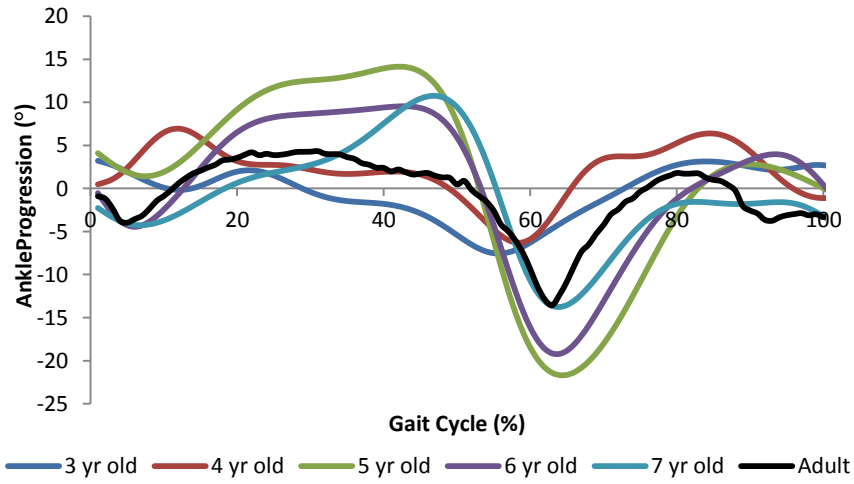

Figure 4.5 Ankle eversion (+) and inversion (-) over 100% of the gait cycle.

4.3.3 GROUND REACTION FORCE

Figure 4.6 show similar GRF's for all the age groups when normalised to body weight so a comparison between the subjects could be made. In Table 4.3 the change between the first peak (heel strike) and the second peak (toe off) shows a difference with age, with this sample there is a trend which shows that during the development to the adult stages there is a larger GRF at toe off instead of heel strike with a difference of -11% at adult from 13% in the 3 year old. The anteroposterior GRF (Figure 4.7) showed a peak in the adult of 2.2 N/kg in the posterior direction and 1.8 N/kg in the anterior. Similar values were found in the other age groups. In the ML (Figure 4.8) direction the 4 year old shows a peak of 1 N/Kg and with a gradual decrease to 0.6 N/Kg at 80%. In the 7 year old a rise to 0.5 N/kg was seen then a decreased GRF before a rise at 80% to 0.41N/Kg.

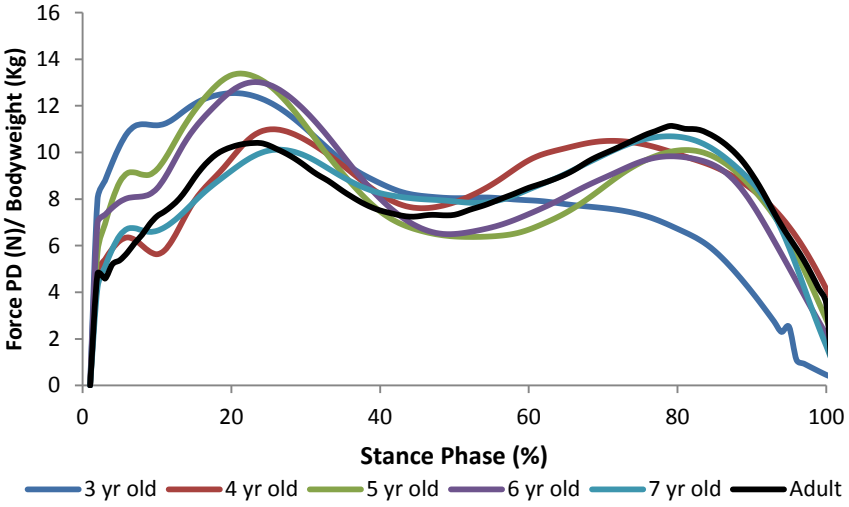

Figure 4.6 Normalised GRF in the Proximal Distal (PD) direction for 100% of the stance phase.

Age	3	4	5	6	7	8	Adult
% Change	13.7	4.2	27.4	20.7	0.0	-2.9	-11.2

Table 4.3 Percentage difference in GRF (Fz) from heel strike to toe off.

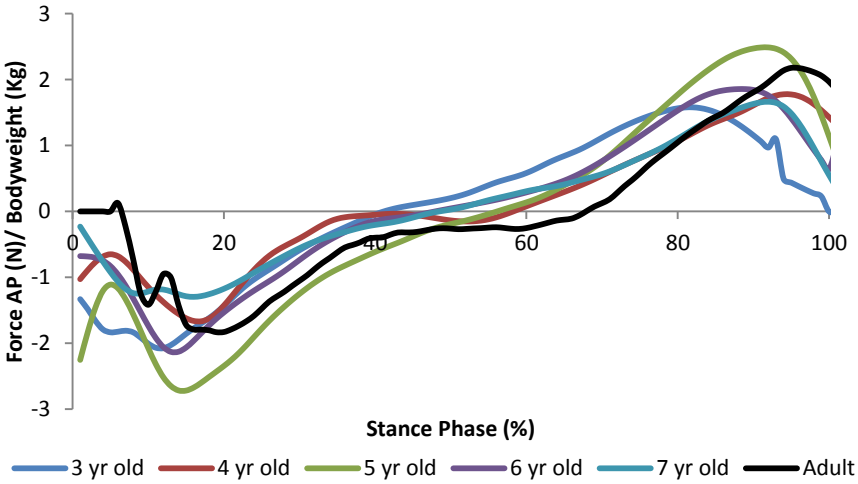

Figure 4.7 Normalised GRF in the anteroposterior direction for all the age groups and adult.

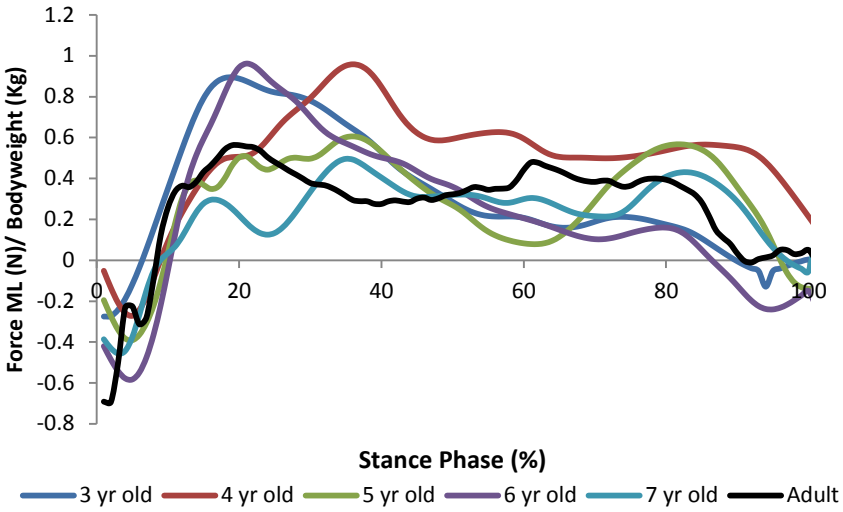

Figure 4.8 Normalised GRF in the mediolateral (ML) direction for all six ages and the adult, throughout 100% of the stance phase.

4.3.4 JOINT MOMENTS

The hip moments (Figure 4.9) show a positive moment initially moving to a negative moment and then decreases further into a negative moment at 80 % of the stance phase. The 3 year old data showed a reduced hip moment compared to the other ages with the highest moment being 0.5Nm/Kg, compared to the highest level of 1Nm/Kg in the other age groups. The knee moments (Figure 4.10) follow a pattern of a negative moment initially then a peak in positive moment at 20-25% there is then a reduction in positive

moment followed by another increase at 90%. The 3 year old had the lowest values at the two peaks of 0.38Nm/kg at the first and 0.18Nm/kg. Whereas the 6 year old had the highest initial peak with a value of 0.82 and the 7 year old showing the highest second peak value of 0.44 Nm/kg. The ankle moment (Figure 4.11) shows a distinct pattern in the 5 to 7 year olds with negative moment initially at around 10% of the stance and then increases to a positive moment until a peak at 75% this then decreases until 0Nm/kg at 100%. In the 3 and 4 year olds there is no negative moment and the increase in moment value is at a flatter rate than the other age groups.

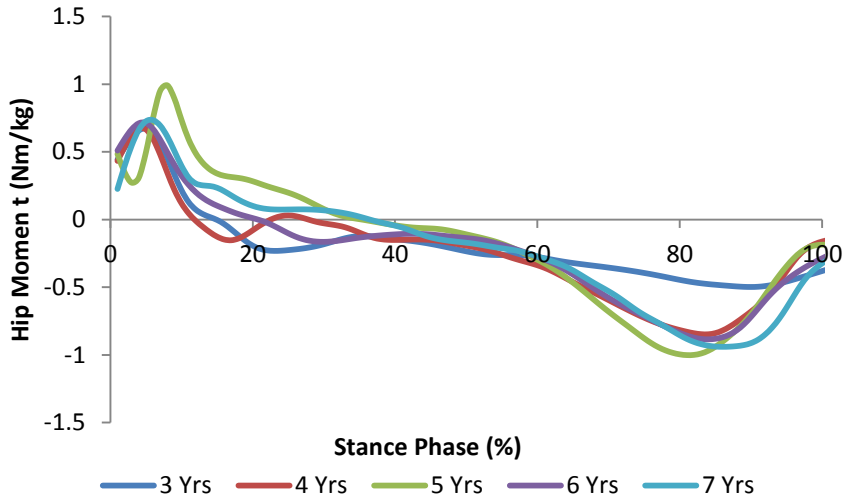

Figure 4.9 Normalised hip moments in the sagittal plane for all age groups. (+extension and –flexion)

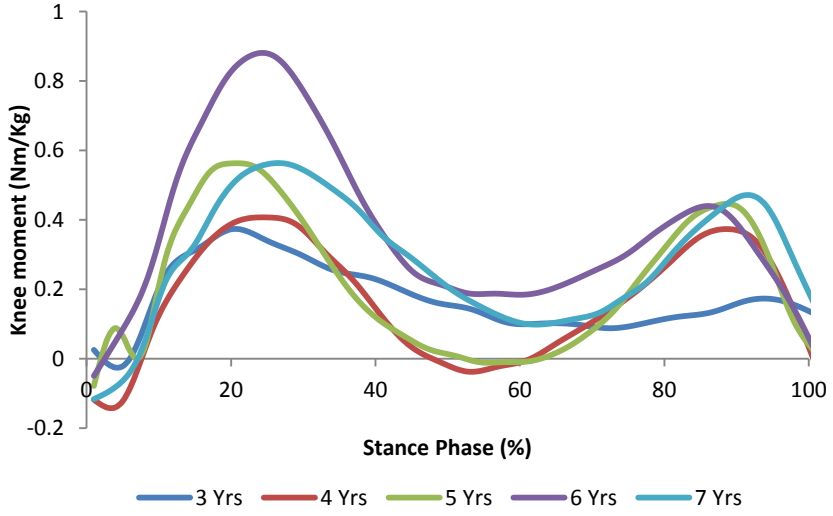

Figure 4.10 Normalised knee moments in the sagittal plane for all age groups. (+extension and –flexion)

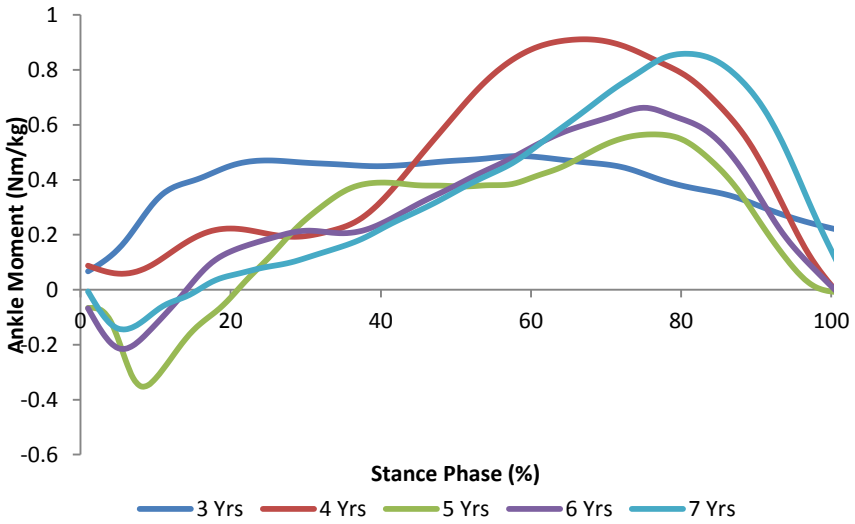

Figure 4.11 Normalised ankle moments of all the age groups are shown throughout the gait cycle. (+plantar flexion and – dorsi flexion).

4.4 DISCUSSION

Changes of gait in children aged 3-7 year olds has been documented in this study, these results are important to inform how the changes, if any, may affect bone development during growth. The data collected in this study is comparable to other research (Source data courtesy of P. Selber, W. de Godoy via the Clinical Gait Analysis normative database) which studied gait analysis at the ages of 4-8 years. A comparison of the average kinematics of the 3-7years old captured children's gait in this thesis and previous work by Selber and Wagner de Godoy can be seen in Figure 4.12 to Figure 4.15.

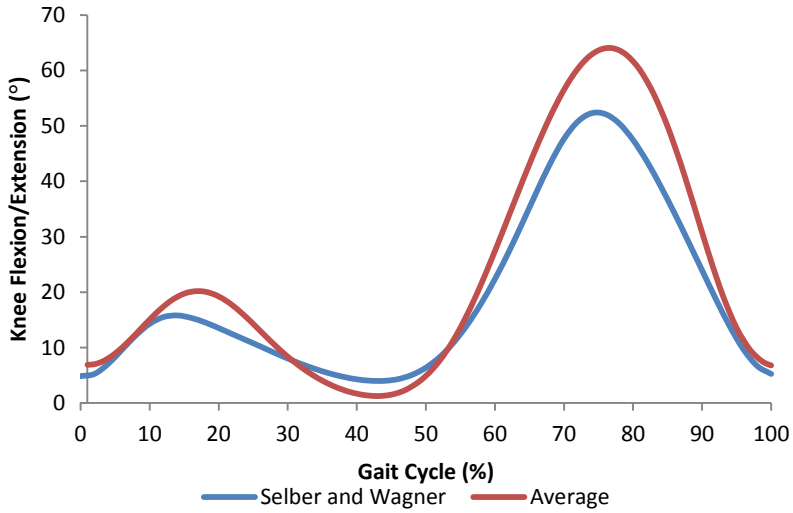

Figure 4.12. Comparison of the knee angle in the sagittal plane between current results (red) and Selber and Wagner (blue).

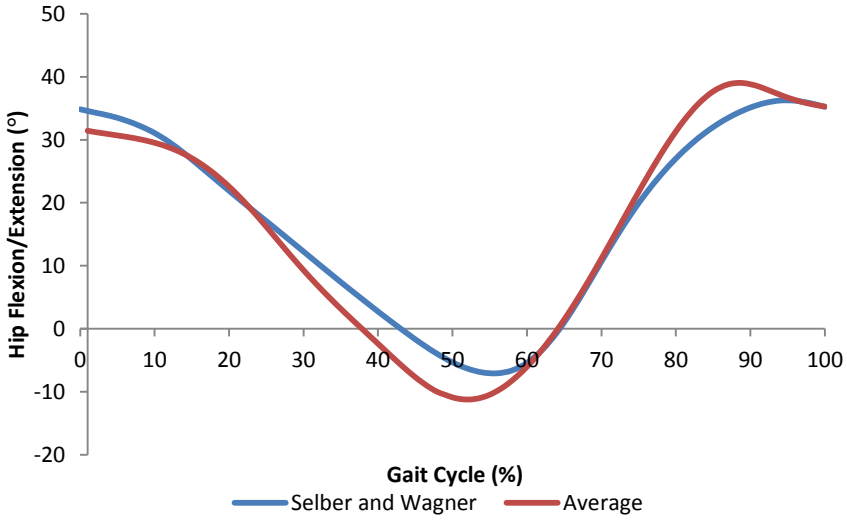

Figure 4.13 Comparison of the hip flexion and extension between current results (red) and Selber and Wagner (blue).

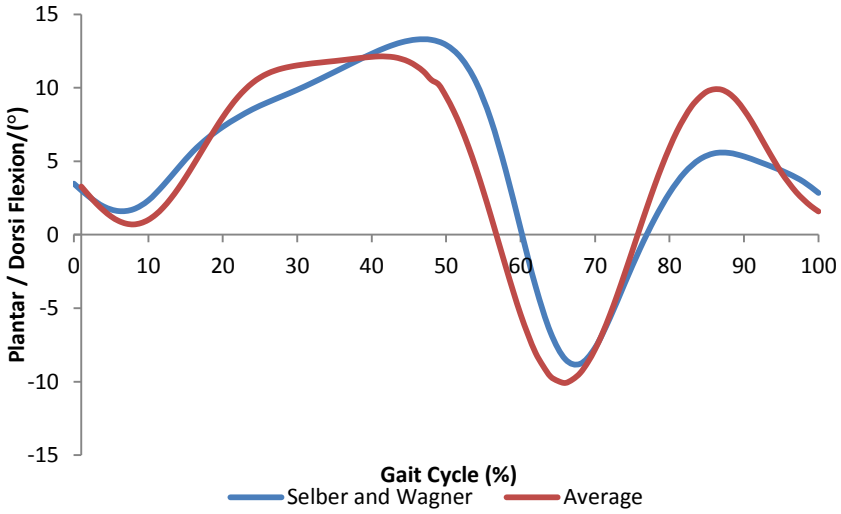

Figure 4.14 Comparison of ankle plantar and dorsi flexion between current results (red) and Selber and Wagner (blue).

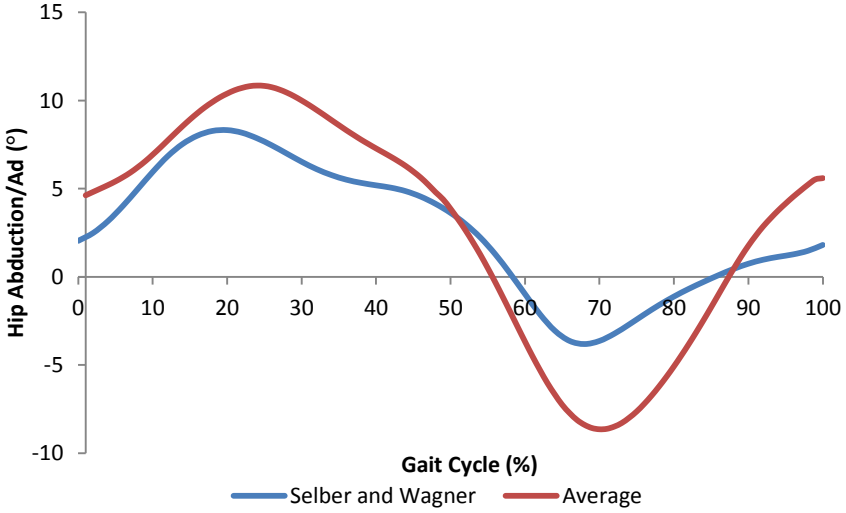

Figure 4.15. Comparisons of hip adduction and abduction between current results (red) and Selber and Wagner (blue).

The temporal spatial parameters were reported to be similar to that seen in previous work (Beck, 1981), with very little change observed in any of the parameters when normalised to height and leg length. Lythgo *et al*, (2011) reported a change in the stance and swing periods of children compared to adults, however in this study the change from a 57% stance phase to a 60% stance in adults was classed as a significant change. This could be due to intrasubject variability (Kirtley, 2006) rather than a result in age differences.

It is important firstly to address the obvious limitations to this current analysis, the greatest of which is the small sample size. However as these results correlate well with previous work which used much larger sample sizes, it is suggested that the collected data, could be deemed to be a representative. Also with the overall aim of this thesis being to load femoral specimens, and the lack of historical knowledge of the specimens to be loaded in the FEA, the accuracy of the gait analysis could never be subject specific.

The present work only considered ages 3-7 years the gait patterns in this age range were seen to be similar. Previous work has also shown that from ages 3 and above, although there is a variation in the values between subjects, kinematic characteristics of a 'mature' gait pattern is followed. It is shown that through the children's age ranges the knee flexion has a normal pattern throughout gait compared adult data. For knee angle, a key area of interest occurs at 15% of the gait cycle where there is slight knee bend ready for the push off phase. Then there is also a large increase in flexion at around 75% which allows for ground clearance and in preparation for heel strike with an almost fully extended leg. The knee flexion angles are in the expected normative range, according to previous studies (Sutherland, 2002) and thus show certain reliability in these results. Similar results were also seen in the hip and ankle in the sagittal plane.

The hip angle in the sagittal plane which shows the flexion and extension angle has been reported to have a peak extension angle of -10 ° at approximately 50 % of the gait cycle, and values in the present study correlate well with this. This peak extension of the leg is seen at the toe off phase of gait cycle and peak flexion is seen at around 10% and 90% of gait cycle. Again these results correlate well with previous studies. The ankle angle in the frontal plane was found to be much lower for both peak inversion and eversion angles in the 3 year old when compared to the other age groups and adult. Chester *et al*, (2006) found differences in the ankle and knee during swing phase, although these were not significant,

therefore this could correlate with the current findings and perhaps maybe an indicator of lack of maturity at this age. All of the other kinematic variables agree with early statements made by Sutherland (1980) proposing that gait maturity is reached by 4 years old in kinematic analysis. The variability between the angle values is relatively large, although this is to be expected as the variations in gait amongst adults is often high and therefore even though the subjects may have attained an accomplished gait pattern, the variability appears to be the comparable to that seen in adults.

Gait cadence decreases from 172 steps/min to 109 steps/min from 3 years through to adulthood likewise step length is increased from 0.74m by 1.49m. Although there were some fluctuations, these findings agree with previous observations of gait changes with age (Pierrynowski and Galea, 2001). In this study the changes in step length and cadence were normalised to show that there was very little difference in these parameters, adding to the suggestion that a mature gait pattern is reached between 3-4 years. Furthermore changes in the contribution of the stance and swing time showed similar values between the ages in a range of 56% - 60% in stance time and 40% - 44% in swing phase. Similarly, Chester *et al* (2006) found no changes in the temporal spatial parameters. Previous studies seem to correlate well with the current findings in which it is observed that the kinematic and temporal spatial parameters appear to follow a mature gait pattern. Although the kinematics have been discussed in terms of development, kinetics is another important aspect that needed to be explored.

If the kinematics during gait development were the only factor affecting bone growth then there would be little change in the developing locomotor skeleton after the age of 4 if it is, as has been suggested, mechanical factors that influence bone growth (Ruff *et al,* 2003a). However because there are changes in the femoral development beyond the age of 4 years of age it may be the kinetics that would influence bone strains to an equal if not greater proportion to that of kinematics. Therefore it may be the changes in kinetics that have an influential role in the developing skeleton during growth.

The GRF changes from a higher heel strike (HS) result in the 3 year old to a higher toe off (TO) in adult may be indicative of an increased control during walking. Oeffinger *et al* (1997) suggested that there is maturation in the concentric actions of the ankle flexors and therefore this would affect such control of HS. This was evident in the current work

showing a possible lack of maturity in the 3 year old subject. GRF in gait analysis allows for inverse dynamics calculations to be performed, with these calculations then allowing joint moments and powers to be produced. Ground reaction force in the mediolateral direction has been seen to be higher in children than that of adults (Cowgill *et al*, 2010). The children's gait in this study was correlated to changes in the diaphysis width and shape of the femur, it was suggested that the mediolateral force increased the bending moment in the femur producing remodelling of the bone, although this was not substantiated by any FE modelling. A number of reasons for this change in the mediolateral force compared to adults were proposed in the study. One concerned the lack of energy efficiency in young children during walking due to poor motor control. One other theory, which also relates to the development of the femur, is the difference in bicondylar angle during development alters the natural centre of gravity and therefore the stance changes to compensate for this. These two compensatory mechanisms discussed seem to be a plausible explanation of the changes noted during gait although further work in the project will attempt to explain these changes through the use of FEA. Further evidence of the poor motor control ability is seen in the lack of knee extension during the stance phase in the 3 year old. Grimshaw *et al* (1998) observed similar gait patterns in subjects between the ages of 10 months and 24 months, and this was attributed to the increased balance when leaving the knee slightly flexed and suggesting that there is a lack of motor control and balance during this immature gait, again which is can be seen in the 3 year old data. This is also observed with a longer double stance phase.

Joint moment patterns help to identify the working mechanisms across joints and furthermore joint powers can be calculated from them, indicating the work load of flexors and extensors. Previous work has also shown that there are differences with age in the moments and powers of joints (Oeffinger *et al*, 1997). In the current study it was seen that the moments in the older children (5-7 years) are consistent with adult moments, however this was not the case in the younger ages. The differences seen in the hip knee and ankle predominantly in the 3 year old, these are distinguished by a definite change in pattern compared to the other age groups. Previous studies have suggested that this is often observed in immature gait patterns which do not have the maturity to produce the joint moments necessary to perform a mature gait. However the 4 year old showed a high ankle moment in the toe off phase of the stance, whereas in the hip and knee the 4 year old has

the lowest recorded values with the exception of the 3 year old. This occurrence can be explained by the theory suggested by Oeffinger *et al* (1997) and again Sutherland (1997), which states that in the younger ages there is a greater dependence on the hip extensors for power in the push off phase than that of the plantar flexors. This could be due to the progression from flat foot and toe walking to a mature gait pattern. The lack of plantar flexor ability to generate power during flat foot walking and toe walking, increases the reliance on the hip extensors for this power. The 5-7 year old hip moment values are of a similar value to that seen in Chester *et al* (2006) in the comparison of kinetics between 3-13 year olds, and again similar values to that of adult hip moments, with values of 0.8Nm/kg being reported (Kirtley, 2006). However in Chester *et al's* work the grouping of 3-4 year olds may have obscured the difference in the results between these ages, which in the present study has been shown to be an important developmental age. The 3 year olds' lack of normative moment patterns may be associated with an immature gait pattern, displaying more flat footed walking and toe walking in some cases (Cioni *et al,* 1993). This can also be seen with the non-mature vertical GRF in the 3 year old where there is a minimal change between the heel strike to toe off peak. These developmental changes in gait may also have a large role to play in the growth and development of the locomotive skeleton due to the changes in the loading. Further findings in the joint moment changes during the development of gait provide further information which may help to explain ontogenetic changes. Joint moments will be discussed in the musculoskeletal modelling chapter (Chapter 6) as the role of different moments will have a greater effect on the computer modelling of muscles through inverse dynamics.

In conclusion, the notable changes and findings in this chapter are in general agreement with previous work which has studied juvenile gait. Apart from the obvious limitation of low subject numbers, the results are comparable to those reported in the literature. The work described in this chapter has provided essential gait data of children at ages relevant to the loads that will be applied to FE modelling further in this research. Although not all of the data will be used, analysis of the gait as age progresses can help to build a picture of gait development. These results will help to explain FEA results by relating any variations in the FE models to the variations found during motion capture and musculoskeletal modelling, as has been discussed in previous work (Cowgill *et al,* 2010).

5 RELIABILITY OF THE MUSCULOSKELETAL MODELS

5.1 INTRODUCTION

The motion capture software (Visual 3D), used for gait analysis, is unable to predict muscle activity to do this the collected data is input into a musculoskeletal modelling software. One such software is AnyBody (www.anybodytech.com), which uses inverse dynamics to derive, amongst other data, muscle forces. Through inverse dynamics joint moments are calculated and then muscle forces are calculated through a linear optimisation technique (for more information see Chapter 2.4).

Breaking down the process by which muscle force data is produced, the reliability of a number of variables need to be tested. As previously discussed, inverse dynamics uses kinematic data and ground reaction force data to produce joint moments. The first reliability test required is examining the kinematic data produced in AnyBody, ensuring this is consistent with the kinematics produced from the motion capture analysis software. Secondly the musculoskeletal models predicted GRF can be compared to the experimental force plate data. Once the kinematic and GRF result have been compared, it can be assumed that the data required produce muscle force is accurate. However the technique used to derive the muscle force data is not possible to test through a simple method of comparison.

Electromyography (EMG) provides detailed information concerning the timing of muscle activity (onset and offset), and further the magnitude of muscular activity when normalised relative to the strength of individual muscles. EMG data cannot be directly compared to muscle force data because of the differing units and therefore the magnitudes cannot be compared. To validate models that are not driven by EMG, there needs to be a method that can correlate force (Newton's) and EMG activity (millivolts), or can convert volts into force. One of the most accurate and methodical approaches was performed by Doorenbosch *et al* (2005). This method collected isometric strength at various speeds and a range of angles in synchronisation with EMG. This would allow the EMG activity of the muscle whilst at various lengths and at different angles which can produce different forces depending on which is most optimum, one limitation with

this method is it is impossible to isolate a singular muscle for strength tests. Cutts (1989) studied the sarcomere length changes during a gait cycle it was found that during gait muscles operate at the peak of where maximum tension can be released. This peak would vary between muscles and subjects.

Due to the inherent difficulty with the collection of EMG data from children, the reliability of the muscle force data will be tested on an adult model. This is an important part of the research so the results that are produced through FEA will have been performed with correctly calculated loads. The aim of the chapter is primarily to test the reliability of the kinematics and the kinetic data against the motion capture data, secondly to compare the muscle force data with EMG data. This will be done by correlating the EMG data and the force data from the AnyBody model to create equal magnitudes so a comparison can be made. The comparisons will be made under the assumption that motion capture of kinematics and kinetics is the gold standard method of measuring human movement and therefore these results will be assumed to be correct.

5.2 METHODS

5.2.1 PROTOCOL

The data that is to be compared to the Anybody was discussed in the previous chapter, for the methods involved in the motion capturing see Chapter 4.

A single male subject (24 years old) was used for the reliability testing. Participant's height (179cm) and mass (76kg) were recorded using a stadiometer and SECA balance scales respectively. Reflective markers were placed over anatomical landmarks according to a Helen Hayes model. Markers were placed over the clavicle, sternum, and the spinous process thoracic 10. Markers were also placed bilaterally on the anterior superior iliac spines, posterior superior iliac spines, thigh, knee, tibia, ankle, heel, 5^{th} metatarsal, and toe. Motion capture data was collected using 10 ProReflex MCU 1000Hz cameras (Qualisys Medical, Sweden). Kinetic data were obtained from three 600mmx900mm AMTI force platforms (AMTI, MA, USA). The force platforms were configured in order to capture 3 consecutive foot contacts. Kinematic data were collected using a sampling frequency of 1000Hz.

Marker trajectories were identified in Qualisys Track Manager and the trials were reduced to full gait cycles only. Kinematic, kinetic, and electromyography data were exported to C Motion Vis 3D (C3d) format. Participant's height and mass data were input to the software and a model was built with hip, thigh, shank, and foot segments. Gait events (heel strike and toe-off) were identified for each of the trials in order to normalise all data to 100% gait cycle (stance and swing). Kinematic data were interpolated and filtered using a low-pass filter with a cut-off frequency of 6Hz. Kinetic data were filtered using a low-pass filter with a cut-off frequency of 25Hz. EMG data were rectified and filtered using a moving root mean square (RMS) with a moving window of 25 frames. All data were inspected visually prior to data compilation. A gait report was produced for each of the participants incorporating the following variables; kinematic, kinetic, and EMG data.

5.2.2 EMG PROTOCOL

EMG data was collected simultaneously with gait motion capture, the data was normalised to the maximum signal (mv) obtained during the Isometric Maximal Voluntary Contractions (iMVC) trials. EMG data were collected unilaterally from the biceps femoris (BF), rectus femoris (RF), tibialis anterior (TA), and gastrocnemius medialis (GM) of the right leg, using an 8-channel portable, wireless EMG system (ME6000, MEGA Electronics Ltd, Finland). Identification of the muscles and skin preparation were performed according to SENIAM standards. The origin and insertion of each muscle were identified in order to identify the appropriate muscle belly. This area was then shaved to remove body hair, and wiped using an alcohol swab to remove any dead skin or body oil. Two circular silver-silver chloride (AgAgCl) electrodes were placed 10mm apart over the muscle belly and one reference electrode was placed over a bony landmark for each of the muscles of interest. Care was taken to avoid crosstalk from myotendinous junctions and adjacent lying muscles. iMVCs were performed for each of the muscles in order to obtain a maximal signal and normalise the EMG. All data were recorded using a 64-channel USB Analog Board, and synchronised via Qualisys Track Manager software.

5.2.3 ISOMETRIC STRENGTH TEST

Isometric strength for 4 muscle groups were recorded, namely the knee flexors and extensors, and ankle plantar flexors and dorsi flexors. The isokinetic dynometer

(Biodex System 3 PRO) was set up so that the subject could perform a maximal contraction and the force could be measured. For knee flexion the initial position was at 60˚ knee extension was at 60˚, and for the ankle plantar flexion and dorsi flexion were set at 90˚ as selected by the protocol on the dynometer. The subject recorded 5 trials of each movement and then the average maximal force was recorded. EMG was collected simultaneously during the maximal strength tests. The dynometer recorded joint torque and therefore force needed to be derived from the torque by rearranging Equation 5.1, and using the collected data presented in Table 5.1.

$$T = rF \sin\theta$$

Equation 5.1 Where T is torque, r is the segment length and θ represents the angle that the force was applied at.

The subject recorded a maximum force 977.6N for the knee flexors and 1655.4N for the knee extensors and 473.8N for the plantar flexors and 183.6N for the dorsi flexors. EMG data was collected during these maximum strength tests providing a maximal EMG reading for the principal agonist muscle in each movement i.e. bicep femoris responsible for knee flexion (Table 5.1). The maximal EMG reading could then be correlated to the maximum force. EMG collected during gait could then be normalised as a percentage of the maximum EMG reading, as a result a force of a muscle could be calculated. For Example; maximum EMG is equal to maximum force; therefore; 10% of maximum EMG during gait is equal to 10% of the maximum force.

Muscle Groups	Segment Length (m)	Angle (°)	Maximum Torque (N/m)	Maximum Force (N)	Maximum EMG (μV)
Knee Flexor	0.43	60	127.8	977.6	514
Knee Extensor	0.43	60	151.1	1655.4	534
Ankle Plantar	0.20	90	82.6	473.8	312
Ankle Dorsi	0.20	90	32.0	183.6	172

Table 5.1 Subject, torque and force data collected from the dynometer testing and maximum EMG values (for the EMG the primary mover was selected for each movement; Knee Flexor- bicep femoris; knee extensor- rectus femoris; plantar flexor- gastrocnemius; dorsi flexor- tibialis anterior).

5.2.4 MUSCULOSKELETAL MODELLING

The repository in AnyBody has vast number of models which can be used without the need for gait analysis input. This is useful when using the muscle data from the model in the repository for analysing a standard adults muscle forces. However to compare the data a subject specific model must be created.

To produce a model in AnyBody a C3d file is needed which can be produced from the motion capture system. The C3d file contains all the motion capture data, which includes anthropometric, marker positions, force data, and EMG data amongst others. The setup of the model, once the C3d file has been loaded, begins with the marker placement. For the captured model to be accurately reproduced in AnyBody the marker positions of the Anybody model need to be moved to the positions of the captured marker positions (Figure 5.1). The set up in AnyBody requires a degree of manual positioning to increase the computational speed of the optimisation of the muscles and for the model to solve all the kinematic and kinetic constraints accurately. However because of this subjectivity in marker positioning it is necessary to see what effect moving the markers has on the results. Therefore a sensitivity test was produced to assess the effects of these changes.

5.2.5 SENSITIVITY OF THE MUSCULOSKELETAL MODELS

5.2.5.1 Protocol

The manual changes that are possible in AnyBody to enable replication of captured data include limb length and limb angle (Figure 5.1)

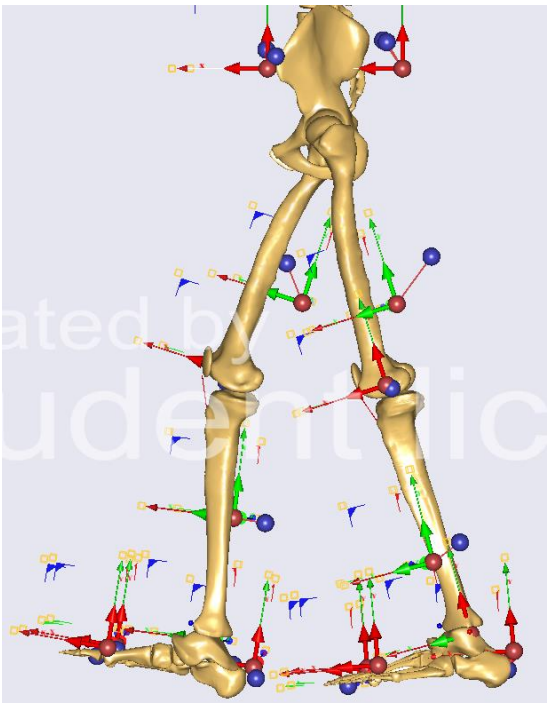

Figure 5.1 AnyBody model of the lower extremity. Showing the AnyBody template markers (red) and the motion capture markers (blue)

In this case an increase of the initial model of 5cm was made to the thigh and shank length and an alteration by +5˚was made to the knee and hip angles. The results of these were compared throughout a full gait cycle.

5.2.5.2 Results

The largest difference between kinematic outputs was found to be 2.1% in hip abduction and adduction values at one instance of the gait cycle (10%) (Figure 5.2). The other data showed very little difference between the models. All other kinematic variables fell below this value of 2.1% difference. This sensitivity study of the changes to increase the speed of optimisation show that there is very little effect on the final kinematics produced and that future models can be adjusted accordingly to increase computational speed.

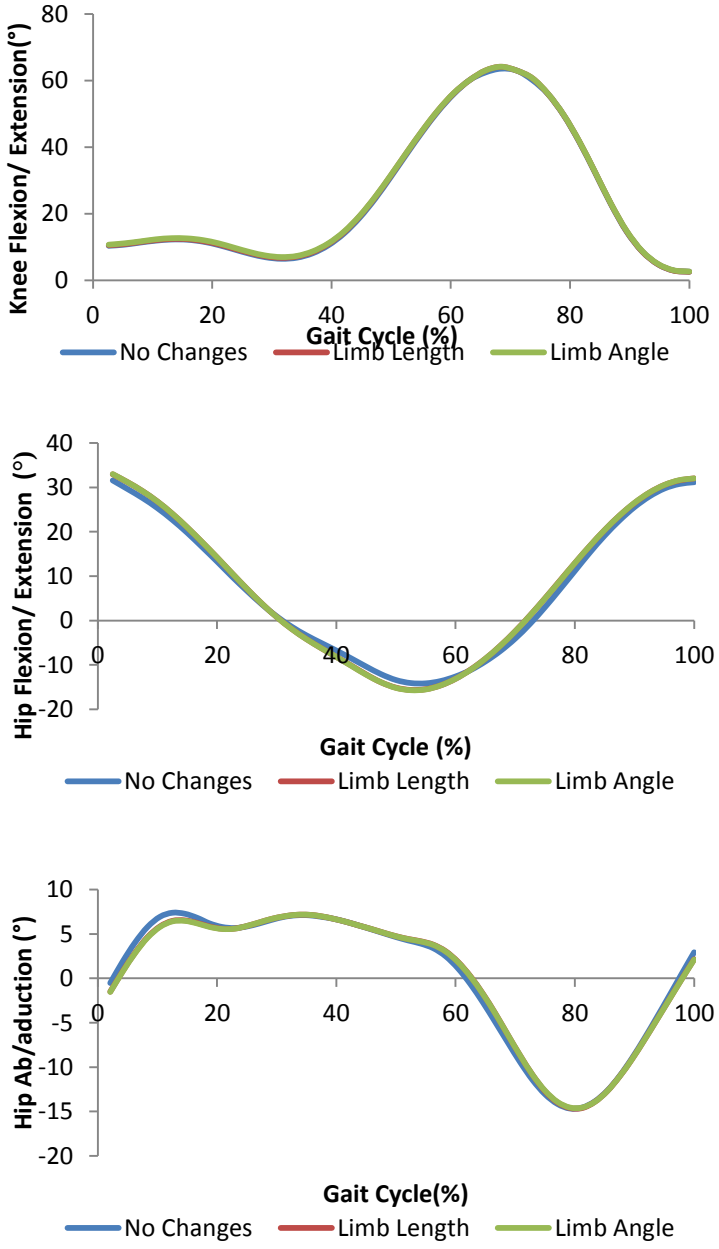

Figure 5.2 Effect of a change in limb length (±5cm) and limb angle (±5°) on the kinematics of the musculoskeletal model.

5.2.6 DATA ANALYSIS

All the kinematic and kinetic data was normalised to 100% of the gait cycle and direct comparisons were made between the kinematic data which was collected from AnyBody and Vis3D. The EMG data collected from the four muscles were compared to EMG provided on the Clinical Gait Analysis (GCA) database (Hof et al 2005) to show the validity of the data collected and then these were compared to the muscle forces produced by AnyBody for onset and offset times and using the methods discussed an EMG to force comparison could be made.

5.3 RESULTS

Due to the different softwares the results may have varied kinematics and kinetics. The differences include fitting the skeletal model to the markers to ensure all kinematic restraints can be resolved in the AnyBody modelling system.

5.3.1 KINEMATICS

In the sagittal plane kinematic differences were observed although the differences were small (Figure 5.3). At the hip during peak flexion a difference of 1.95° and at peak extension 0.87° was observed. These values were similar throughout the gait cycle. In the knee, differences at peak extension values of 3.2° were seen and peak flexion was 11.23° and again this was similar throughout. In the ankle, where plantar flexion peaked at 17.08° in Vis3D, the Anybody model was much higher with an angle of 25.67° although a similar dorsi flexion angle was seen to occur with values of -0.16° and -1.91° in Vis3D and Anybody respectively.

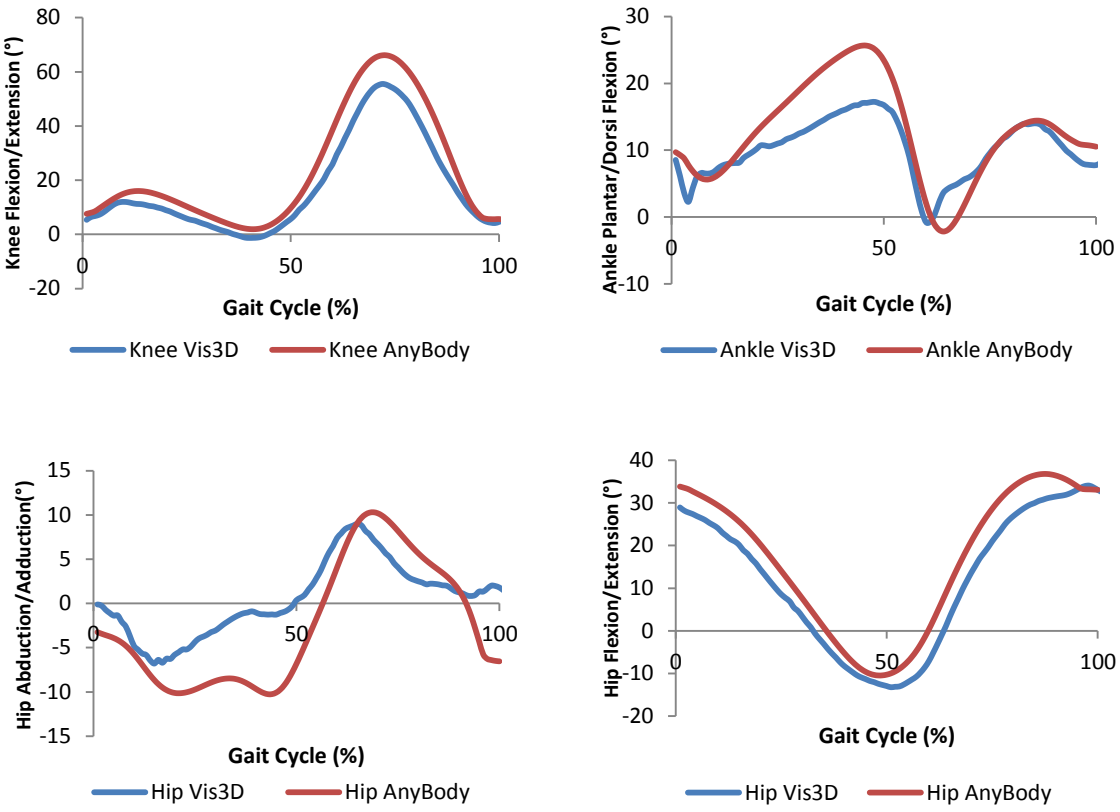

Figure 5.3 Comparison of kinematics data between AnyBody (red) and Vis3D (blue).

5.3.2 KINETICS

Examining the GRF in Figure 5.4 the Z (PD) direction sustains a similar value throughout the gait cycle. with peaks of 10.11N/Kg and 10.07 N/Kg being observed at heel strike in the AnyBody model and Vis3D respectively, again at toe off comparative values of 10.4N/Kg and 10.56N/Kg were seen, showing a high level of agreement in the vertical force. In the Y direction the ML force is shown, the AnyBody data shows a slightly larger peak at 20% of the gait cycle by 0.04N/Kg. Whilst the rest of the data seems to correspond well. In the X (A/P) data showed a consistent pattern between the two methods and show very similar values throughout the gait cycle. The peaks are at the same time as the Z and Y graphs during gait cycle which correlate with HS and TO.

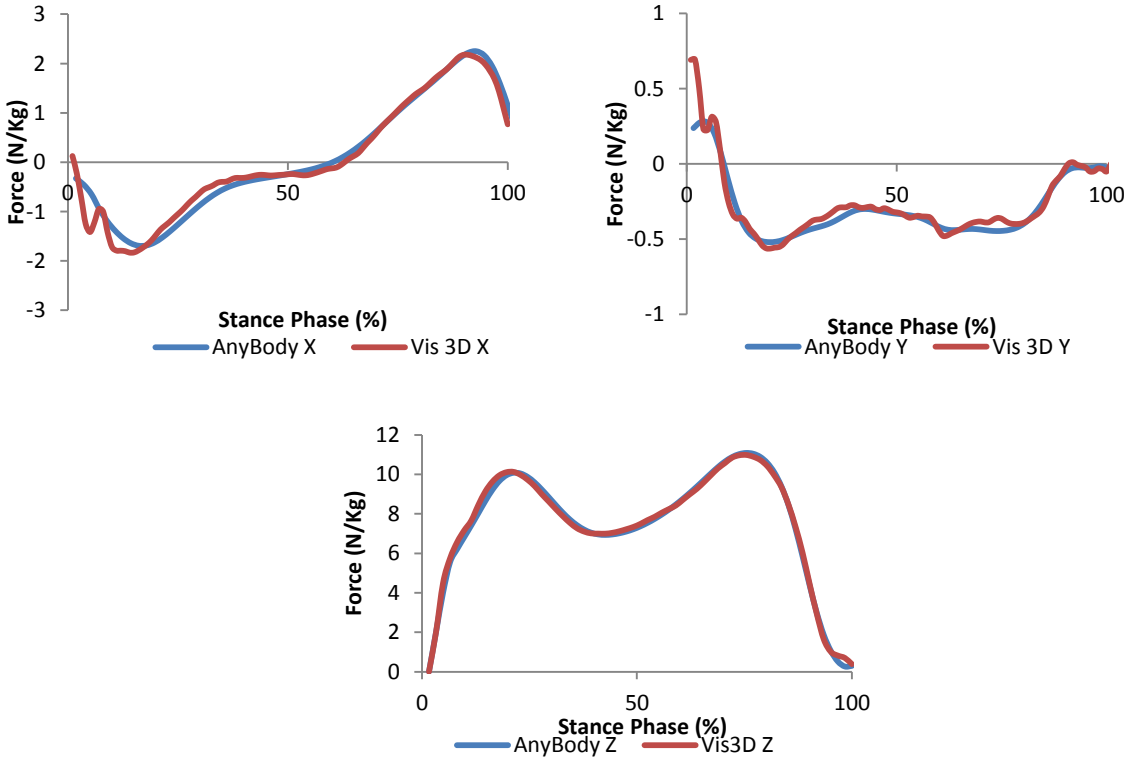

Figure 5.4 Comparison between the Vis3D (measured) and AnyBody (predicted) ground reaction forces in the X, Y and Z directions

5.3.3 EMG AND MUSCLE FORCE COMPARISON

The data presented shows measured EMG data for four muscles (bicep femoris, rectus femoris, gastrocnemius and tibialis anterior), EMG from 8 muscles collected by Hof *et al*, (2005) (four previously mentioned and also including; vastus lateralis, vastus medialis, gluteus maximus and gluteus medius) and the predicted AnyBody muscle data for the same 8 muscles (Figure 5.5 and Figure 5.6). Overall the results show good correlation between the three data sets. In the gastrocnemius a peak activity and muscle force of 1790N was observed at 40% and the EMG data showed values of 181.3µV in the collected data and 177.2µV from Hof *et al's* data. Tibialis anterior showed similar activity times however values differed between the collected and published work. Initial peak during loading response phase was 245.3µV and 33.9µV for Hof *et al's* data and collected EMG, respectively. The muscle forces correlated well with the peak forces being achieved at 1% and 98% of the gait cycle. The bicep femoris at 42% showed similar peaks between Hof *et al* data and muscle force data, the collected data showed no peak at this stage. At 94% all 3 data sets showed muscle activation. In the rectus

femoris collected EMG showed a much larger initial peak, 127µV, than that of the published work. The secondary peak, observed at 59%, were much closer matched with values of 109.0µV and 74.1µV for the collected data and Hof *et al's,* respectively. The muscle force data showed three peaks throughout the gait cycle correlating with the peaks in the EMG.

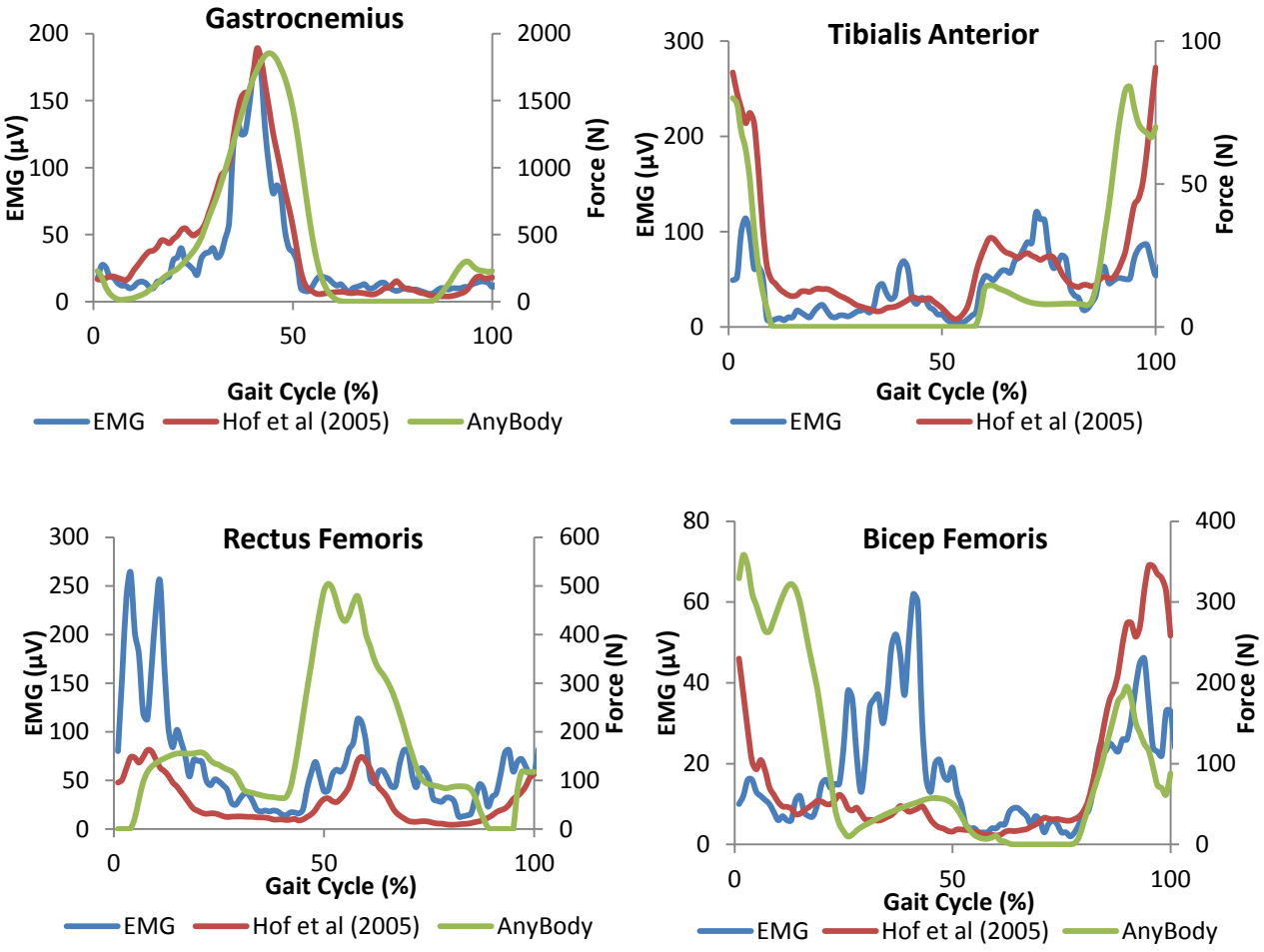

Figure 5.5 Collected EMG data (blue), EMG data from the literature (red) and predicted muscle force data for four muscles throughout 100% of the gait cycle.

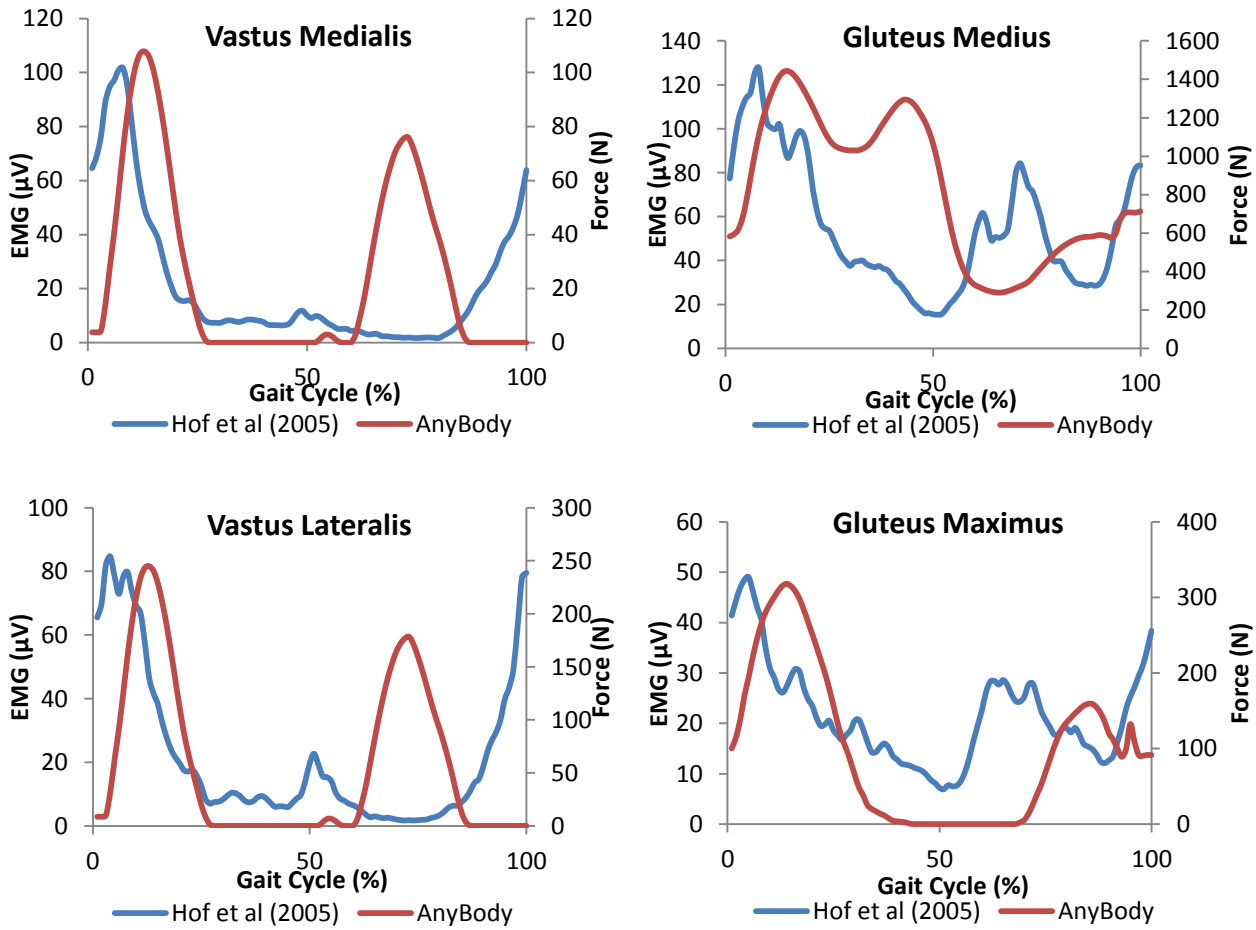

Figure 5.6 Reported EMG data (Hof *et al*, 2005) (blue) against 4 muscle forces collected from AnyBody (red) throughout 100% of the gait cycle.

5.3.4 EMG TO FORCE

A simple method was used to convert the EMG recordings during gait to muscle force data. EMG data was recorded during a maximal force test using an isokinetic dynometer (Chapter 5.2.3). This provided a maximal force (100%) and a maximal EMG reading from the tested muscle group. The EMG value recorded during gait was expressed as a percentage of the EMG activity produced during maximal force. Using the maximal force values to normalise the EMG a conversion to force was possible.

The AnyBody model in the rectus femoris had a maximum value of 490N at 51% of the gait cycle which was sustained, whereas in the EMG model of 49 N but only a brief spike was produced much earlier in the gait cycle at 4%. The bicep femoris EMG model at maximum value of 12N at 40% whereas the AnyBody model produced a much larger force of 358N at 2% of the gait cycle. The tibialis anterior showed a peak force of 80N (Figure 5.7) produced from the AnyBody model and a peak of 37N from the EMG model both at ~5% of the gait cycle. In the gastrocnemius the EMG model showed a peak of 98N and the AnyBody model produced a maximum force of 179N. The EMG model peaked at 40% of the gait cycle and the AnyBody model at 60%

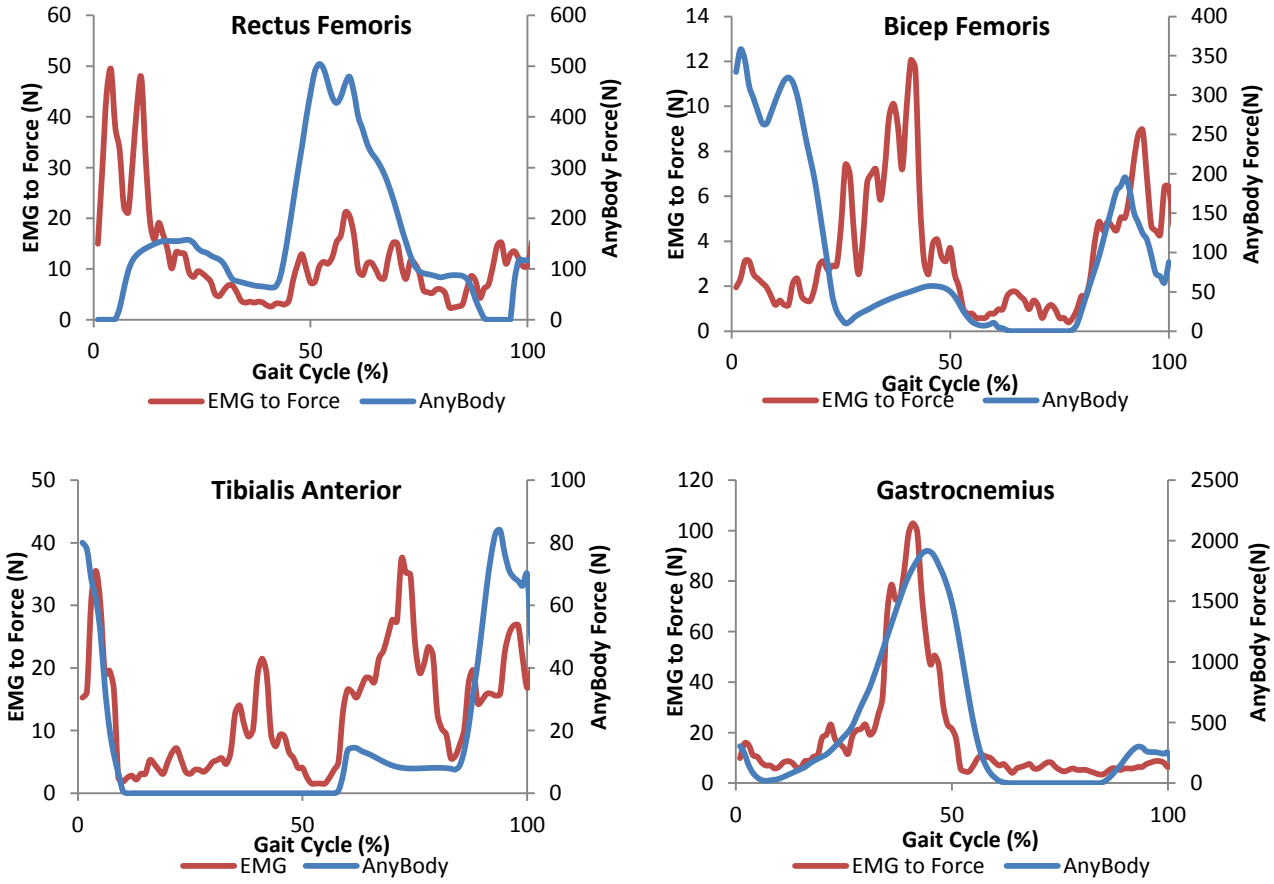

.

Figure 5.7 Showing four muscles for EMG to Force results (red) and muscle forces produced from AnyBody (blue) during 100% of the gait cycle.

5.4 DISCUSSION

The main aim of this chapter was to explore whether using musculoskeletal modelling is a reliable method to simulate human movement and if it is possible to attain reliable muscular forces for further use in FEA. The overall findings show that some comparison can be made between the motion capture and the musculoskeletal modelling software. The method used to validate muscle force against EMG was not a success and further methods need to be investigated. The results and the implications of these results are to be discussed.

5.4.1 KINEMATICS

Kinematic results revealed that AnyBody can produce accurate results in some instances when compared to Vis3D, which is a standardised method of analysing gait. Although the kinematics had different magnitudes, the times at which events such as peak angles coincided between the models. This indicates the muscles would be firing at the same time in each model just at a different intensity and thus the onset and offset of the EMG and muscle activity would not be different. This issue will need to be addressed when considering the muscle angles which can affect loading of the skeletal system.

5.4.2 KINETICS

GRF results were shown to be very similar between the two software's which is to be expected as the same C3d file was used in both. This C3d file contains the raw data collected from the force platforms, therefore any discrepancies seen between the two softwares will be a result from the filtering and interpolating methods used between the two methods. Therefore using AnyBody rather than Vis3D for motion capture analysis is accurate up to the point where Vis3D reaches its modelling capabilities. Which gives AnyBody software a good platform to perform the more advanced modelling of muscles.

5.4.3 EMG ONSET AND OFFSET

The EMG data obtained from the GCA normative database and from Hof *et al* (2005) were taken over a full gait cycle for 8 muscles, the descriptions of which were matched to the AnyBody data (Figure 5.1). As expected the results correlated well due to the

normative values of both data sets and therefore the EMG data can be compared to the muscle activity which is produced in the AnyBody model but was not collected during the present studies analysis. Although the muscle forces show a high correlation and similar peaks to the onset and offset levels of EMG it is hard to discuss the EMG data and the muscle activity with true reliability. This is due to the non-comparable units of measure, whilst EMG is presented in millivolts AnyBody cannot replicate this measurement and uses force or percentage activity. This limitation is common practice in research when discussing the reliability and values of EMG data. It is also possible that the delays observed between the muscle force peak and EMG peaks are due to the muscle force delay by 50ms to 200ms compared to EMG (Hof *et al*, 2002). The gastrocnemius showed a large force of 1970N, however this is within the range of an accepted maximum muscle force in an adult (Buchanan *et al*, 2004). Similarly, other muscle forces that were computed were safely within their ranges of maximal force.

5.4.4 EMG TO FORCE- ISOMETRIC TESTING

A number of methods have been employed to enable a relationship between EMG and muscle force these include EMG to Force relationship (Heintz *et al*, 2007) and comparisons of metabolic output (Bisi *et al*, 2011). The approach that was taken in this study was to use EMG data collected during a maximal muscle test and relate this to the force produced (Figure 5.7). Therefore a maximal EMG reading can be related to the percentage activity seen during gait and correlated with the muscle force data. These results provide an estimate of the force produced. However this technique has a number of limitations apart from the EMG collection. The inability to collect maximal strength from a singular muscle is a significant limitation, the strength data collected for what would be the rectus femoris would actually be an accumulation of all the knee extensors due to the protocol used in the maximal strength test.

The data presented demonstrates a degree of accuracy of the musculoskeletal model when compared to the EMG data on the four chosen muscles. These four muscles were chosen because of their extensive activity during gait. Because of the inability of EMG to produce data from eccentric muscle contraction and for only superficial muscle, then more extensive results would be difficult to obtain.

5.5 CONCLUSION

The errors between the results may be due to the inaccuracies in matching up the AnyBody markers with the C3d markers. This would affect the kinematics, creating a systematic error that would affect the moments, powers and muscles to a similar degree, as these are derived from the kinematics. Although because the GRF is correctly reported in AnyBody this will reduce any further error. This chapter can help to enhance the use of musculoskeletal models by showing some level of reliability. The EMG to force method may have been the reason why the results did not show extensive reliability, rather than AnyBody producing inaccurate muscle force data. As previously mentioned the use of musculoskeletal models can help with muscular data capture in those that it is difficult to collect EMG from, these demographics include the young, old and obese. Precaution may need to be taken when transferring the results to the young as scaling the models to a small model may cause problems, this will be the direction of future work using AnyBody.

6 MUSCULOSKELETAL MODELLING

6.1 INTRODUCTION

Following the reliability testing of the AnyBody musculoskeletal modelling software (Chapter 5) the results of the children's musculoskeletal modelling can be explored. Musculoskeletal modelling of children under the age of 6 years old (Carriero *et al*, 2009) has not been performed before, as far as the author is aware. The present study aims to analyse any differences observed between the variables that are not able to be compared through the sole use of motion capture software. The variables to be assessed include all 24 muscles that have insertion and origins in the proximal section of the femur and also the joint reaction forces (JRF) in the femoral head will be analysed. The results will be compared between each age group and then the adults will be compared to previous data in the literature. This will develop an understanding of differences in muscle forces and JRF's between age groups as gait matures. The muscle and joint reaction forces that are produced in this chapter will be applied to finite element models. Finally these results will be used to explain any strain distribution variations observed between models during FEA.

6.2 METHOD

6.2.1 PROTOCOL

The protocol for data collection and building the adult musculoskeletal model in AnyBody can be seen in Chapter 5. The same method that was used to build the adult model was used for the children's. The model was created by isotropically scaling a generic adult model, based on height, from the AnyBody modelling repository. The subjects for the children's musculoskeletal models were the same used in the gait analysis (Chapter 4), the ages for these subjects were 3-7 years old. A C3d file created through motion capture, containing marker positions and force plate data, was inputted to AnyBody. The children's data was collected in a different laboratory with different force plates it was necessary to make changes to represent this in the AnyBody software. Once this was performed the kinematic and inverse dynamic optimisations were able to be performed by the AnyBody software. Through this method, amongst other data, muscle forces, lines of action and joint reaction forces can be derived.

6.2.2 DATA ANALYSIS

All data was normalised to 100% of the gait cycle so that a comparison of the standardised gait cycle could be made to previous data and between subjects. The results provided from the AnyBody musculoskeletal modelling software were then exported into Microsoft Excel for analysis of muscle forces and joint kinematics. To test for significance of the kinematic data a One Way ANOVA was performed and a transformation log was applied so that the data was normally distributed. Significance was defined at a level of $p>0.05$.

6.3 RESULTS

To facilitate comparison to other studies, key events in the gait cycle were needed to be identified. Previous musculoskeletal modelling studies have used the double support phase of stance (45-60% gait cycle) however this gait data was not available for comparison (Duda 1997 and Speirs, *et al*, 2007). During this study a combination of two studies (Duda, 1997; Dalstra and Huiskes, 1995) were employed so that a full review of the key stages in the gait cycle can be explored. These stages were 2%, 10%, 30%, 45%, 52%, 63%, 70%, 85%, 98%, to coincide with key phases in the gait cycle; initial contact, double support, mid stance, toe off, pre swing, mid swing and end swing.

6.3.1 KINEMATIC RESULTS

The kinematic results showed a number of significant differences between different age groups at a level of $p<0.05$ (Table 6.1). At 2 % of the gait cycle, the 3 year old, compared to the other age groups, showed a higher value in hip rotation, knee flexion and extension, and in both ankle plantar flexion and ankle eversion at a significant level. At 10% of the gait cycle, significant differences were found in the 3 year old when compared to the 4 year old, 7 year old and adult in hip rotation. Also in ankle flexion for the 3 year old compared to the 5 year old. At 30% significant differences were found in the hip flexion and extension angles between the 3, 5, 6, and 7 year old. At 45% 3 year old hip abduction and adduction was seen to be significantly less than the other age groups. At 52% hip rotation was shown in the adult to be lower than the other ages at a significant level of $p>0.05$. This was also seen at 63% and 85% of the gait cycle. Also at 85% of the gait cycle the 3 year old had a significant lower hip flexion angle and a significantly higher plantar flexion angle. At 98% of the gait cycle significances were

found in the plantar flexion for the 3 year old and 5 year old and for the ankle eversion the adult showed significant differences.

	Joint Angle (°)	3 yrs.	4 yrs.	5 yrs.	6 yrs.	7 yrs.	Adult
2%	Hip Flex/Extension	32.76	33.90	33.81	34.54	34.09	36.67
	Hip Ab/Adduction	2.24	0.73	1.70	1.99	-0.17	-0.58
	Hip Rotation	-30.50*+	-17.16	-20.80*	-15.85	-17.32	-9.65*
	Knee Flex/Extension	10.73*+	10.42	9.39	9.96	6.54*	8.23
	Ankle Plant/ Dorsi	25.61*+	24.95	23.49*	22.15	17.07	14.47*
	Ankle Eversion	10.62*	12.78	9.62	6.64	13.80	26.62*
10%	Hip Flex/Extension	30.01	31.55	30.40	31.08	30.84	32.82
	Hip Ab/Adduction	-1.16	-1.46	-0.19	0.45	-0.80	-2.45
	Hip Rotation	-28.29*+	-7.49*	-13.98	-15.42	-8.08*	1.84*
	Knee Flex/Extension	17.30	16.72	14.58	14.50	10.49	10.59
	Ankle Plant/ Dorsi	23.93*+	22.45	20.70*	20.23	14.89	13.15*
	Ankle Eversion	5.52	-1.40	4.83	0.60	4.65	17.62
30%	Hip Flex/Extension	4.34*+a	5.22	5.55*ab	6.06	6.99	11.06*+ab
	Hip Ab/Adduction	-5.70	-6.13	-5.28	-4.90	-5.33	-6.41
	Hip Rotation	-27.89	-15.62	-14.15	-19.10	-15.69	-4.12
	Knee Flex/Extension	10.93*	9.65	11.12*	10.35*	8.57*+	10.86
	Ankle Plant/ Dorsi	29.56*	29.48	31.37	29.65	27.72	25.33*
	Ankle Eversion	2.18	-5.23*	-0.10	-2.44*	2.48	13.49*+
45%	Hip Flex/Extension	-11.64	-9.93	-9.90	-9.42	-8.70	-9.14
	Hip Ab/Adduction	-1.72*	-2.83	-2.32*	-1.37*	-0.72*	-0.10*+
	Hip Rotation	-32.54	-31.16	-20.89	-23.57	-24.14	-12.54
	Knee Flex/Extension	4.20	2.99	4.06	3.38	2.17	0.95
	Ankle Plant/ Dorsi	21.98	22.33	29.22	27.25	29.54	27.32
	Ankle Eversion	4.72	-0.49	-3.43*	0.03	2.65	13.40*
52%	Hip Flex/Extension	-14.61	-12.29	-12.07	-11.93	-11.84	-11.36
	Hip Ab/Adduction	2.64	0.75	0.86	1.21	1.64	3.19
	Hip Rotation	-36.10*	-39.04*	-24.55	-25.65	-28.02*	-11.67*+
	Knee Flex/Extension	9.61	11.09	12.21	10.96	8.86	8.79
	Ankle Plant/ Dorsi	15.30	13.62	21.51	19.26	22.13	20.20
	Ankle Eversion	6.05	2.11	-2.81*	0.00	3.84	12.88*
63%	Hip Flex/Extension	-4.19	0.39	1.72	1.18	0.97	1.06
	Hip Ab/Adduction	12.87	12.93	12.70	12.35	12.59	10.98
	Hip Rotation	-31.79*	-29.85*	-27.42*	-26.63*	-25.13*	6.03*+
	Knee Flex/Extension	37.97	43.82	45.88	43.83	42.60	38.88
	Ankle Plant/ Dorsi	5.67	4.10	5.26	2.62	-2.05	-7.04
	Ankle Eversion	7.31	5.21	0.64	0.92	6.52	11.11
70%	Hip Flex/Extension	8.85	13.73	15.74	15.15	15.38	15.96
	Hip Ab/Adduction	15.70	17.15	16.93	17.50	18.19	13.72
	Hip Rotation	-26.26	-20.23	-26.48	-26.63	-17.63	8.88
	Knee Flex/Extension	56.13	61.75	64.88	63.74	65.49	58.60

	Ankle Plant/ Dorsi	12.33	12.71	10.47	7.45	0.44	-6.40
	Ankle Eversion	5.18	1.45	1.34	0.30	2.66	7.68
85%	Hip Flex/Extension	32.87*+	36.16*	39.49*	41.17	43.41	46.07
	Hip Ab/Adduction	6.58	7.99	8.47	10.45	11.09	7.34
	Hip Rotation	-21.86	-12.19	-18.42	-21.31	-8.94	3.96
	Knee Flex/Extension	44.53	45.18	50.82	54.63	61.71	52.31
	Ankle Plant/ Dorsi	31.99*+	30.47*	27.61*	25.38	21.02*	17.67*
	Ankle Eversion	7.69*	-1.04	10.55*	2.01*	1.36	15.41*+
98%	Hip Flex/Extension	35.68	37.14	36.37	37.37	38.04	40.54
	Hip Ab/Adduction	-0.64	-1.41	-0.32	1.43	2.40	0.77
	Hip Rotation	-27.89	-15.82	-15.98	-17.78	-17.68	-16.84
	Knee Flex/Extension	6.07	6.14	8.83	11.18	11.46	9.65
	Ankle Plant/ Dorsi	23.33*+a	20.77*a	19.77	17.24*+b	16.93	12.50*ab
	Ankle Eversion	13.27*	8.14*	13.14*	5.77*	12.44*	31.86*

Table 6.1 Lower extremity kinematic results at the identified key stages of gait for six variables. A negative value represents extension, internal rotation, abduction and ankle plantar flexion and eversion. *denotes significance (<0.05), + denotes where the significance is to (a or b).

6.3.2 MUSCLE FORCES

Some significant differences in the muscle force were found in all age groups Table 6.2 to Table 6.10 explores these differences and at which stage of the gait cycle they were observed. Full data of the muscle forces can be seen in Appendix V.

2% (N/Kg)	3 yrs.	4 yrs.	5 yrs.	6 yrs.	7 yrs.	Adult
Gracilis	0.196*	0.610	0.289	0.223	0.316	0.000*

Table 6.2 Muscle forces for the different age groups at 2% of the gait cycle. *denotes significance (<0.05).

10% (N/Kg)	3 yrs.	4 yrs.	5 yrs.	6 yrs.	7 yrs.	Adult
Quadratus Femoris	0.115*	0.091	0.522*	0.116*	0.225	0.020*
Semimembranosus	3.535*	8.129	2.366	1.061*	0.531	0.000*

Table 6.3 Muscle forces for the different age groups at 10% of the gait cycle. *denotes significance (<0.05), + denotes where the significance is to.

30% (N/Kg)	3 yrs.	4 yrs.	5 yrs.	6 yrs.	7 yrs.	Adult
Quadratus Femoris	0.255*	0.000	0.195	0.112	0.110	0.000*
Gracilis	0.256*	0.177*	0.234	0.104	0.295	0.000*+
Gluteus Medius	3.970	5.252	5.922	3.744	6.445	16.943*
Bicep Femoris	1.077*a	3.385*+b	0.690*b	0.178*ab	0.216*b	0.319*b
Semimembranosus	0.981*+a	0.000*+b	0.011*ab	0.026*a	0.000*ab	0.000*ab

Table 6.4. Muscle forces for the different age groups at 30% of the gait cycle. *denotes significance (<0.05), + denotes where the significance is to (a or b).

45% (N/Kg)	3 yrs.	4 yrs.	5 yrs.	6 yrs.	7 yrs.	Adult
Rectus Femoris	1.597	0.000*+	1.778*	1.234*	1.595*	3.340*
Bicep Femoris	0.476	1.575*+a	0.316*a	0.375	0.157*+ab	0.752*b

Table 6.5 Muscle forces for the different age groups at 45% of the gait cycle. *denotes significance (<0.05), + denotes where the significance is to (a or b).

52% (N/Kg)	3 yrs.	4 yrs.	5 yrs.	6 yrs.	7 yrs.	Adult
Gracilis	0.534*	0.088*	0.511*	0.614*	0.485*	0.030*+
Iliacus	1.893	0.538*+	2.160	2.637*	2.314	2.749*
Psoas Major	0.831*	2.756	2.240	2.210*	3.168	8.136*+

Table 6.6. Muscle forces for the different age groups at 52% of the gait cycle. *denotes significance (<0.05), + denotes where the significance is to.

63% (N/Kg)	3 yrs.	4 yrs.	5 yrs.	6 yrs.	7 yrs.	Adult
Vastus Lateralis	0.239	0.891	0.000*	0.008	0.001	0.630*
Vastus Medialis	0.109	0.404*	0.000*+	0.003	0.000	0.289*
Gracilis	0.612*ab	0.002*+a	0.566*ab	0.378*ab	0.407*ab	0.000*+ba
Iliacus	1.929*	0.062*+	2.169*	1.659*	1.902*	1.242*
Satorius	2.001*	0.000*+	2.561*	1.555*	1.836*	1.345*

Table 6.7. Muscle forces for the different age groups at 63% of the gait cycle. *denotes significance (<0.05), + denotes where the significance is to (a or b).

70% (N/Kg)	3 yrs.	4 yrs.	5 yrs.	6 yrs.	7 yrs.	Adult
Pectineus	0.1571*	0.0000	0.1928*	0.2264*	0.1975*	0.0000*+
Adductor Brevis	0.1774*	0.0000	0.2338	0.3249	0.2197	0.0000*
Adductor Longus	0.5586*	0.0000	0.6144	0.8171	0.5966	0.0000*
Gracilis	0.1125*	0.0000	0.1651	0.2284	0.1357	0.0000*

Table 6.8 Muscle forces for the different age groups at 70% of the gait cycle. *denotes significance (<0.05), + denotes where the significance is to.

85% (N/Kg)	3 yrs.	4 yrs.	5 yrs.	6 yrs.	7 yrs.	Adult
Semimembranosus	1.074*	0.000	0.265	0.108	0.144	0.000*
Psoas Major	0.378	0.000*+	0.345*	0.532*	1.289*	5.634*

Table 6.9 Muscle forces for the different age groups at 85% of the gait cycle *denotes significance (<0.05), + denotes where the significance is to.

98% (N/Kg)	3 yrs.	4 yrs.	5 yrs.	6 yrs.	7 yrs.	Adult
Semimembranosus	1.134*	0.000	0.407	0.604	0.526	0.000*

Table 6.10 Muscle forces for the different age groups at 98% of the gait cycle. *denotes significance (<0.05), + denotes where the significance is to.

Table 6.2 to Table 6.10 show muscle forces (N/kg) for the muscles found to be significant at the following times during the gait cycle, 2%, 10%, 30%, 45%, 52%, 63%, 70%, 85%, 98%. Significant values were defined at a value of p>0.05.

Figure 6.1 to Figure 6.3 explore the muscle forces that were found to be significant for all ages over 100% of the gait cycle, comparisons between all ages will be made in the discussion. The differences in the 3 year old data were identified at 2% in the gracilis, 10% in the quadratus femoris and semimembranosus, 30% the quadratus femoris, semimembranosus and bicep femoris. At 70% the adductor brevis, adductor longus and the gracilis, at 85% and 98% the semimembranosus were all identified as having significant differences. At 30% the 4 year old showed significances in the bicep femoris and semimembranosus, whilst the rectus femoris was significant at 45% and the iliacus at 52%. The vastus medialis, gracilis, iliacus and satorius were significant at 63% and at 85% the psoas major showed significance. The 5 year old showed significance at 63% in the vastus medialis and no significance was found in the 6 year old. The 7 year old showed significance at 45% of the gait cycle in the bicep femoris. In the adult the following significances were found at 10% in the quadratus femoris, at 30% in the gracilis and gluteus medius. At 52% the gracilis and psoas major showed significances and the vastus lateralis, gracilis and the bicep femoris at 63% and at 70% the pectineus showed significance at a level of $p<0.05$. The gluteus medius muscle force was highest in the adult, with peaks occurring during the start of single stance phase and at 47% in preparation for swing phase, the lowest force was observed in the 3 and 4 years old. Gluteus minimus had two peaks of activity, the highest force in the adult and 7 year old was at the second peak (45% of the gait cycle). The initial peak (15%) was highest in the 3 year old. Average hip abductor force showed peaks were of varied values but the

shape was similar (peaks at 15% and 45% of gait cycle) except for the 3 year old where only one peak was observed followed by a plateau.

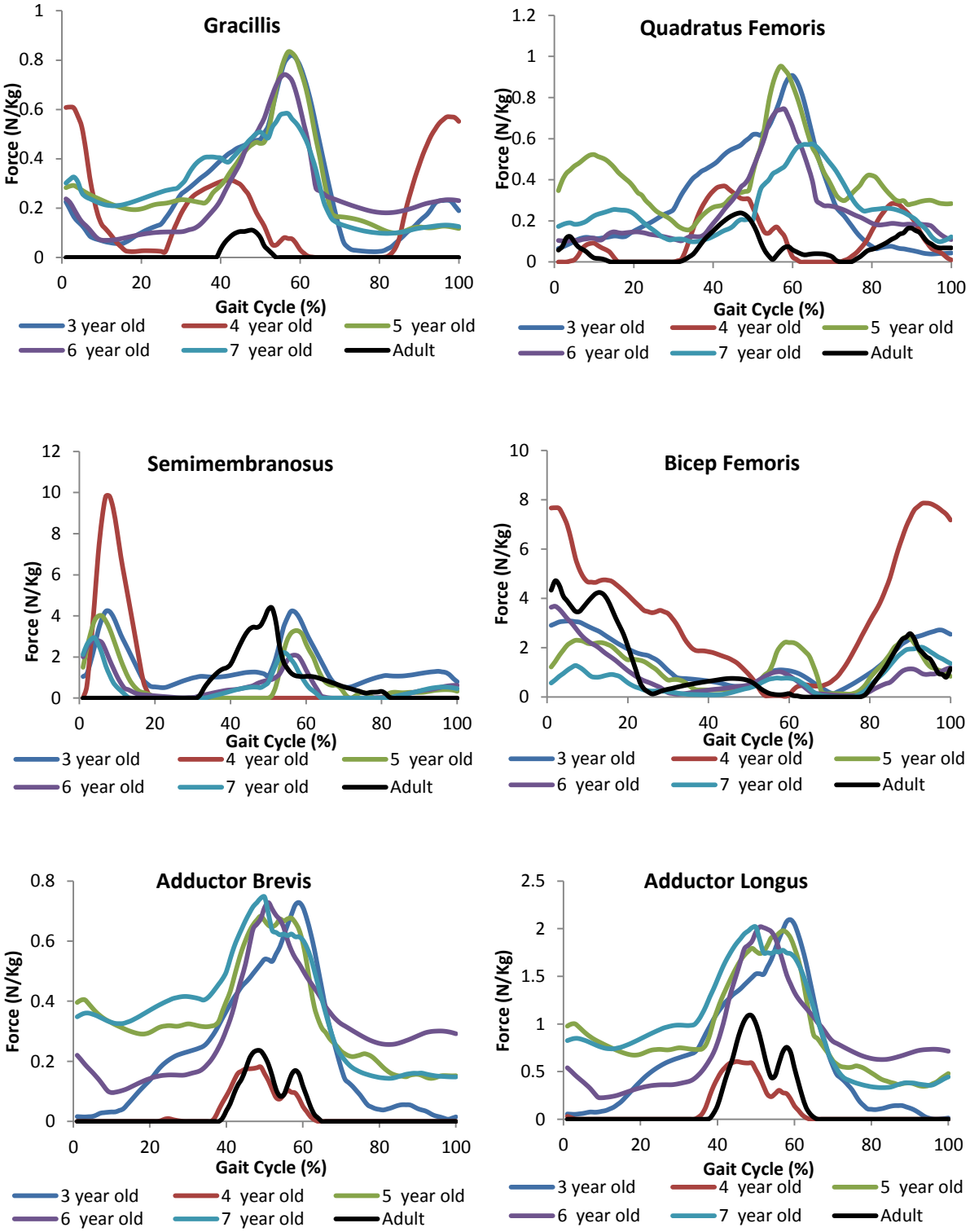

Figure 6.1 Muscle activity normalised to body weight for all ages during 100% gait cycle for children and adult.

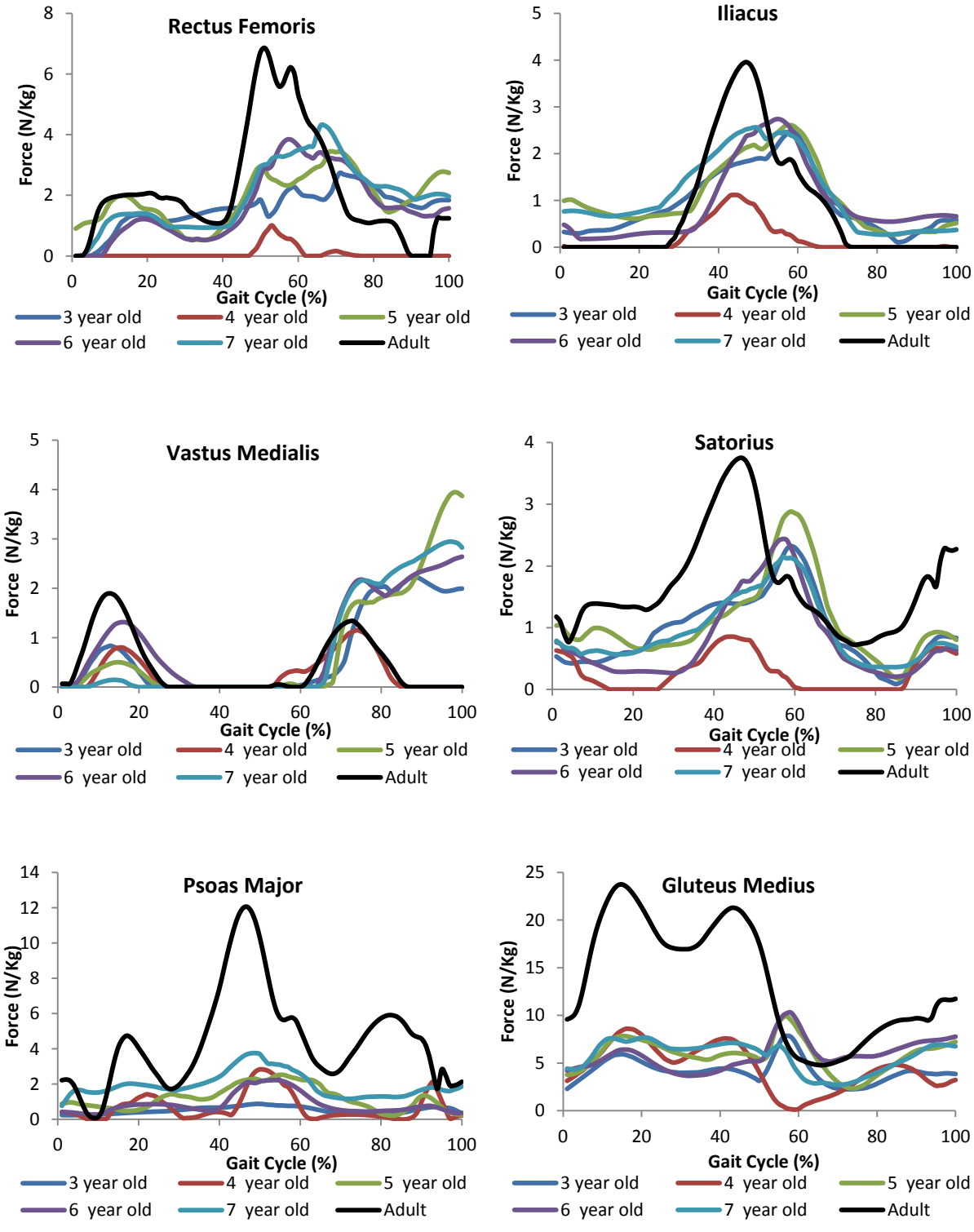

Figure 6.2 Muscle activity normalised to body weight for all ages during 100% gait cycle for children and adult.

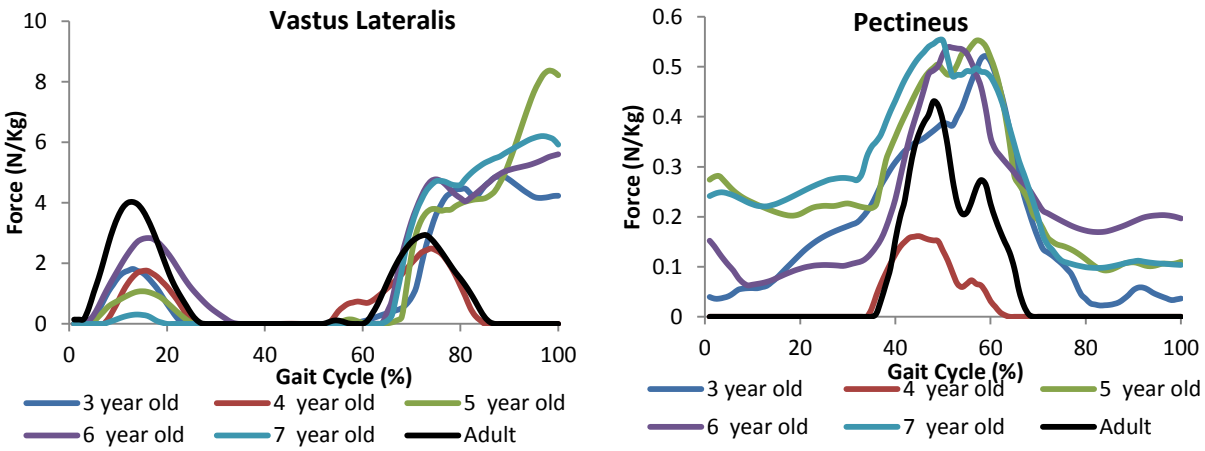

Figure 6.3 Muscle activity normalised to body weight for all ages during 100% gait cycle for children and adult.

6.3.3 JOINT REACTION FORCE

Other than muscle force data AnyBody can calculate JRF which cannot be directly obtained from motion capture. The results for the hip joint were analysed in three directions, for 100% of the gait cycle.

	3 yrs.	4 yrs.	5 yrs.	6 yrs.	7 yrs.	Adult
RhZ (N)	594	644	1266	514	1299	1938
RhY (N)	-300	-253	-716	-102	-705	-343
RhX (N)	-163	-167	-377	-106	-460	-203
Rh (N)	685	712	1503	534	1548	1979
Rh (% Body Weight)	537	412	613	294	480	265

Table 6.11 Resulting forces at the femoral head for the five age groups and adults. RhZ shows the force in the proximal distal direction, RhY shows the force in anterior posterior direction, RhX shows the force in the mediolateral direction. Rh shows the total resultant hip force.

Resulting forces from the hip during single leg stance (20% of gait cycle) are shown in Table 6.11. As expected the adult has the highest resultant force at the hip with values of 1979N with the 7 year old showing the second highest with a value of 1548 N.

6.4 DISCUSSION

The primary goal of musculoskeletal modelling of the adults and children's gait was to produce muscle loads for use in finite element analysis on the femora of the relevant age group (Chapter 7). However the results need to be discussed so that it is possible to identify any differences in the muscle activity and joint contact forces between the ages.

6.4.1 KINEMATIC DATA

Kinematic data from the children's motion analysis has been discussed extensively Chapter 4 and it was shown that the AnyBody modelling system could successfully replicate motion capture data in Chapter 5. Therefore the kinematic data does not need to be discussed in great detail again. However the gait kinematics which the muscle forces are derived from can help to inform and explain any changes in the muscle forces. Therefore the kinematic data represented here (Table 6.1) will be discussed in relation to muscle forces produced.

6.4.2 MUSCLE VS ANGLES

Muscle activity can be expected to occur at the same time as an action is performed, for example, when peak knee flexion is produced it would be expected that there would be an activation of the bicep femoris, this being the muscle associated with this movement. The grouping of the muscles in this study was chosen to represent the muscles that produce hip flexion/extension, abduction/adduction, internal/external rotation and knee flexion/extension. The predicted muscle activity showed good agreement with the measured angles by producing a force prior to when the movement reaches peak angle in the adult data, as shown in Figure 6.4 to Figure 6.7. During knee extension muscle forces of the vastus medialis, vastus intermedius and the vastus lateralis show prominent muscle forces. Although the rectus femoris is a large contributor to knee extension it does not show a force as distinguishably responsible for this action. This is due to the rectus femoris also being a contributor to hip flexion, which is coincident to knee extension during gait and therefore the rectus femoris is multifactorial helping to perform two different actions simultaneously. This is not just seen in the rectus femoris with hip and knee flexion. It can also help to explain any discrepancies seen within the results in relation to the kinematic angles. Due to a secondary role that the muscle plays, or even a tertiary role which is seen in the semimembranosus as a knee flexor, hip extensor and internal rotator. A number of muscles have been observed to be responsible for multiple movements in this study. It is necessary to further explore this, the movements involved in gait need to be broken down so that it is possible to see

which movements occur simultaneously and therefore explain the simultaneous contraction of some muscles (Table 6.12).

Gait Cycle	Hip Flex/Ext	Muscles	Hip Rotation	Muscles	Knee Flex/Ext	Muscles
10%	Flexion	Rectus Femoris			Extension	Rectus Femoris
70%	Flexion	Satorius, Semimem	Internal rotation	Semimembranosus	Flexion	Semimembranosus, Satorius

Table 6.12 Muscles performing simultaneous actions during the gait cycle at the key stages selected.

As can be seen from the muscles that correlate to key movements in the hip and knee there is multiple interactions. Although the muscles will be activated for longer than when the angle is at its peak it is still possible to see that the activity of the muscle is related to generating the movement (Figure 6.4 to Figure 6.7). Muscles also play a large stabilizing role during gait which would also provide a discrepancy when isolating the muscles for one particular motion. The gluteus medius secondary function is to act as a stabilising muscle for the hip (Gray, 1858) therefore the muscle may be active but would not be correlated with any movement. Conversely movement that occurs at the joint are not always necessarily the result of muscle contractions. For example the flexion of the knee is not always performed by the knee flexors but can be created by momentum after toe off, therefore the muscle would play a controlling role rather than that of a contracting role. This would have great effect on the loading of the bone which would need to be explored. The values in the bicep femoris may have a lower than expected muscle force because AnyBody as a musculoskeletal modelling system only produces forces from concentric contractions and therefore the eccentric action of the bicep femoris before heel strike would not be represented as active in the musculoskeletal model.

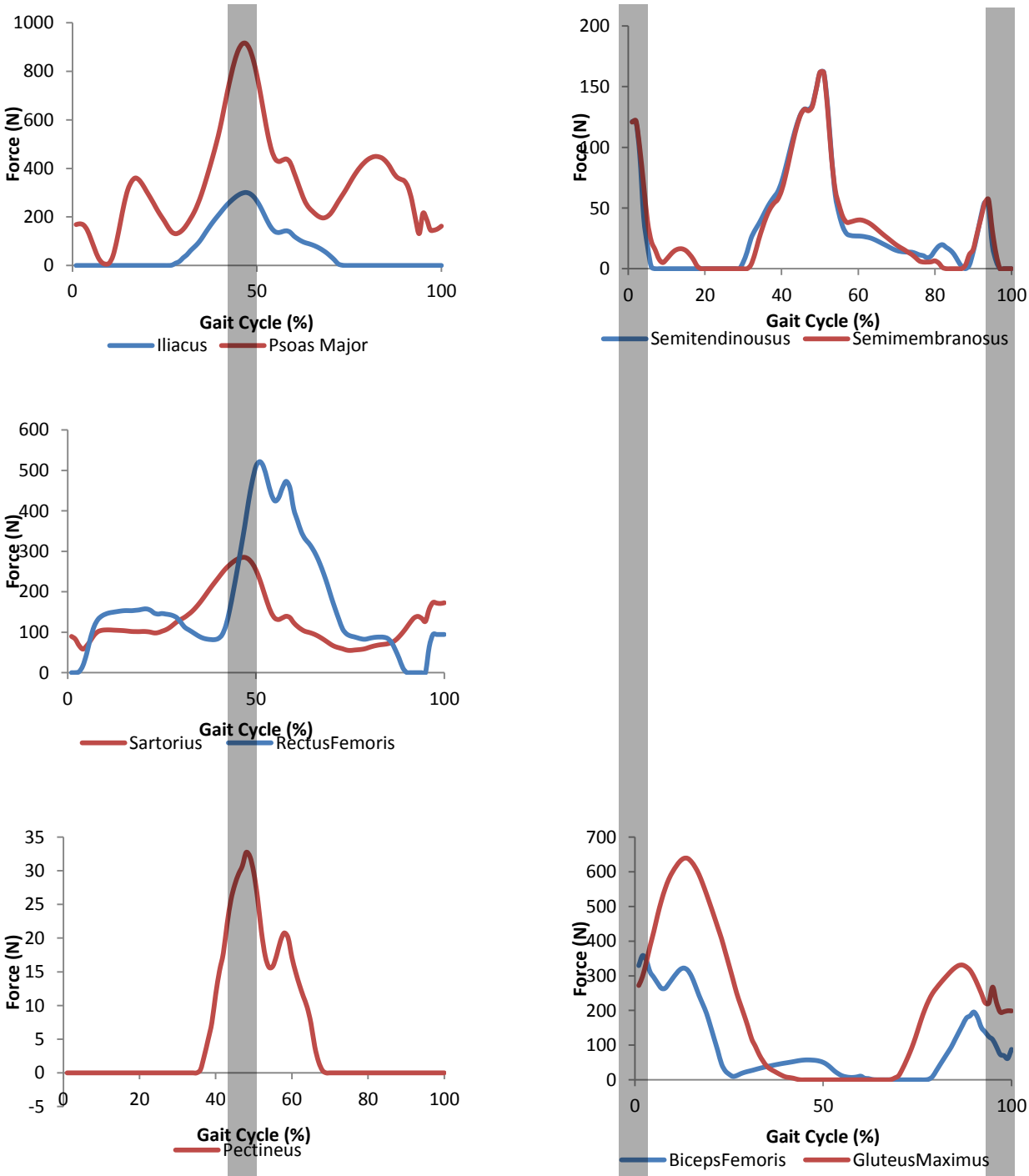

Figure 6.4 Hip Flexor and extensor muscles correlating to changes in joint angles of the adult subject. Grey area highlighting areas of peak angles.

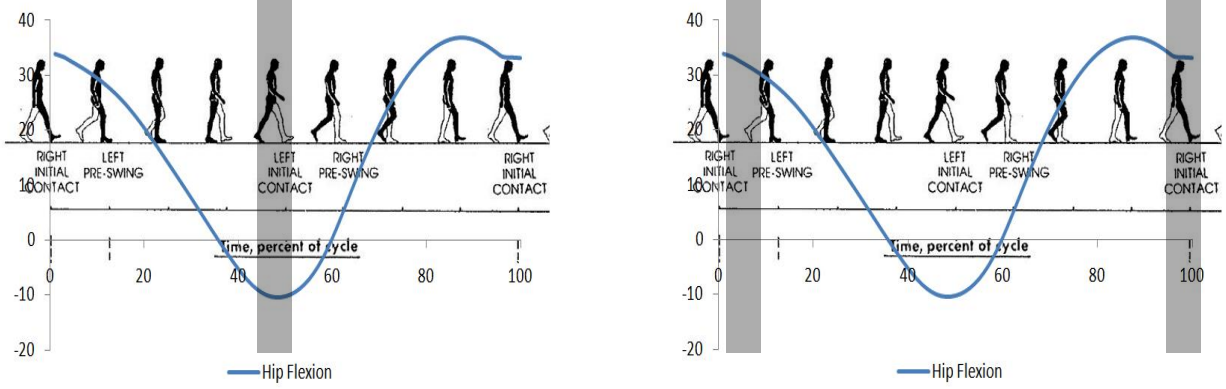

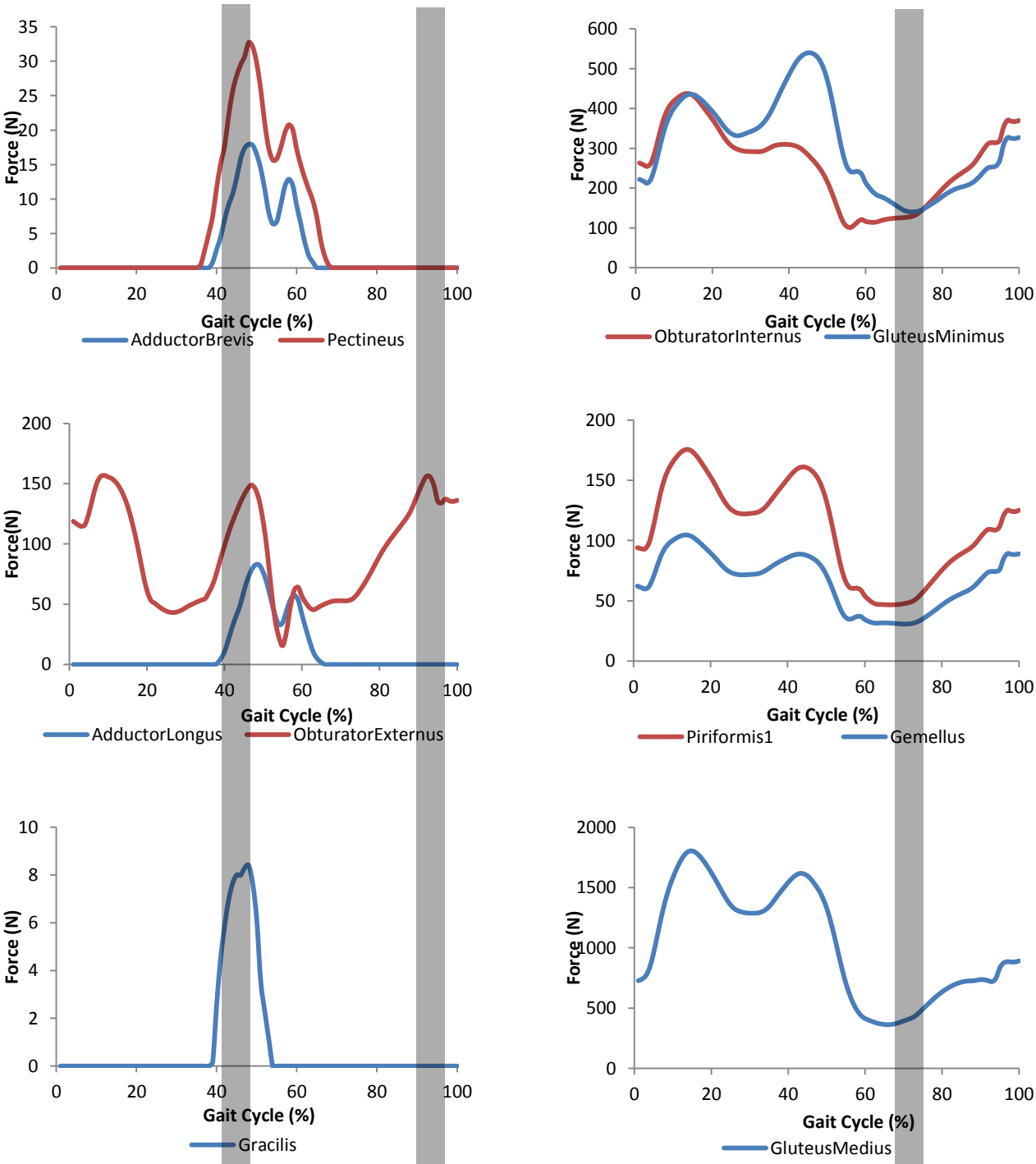

Figure 6.5 Hip adductor and abductor muscles correlating to changes in joint angles of the adult subject. Grey area highlighting areas of peak angles.

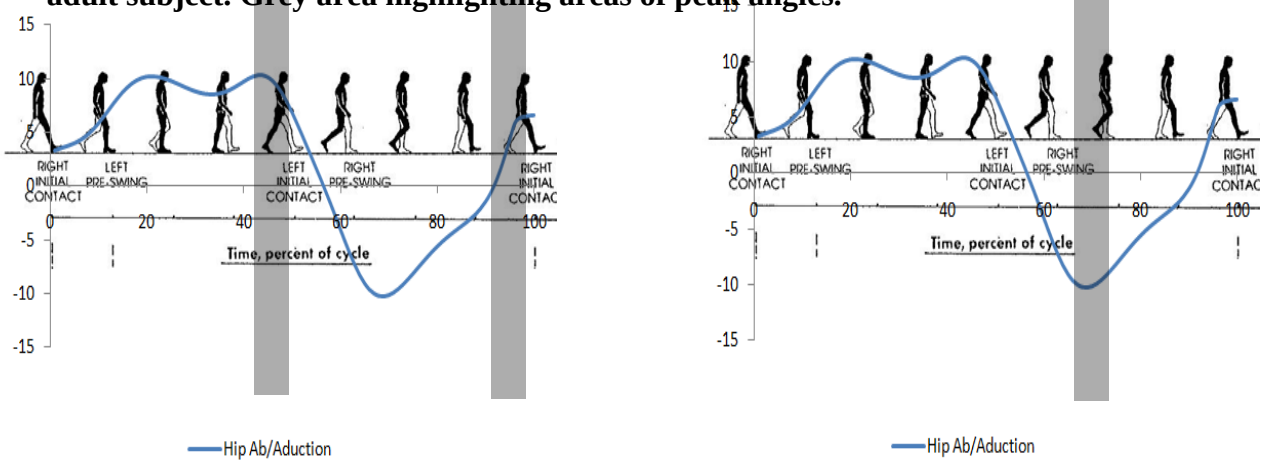

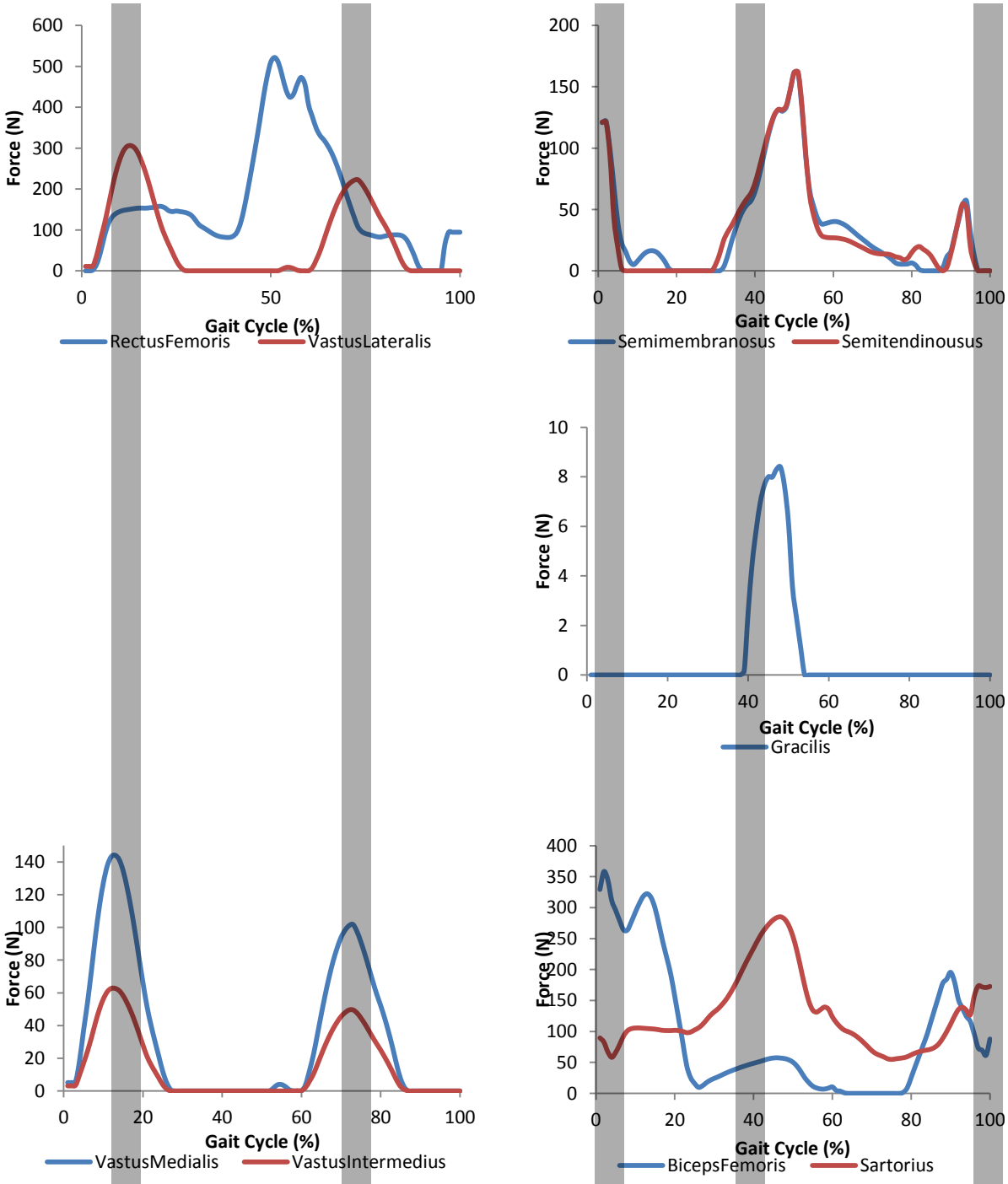

Figure 6.6 Knee flexor and extensor muscles correlating to changes in joint angles of the adult subject. Grey area highlighting areas of peak angles.

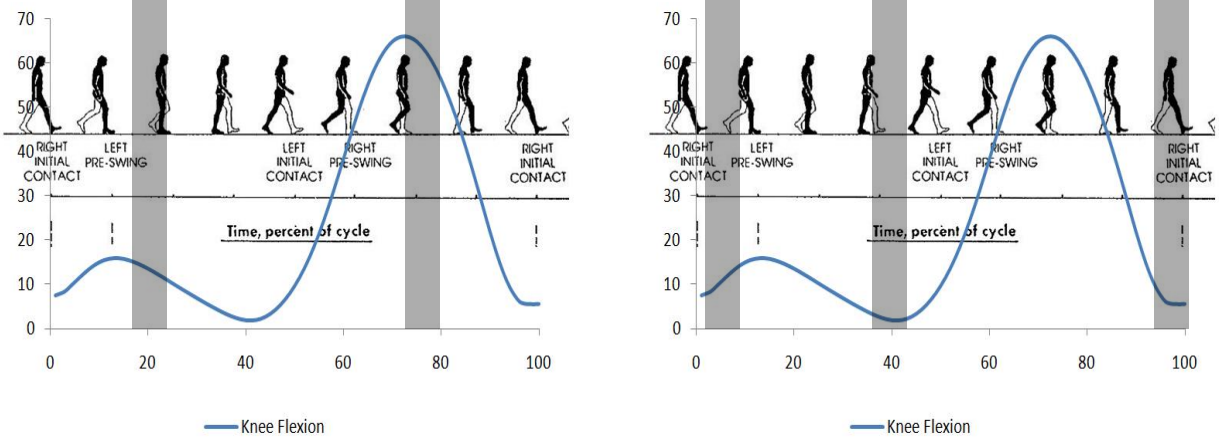

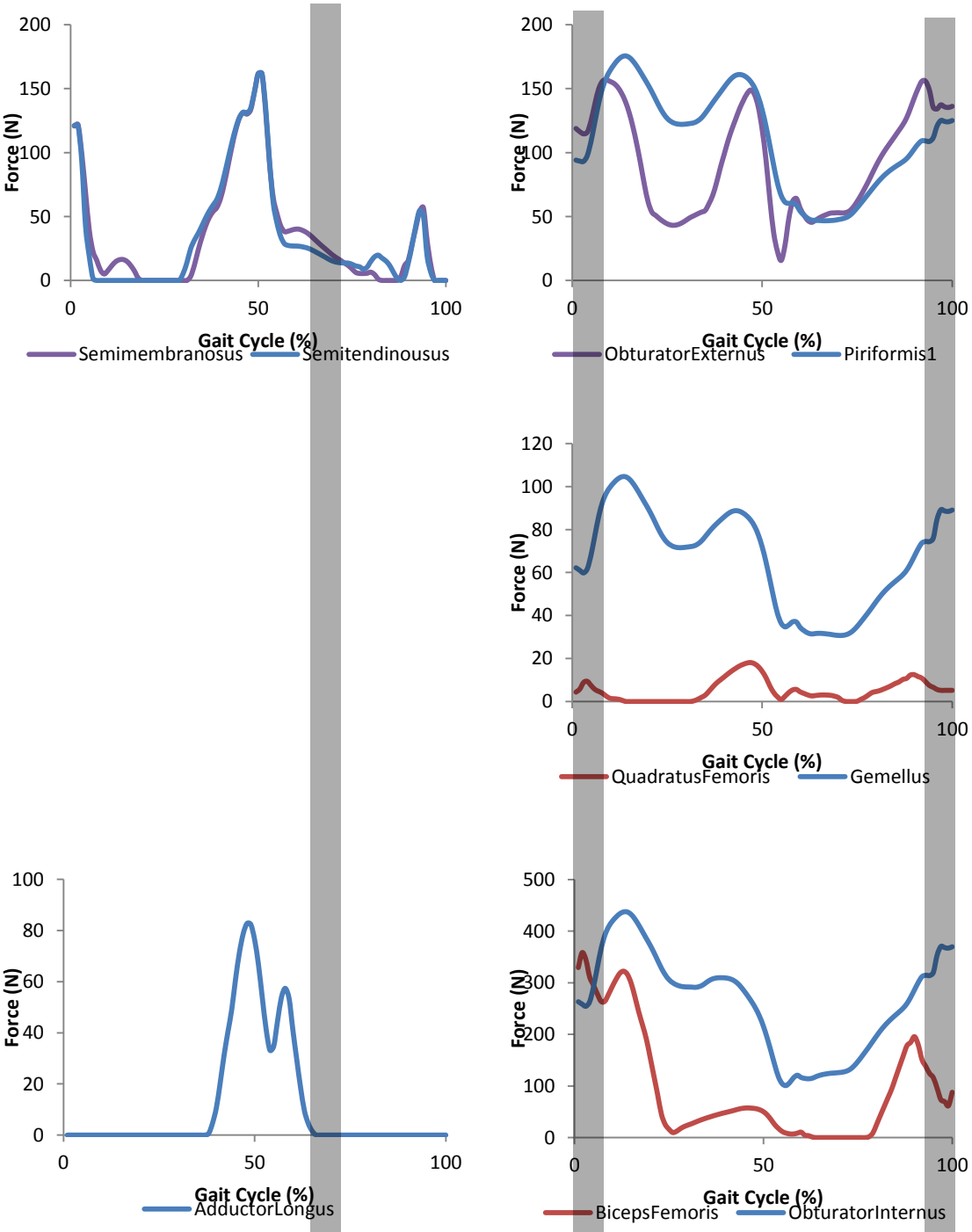

Figure 6.7 Hip internal and external muscles compared to joint angles of the adult subject.. Grey area highlighting areas of peak angles.

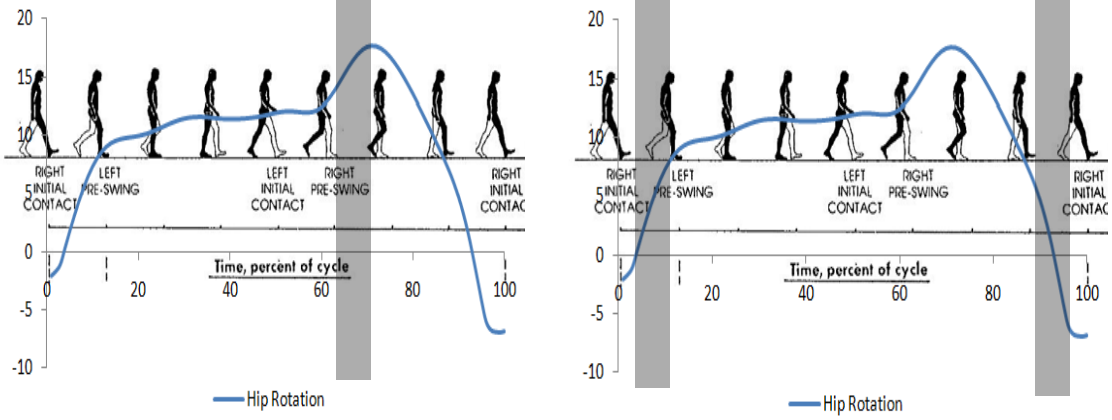

6.4.3 COMPARISON OF PREDICTED MUSCLE FORCES WITH THE LITERATURE

Muscle forces produced by the AnyBody musculoskeletal modelling system can be compared against other musculoskeletal modelling data. Phillips (2009) compared their data produced for linear and non-linear muscle optimisations against Heller *et al's* (2001) data. For the purpose of this study the same comparison was made between the present results, Heller *et al* (2001) and the linear free boundary condition model of Phillips (2009), however all the data was normalised to bodyweight. From the adult muscle forces, as a general observation the results, were higher than the forces seen in both the Phillips et al and the Heller *et al* studies, albeit within an acceptable range. At 20% of the gait cycle the adult in the current study showed a value of 2.07N/kg compared to 1.81N/kg in Heller *et al's* work (Table 6.13) and in the 3 year old a value of 1.31N/kg, showing similar values independent of age in these particular muscles. The differences found could be attributed to the variations in the point in the gait cycle at which the data was analysed as the exact timing of the gait cycle was not reported in these papers, but only at the peak hip contact (approximately 20% of the gait cycle according the findings of the present study). Inter subject variability in movement patterns could lead to mistiming of muscle activity between subjects.

20%	Heller	Phillips	3 yrs.	4 yrs.	5 yrs.	6 yrs.	7 yrs.	Adult
Abductors			6.74	9.28	9.16	7.06	9.42	26.53
	10.14	11.62	(-3.4)	(-0.86)	(-0.98)	(-3.08)	(-0.72)	(+16.39)
Bicep			1.95	4.15	1.51	1.07	0.58	2.06
Femoris	0.00	2.26	(-0.31)	(+1.89)	(-0.75)	(-1.19)	(-1.68)	(-0.2)
Iliopsoas			1.00	1.24	1.16	1.13	2.74	4.05
	0.00	0.64	(+0.36)	(+0.6)	(+0.52)	(+0.49)	(+2.1)	(+3.41)
Piriforms			0.43	0.41	0.78	0.47	0.65	2.01
	0.00	0.49	(-0.06)	(-0.08)	(+0.29)	(-0.02)	(+0.16)	(+1.52)
Vastus			0.66	1.23	0.71	2.37	0.00	1.84
Lateralis	0.95	0.00	(-0.29)	(+0.28)	(-0.24)	(+1.42)	(-0.95)	(+0.89)
Vastus			0.31	0.56	0.33	1.10	0.00	0.87
Medialis	2.01	0.00	(-1.7)	(-1.45)	(-1.68)	(-0.91)	(-2.01)	(-1.14)
Rectus			1.31	0.00	1.54	1.20	1.39	2.07
Femoris	1.81	0.00	(-0.5)	(-1.81)	(-0.27)	(-0.61)	(-0.42)	(+0.26)

Table 6.13 Comparison of muscle forces predicted by the current study, Heller *et al,* (2001) and Phillips (2009). Heller and Phillips results divided by body weight of 85Kg and 102kg respectively.

Further comparison can be made between Polgar *et al* (2003b) (Table 6.14) and Jonkers (2008) (Table 6.15) their muscle forces were provided for 10%, 15% respectively.

10%	Polgar	3 yrs.	4 yrs.	5 yrs.	6 yrs.	7 yrs.	Adult
Piriforms	0.10	0.47 (+0.37)	0.52 (+0.42)	0.75 (+0.65)	0.51 (+0.41)	0.69 (+0.59)	2.09 (+1.99)
Obturator Internus	0.10	1.39 (+1.29)	1.28 (+1.28)	2.11 (+2.01)	1.23 (+1.77)	1.77 (+1.67)	5.51 (+5.41)
Quadratus Femoris	0.07	0.12 (+0.05)	0.09 (+0.09)	0.52 (+0.45)	0.12 (+0.05)	0.22 (+0.15)	0.02 (-0.05)
Vastus Medialis	0.40	0.71 (+0.31)	0.34 (-0.06)	0.36 (-0.04)	0.84 (+0.44)	0.08 (-0.32)	1.67 (+1.27)
Bicep Femoris	0.07	2.88 (+2.81)	4.68 (+4.61)	2.18 (+2.11)	2.29 (+2.22)	0.95 (+0.88)	3.85 (+3.78)
Gluteus Maximus	0.33	2.96 (+2.63)	4.12 (+3.79)	3.20 (+2.87)	2.71 (+2.38)	2.61 (+2.28)	7.90 (+7.57)

Table 6.14 Muscle force (N/kg) compared to Polgar *et al,* (2003b).

15%	Jonkers	3 yrs.	4 yrs.	5 yrs.	6 yrs.	7 yrs.	Adult
Iliacus	3.09	0.43 (-2.66)	0.00 (-3.09)	0.65 (-2.44)	0.22 (-2.87)	0.68 (-2.41)	0.00 (-3.09)
Psoas	1.71	0.34 (-1.37)	0.73 (-0.98)	0.54 (-1.17)	0.68 (-1.03)	1.89 (+0.18)	4.11 (+2.4)
Quadratus Femoris	0.18	0.13 (-0.05)	0.02 (-0.16)	0.46 (+0.28)	0.15 (-0.03)	0.26 (+0.08)	0.00 (-0.18)
Piriforms	4.03	0.60 (-3.43)	0.65 (-3.38)	0.89 (-3.14)	0.57 (-3.46)	0.67 (-3.36)	2.30 (-1.73)
Gluteus Maximus	7.21	2.73 (-4.48)	5.05 (-2.16)	3.52 (-3.69)	2.90 (-4.31)	2.52 (-4.69)	8.27 (+1.06)
Gluteus Minimus	14.55	1.69 (-12.86)	1.32 (-13.23)	1.88 (-12.67)	1.40 (-13.15)	1.69 (-12.86)	5.73 (-8.82)
Gluteus Medius	0.96	5.87 (+4.91)	8.16 (+7.2)	7.76 (+6.6)	6.32 (+5.36)	7.46 (+6.5)	23.67 (+22.71)

Table 6.15 Comparisons of muscle forces (N/kg) to that observed by Jonkers *et al* (2008). These gait percentages were used as they are at a peak hip contact force.

The results of comparisons between Jonkers *et al,* (2008) and Polgar *et al*, (2003b) and the present results show some similar values between this model and the musculoskeletal models produced in their studies. Large differences were also observed, most notably in the gluteus medius a difference of 22.71N/kg was seen at 15% of the

gait cycle. The difference here may be the early contraction of the gluteus medius in preparation for single support phase in the current model as shown in Table 6.15. Also in the gluteus minimus a reduced force was produced in the present model which may indicate that as the minimus and medius perform similar movements, in the optimisation there is an increased reliance on the medius rather than the minimus. Between the current work and Polgar *et al,* (2003b) some big differences were observed. In general the current models muscle forces were much higher, for example the gluteus maximus force was over 20 times greater. However, Polgar *et al's* model was based on an older mathematical model produced by Brand *et al,* (1986) which may not be as complex as the AnyBody model and therefore this maybe the cause of the large discrepancies. This would also explain why the current results are closer to previous research, both the Heller and Phillips models, which are of a similar complexity. Jonkers *et al's* (2008) work used a muscle minimising algorithm for the optimisation, which may have produced different muscle activities. These may have caused the discrepancies between the results, however all of the data from the present study are within the maximal muscle force values (Horsman *et al,* 2005).

6.4.4 CHILDREN'S MUSCULOSKELETAL MODELLING

The main aim of this chapter in the thesis was to assess the changes that occur in the muscle activity and force between the ages of 3-7 years, with the aim of applying them to the FE models. The gait data was assessed at key stages during the gait cycle as identified in previous studies (Duda, 1997; Dalstra and Huiskes, 1995). Musculoskeletal modelling of the children's gait showed some significant differences between the age groups in both the kinematics and muscle forces. No previous studies have built musculoskeletal models of children and therefore comparison of these results will be made with adult data. Previous work has suggested what may occur in the muscle patterns of children during gait (Oeffinger *et al,* 1997) and therefore the results will be discussed in relation to this.

The 3 year old kinematic data showed the most significant data points, with 60% of the significance being found at this age. The data also showed significant kinematics values during early and late stages of the gait cycle, compared to other age groups. This would have affected the muscle values of the hip irrespective of whether the hip kinematics were significantly different due to the inverse dynamic procedure used to derive the

muscle forces. In reality it would be incorrect to assume that exactly the same relationship is formed. However changes in the kinematics of the ankle can lead to changes in muscular activity further up the kinematic chain. During ground clearance, for example, with a smaller dorsi flexion angle an increased hip angle could be adopted to stop dragging of the foot during gait. Therefore this would change the muscular activity at the hip due to a change at the ankle. The reliability of the children's muscle data cannot be compared to other literature as this is the first of its kind that has been produced. The muscle force data shown in Figure 6.1 to Figure 6.3 found that between all age groups similar muscle force activities are present. This is unsurprising due to the similarities in the kinematics and GRF. However there are a number of significant differences.

The patterns of the muscle forces show large similarities with reference to their activity and muscle forces produced when normalised to BW. As an overall trend the hip flexors, abductors, and external rotators are much larger in the adult models. The psoas major showed a value of 12N/kg at 50% of the gait cycle whereas the next highest force produced was by the 7 year old with a force not exceeding 3N/kg. Compared to the 3 year old where a value of 0.9N/Kg was produced. Along with the observed changes in hip kinematics at 45% of the gait cycle, where the 3 year old has a much larger rotation and flexion angle. An explanation of the reduced force is possible; the gait pattern of the 3 year old did not require more hip flexion at the stage when the adult model did. Therefore the reason for a the lower force is perhaps that the 3 year did not require more movement in this joint therefore a large force by the psoas major was not required. Also considering the uni-modal activity in the gluteal muscles for the 3 year old, it is possible to surmise that this difference is due to a supporting/stability role played by the abductor muscles at this age (Hallemans *et al*, 2005), rather than a larger role in movement producing force as is seen in older age groups.

In the present study the semimembranosus was shown as highly significant muscle for the 3 year old, whose action extends the hip and flexes the knee. This increased force in the muscle when compared to the other ages can be explained by a greater reliance on the hip muscle during the push off phase of gait. This was suggested by Oeffinger *et al* (1997) as a possible change due to the lack of neuromuscular maturity in the plantar flexors to generate sufficient force at this stage in gait. Further findings in the present study show there was a significant difference seen in the 3 year old models hip adductors at 70% of the gait cycle which coincides with peak abduction of the hip

which is higher than the other age groups. The increased abduction in the 3 year old maybe as a result of the larger neck shaft angle (NSA) compared to the other age groups (Scheuer and Black, 2005), which has been reported to affect muscle activity (Scheys *et al*, 2011), however it is not possible to model NSA change in AnyBody. As a result the differences seen may have been a result of the altered kinematics captured during gait. However it is also possible that these altered kinematics would result in a change in the NSA and therefore the muscle forces observed would explain the relationship between these altered kinematics and the change in NSA.

Although the musculoskeletal modelling system reports the variations in gait kinematics and kinetics, there is a limitation with this method, as AnyBody uses a scaling technique to account for changes in height and body mass and does not account for the geometric shape changes of bone during growth which may affect the lines of action of the muscles. The form of the femur changes dramatically from prenatal to 3 years (Chapter 2.1) and from 3 years to skeletal maturity the shape of the femur adapts but at a significantly slower development rate. From three to four years a number of changes can be observed including an increase in bicondylar angle and neck shaft angle. The lines of action of the muscles would be changed due to this change in structure and therefore affect the loading on the bone and the role of the muscle. The change in the role of the muscle would be a resultant factor of the change in shape of the femur. For instance, considering the muscles that attach into the greater trochanter from the pelvis which are predominantly hip abductors, when a change in the neck angle occurs (Lenaerts *et al*, 2008) the abductor muscles would change their line of action and therefore change their ability to perform their abduction movement. O'Brien *et al* (2009) found that in pre pubertal children the muscle moment arms of the knee cannot be scaled down from adults as they have a change in proportion, therefore this would not produce the correct muscle forces. Other than work by O'Brien *et al*, (2009; 2010) there has been little work performed on the changes in geometry of the juvenile femur in relation to the muscle moment arm, however there has been work produced to study the effect of changes in NL and NSA in the adult femur (Delp, 1994; Lenaerts *et al*, 2008). Although these skeletal changes cannot be modelled in AnyBody without the use of MRI, Lenaerts *et al* (2008) reported that the increases in NSA result in an increased hip abductor activity (gluteus maximus and minimus). However during this work there was no subject specific gait analysis and therefore the changes in kinematics resulting from a change in muscle activity were not able to be considered. The effect of this lack

of ability to change the geometry of the femur in the children's modelling will be discussed in greater detail in the FEA chapter of this thesis.

The 4 year old data showed a number of significant differences, in terms of maturity the 4 year old is said to have an adult like gait pattern and therefore the differences observed here may not correlate well with this. However this may be due to geometrical changes in the 4 year old femur and therefore subject specific models may need to be produced. What is not clear in this study, or any other, is how the muscles activity patterns change due to growth to maintain an adult like gait pattern. If the muscles were to produce a consistent pattern of activity during growth through to adulthood. Then due changes in the moment arm lengths caused by the changes in geometry of the femur, the gait kinematics would alter. Therefore it is would be necessary for the muscle activity to vary during growth to account for the different in muscle geometry. To assess this a longitudinal study may be required using subject specific musculoskeletal models including geometrical positioning of bones and muscles.

6.4.5 MEASURED JOINT REACTION FORCE

Adult joint contact forces for the hip were found to be similar to those of Bergmann *et al,* (2001) and Phillips, (2009) (Table 6.16).

Model	RhX (N)	RhY(N)	RhZ (N)	Rh (N)
Adult	-343	-203	-1938	1979
Bergmann *et al,* (2001)	-140	-130	-2211	2216
Phillips *et al,* (2009)	-342	-11	-2020	2048

Table 6.16 Measured joint reaction forces compared to *in vivo* data (Bergmann *et al,* 2001) and forward dynamic model (Phillips, 2009)

Values in the Y direction of -203N showed a much higher value than the linear model in Phillips *et al,* (2009) (-11N) but were of a similar magnitude to Bergmann *et al,* (2001) (-130N). The forces in the X showed the opposite and had closer values to Phillips than Bergmann. In the Z direction a maximum difference of 191N was observed. These values are well within an accepted range observed between subjects in previous papers. When comparing the total resultant force (Rh) the present study had a value of 265%BW comparing well to 204%BW of the Phillips model and 226%BW of the *in*

vivo measurements by Bergmann *et al,* (2001). A comparison of the JRF shows relatively normal values although it is noted that large variances in the JRF have been observed in many other papers (Jonkers *et al,* 2008; Lenaerts *et al,* 2008). This can be attributed to differences in kinematics and kinetics of the subjects.

In the children however, a much larger JRF was observed with forces of 537% BW and 613% BW being seen in the 3 year old and 5 year old respectively. These values are much higher than those observed in the adult. However a large variability has been observed in the JRF between similar age groups, so it may not be correct to conclude that this is due to age differences. In a study (Bergmann *et al,* 2001) of fairly homogenous subjects a difference was found of up to 110% BW in hip joint contact force between subjects in normal walking. This large variability between subjects makes it difficult for comparisons to be made. Further to this in the 5 year old a faster walking speed was identified, it has been reported that an increased speed can increase JRF. Bergmann *et al,* (2001) showed an increase of 18% bodyweight by increasing speed, so this may indicate why a higher JRF was observed in the 5 year old when compared to the other age groups.

As previously reported, the 3 year old gait data has been shown to be significantly different to that observed in the other age groups, this is also observed in the JRF. A much larger resultant force BW percentage was found. Bergmann *et al,* (2004) found that in response to a stumble there is a very large increase in JRF. It was reported that during a stumble one subject's JRF increased from 400% BW to 870% BW which is over double the normal walking JRF. Stumbling can be seen as a lack of control during gait, this lack of control is also observed in immature gait (Chester *et al,* 2005). It is possible that this is the reason for the much larger JRF seen in the 3 year old, explaining the differences in the 3 year old kinematics that were observed (Chapter 6). Although this was not in agreement with previous studies (Sutherland *et al,* 1980). Furthermore the lack of subject specific geometrical modelling may have resulted in the increased mediolateral, Rx, and anteroposterior, Ry, JRF in the children. This was found by Lenaerts *et al,* (2008) where an increase mediolateral force and resultant force angle of the hip was observed when subject specific geometries were not modelled correctly. A number of limitations have to be addressed when discussing these results, firstly muscle forces derived from inverse dynamics are calculated from adult segment mass data (Winter, 1991). Jensen *et al* (1989) identified that the bone density of children is less than that observed in adults and therefore the muscles forces may be incorrectly derived.

However this limitation would be difficult to correct without the correct segment masses. Collecting the correct masses and measuring BMD would be beyond the scope of this research but an area of interest for future work. Secondly, the lack of subject specific geometrical modelling could affect the muscle forces. However it was not possible to model this in the current study and any changes to the muscle moment arms would not take into account subject specific gait. The subjects' gait was deemed more important in this study than the geometrical positioning, but future work would be inclined to try and take both of these variables into account.

The novel findings of the musculoskeletal modelling indicate that there are difference between the muscle forces produced in children's musculoskeletal modelling compared to each other and adults. Most significantly an immature gait pattern was observed in the 3 year old subject, which could play a role on the structure of bone at this age. The next stage is to test what role these differences play on the stress and strain of age specific femur models through the use of finite element analysis by applying the loads obtained in this chapter to the computer models created in Chapter 3.

7 FINITE ELEMENT ANLAYSIS

7.1 INTRODUCTION

All previous work in this thesis has provided the knowledge and materials necessary to complete this chapter. These being Chapter 3; developing the 3D models, Chapter 4; collecting the gait data from adult and juvenile subjects, Chapter 6; building of musculoskeletal models. Therefore this chapter will bring the results of these chapters together to present the main findings of this thesis. The mechanical response of the adult and a series of juvenile proximal femora constructed in Chapter 3, when experiencing the loading detailed in Chapter 7, was compiled in a series of FE analyses. The stresses and strains observed during this analysis will be evaluated and any differences will be explained with regard to the boundary conditions and geometrical differences of the model.

7.2 MODEL CONSTRUCTION

FEA was performed in ANSYS, and based on tetrahedral meshes generated within AMIRA, which were created through converting the digitised proximal femur reconstructions into polygon surface models. In all cases, the tetrahedral element parameters were adjusted to the software recommended aspect ratio and tetrahedral quality, in order to ensure the highest mesh quality possible. Solid 10-noded tetrahedral elements (SOLID 92) were modelled to represent trabecular bone, cartilage (if present) and the medullary canal. 4-noded shell elements (SHELL 63) clad around the structural exterior replicating cortical bone, shell elements did not cover the exterior regions where trabecular bone would connect to cartilage. This aimed to replicate the structure of an ossifying femur. The thickness of the cortical shell was estimated from that reported by Goldman *et al*, (2009) (Table 7.1).

Cortical Area (mm)	2 yr old	5 yr old	9 yr old	7 yr old	Adult
P	4.39	3.79	5.09	4.44	9.22
PM	3.8	3.46	5.1	4.28	7.03
M	3.32	3.2	4.27	3.735	6.79
AM	3	3.07	4.33	3.7	6.24
AM	2.7	2.78	4.59	3.685	5.61
AL	2.88	2.78	5.03	3.905	6.83
L	2.96	3.06	4.447	3.7535	6.76
PL	3.84	3.21	4.55	3.88	6.21
Cortical Average	3.36	3.17	4.68	3.92	6.84

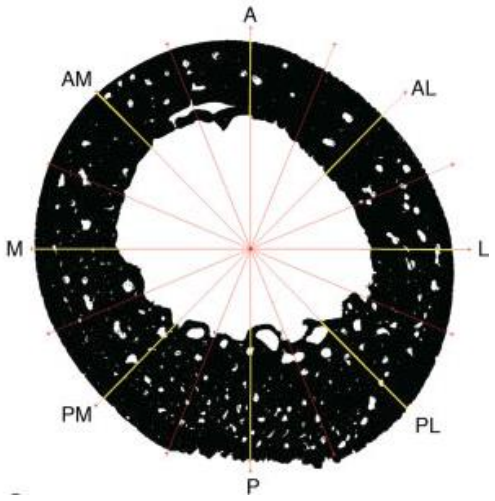

Table 7.1 shows the observed cortical thickness (mm) of the midshaft of the femur by Goldman et al 2009) in various age groups. The defined areas of the cortical thickness as defined by Goldman et al. Abbreviations for radial lines as follows: A, anterior; AL, anterior lateral; L, lateral; PL, posterior lateral; P, posterior; PM, posterior medial; M. medial; AM, anterior medial;

All femora were represented as a linear elastic material and each femora had varied material properties according to literature. These material properties will be reported in later sections.

7.3 LOADING CONDITIONS

The loading applied to the model were the muscle and joint forces calculated in Chapter 6. Only walking was modelled, although it should be noted that other activities are undertaken by humans on a daily basis; for example, stair climbing, running, sitting upright, sit to stand. However, walking loads are used frequently in FE models and results can be compared to the findings of previous literature.

The muscle loads were defined as distributed loads over the surface nodes within muscular origin sites, which were identified using the descriptions of Scheuer and Black (2000), Gray (1991) and Sobotta (2006) (Figure 7.1). The muscle locations for the juvenile models seen in Figure 7.4 and Figure 7.8 were more difficult than the adult model due to the lack of literature detailing these locations and the lack of fully established and anatomical landmarks. However, the landmarks which were available were used as reference points to apply the muscles, then the applied muscles were used to position surrounding muscles.

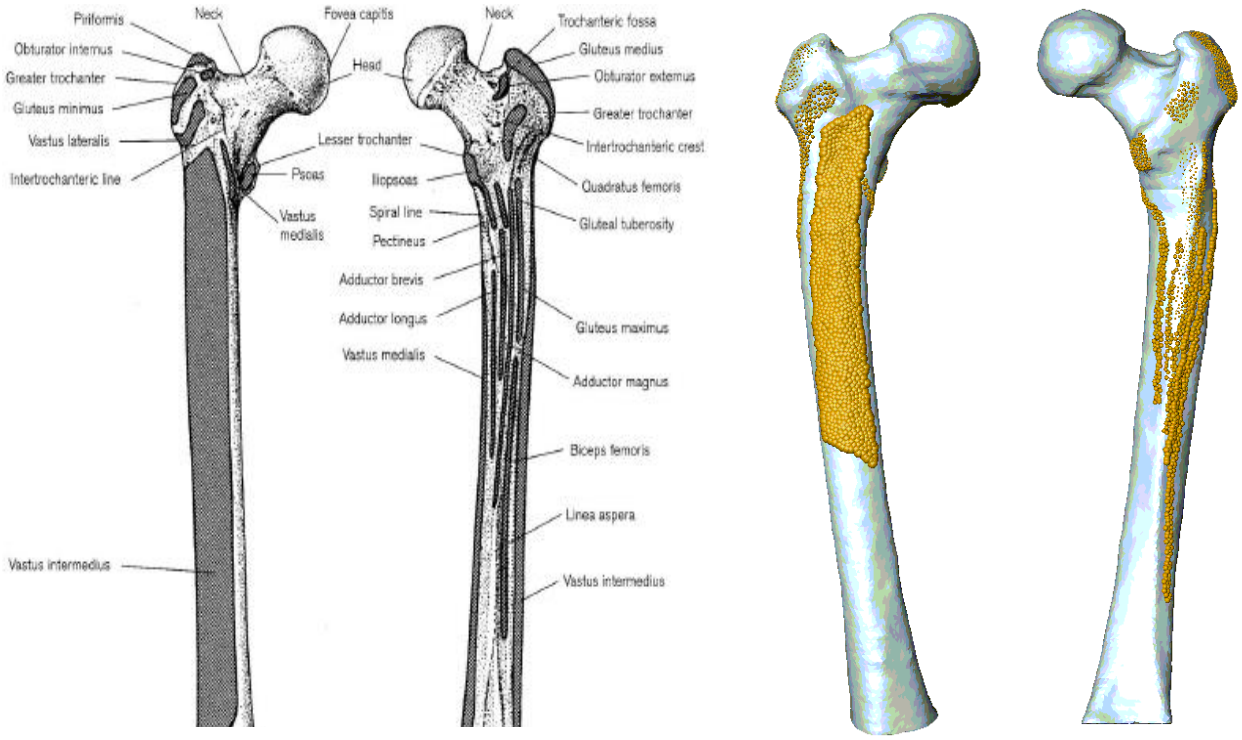

Figure 7.1 The attachment sites for muscles on the femur from literature a) Scheuer and Black; and b) landmarked on the 3D model.

Identification of origin and insertion points and therefore mapping of the muscles was most difficult in the younger specimens as they did not have the landmarks which correlate with the adult models. However a number of insertion points were apparent, one such is the lesser trochanter. The identification of this allowed a number of muscles to be mapped, which then enabled the orientation of these muscles, other muscles could be mapped accordingly. The psoas major was an exception because the insertion was on the iliacus muscle. The psoas major forces were added to the forces applied from the iliacus as a combined muscle known as iliopsoas or the dorsal hip muscle. The location of the muscles' origin and insertion points would be dependent on the model created from AnyBody and at which point during the gait cycle was being modelled. From AnyBody 25 muscles with 127 lines of actions were selected, which attach into the proximal femur. From these 127 lines of action, where each muscle would contain up to 8, it was possible to group them into singular ones and the mid line of action for each muscle was selected. This left the 25 muscles with 30 lines of action. The lines of action were calculated through vector mechanics between the coordinates of the origin, insertions or via points (produced in AnyBody), for each muscle at the following gait cycle points 2%, 10%, 20%, 30%, 45%, 70% and 98%. A force in the 3 directions, x, y and z, was calculated and applied to the FEM. The forces that were applied during these loading conditions were age specific loads calculated from the musculoskeletal models produced in Appendix V. The changes in the line of action can be seen in Figure 7.2. It is possible to see how the direction that the muscle would be acting in at each of the 7 stages of gait, which are being studied, for the 3 different models changes throughout.

a) Adult

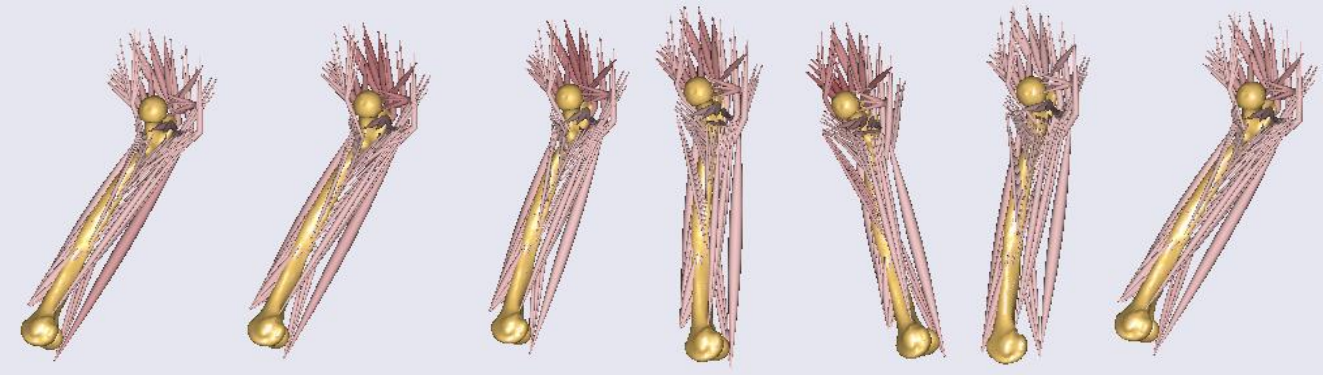

b) 7 Year Old

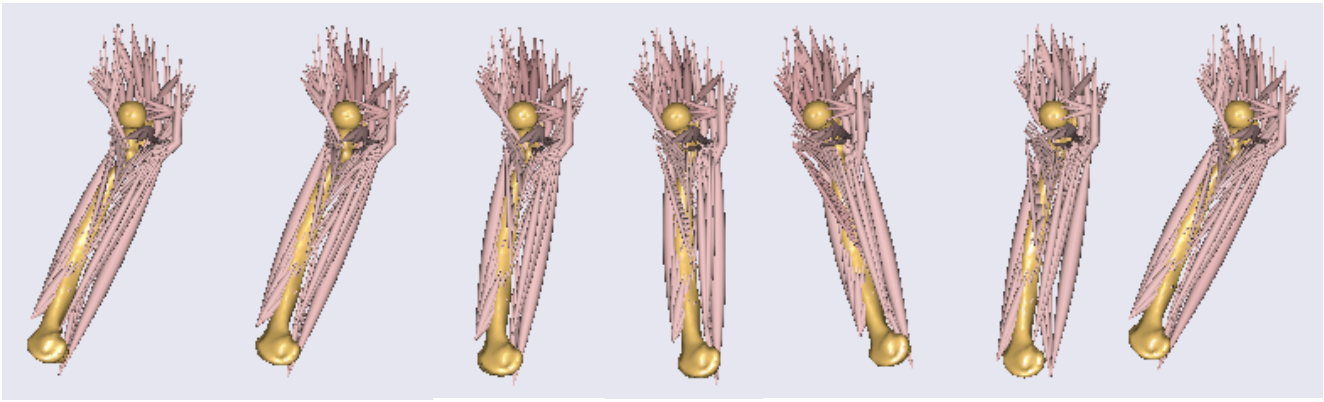

c) 3 Year Old

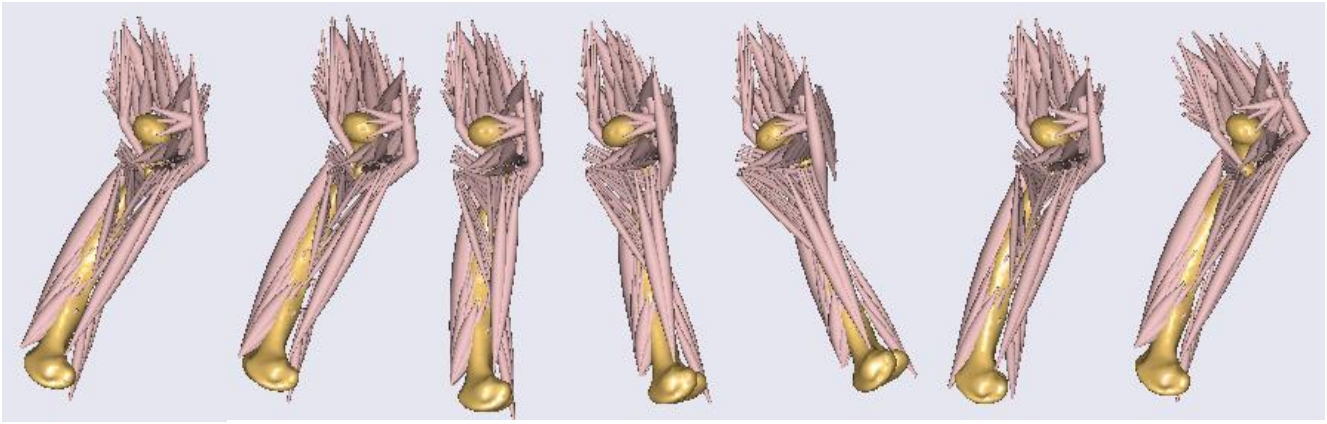

Figure 7.2 illustrates the changes of the muscle lines of action during gait at the seven analysed stages (2%, 10%, 20%, 30%, 45%, 70% and 98%.) for the three different models a) adult, b) 7 year old, and c) 3 year old.

This study is only modelling the proximal portion of the femur and therefore physiological constraints were difficult to replicate. However Polgar *et al,* (2003) showed that constraining the femur at the most distal nodes in all DOF, proved to provide the most physiologically representative strain distributions, therefore each model was constrained in such a manner.

7.4 ANALYSIS OF THE RESULTS

The trabecular bone and cortical bone were analysed observing von Mises strains and stresses to evaluate any changes as the femur develops and grows. As reported previously the predicted stress and strains are to be examined from a number of stages during the gait cycle.

Beyond this analysis a method detailed in Curtis *et al*, (2011) where peak strains for each element over the full gait cycle, are to be calculated and cumulatively presented on a strain plot of the femur. Each individual element experiences a different strain under the different loading conditions. The highest strain experienced by each individual element, irrespective of the loading condition is displayed in the cumulative stress model. This will allow a full understanding of the peak cumulative strains that are present during a full gait cycle, which has not been reported previously. This method has, to this researchers' knowledge, never been performed on a femur before. Previous work has applied peak muscle forces observed throughout the gait cycle on a single FE model of the femur (Taylor *et al,* 1996) or used single load cases from specified stages in the gait cycle (Duda, 1997). These methods only allow the researchers to observe strains occurring in one instance of loading. As the morphology of the femur is thought to be determined by the overall loads it experiences throughout daily living, then the approach described in this work will allow for a much more accurate and comprehensive description of the impact on the femur that this cumulative loading causes.

Strain/stress magnitudes were also analysed to observe if they fell within a remodelling limit of bone as reported in the literature (Martin, 2000). This would ensure the loads did not exceed those experienced during physiological loading. The stress/strain plots between the different phases of gait cycle will have a large variation of magnitude because of the

differences in loading. Where the later stages of gait cycle (swing phases) the femur is relatively unloaded. Therefore the contour ranges on each phase of the gait cycle will be varied to account for this.

7.5 PROTOCOL

Because each model would have a different behaviour due to the different stages of development, they had to be assessed as an individual model rather than a generic mesh and material property given to them all. However, the loading geometry and stages of gait cycle which are used will be the same for each model. The loading regime can be discussed as a generalised approach for all models. The differences in the loading regime will be the forces which were calculated using the age specific musculoskeletal models (Chapter 6).

Only the proximal part of the femur was modelled in this study, due to the difficulties of re articulating the femora (Chapter 3). It was decided that the distal end of the femur would be dis-regarded to simplify the task of rebuilding the femora. The length of the femur (FL) to be modelled (75% of the full femur) can be seen in Table 7.2 along with the femur width (FW) and femur depth (FD) as defined in Figure 7.3.

Model	Full Femur Length (mm)	Modelled femur length (mm)	Femur Depth (mm)	Femur Width (mm)
3 year old	210.29	153.90	40.97	25.37
7 year old	300.60	232.40	53.40	27.53
Adult	430.30	345.53	97.68	43.50

Table 7.2 Shows the length of a full femur (Anderson *et al,* 1964) and the length of the femur being modelled along with femoral depth and width for the specified ages.

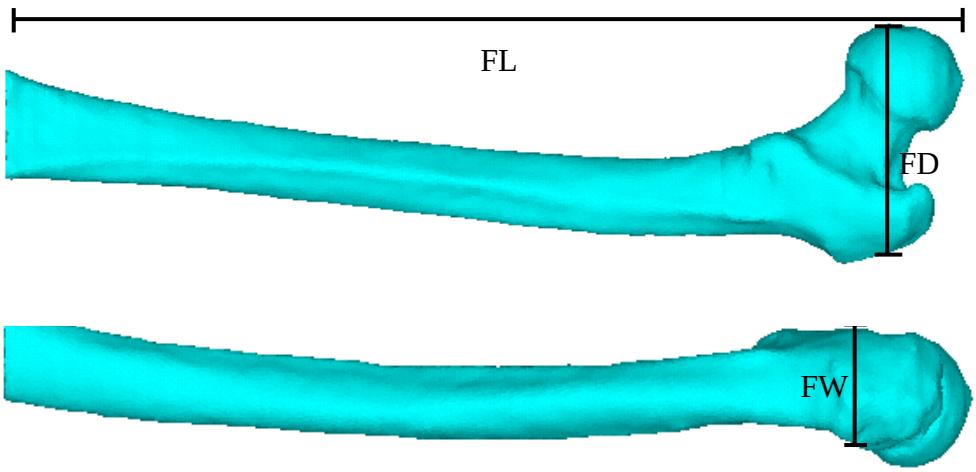

Figure 7.3 Adult femur with the definitions of femur length (FL), femur depth (FD) and femur width (FW).

It was necessary to assess each model differently due to the developmental changes which occur during the growth of the femur. The geometrical shape of the femur will play a role in the type of mesh, and the material properties will change according to the age of, and the amount of cartilage present in the, juvenile models. Therefore each model is represented differently. The prenatal model did not undergo FEA because of the difficulty in producing a realistic loading regime, although future work continuing on from Appendix III will use the digitised model.

All models underwent a convergence test prior to the FEA, the models converged at 210482 elements, 224382 elements and 234809 elements for 3 year old, 7 year old and adult model, respectively. The models had a simple loading regime and were constrained at the distal nodes. The same geometric location of 8 elements, and the 10 adjacent elements were averaged and analysed. Convergence of the models was satisfactory and these results are discussed in greater depth in Appendix VI.

The cortical von Mises stress and trabecular strains of the femoral head were analysed for all models. To ensure the models reacted in a physiological manner and the loading regimes were correct, the adult model analysis was compared against literature (Wagner, *et al* 2010). Comparisons between each model were made for locations of the peak von Mises stresses and peak trabecular strains, subsequently relating these to the development of the femoral morphology. In the 3 and 7 year old models the cartilage was unselected for the

analysis of the results. The high magnitudes of stress/strain that would be observed in the low Young's Modulus material would obscure the contour ranges used for analysis of the higher Young's Modulus material, bone.

7.6 3 YEAR OLD

The 3 year old was modelled with 94838 volumetric elements for trabecular, 5305 cartilage and 110339 for the medullary canal (Figure 7.4a). Cortical bone was modelled with 18083 shell elements with a thickness of 3.36mm, based on (Goldman *et al*, 2009) and the proximal part modelled with a thickness of 1.68mm (Silvestri and Ray, 2009). The loading applied to the model was described previously in Chapter 6 and where the muscle forces were applied can be seen below (Figure 7.4. a) The FEA model of the anterior and posterior of the 3 year old proximal femur containing 210482 10-node tetrahedral elements and 18083 6-node shell elements

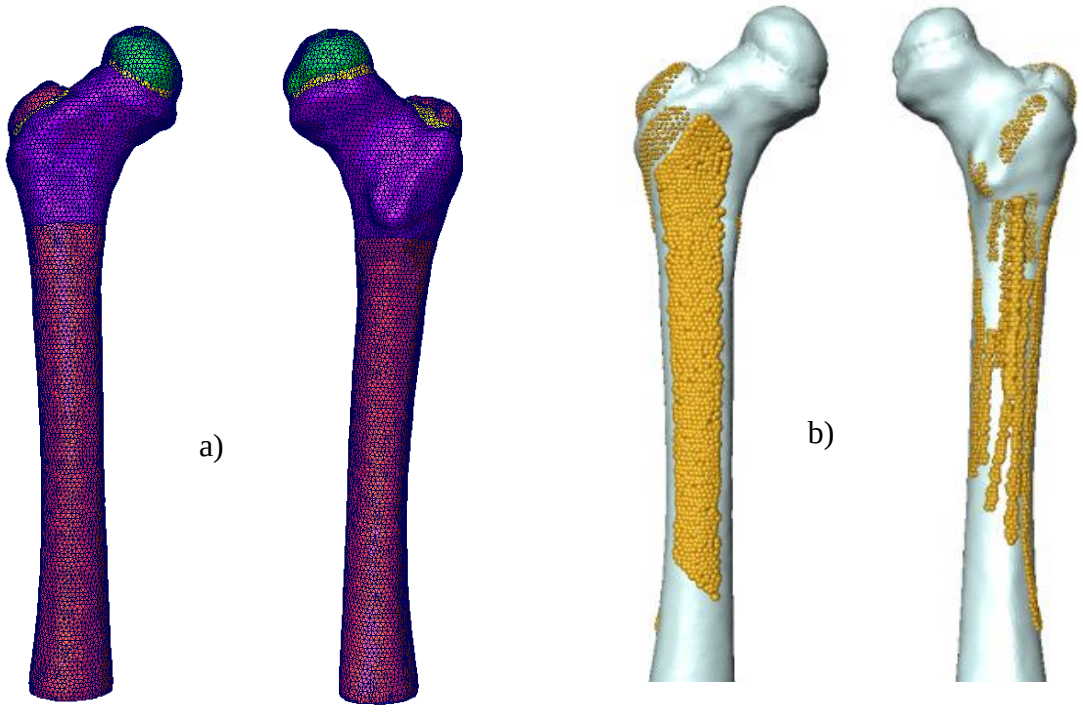

Figure 7.4. a) The FEA model of the anterior and posterior of the 3 year old proximal femur containing 210482 10-node tetrahedral elements and 18083 6-node shell elements. b) The attachment sites for muscles on the femur landmarked on the 3D model.

Material properties were assigned to the model as follows: 11500E (v = 0.3) and 345E (v = 0.3), to represent cortical and trabecular bone respectively. Cartilage and medullary canal were also assigned 108E (v = 0.34) and 5E (v = 0.3) respectively (Appendix II).

7.6.1 STRESS DISTRIBUTION ASSOCIATED WITH GAIT LOADING

Cortical von Mises stress distribution, produced by the applied muscular loading (Appendix V), were the largest magnitudes during, 10%, 20% and CS load cases (Figure 7.5a, b and d), with stresses in the proximal femur exceeding 15.5MPa. The lowest stress was observed during 70% of the gait cycle (Figure 7.5c) showing peak stresses of 0.9MPa. The peak stresses observed were in a similar concentration in all load cases and were on the distal portion of the femoral neck. Another peak area of stress observed in all load cases was on the posterior portion of the neck, where as a region of low stress was observed on the anterior. The stresses observed in the later stages of the gait cycle (70%) were much lower as this is in the swing phase of gait, absent of force generated from foot contact with the floor. Greater uniformed stresses were observed during the swing phases. In particular the lesser trochanter during the stance phases was a low area of stress, in the swing phases, although still low, the lesser trochanter was a more uniformed with the surrounding areas. The maximal structural deformation observed during analysis was 1.2%, 2.6% and 1.9% in FL, FD, and FW, respectively.

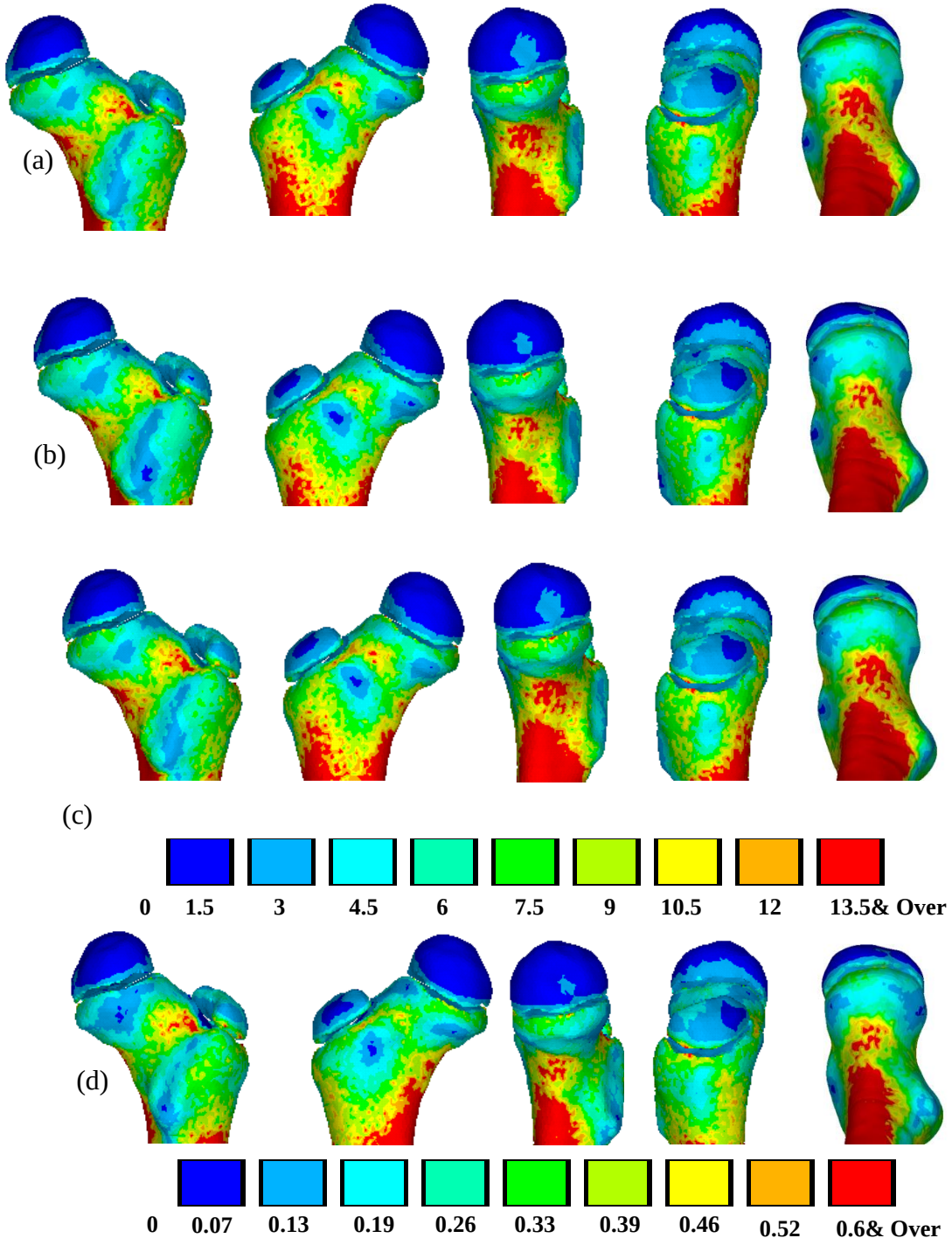

Figure 7.5 The cortical von Mises stress distribution of the 3 year old proximal femur produced by the musculoskeletal model loading at (a) 10%, (b) 20%, (c) the cumulative stress model and (d) 70% of the gait cycle.

The highest strains were observed where the cartilage was in contact with the bone, as would be expected. The cumulative stress (CS) model produced strain magnitudes of 3600με on the posterior and anterior aspects of the femoral neck. However a concentration of peak strain was observed on the distal portion of the neck with values exceeding 5400με. This peak strain area was present in all phases of the gait cycle and moved from anterior to posterior throughout. Single support phase of the gait cycle produced the highest strain, these were in the 10% and 20% load cases with strain values of >6000με. The lowest strains were produced at 70% of the gait cycle, where values in the femoral head did not exceed 250με, and with large areas of the head and neck not exceeding 150με. The high stress was still present on the distal portion of the neck but had dissipated to a more posterior position. In all load cases the lesser trochanter had relatively low strains, in the CS case the values did not exceed 1200με. A reduction in the overall strain was observed as double support phase of gait is initiated (Figure 7.7c).

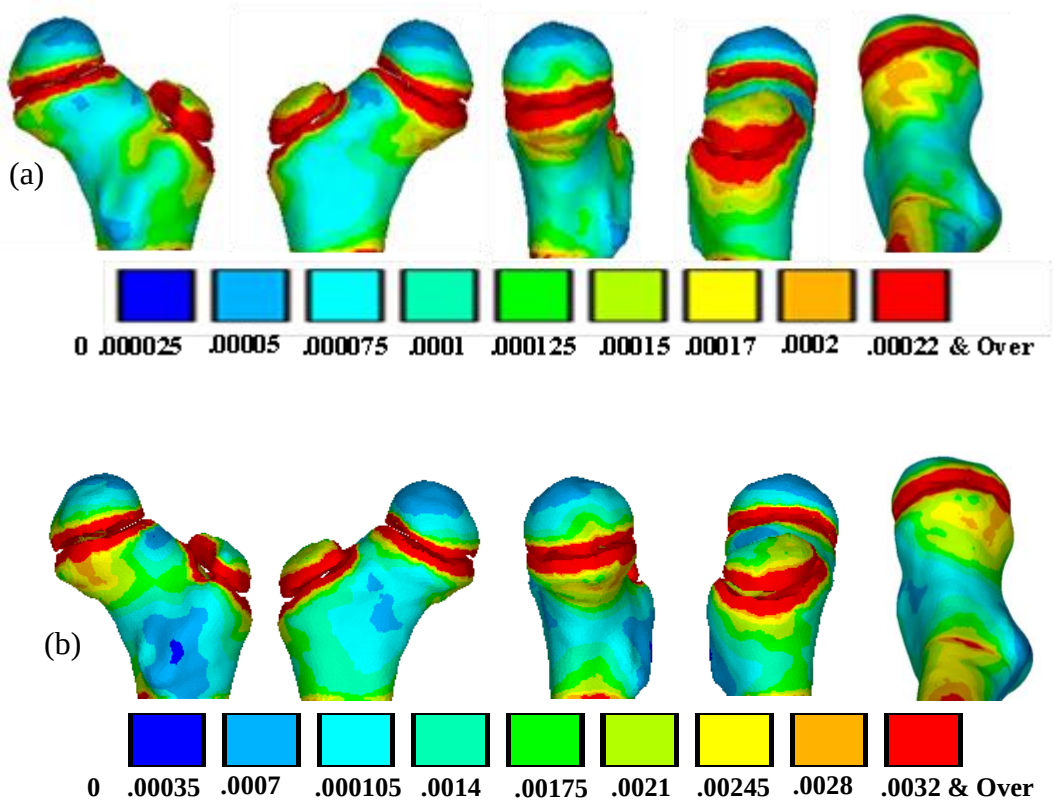

Figure 7.6 The trabecular von Mises strain distribution of the 3 year old femoral head produced by the musculoskeletal model loading at (a)70% of the gait cycle and (b) the cumulative stress model.

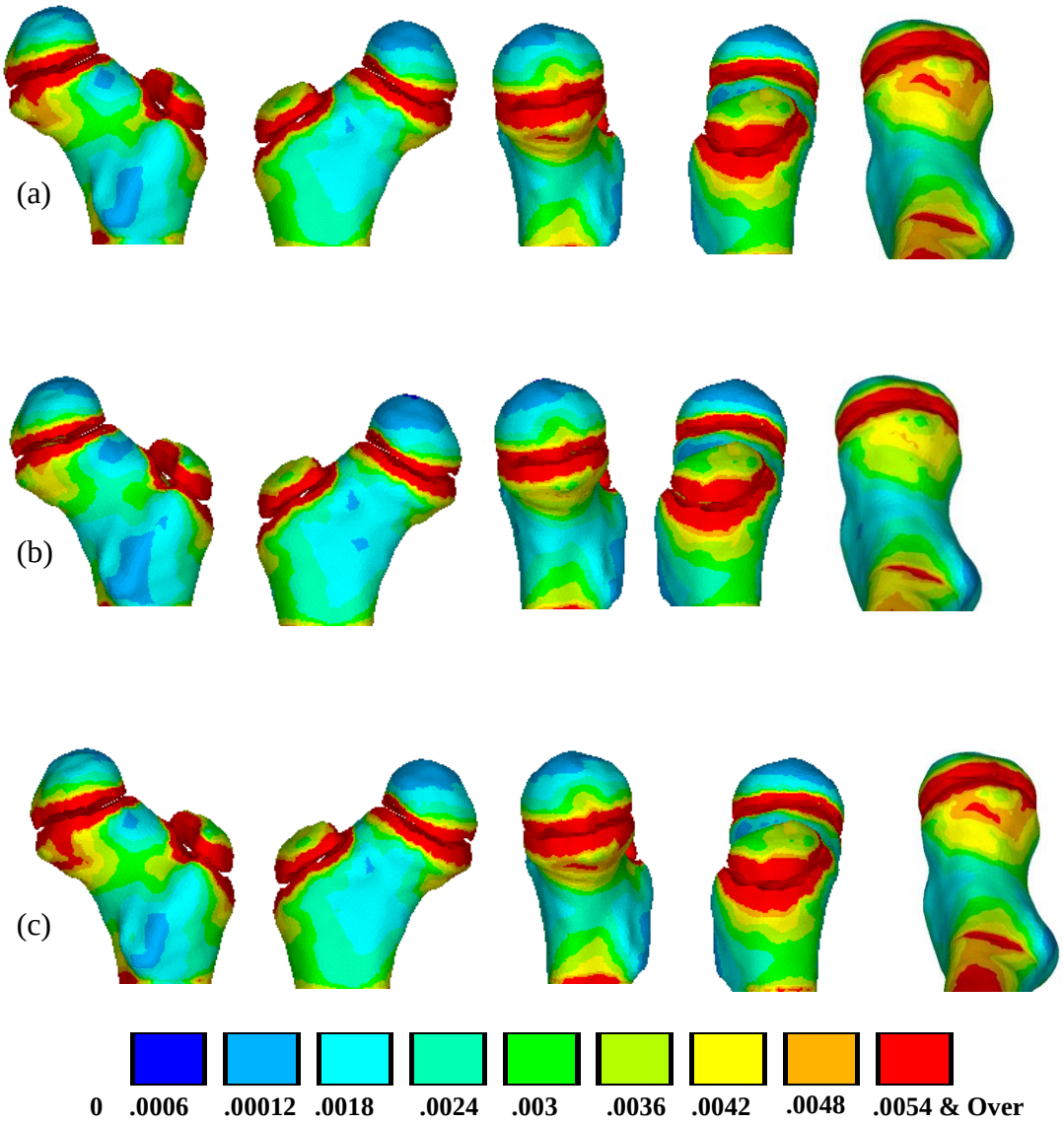

Figure 7.7 The trabecular von Mises strain distribution of the 3 year old femoral head produced by the musculoskeletal model loading at (a) 10%, (b) 20%, (c) 45%,

7.7 7 YEAR OLD

The 7 year old was modelled with 84434 volumetric elements for trabecular, 4718 cartilage and 135230 for the medullary canal (Figure 7.8a). Cortical bone was modelled with 21064 shell elements with a thickness of 3.92mm, based on (Goldman *et al,* 2009) and the proximal part modelled with a thickness of 1.96mm (Silvestri and Ray, 2009). The loading

applied to the model was described previously in Chapter 6 where the muscle forces were applied can be seen below (Figure 7.8b).

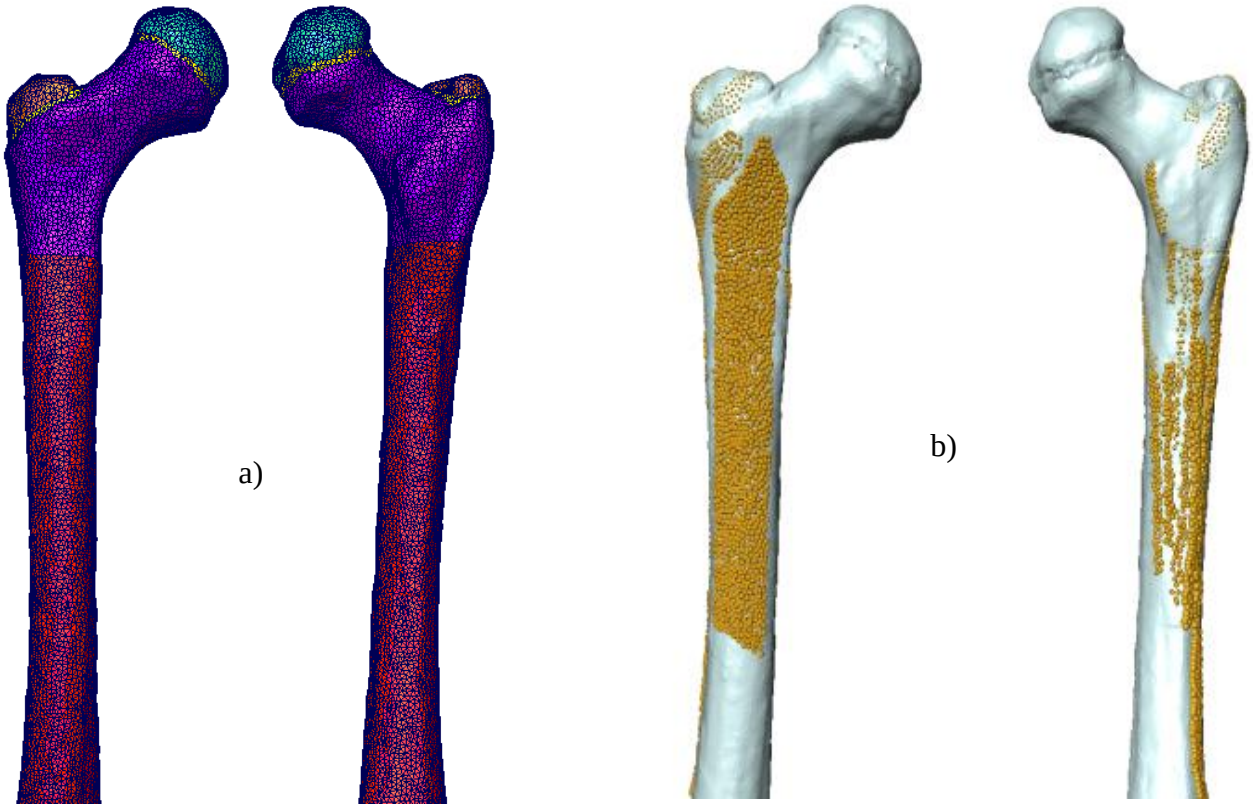

Figure 7.8 The FEA model of the anterior and posterior of the 7 year old proximal femur containing 224382 10-node tetrahedral elements and 21064 6-node shell elements. b) The attachment sites for muscles on the femur landmarked on the 3D model.

Material properties were assigned to the model as follows: 11500E (v = 0.3) and 345E (v = 0.3) to represent cortical and trabecular bone respectively, and cartilage and medullary canal were assigned 108E (v = 0.34) and 5E (v = 0.3) respectively (Appendix II).

7.7.1 STRESS DISTRIBUTION ASSOCIATED WITH GAIT LOADING

As observed in the 3 year old, model the highest stresses were observed during 10% and 20% of the gait cycle. The magnitude of the stresses were similar to those observed in the 3 year old model, with the maximal stress values in the proximal femur being 13.5MPa in the CS compared to 15.5MPa in the younger model. Also, as in the 3 year old model, the highest magnitude of stress is observed on the neck of the femur. As the gait cycle progresses, the concentration of the stress which is on the distal portion of the femoral neck, moves anteriorly towards the lesser trochanter. An exception to this was observed in the 70% load case where there was no area of high stress on the neck. The 70% load case showed a maximal stress of 2.25MPa on the lateral portion of the proximal femur. The lowest areas of stress were seen in the distal epiphyses in all load cases. The maximal displacement of the 7 year old model were calculated as FL, 0.3%; FD, 1.5%; FW, 1.2%.

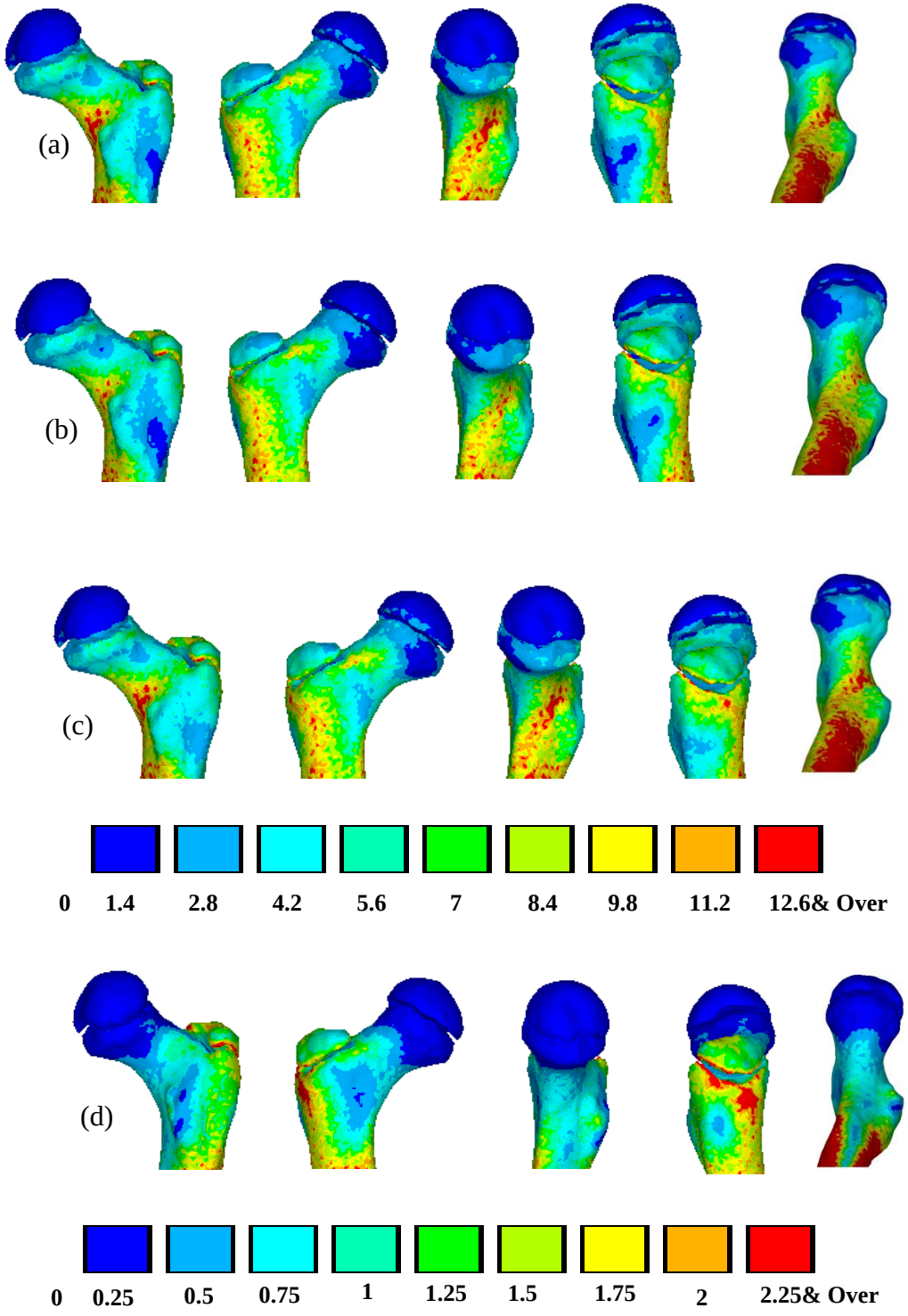

Figure 7.9 The cortical von Mises stress distribution of the 7 year old proximal femur produced by the musculoskeletal model loading at (a) 10%, (b) 20%, (c) the cumulative stress model and (d) 70% of the gait cycle.

The highest trabecular strain of the in the femoral head in the 7 year old model was shown to be 5655με in the 10% and 20% load cases (Figure 7.10), the same as observed in the 3 year old. Much of the GT was under a high magnitude of strain, 3500με, and the majority of the head being under 2400με. These values are much higher than that observed in the 3 year old model. In the CS strain magnitudes of 4000με and over were experienced. As in the 3 year old model a concentration of stress was found in the distal portion of the neck. This concentration was located posteriorly compared to the younger model which had a more anterior position. Strain on the anterior aspect did not exceed 1600με, whereas the posterior experienced values of 2800με. The 70% and 98% load case again experienced the lowest peak strain, with values generally below 500με. The GT experienced the highest strain, and the strain concentration observed in the distal portion of the neck during the stance phase load cases, was not present during the swing phase load cases.

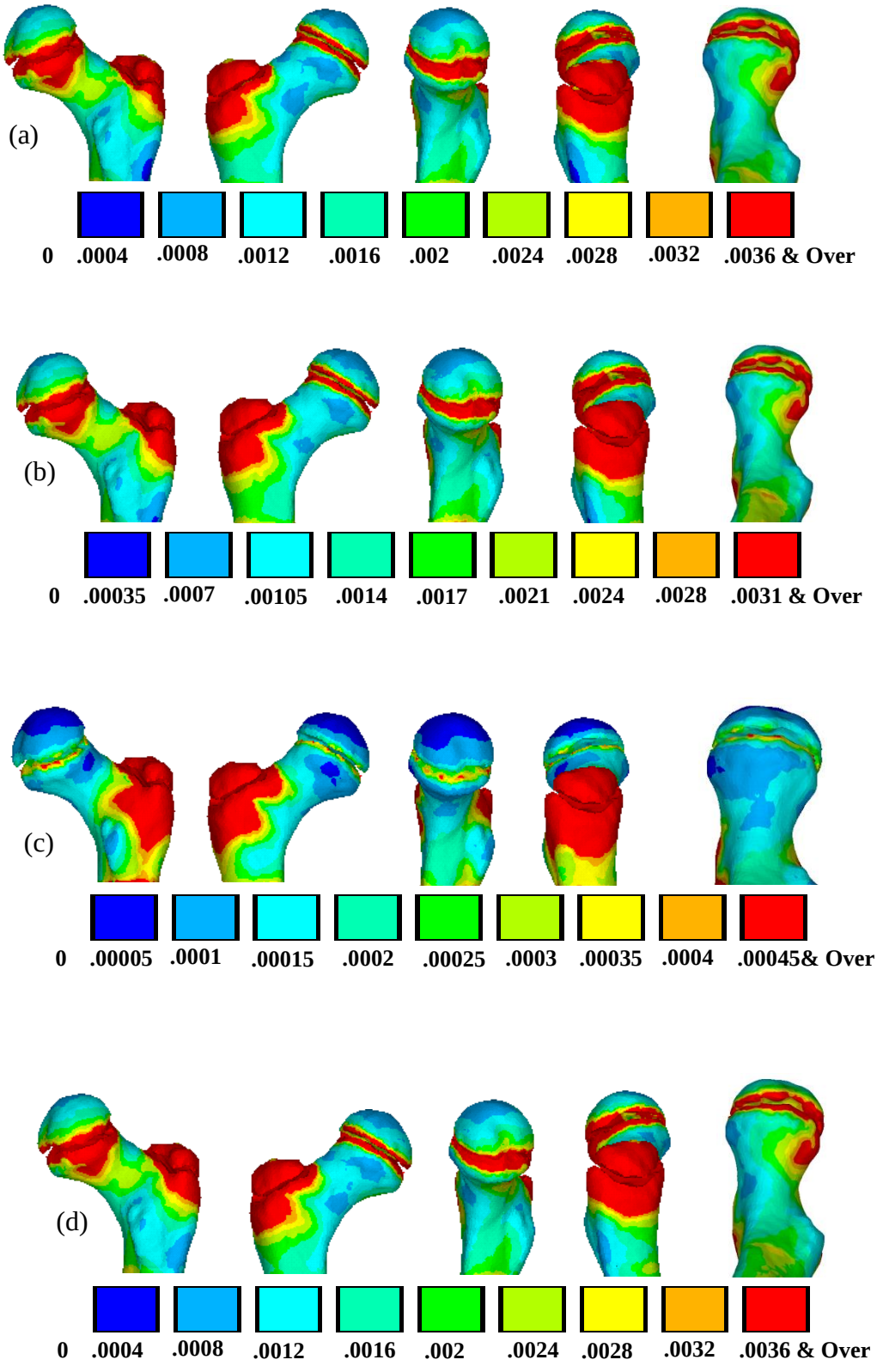

Figure 7.10 The trabecular von Mises strain distribution of the 7 year old femoral head produced by the musculoskeletal model loading at (a) 10%, (b) 20%, (c) 70% of the gait cycle and (d) the cumulative stress model.

7.8 ADULT

The adult model of the proximal part of the femur was performed for comparisons to be made to the FEA of the juvenile proximal femurs. This model will also be compared to FEA of the femur in literature, to validate the boundary conditions that are consistent through all the models. The adult proximal femur was modelled with 111382 volumetric elements for trabecular, and 1234427 for the medullary canal (Figure 7.11). Cortical bone was modelled with 22572 shell elements with a thickness of 6.83mm, based on (Goldman *et al*, 2009) and the proximal part modelled with a thickness of 3.41mm (Silvestri and Ray, 2009). The loading applied to the model was described previously.

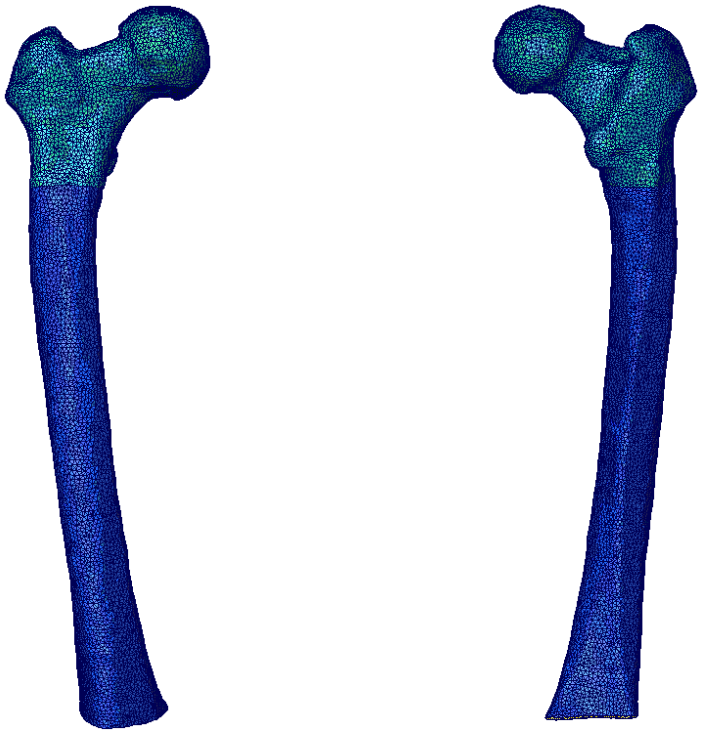

Figure 7.11 The FEA model of the anterior and posterior of the Adult proximal femur containing 234809 10-node tetrahedral elements and 22572 6-node shell elements.

Material properties were assigned to the model as follows 17000E (v = 0.3) and 1000E (v = 0.3) to represent cortical and trabecular bone respectively, and medullary canal were assigned 10E (v = 0.3) respectively (Appendix II).

7.8.1 STRESS DISTRIBUTION ASSOCIATED WITH GAIT LOADING

The cortical von Mises stress in the adult femur showed higher magnitudes of stress compared to the 7 and 3 year old models. With peak values in the adult model exceeding 44MPa, the highest stresses were found in the 45% model, except the cumulative stress model, compared to the juvenile femora models where the 10% model was found to produce the highest stress. The areas of peak stresses in the CS load case can be seen on the distal portion of the neck (Figure 7.12). Other areas of high stress magnitude observed in all load cases were on the proximal posterior portion of the neck, with a low area of stress on the anterior portion. Similar to the juvenile models the greater trochanter and femoral head were relatively unstressed. The 70% load case had the lowest stress magnitudes with a maximum of 2.7MPa, although the areas of peak stress were similar to the other load cases which were not observed in the juvenile models. Maximal displacements of the adult model were calculated as FL, 2.9%; FD, 5.5%; FW, 4.9%.

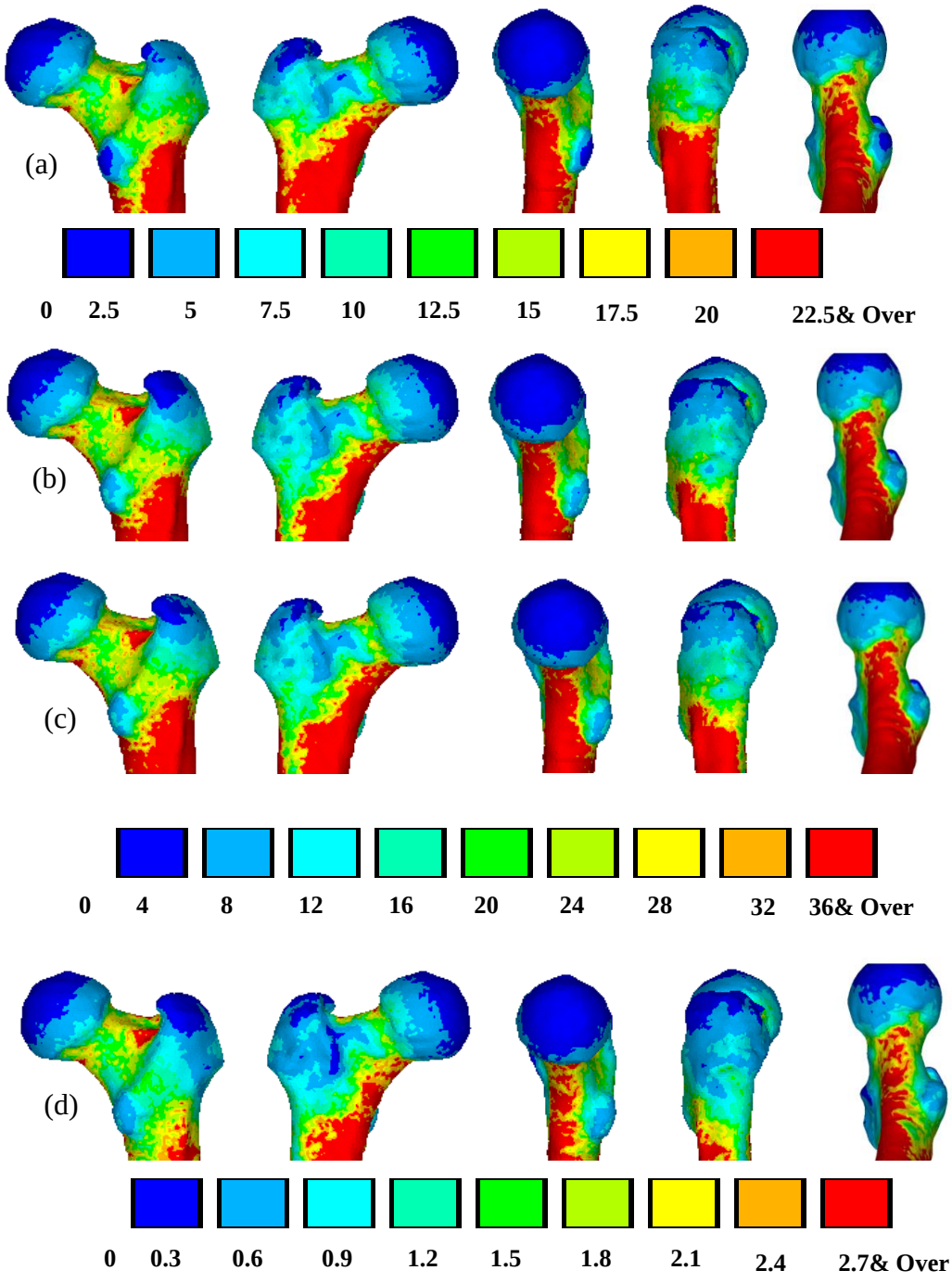

Figure 7.12 The cortical von Mises stress distribution of the 7 year old proximal femur produced by the musculoskeletal model loading at (a) 10%, (b) 45%, (c) CS load case and (d) 70% of the gait cycle.

Von Mises strain on the trabecular was found to be the highest in the CS model and in the 45% gait cycle load case compared to the juvenile models where the highest strains were found in the 20% gait cycle load case (Figure 7.13). Compared to the juvenile models, the GT showed a much lower strain, possibly due to the fusion of the GT and therefore the lack of a cartilaginous growth plate. The highest concentration of strain was observed in the intertrochanteric notch. The average strains in the femoral head were generally higher in the adult, no less than 4500με compared to the 3500με in the 7 year old. This is disregarding the high strain on the intertrochanteric notch. All the models have shown a higher level of strain on the posterior side of the head and the lowest over strains have been in the 70% and 98% load cases (Figure 7.14), due to the reduced hip force during the swing phase.

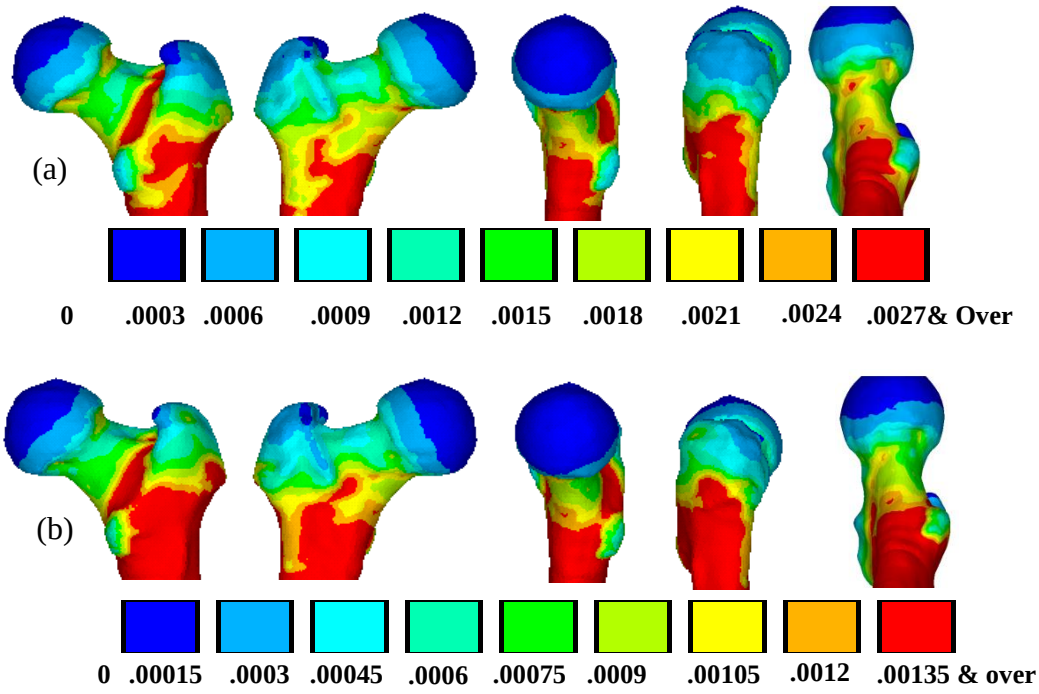

Figure 7.13 The trabecular von Mises strain distribution of the adults femoral head produced by the musculoskeletal model loading at (a) 10% and (b) 20% of the gait cycle.

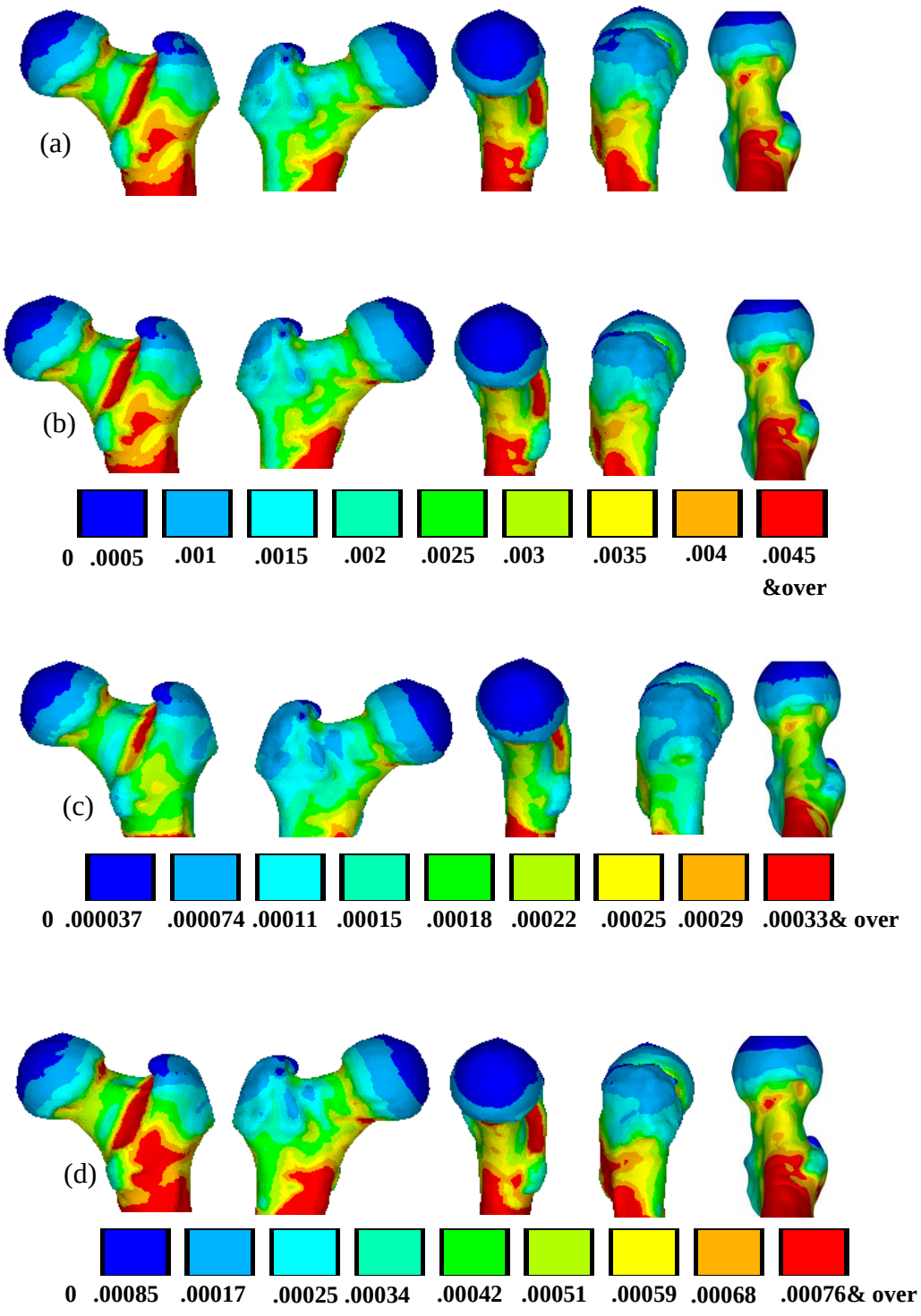

Figure 7.14 The trabecular von Mises strain distribution of the adults femoral head produced by the musculoskeletal model loading at (a) 45%, (b) the cumulative strain model, (c) 70% and (d) 98% of the gait cycle.

7.9 COMPARISON OF FINITE ELEMENT MODELS

7.9.1 GROWTH PLATE COMPARISON

FEA of the juvenile femur has never been performed to this extent before, although Carriero *et al,* (2011) studied the effect of gait loading on the growth plate of the femoral head. This work could be used to assess the loading of the FEM in the current study. The results produced by Carriero *et al,* are reproduced in Figure 7.15 alongside the growth plate of the 3yr old model.

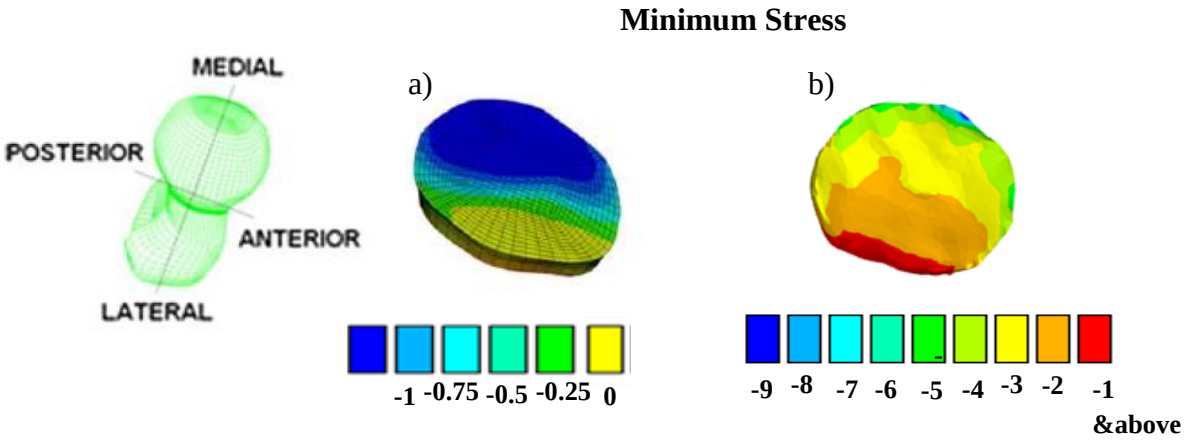

Figure 7.15 Growth plate of the femoral head showing minimum principle stress for a healthy 6 year old reported by Carriero *et al,* (2011) and the 3 year old growth plate from the present study.

The model shows high compressive stress towards the lateral aspect of the growth plate reproducing the results observed in the literature. The comparison between these two studies is made between two cumulative models. However the current model is an accumulation model of the peak stresses (CS model) throughout the gait cycle. Whereas the literatures model shows a stress plot produced a loading regime modelling the peak forces produced over a gait cycle. Despite these differences a comparison is able to be made. The largest stresses in both models were found to be towards the lateral side of the growth plate dispersing towards the medial side in a fairly consistent pattern. Carriero *et al,* (2010)

reported the results would indicate that normal growth would occur through these patterns of stress. Therefore it can be assumed the loading on the current model also correct. However the loading on the present study was more comprehensive than Carriero's model and therefore the differences in the magnitude of the stress may be as a result of this.

7.9.2 ADULT MODEL COMPARISON

The adult model can be compared visually to the data in the literature to show if the results are valid. Figure 7.16 compares the von Mises stress distribution in an adult femur at 10% and 45% of a full gait cycle between the current model and Wagner *et al,* (2010). Both models were constrained in the same manner and load cases were taken from AnyBody musculoskeletal modelling software.

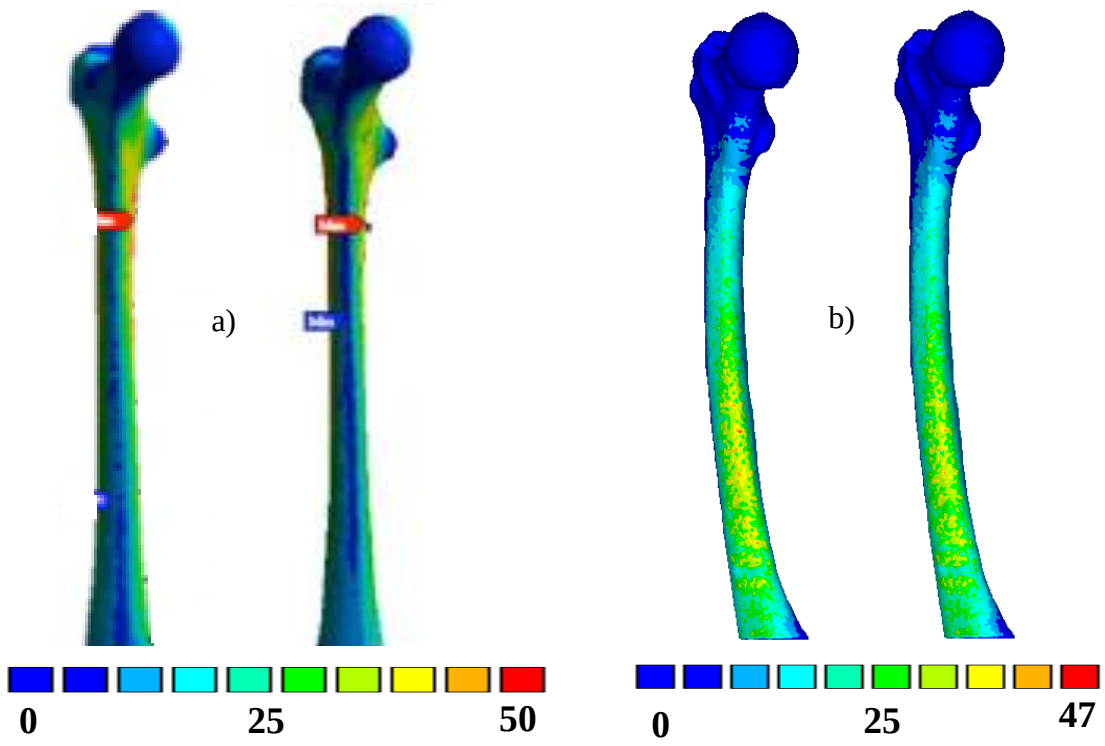

Figure 7.16 Comparison of the von Mises stress distribution between literature (a) and the current study (b) at 10% and 45% of the gait cycle.

The strain magnitudes in the current model are also much lower in comparison. This validation was inconclusive although stress distribution was similar to what has been reported in the literature. The orientation of the stress had minimal differences, these

variations may be due to the geometrical differences of the models. From Figure 7.16 it is clear to see that there is much more anteversion in the current study's model.

7.10 DISCUSSION

Throughout this thesis a number of differences between the studied age groups have been made apparent. This includes the changes in joint moments and GRF of the 3 year old during gait analysis, and the discoveries of such, along with this FEA, can help to develop an understanding of the development of the juvenile femur. The FEA performed in this chapter utilised the results and outcomes from previous chapters. The aim was to identify high and low concentrations of stress that are produced due to loading the femur undergoes throughout the age specific gait cycle. Each model was analysed at 7 stages of the gait cycle; 2%, 10%, 20%, 30%, 45%, 70% and 98%; furthermore, a unique analysis was used to observe the stress the femur experiences during the full gait cycle. These results provided a comprehensive overview of the mechanical stress which is experienced throughout growth and development.

The comparison models in this chapter showed that the loading of the femur and the stresses achieved in all models were comparable to literature. The only comparison possible for the juvenile models was by comparing stresses observed in the cartilaginous growth plate of the femoral head. These results showed the distribution in the growth plate were similar to Carriero *et al's* (2011) study, indicating that the hip loading was correct. The muscle loading is very difficult to validate, although the muscle forces derived in Chapter 5 and 6 would imply that the loading regime is correct. The comparison of the adult model when compared to Wagner *et al,* (2010) (Figure 7.16) had differences however these could be due to geometrical differences in the adult femur. The effect of geometry has been discussed in the literature review (Chapter 2.5.1), where Lenaerts *et al* (2008) compared three different models and found their differing geometries affected the stress distribution. This is apparent with the comparison model, however the magnitudes of stress observed in both models were much lower in the current model, but the distributions were not entirely dissimilar. The comparison was not convincing, however further comparisons to the literature will be made throughout this discussion to ensure the findings are comparable to literature.

Generalising the results the models show some similarities and differences in the distribution of the stress and strains. The areas which have a high magnitude of stress are in similar locations in all models but some differences occur in how the stress dissipates from the peak area and also some differences in the magnitudes of stress between the swing and stance phase for each model. These differences and similarities are to be discussed in relation to the applied forces.

The novel method of analysing cumulative stress between the models can give a comprehensive view of the peak strain experienced during the full gait cycle. The adult model showed a different concentration of stresses compared to the juvenile femora. In the adult model the peak stresses were found to be on the intertrochanteric notch, whereas in the juvenile models the peak stresses were found on the greater trochanter and around the growth plate of the femoral head, despite the cartilage being removed from the analysis. These could be an artefact from the lower Young's modulus applied to the cartilage and the high stress is a result from the force being transferred to the bone through the cartilage, therefore the high strains found here may not be accurate. Another high concentration of strains in the femoral head from the cumulative strain was found on the distal portion of the femoral neck in all models. The variation in the position of this strain changed from the juvenile models to the adult, with a more posteriorly positioned strain in the adult model and anteriorly in the juvenile models. This may be indicative of an effect from the loading applied to the models, the specifics of which will be discussed in this section. The advantage of using this cumulative stress method allows the researcher to identify peak stress distributions in all models irrelevant of the load case, providing an overall view of the loaded femur.

Data obtained for the trabecular strain of the femoral neck compared well to findings in the literature. Klodowski *et al,* (2012) studied the strains in the femoral neck during walking, and found that the lateral aspect of the femur during peak hip contact, reached strains of 1020με and in swing phase values of 200-400με being observed. In the present study, the lateral aspect of the neck showed values of 1200με at peak hip contact and 180-440με during swing phase. The juvenile femora showed much larger strain levels, this however could be due to the cartilage in this region of the femur, therefore this comparison is difficult to make. In the adult model of the femur the peak areas of stress were located in

similar areas during all load cases. However the juvenile models showed varied peak areas of stress. In the 3 year old the peak load on the distal portion of the femoral neck moved anteriorly as the gait cycle progresses. Similarly, the 7 year old model showed the same anterior movement of the peak stress area which is interesting because the muscle force patterns and JRF were not significantly different to the muscle forces in the adult. This may indicate that the bone in the juvenile is not entirely adapted to the changes in load experienced throughout the gait cycle, whereas the adult model is and thus the peak areas of stress remain located in the same position. It could be used to explain the morphological changes in the femur observed during growth between these ages. Previous studies have suggested low habitual loading levels have the ability to remodel bone as well as large load levels (Rubin *et al*, 2002). Therefore despite the loading patterns varying during the swing phase of gait, where stress and strains are low, the areas of peak stress may still contribute to the remodelling of the femur during swing phase. Furthermore comparison between the highest areas of stress during stance and swing phase reveal that the 3 year old, compared to the other models, has a much higher stance/swing difference. It could be said because of this, that the stance phase is one of the most important phases for driving bone development. Therefore in younger age groups it may be possible that the increased double support phase (Lythgo, 2011) may help to increase the bone development and explain the initial high rate the femur develops at before decreasing in speed with age. The temporal spatial parameters such as stance time and double support time may be the driving force of the rate of development, whereas the changes in kinetic and muscle force data could give the direction in which the development occurs.

The 3 year old and the 7 year old showed a higher overall strain at 10% and 20% of the gait cycle compared to the adult where the peak strain was found at 45% of the gait cycle. As discussed more extensively in Chapter 6, the explanation could be due to an immature gait pattern and a lack of control in the initial foot contact. As the largest strain was found in the 3 year old, again this would agree with the JRF force of the hip produced in the musculoskeletal analysis, where the largest value of 537% BW was found in the 3 year old compared to the adults value of 265% BW. The strains in the femoral head of the 3 year old were found to be above the physiological ranges of bone formation as reported by Martin (2000) however this could be due to the larger JRF's observed. The effect of these large

strains, according the Martin's remodelling model (Figure 2.2), would have put the remodelling rate into overload and possibly damaged the bone.

The results of the present study revealed similarities in stress/strain of the different models. This could be because all the models are optimised, to the same extent as each other, to the individual loads that are being applied to them and therefore no major differences. For instance, all models are highly stressed at the femoral neck and at the intertrochanteric notch, and low stress is observed on the middle part of the anterior portion of the femoral neck. in the stress/strain distributions would be expected. However, as the 7 year old model showed some differences specifically during stance and at the femoral neck. During the gait cycle the 7 year old model showed the largest differences between the stance and swing phase, during the stance phase the stress in the femoral neck was oriented centrally and dissipates posteriorly to the lesser trochanter. However during the swing phase there is no stress in this area of the femur and instead there is a high stress observed in the lateral portion of the neck in an anterior position. This is different to the adult and 3 year old models where there is still a large portion of the femoral neck under high stress during the swing phase and during the stance phase, as the stress is focused much more anteriorly when compared to the 7 year old model. This may be due to the similarity of the gait pattern to that of the adult model and therefore because the 7 year old model still had geometrical differences but was been loaded very similar the differences maybe where the model was not optimised as the adult femur. For future work it would be insightful to see if this was the case by loading the juvenile models with adult loading patterns. It would be expected that the models would have higher stresses as they would not be adapted to the loads of a different gait pattern. Recent work by Djuric *et al* , (2012) analysed changes of trabecular and cortical bone in the proximal femur as age progresses; from one month to 14 years. It was observed that the structure of the femur changes dramatically up until the age of 3 years, internally and externally, and these changes were hypothesised to be associated with changes in locomotion. Further still trabecular, eccentricity was observed to be higher in the medial portion of the neck, which was proposed to be a bone adaptive response to loading. As was the case in the present results, high strains were found on the medial portion of the neck, suggesting an area of high bone growth. The results in this FEA appear to fit well with the literature with regards to what occurs *in vivo.*

No work prior to this thesis has evaluated the stress and strain patterns of the femur during development and growth in a range of ages and using age specific gait. The analysis has revealed that the stress distribution is similar between the models, which could infer that the models are each equally optimised to deal with the loads that are experienced during walking despite the geometrical differences. It is however unclear whether gait maturation would drive these changes but the difference in locomotion seemed to, from these results, have some effect on the loading of the femur. This needs to be explained in terms of how this may affect the growth and development at this stage. Beyond the age of 3 years the ossification of the femur is less dramatic than that seen in early stages, although the structural shape is very dynamic and these results would seem to suggest gait changes play a role in this. However, this is dependent on how typical the gait pattern is of the 3 year old analysed in this study. This FEA has produced some differences between the different ages of femora in the stress and strain observed. However there are a number of obvious limitations to the models. Firstly is one which was brought to attention in Chapter 6. The moment arms of the muscle line of action from the musculoskeletal modelling would have been affecting moment arm and thus the force of the muscles applied to the model. The lack of ligamentous structures applied in this model, according to literature, would have had an effect on the results. Pauwels (1980) stated that the application of the ligaments moved the vector of the stress in the vertical axis to the centre of the diaphysis resulting in a compressive stress in the shaft of the femur. In the current study due to the automated process of the musculoskeletal modelling, then the force applied by the ligaments would be difficult to compute, however this may be necessary to gather more accurate results.

8 CONCLUSION

This thesis aimed to investigate the mechanical loading that the human proximal femur undergoes during growth and development, and evaluate the stress and strains which are apparent. These stresses and strains are a product of the loads experienced during activities of daily living at different stages of bipedal locomotion development. Ontogenetic studies have shown that there are similarities between the loads experienced during gait and the bone structure observed in the femur. However no study had, up until now, analysed the growth of the femur throughout bipedal locomotion development. Evaluation of the stresses and strains of the femur at three stages of femoral development revealed that each model was as structurally adapted to deal with the applied loads as the other models.

Digitisations of the cadaveric specimens were difficult due to the dry nature of the specimens. The models constructed from two separate sources, MRI and CT scans, were developed with good accuracy but ideally the models would have been one entity. Much of the work performed at this stage could have been more efficient with access to specimens in their entirety. Regardless, the aims of this chapter were fulfilled and fully articulated specimens were able to be modelled and subsequent modelling took place.

Gait analysis of the children revealed that there is very little difference in the kinematics between children and adults. Although the subject numbers were low, the results were comparable to previous results in the literature, and thus deemed a true representative of children's gait. The kinetic analysis however showed some differences in the GRF's with the 3 year old producing higher forces in the heel strike compared to toe off, opposite to the other models. Further results of the joint moments, again in the 3 year old, revealed a different pattern of force during the gait cycle compared to the older subjects. The GRF and joint moments suggest an immature gait is still adopted by the 3 year old subject used in the current study, this agrees with previous research.

Musculoskeletal modelling of children's gait was performed to derive muscle forces to be used in the FEA. Musculoskeletal modelling of children was a novel result which had previously not been performed on children under the age of 6 years. These results revealed that the 3 year old showed the most significant muscle activity when compared to the other children's data and the adults. Specifically hip flexor and abductor forces were seen to

significantly differ from all other age groups. The differences observed in the modelling results supported the gait analysis conclusion that the 3 year old subject had an immature gait pattern. These results had important implications on how the model was loaded during FEA and what the outcome of the analysis was.

The finite element analysis revealed that the varying gait patterns and muscle activity produced similar predicted von Mises stress/strain distributions in the 3 year old, 7 year old and adult models. From this it could be surmised that each model is as adapted to the loads that it experiences during gait as the other models, irrelevant of age. Because of the differences observed in the muscle forces, which were applied to the models, it could further be said that the femur needs the maturation of gait to take place to develop its structure from a juvenile to an adult femur. It is suggested future work should load the 3 year and 7 year old model with adult muscle force's and JRF's to discover what effect this would have on the stresses and strains in the femur. This would reveal if the femur is structurally adapted to any type of physiological loading or if in fact it is adapted to a specific type of physiological loading i.e. age specific. A question of how mechanical influence effects bone development during growth could then be tested. Concentrations of high stress in the trabecular bone were observed on the distal portion of the neck of the femur which is a result of the hip loading. This high area of stress is expected because it is an area of dense trabecular bone, present because of this mechanical influence. The small differences found between the models were how the peak areas of stress dissipated as the stages of gait progressed. Anterior movement of the peak stresses were observed in the 3 year old and 7 year old models, whereas in the adult the location remained the same throughout. This could be an indication that the juvenile models were still not fully adapted to these loads and that this variation in stress and strain could be the driver of further adaptation of bone structure.

The magnitudes of strain observed in the femur were higher than the accepted physiological rate (Martin, 2000), this could be due to the necessity of a larger strain rate to promote bone modelling. However it is much more likely that the models require a more physiological loading regime including ligaments and other soft tissue that are imperative to the function of the femur. Greater variability in the strain patterns may have been observed if the research modelled more dramatic changes of locomotion i.e. crawling to walking. The

subtle changes leading from an immature gait pattern to a mature gait pattern make it difficult to make solid conclusions from these findings.

A number of limitations to this research did not allow for some interesting areas of work to be performed which would have added to the thesis. These areas of work will be discussed as future directives but first it is important to discuss what these limitations are. Primarily the specimens initially used for modelling were dry (missing cartilage) and this, as discussed previously, would not allow full FEA to be performed. A number of methods were explored to produce a full model from these specimens, these included the work produced in Appendix III. Once the fully articulated specimens were acquired the methods were no longer required. But this work had reduced the available time left to produce the models for FEA. Thus reducing the time available to perform an extensive FEA i.e. FEA of running movement. Similarly the musculoskeletal modelling was time restrictive due to the software (AnyBody) being in the early stages of development and therefore the use of the software was more difficult and more time consuming than anticipated. Due to software development this limitation would now be eradicated.

9 FUTURE WORK

Although this study was successful at evaluating the stresses and strains experienced in the femur from an immature gait pattern through to a mature gait pattern further ages need to be explored. A greater understanding of the development of the femur would be made when studying different forms of locomotion within the attainment of bipedal locomotion. These would include, but not only extend to, crawling and the initial stages of independent standing. Further still different forms of bipedal locomotion should be analysed for all ages, such as running. Initial work has been performed building musculoskeletal models of an adult running (Figure 9.1). This should be extended to other activities such as stair walking and jumping.

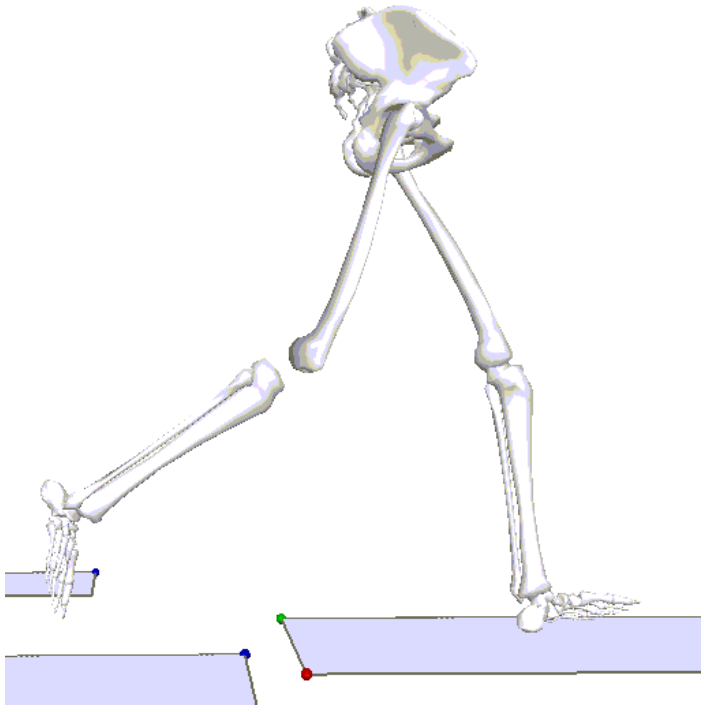

Figure 9.1 Motion capture image of human running.

The present work offered a comprehensive overview of developing locomotion, however further work is needed. This in depth analysis of human locomotion would, if produced in full, show how the femur is developed. Hammer (2010), whilst studying the trabecular

growth in the femur, stated that the trabecular lines, referred to as principle tensile group, are in fact responsible for transferring the compressive stress during a squat. Therefore an analysis of full human movements would confirm this theory.

The musculoskeletal modelling of children is required to be more specific so that true geometries of bones and lines of action of muscles can be modelled in FEA, this could be produced through the use of MRI. It has the ability to not only allow digitisation of the bone structure, but it is also possible to identify the soft tissue structures which could be useful in developing subject specific models. With extra information the musculoskeletal models would be more specific than those used in the current work, which inevitably are scaled adult models. To increase the subject specificity the participants that are recruited for MRI scans could have their gait analysed and the true loading regime on the bones would be available. These future work suggestions could be produced with more time and resources, but to fully understand the growth of bone, subject specific and longitudinal studies need to be analysed. This would require research to follow subjects throughout growth and development taking, measurements and gait analysis at intervals to match the bone development to the gait pattern.

The work in Appendix III, as stated, is not complete and therefore this area of work will be continued. The goal of the research is to show that osteogenesis can occur under a compressive state. From the successful simulation of ossification in the simply loaded 2D models through a number of developmental stages, a more complex 3D model will be produced. Using the FE model developed in Chapter 3 the development of the femur throughout growth will be simulated under the assumption that compression will encourage bone growth.

Work in prenatal and neonatal development would be a valuable direction for future work. Quantifying movements in the very young and *in utero* would however be a very difficult task because the movements are very different to gait patterns. Thus the differences between adults mechanically induced growth and prenatal /neonatal would be easier to identify. *In utero* analysis of movement would require the use of 4D ultrasonography and even then to quantify the movements would be difficult. Capturing movements at neonatal age would be very time consuming. The difficulty would be collecting clean force plate data that musculoskeletal modelling could be computed from. This task would require

specialist force plates, to capture small strides, but with the correct equipment the change from crawling to bipedal locomotion could be captured, allowing for FEA to be performed identifying the different stresses the femur would experience under different forms of locomotion.

Finally, addressing future work which could be performed on the FEA would involve the sensitivity of the models used. One element of the models which perhaps would be important and need to be age specific is the thickness of the cortical shell. In the current study the thickness was estimated from previous literature (Chapter 7). However to get more accurate results, a number of methods in future could be employed, one of these can be seen in Figure 9.2. This would involve taking cross sections of the scanned specimen at regular intervals and measuring the cortical thickness to improve the accuracy of modelling in FEA.

.

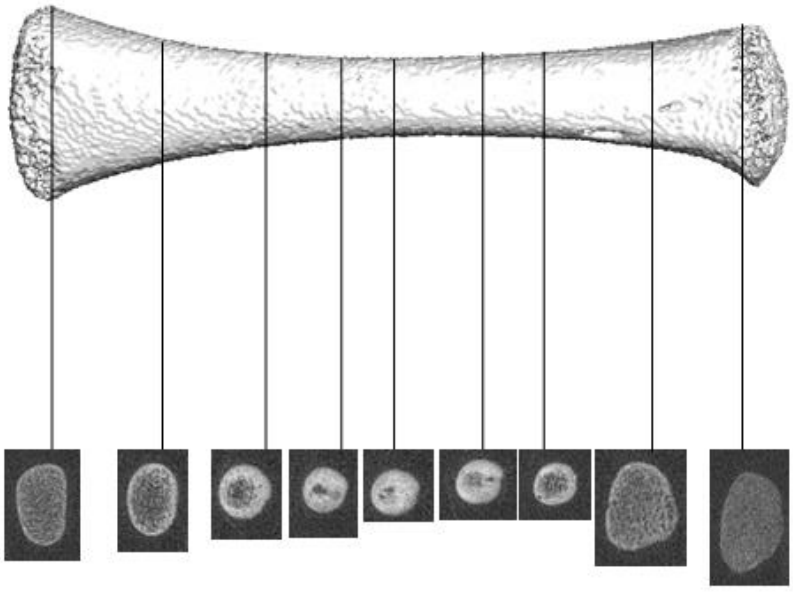

Figure 9.2 Cross section images of a prenatal femur, identifying the cortical shell thickness.

REFERENCES

ANDERSON, M., MESSNER, M. B. & GREEN, W. T. 1964. Distribution of Lengths of the Normal Femur and Tibia in Children from One to Eighteen Years of Age. *J Bone Joint Surg Am,* 46**,** 1197-202.

ALMI, R, C., BALL, R, H., WHEELER, M, E. 2006. Human Fetal and Neonatal Movement Patterns: Gender Differences and Fetal-to-Neonatal Continuity, *Dev Psychobiol* 38, 252-273.

ASSAIANTE, C. 1998. Development of locomotor balance control in healthy children. *Neuroscience and Biobehavioral Reviews,* 22**,** 527-532.

BARBU-ROTH, M., ANDERSON, D. I., DESPRES, A., PROVASI, J., CABROL, D. & CAMPOS, J. J. 2009. Neonatal stepping in relation to terrestrial optic flow. *Child Dev,* 80**,** 8-14.

BAYRAKTAR, H. H., MORGAN, E. F., NIEBUR, G. L., MORRIS, G. E., WONG, E. K. & KEAVENY, T. M. 2004. Comparison of the elastic and yield properties of human femoral trabecular and cortical bone tissue. *Journal of Biomechanics,* 37**,** 27-35.

BECK, R. J., ANDRIACCHI, T. P. & KUO, K. N. 1981. Changes in the gait patterns of growing children. *Journal of Bone and Joint Surgery - Series A,* 63**,** 1452-1457.

BERGER, S. E., THEURING, C. & ADOLPH, K. E. 2007. How and when infants learn to climb stairs. *Infant Behav Dev,* 30**,** 36-49.

BERGER, W., QUINTERN, J. & DIETZ, V. 1987. Afferent and efferent control of stance and gait: Developmental changes in children. *Electroencephalography and Clinical Neurophysiology,* 66**,** 244-252.

BERGMANN, G., DEURETZBACHER, G., HELLER, M., GRAICHEN, F., ROHLMANN, A., STRAUSS, J. & DUDA, G. N. 2001. Hip contact forces and gait patterns from routine activities. *J Biomech,* 34**,** 859-71.

BISI, M. C., STAGNI, R., HOUDIJK, H. & GNUDI, G. 2011. An EMG-driven model applied for predicting metabolic energy consumption during movement. *Journal of Electromyography and Kinesiology,* 21**,** 1074-1080.

BITSAKOS, C., KERNER, J., FISHER, I. & AMIS, A. A. 2005. The effect of muscle loading on the simulation of bone remodelling in the proximal femur. *J Biomech,* 38**,** 133-9.

BONNEAU, N., SIMONIS, C., SERINGE, R. & TARDIEU, C. 2011. Study of femoral torsion during prenatal growth: Interpretations associated with the effects of intrauterine pressure. *American Journal of Physical Anthropology,* 145**,** 438-445.

BOYLE, W. J., SIMONET, W. S. & LACEY, D. L. 2003. Osteoclast differentiation and activation. *Nature,* 423**,** 337-342.

BRAND, R. A., CROWNINSHIELD, R. D., WITTSTOCK, C. E., PEDERSEN, D. R., CLARK, C. R. & VAN KRIEKEN, F. M. 1982. MODEL OF LOWER EXTREMITY MUSCULAR ANATOMY. *J BIOMECH ENG TRANS ASME,* V 104**,** 304-310.

BULANDRA, A., GIELECKI, J. S., LECIEJEWSKA, I., KARASZEWSKI, P. & SIEROŃ, D. 2003. Digital-image analysis of the femoral shaft/neck angle in human foetuses. *Folia Morphologica,* 62**,** 415-417.

CARPENTER, R. D. & CARTER, D. R. 2008. The mechanobiological effects of periosteal surface loads. *Biomechanics and Modeling in Mechanobiology,* 7**,** 227-242.

CARRIERO, A., JONKERS, I. & SHEFELBINE, S. J. 2010. Mechanobiological prediction of proximal femoral deformities in children with cerebral palsy. *Comput Methods Biomech Biomed Engin***,** 1.

CARRIERO, A., ZAVATSKY, A., STEBBINS, J., THEOLOGIS, T. & SHEFELBINE, S. J. 2009. Determination of gait patterns in children with spastic diplegic cerebral palsy using principal components. *Gait Posture,* 29**,** 71-5.

CARTER, D. R. & BEAUPRÉ, G. S. 2001. *Skeletal function and form : mechanobiology of skeletal development, aging, and regeneration,* Cambridge ; New York, Cambridge University Press.

CARTER, D. R., VAN DER MEULEN, M. C. & BEAUPRE, G. S. 1996. Mechanical factors in bone growth and development. *Bone,* 18**,** 5S-10S.

CARTER, D. R. & WONG, M. 1988a. Mechanical stresses and endochondral ossification in the chondroepiphysis. *J Orthop Res,* 6**,** 148-54.

CARTER, D. R. & WONG, M. 1988b. The role of mechanical loading histories in the development of diarthrodial joints. *J Orthop Res,* 6**,** 804-16.

CHESTER, V. L., TINGLEY, M. & BIDEN, E. N. 2006. A comparison of kinetic gait parameters for 3-13 year olds. *Clinical Biomechanics,* 21**,** 726-732.

CIONI, G., DUCHINI, F., MILIANTI, B., PAOLICELLI, P. B., SICOLA, E., BOLDRINI, A. & FERRARI, A. 1993. Differences and variations in the patterns of early independent walking. *Early Human Development,* 35**,** 193-205.

COWGILL, L. W., WARRENER, A., PONTZER, H. & OCOBOCK, C. 2010. Waddling and toddling: The biomechanical effects of an immature gait. *American Journal of Physical Anthropology,* 143**,** 52-61.

CRISTOFOLINI, L., JUSZCZYK, M., TADDEI, F. & VICECONTI, M. 2009. Strain distribution in the proximal human femoral metaphysis. *Proc Inst Mech Eng H,* 223**,** 273-88.

CRISTOFOLINI, L., VICECONTI, M., CAPPELLO, A. & TONI, A. 1996. Mechanical validation of whole bone composite femur models. *J Biomech,* 29**,** 525-35.

CRISTOFOLINI, L., VICECONTI, M., TONI, A. & GIUNTI, A. 1995. Influence of thigh muscles on the axial strains in a proximal femur during early stance in gait. *J Biomech,* 28**,** 617-24.

CROWNINSHIELD, R. D. & BRAND, R. A. 1981. A physiologically based criterion of muscle force prediction in locomotion. *Journal of Biomechanics,* 14**,** 793-801.

CROWNINSHIELD, R. D., JOHNSTON, R. C., ANDREWS, J. G. & BRAND, R. A. 1978. A biomechanical investigation of the human hip. *Journal of Biomechanics,* 11**,** 75-85.

CULMANN, K., 1866. Die Graphische Statik. Verlag von Meyer & Zeller, Zurich, Switzerland.

CURTIS, N., JONES, M. E. H., SHI, J., O'HIGGINS, P., EVANS, S. E. & FAGAN, M. J. 2011. Functional relationship between skull form and feeding mechanics in sphenodon, and implications for diapsid skull development. *PLoS ONE,* 6.

CUTTS, A. 1989. Sarcomere length changes in muscles of the human thigh during walking. *Journal of Anatomy,* 166**,** 77-84.

DALSTRA, M., HUISKES, R. & VAN ERNING, L. 1995. Development and validation of a three-dimensional finite element model of the pelvic bone. *Journal of Biomechanical Engineering,* 117**,** 272-278.

DELP, S. L. 1994. Transfer of the rectus femoris: Effects of transfer site on moment arms about the knee and hip. *Journal of Biomechanics,* 27**,** 1201-1211.

DELP, S. L., LOAN, J. P., HOY, M. G., ZAJAC, F. E., TOPP, E. L. & ROSEN, J. M. 1990. An interactive graphics-based model of the lower extremity to study orthopaedic surgical procedures. *IEEE Transactions on Biomedical Engineering,* 37**,** 757-767.

DOORENBOSCH, C. A. M., JOOSTEN, A. & HARLAAR, J. 2005. Calibration of EMG to force for knee muscles is applicable with submaximal voluntary contractions. *Journal of Electromyography and Kinesiology,* 15**,** 429-435.

DOUBE, M., WIKTOROWICZ-CONROY, A., CHRISTIANSEN, P., HUTCHINSON, J. R. & SHEFELBINE, S. 2009. Three-dimensional geometric analysis of felid limb bone allometry. *PLoS One,* 4**,** e4742.

DUDA, G. N., HELLER, M., ALBINGER, J., SCHULZ, O., SCHNEIDER, E. & CLAES, L. 1998. Influence of muscle forces on femoral strain distribution. *J Biomech,* 31**,** 841-6.

DUDA, G. N., SCHNEIDER, E. & CHAO, E. Y. S. 1997. Internal forces and moments in the femur during walking. *Journal of Biomechanics,* 30**,** 933-941.

EDWARDS, W. B., GILLETTE, J. C., THOMAS, J. M. & DERRICK, T. R. 2008. Internal femoral forces and moments during running: implications for stress fracture development. *Clin Biomech (Bristol, Avon),* 23**,** 1269-78.

ERDEMIR, A., MCLEAN, S., HERZOG, W. & VAN DEN BOGERT, A. J. 2007. Model-based estimation of muscle forces exerted during movements. *Clinical Biomechanics,* 22**,** 131-154.

FISK, J, A., 2004. Evaluating the accuracy of knee kinematics measured in six degrees of freedom using surface markers, *Unpublished. Masters Thesis, University of Pittsburgh.*

FORSSBERG, H. 1985. Ontogeny of human locomotor control. I. Infant stepping, supported locomotion and transition to independent locomotion. *Experimental Brain Research,* 57**,** 480-495.

FOX, J. C. & KEAVENY, T. M. 2001. Trabecular eccentricity and bone adaptation. *J Theor Biol,* 212**,** 211-21.

FROST, H. M. 1987. Bone "mass" and the "mechanostat": a proposal. *Anat Rec,* 219**,** 1-9.

FROST, H. M. 1990. Skeletal structural adaptions to mechanical usage (SATMU): 2. Redefining Wolff's law: The remodeling problem. *Anatomical Record,* 226**,** 414-422.

GANLEY, K. J. & POWERS, C. M. 2005. Gait kinematics and kinetics of 7-year-old children: A comparison to adults using age-specific anthropometric data. *Gait and Posture,* 21**,** 141-145.

GARCES, G. L. & SANTANDREU, M. E. 1988. Longitudinal bone growth after sciatic denervation in rats. *J Bone Joint Surg Br,* 70**,** 315-8.

GARDNER, E. & GRAY, D. J. 1970. The prenatal development of the human femur. *Am J Anat,* 129**,** 121-40.

GARGIULO, P., REYNISSON, P. J., HELGASON, B., KERN, H., MAYR, W., INGVARSSON, P., HELGASON, T. & CARRARO, U. 2011. Muscle, tendons, and bone: Structural changes during denervation and fes treatment. *Neurological Research,* 33**,** 750-758.

GLARD, Y., JOUVE, J. L., PANUEL, M., ADALIAN, P., TARDIEU, C. & BOLLINI, G. 2005. An anatomical and biometrical study of the femoral trochlear groove in the human fetus. *J Anat,* 206**,** 411-3.

GLITSCH, U. & BAUMANN, W. 1997. The three-dimensional determination of internal loads in the lower extremity. *J Biomech,* 30**,** 1123-31.

GRAY, H., WARWICK, R. & WILLIAMS, P. L. 1973. *Gray's anatomy,* London, Longman.

GRIMSHAW, P. N., MARQUES-BRUNA, P., SALO, A. & MESSENGER, N. 1998. The 3-dimensional kinematics of the walking gait cycle of children aged between 10 and 24 months: Cross sectional and repeated measures. *Gait and Posture,* 7**,** 7-15.

GROSS, T. S., POLIACHIK, S. L., PRASAD, J. & BAIN, S. D. 2010. The effect of muscle dysfunction on bone mass and morphology. *Journal of Musculoskeletal Neuronal Interactions,* 10**,** 25-34.

HALLEMANS, A., DE CLERCQ, D., OTTEN, B. & AERTS, P. 2005. 3D joint dynamics of walking in toddlers: A cross-sectional study spanning the first rapid development phase of walking. *Gait and Posture,* 22**,** 107-118.

HAMMER, A. 2002. Triangular structure of the proximal femur. *Clin Anat,* 15**,** 210-6.

HAMMER, A. 2010. The structure of the femoral neck: A physical dissection with emphasis on the internal trabecular system. *Annals of Anatomy,* 192**,** 168-177.

HEIMKES, B., POSEL, P., PLITZ, W. & JANSSON, V. 1993. Forces acting on the juvenile hip joint in the one-legged stance. *J Pediatr Orthop,* 13**,** 431-6.

HEINTZ, S. & GUTIERREZ-FAREWIK, E. M. 2007. Static optimization of muscle forces during gait in comparison to EMG-to-force processing approach. *Gait Posture,* 26**,** 279-88.

HELLER, M. O., BERGMANN, G., DEURETZBACHER, G., CLAES, L., HAAS, N. P. & DUDA, G. N. 2001a. Influence of femoral anteversion on proximal femoral loading: measurement and simulation in four patients. *Clin Biomech (Bristol, Avon),* 16**,** 644-9.

HELLER, M. O., BERGMANN, G., DEURETZBACHER, G., DURSELEN, L., POHL, M., CLAES, L., HAAS, N. P. & DUDA, G. N. 2001b. Musculo-skeletal loading conditions at the hip during walking and stair climbing. *J Biomech,* 34**,** 883-93.

HENDERSON, J. H. & CARTER, D. R. 2002. Mechanical induction in limb morphogenesis: The role of growth-generated strains and pressures. *Bone,* 31**,** 645-653.

HENNESSY, M. J., DIXON, S. D. & SIMON, S. R. 1984. The development of gait: a study in African children ages one to five. *Child development,* 55**,** 844-853.

HERIZA, C. B. 1988. Comparison of leg movements in preterm infants at term with healthy full-term infants. *Physical Therapy,* 68**,** 1687-1693.

HILLMAN, S. J., STANSFIELD, B. W., RICHARDSON, A. M. & ROBB, J. E. 2009. Development of temporal and distance parameters of gait in normal children. *Gait and Posture,* 29**,** 81-85.

HOF, A. L., ELZINGA, H., GRIMMIUS, W. & HALBERTSMA, J. P. K. 2002. Speed dependence of averaged EMG profiles in walking. *Gait and Posture,* 16**,** 78-86.

HOF, A. L., ELZINGA, H., GRIMMIUS, W. & HALBERTSMA, J. P. K. 2005. Detection of non-standard EMG profiles in walking. *Gait and Posture,* 21**,** 171-177.

HUISKES, R. 1990. The various stress patterns of press-fit, ingrown, and cemented femoral stems. *Clinical Orthopaedics and Related Research***,** 27-38.

HUISKES, R. 2000. If bone is the answer, then what is the question? *Journal of Anatomy,* 197**,** 145-156.

ISAAC, B., VETTIVEL, S., PRASAD, R., JEYASEELAN, L. & CHANDI, G. 1997. Prediction of the femoral neck-shaft angle from the length of the femoral neck. *Clin Anat,* 10**,** 318-23.

JAVAID, M. K., LEKAMWASAM, S., CLARK, J., DENNISON, E. M., SYDDALL, H. E., LOVERIDGE, N., REEVE, J., BECK, T. J. & COOPER, C. 2006. Infant growth influences proximal femoral geometry in adulthood. *J Bone Miner Res,* 21**,** 508-12.

JENG, S. F., CHEN, L. C. & YAU, K. I. T. 2002. Kinematic analysis of kicking movements in preterm infants with very low birth weight and full-term infants. *Physical Therapy,* 82**,** 148-159.

JENKINS, S. E., HARRINGTON, M. E., ZAVATSKY, A. B., O'CONNOR, J. J. & THEOLOGIS, T. N. 2003. Femoral muscle attachment locations in children and adults, and their prediction from clinical measurement. *Gait Posture,* 18**,** 13-22.

JENSEN, R. K. 1989. Changes in segment inertia proportions between 4 and 20 years. *Journal of Biomechanics,* 22**,** 529-536.

JONKERS, I., SAUWEN, N., LENAERTS, G., MULIER, M., VAN DER PERRE, G. & JAECQUES, S. 2008. Relation between subject-specific hip joint loading, stress distribution in the proximal femur and bone mineral density changes after total hip replacement. *J Biomech,* 41**,** 3405-13.

KELLER, T. S., WEISBERGER, A. M., RAY, J. L., HASAN, S. S., SHIAVI, R. G. & SPENGLER, D. M. 1996. Relationship between vertical ground reaction force and speed during walking, slow jogging, and running. *Clinical Biomechanics,* 11**,** 253-259.

KERRIGAN, D. C., TODD, M. K., DELLA CROCE, U., LIPSITZ, L. A. & COLLINS, J. J. 1998. Biomechanical gait alterations independent of speed in the healthy elderly: Evidence for specific limiting impairments. *Archives of Physical Medicine and Rehabilitation,* 79**,** 317-322.

KHARB, A., SAINI, V., JAIN, Y, K., DHIMAN, S. 2011. A review of gait cycle and its parameters. *International Journal of Computational Engineering & Management,* 13, 78-83.

KIM, J. E., LI, Z., ITO, Y., HUBER, C. D., SHIH, A. M., EBERHARDT, A. W., YANG, K. H., KING, A. I. & SONI, B. K. 2009. Finite element model development of a child pelvis with optimization-based material identification. *J Biomech,* 42**,** 2191-5.

KIMURA, T., YAGURAMAKI, N., FUJITA, M., OGIUE-IKEDA, M., NISHIZAWA, S. & UEDA, Y. 2005. Development of energy and time parameters in the walking of healthy human infants. *Gait and Posture,* 22**,** 225-232.

KIRTLEY, C. 2005. *Clinical gait analysis : theory and practice,* Edinburgh ; New York, Elsevier.

KLEIN HORSMAN, M. D., KOOPMAN, H. F., VAN DER HELM, F. C., PROSE, L. P. & VEEGER, H. E. 2007. Morphological muscle and joint parameters for musculoskeletal modelling of the lower extremity. *Clin Biomech (Bristol, Avon),* 22**,** 239-47.

KO, C. H., TSE, P. W. & CHAN, A. K. 2006. Risk factors of long bone fracture in non-ambulatory cerebral palsy children. *Hong Kong Med J,* 12**,** 426-31.

KUIPER, J. H. & HUISKES, R. 1996. Friction and stem stiffness affect dynamic interface motion in total hip replacement. *J Orthop Res,* 14**,** 36-43.

KUMMER B., 2005. *Biomechanik*. Deutsche Ärzte-Verlag, Köln.

KURJAK, A., POOH, R. K., MERCE, L. T., CARRERA, J. M., SALIHAGIC-KADIC, A. & ANDONOTOPO, W. 2005. Structural and functional early human development assessed by three-dimensional and four-dimensional sonography. *Fertility and Sterility,* 84**,** 1285-1299.

LAI, Y. M., QIN, L., YEUNG, H. Y., LEE, K. K. & CHAN, K. M. 2005. Regional differences in trabecular BMD and micro-architecture of weight-bearing bone under habitual gait loading--a pQCT and microCT study in human cadavers. *Bone,* 37**,** 274-82.

LAND, C. & SCHOENAU, E. 2008. Fetal and postnatal bone development: reviewing the role of mechanical stimuli and nutrition. *Best Pract Res Clin Endocrinol Metab,* 22**,** 107-18.

LEE, C.A. & EINHORN, T.A., 2001. *The Bone Organ System: Form and Function.* In: *Osteoporosis.* Second Edition, Edited by Marcus R, Feldman D, Kelsey J. San Diego,CA.

LENAERTS, G., DE GROOTE, F., DEMEULENAERE, B., MULIER, M., VAN DER PERRE, G., SPAEPEN, A. & JONKERS, I. 2008. Subject-specific hip geometry affects predicted hip joint contact forces during gait. *J Biomech,* 41**,** 1243-52.

LU, T. W., TAYLOR, S. J., O'CONNOR, J. J. & WALKER, P. S. 1997. Influence of muscle activity on the forces in the femur: an in vivo study. *J Biomech,* 30**,** 1101-6.

LYTHGO, N., WILSON, C. & GALEA, M. 2011. Basic gait and symmetry measures for primary school-aged children and young adults. II: Walking at slow, free and fast speed. *Gait and Posture,* 33**,** 29-35.

MARIEB, E. N. 2004. *Human anatomy & physiology*, New York, Pearson Education.

MARTIN, R. B. 2000. Toward a unifying theory of bone remodeling. *Bone,* 26**,** 1-6.

MILLER, F., SLOMCZYKOWSKI, M., COPE, R. & LIPTON, G. E. 1999. Computer modeling of the pathomechanics of spastic hip dislocation in children. *J Pediatr Orthop,* 19**,** 486-92.

MILLER, M. E. 2003. The bone disease of preterm birth: a biomechanical perspective. *Pediatr Res,* 53**,** 10-5.

MODLESKY, C. M., SUBRAMANIAN, P. & MILLER, F. 2008. Underdeveloped trabecular bone microarchitecture is detected in children with cerebral palsy using high-resolution magnetic resonance imaging. *Osteoporos Int,* 19**,** 169-76.

MORIMOTO, N., DE LEÓN, M. S. P. & ZOLLIKOFER, C. P. 2011. Exploring Femoral Diaphyseal Shape Variation in Wild and Captive Chimpanzees by Means of Morphometric Mapping: A Test of Wolff's Law. *Anatomical Record,* 294**,** 589-609.

MUNIH, M. & KRALJ, A. 1997. Modelling muscle activity in standing with considerations for bone safety. *J Biomech,* 30**,** 49-56.

MUNIH, M., KRALJ, A. & BAJD, T. 1992. Bending moments in lower extremity bones for two standing postures. *J Biomed Eng,* 14**,** 293-302.

MURRAY, P.D.F., 1936. *Bones: A Study of the Development and Structure of the Vertebrate Skeleton*. Cambridge University Press, Cambridge, UK. In: SKEDROS AND BAUCOM. 2007.

NEWELL, R. L. M. 1997. The calcar femorale: A tale of historical neglect. *Clinical Anatomy,* 10**,** 27-33.

NORKIN, C.C. AND P.K. LEVANGIE. 1983. *The hip complex. In Joint Structure and Function*. Philadelphia.

O'BRIEN, T. D., REEVES, N. D., BALTZOPOULOS, V., JONES, D. A. & MAGANARIS, C. N. 2009. Moment arms of the knee extensor mechanism in children and adults. *Journal of Anatomy,* 215**,** 198-205.

O'BRIEN, T. D., REEVES, N. D., BALTZOPOULOS, V., JONES, D. A. & MAGANARIS, C. N. 2010. Mechanical properties of the patellar tendon in adults and children. *Journal of Biomechanics,* 43**,** 1190-1195.

OEFFINGER, D.J., AUGSBURGER, S., CUPP, T., (1997) Age Related Changes In Able-Bodied Populations. *Gait and Posture,* 5**,** 155-156.

ÖHMAN, C., BALEANI, M., PANI, C., TADDEI, F., ALBERGHINI, M., VICECONTI, M. & MANFRINI, M. 2011. Compressive behaviour of child and adult cortical bone. *Bone,* 49**,** 769-776.

OSBORNE, D., EFFMANN, E., BRODA, K. & HARRELSON, J. 1980. The development of the upper end of the femur, with special reference to its internal architecture. *Radiology,* 137**,** 71-6.

PANATTONI, G. L., D'AMELIO, P., DI STEFANO, M. & ISAIA, G. C. 2000. Ossification centers of human femur. *Calcif Tissue Int,* 66**,** 255-8.

PARFITT, A, M., 2008. Pathophysiology of bone fragility. In *Proceedings of the Fourth International Symposium on Osteoporosis.*

PAUWELS, F.,1980. *Biomechanics of the Locomotor Apparatus*: *Contributions on the Functional Anatomy of the Locomotor Apparatus*. New York: Springer.

PEDERSEN, D. R., BRAND, R. A., CHENG, C. & ARORA, J. S. 1987. DIRECT COMPARISON OF MUSCLE FORCE PREDICTIONS USING LINEAR AND NONLINEAR PROGRAMMING. *Journal of Biomechanical Engineering,* 109**,** 192-199.

PHILLIPS, A. T. 2009. The femur as a musculo-skeletal construct: a free boundary condition modelling approach. *Med Eng Phys,* 31**,** 673-80.

PIEK, J. P. 1996. A quantitative analysis of spontaneous kicking in two-month-old infants. *Human Movement Science,* 15**,** 707-726.

PIERRYNOWSKI, M. R. & GALEA, V. 2001. Enhancing the ability of gait analyses to differentiate between groups: Scaling gait data to body size. *Gait and Posture,* 13**,** 193-201.

POLGAR, K., GILL, H. S., VICECONTI, M., MURRAY, D. W. & O'CONNOR, J. J. 2003a. Development and numerical validation of a finite element model of the muscle standardized femur. *Proc Inst Mech Eng H,* 217**,** 165-72.

POLGAR, K., GILL, H. S., VICECONTI, M., MURRAY, D. W. & O'CONNOR, J. J. 2003b. Strain distribution within the human femur due to physiological and simplified loading: finite element analysis using the muscle standardized femur model. *Proc Inst Mech Eng H,* 217**,** 173-89.

QIAN, J. G., SONG, Y. W., TANG, X. & ZHANG, S. 2009. Examination of femoral-neck structure using finite element model and bone mineral density using dual-energy X-ray absorptiometry. *Clin Biomech (Bristol, Avon),* 24**,** 47-52.

RAMOS, A. & SIMÕES, J. A. 2006. Tetrahedral versus hexahedral finite elements in numerical modelling of the proximal femur. *Medical Engineering and Physics,* 28**,** 916-924.

RIBBLE, T. G., SANTARE, M. H. & MILLER, F. 2001. Stresses in the growth plate of the developing proximal femur. *Journal of Applied Biomechanics,* 17**,** 129-141.

ROBERTSON, D. G. E. & WINTER, D. A. 1980. Mechanical energy generation, absorption and transfer amongst segments during walking. *Journal of Biomechanics,* 13**,** 845-854.

RODRIGUEZ, J. I., PALACIOS, J., GARCIA-ALIX, A., PASTOR, I. & PANIAGUA, R. 1988. Effects of immobilization on fetal bone development. A morphometric study in newborns with congenital neuromuscular diseases with intrauterine onset. *Calcif Tissue Int,* 43**,** 335-9.

ROUX, W., 1912. Anpassungslehre, Histomechanik,Histochemie. Mit Bemerkunngen uber die Entwicklung und Formgestaltung der Gelenke [Adaptation, Histomechanics, Histochemistry. With Comments on the Development and Morphology of the Joints]. Virchows Arch 207: 168-209

RUBIN, C., TURNER, A. S., MULLER, R., MITTRA, E., MCLEOD, K., LIN, W. & QIN, Y. X. 2002. Quantity and quality of trabecular bone in the femur are enhanced by a strongly anabolic, noninvasive mechanical intervention. *J Bone Miner Res,* 17**,** 349-57.

RUDMAN, K. E., ASPDEN, R. M. & MEAKIN, J. R. 2006. Compression or tension? The stress distribution in the proximal femur. *Biomed Eng Online,* 5**,** 12.

RUFF, C. 2003a. Growth in bone strength, body size, and muscle size in a juvenile longitudinal sample. *Bone,* 33**,** 317-29.

RUFF, C. 2003b. Ontogenetic adaptation to bipedalism: age changes in femoral to humeral length and strength proportions in humans, with a comparison to baboons. *J Hum Evol,* 45**,** 317-49.

RUFF, C. 2007. Body size prediction from juvenile skeletal remains. *American Journal of Physical Anthropology,* 133**,** 698-716.

RYAN, T. M. & KROVITZ, G. E. 2006. Trabecular bone ontogeny in the human proximal femur. *J Hum Evol,* 51**,** 591-602.

SCHEUER, L. & BLACK, S. M. 2000. *Developmental juvenile osteology,* San Diego, CA, Academic Press.

SCHEUER, L. & BLACK, S. M. 2005. *The juvenile skeleton,* London ; San Diego, Calif., Elsevier Academic Press.

SCHEYS, L., DESLOOVERE, K., SUETENS, P. & JONKERS, I. 2011. Level of subject-specific detail in musculoskeletal models affects hip moment arm length calculation during gait in pediatric subjects with increased femoral anteversion. *Journal of Biomechanics,* 44**,** 1346-1353.

SCHEYS, L., JONKERS, I., LOECKX, D., MAES, F., SPAEPEN, A. & SUETENS, P. 2006. Image based musculoskeletal modeling allows personalized biomechanical analysis of gait.

SCHEYS, L., VAN CAMPENHOUT, A., SPAEPEN, A., SUETENS, P. & JONKERS, I. 2008. Personalized MR-based musculoskeletal models compared to rescaled generic models in the presence of increased femoral anteversion: effect on hip moment arm lengths. *Gait Posture,* 28**,** 358-65.

SCOTT, J. H. 1957. Muscle growth and function in relation to skeletal morphology. *Am J Phys Anthropol,* 15**,** 197-234.

SELBER, P., DE GODOY, W. Childrens Gait Data, via the Clinical Gait Analysis Normative Database.

SERRAT, M. A., RENO, P. L., MCCOLLUM, M. A., MEINDL, R. S. & LOVEJOY, C. O. 2007. Variation in mammalian proximal femoral development: comparative analysis of two distinct ossification patterns. *J Anat,* 210**,** 249-58.

SHEFELBINE, S. J. & CARTER, D. R. 2004a. Mechanobiological predictions of femoral anteversion in cerebral palsy. *Ann Biomed Eng,* 32**,** 297-305.

SHEFELBINE, S. J. & CARTER, D. R. 2004b. Mechanobiological predictions of growth front morphology in developmental hip dysplasia. *J Orthop Res,* 22**,** 346-52.

SHEFELBINE, S. J., TARDIEU, C. & CARTER, D. R. 2002. Development of the femoral bicondylar angle in hominid bipedalism. *Bone,* 30**,** 765-70.

SILVESTRI, C. & RAY, M. H. 2009. Development of a finite element model of the knee-thigh-hip of a 50th percentile male including ligaments and muscles. *International Journal of Crashworthiness,* 14**,** 215-229.

SIMOES, J. A., VAZ, M. A., BLATCHER, S. & TAYLOR, M. 2000. Influence of head constraint and muscle forces on the strain distribution within the intact femur. *Med Eng Phys,* 22**,** 453-9.

SISIAS, G., PHILLIPS, R., LANGTON, C.M., DOBSON, C. A., FAGAN, M. J., GANNEY, P.S., 2001. DXA to FEM Converter 2.

SODERBERG, G. L. & DOSTAL, W. F. 1978. Electromyographic study of three parts of the gluteus medius muscle during functional activities. *Physical Therapy,* 58**,** 691-696.

SOMMERFELDT, D. & RUBIN, C. 2001. Biology of bone and how it orchestrates the form and function of the skeleton. *European Spine Journal,* 10**,** S86-S95.

SPEIRS, A. D., HELLER, M. O., DUDA, G. N. & TAYLOR, W. R. 2007. Physiologically based boundary conditions in finite element modelling. *J Biomech,* 40**,** 2318-23.

SPOOR, C. W., VAN LEEUWEN, J. L., DE WINDT, F. H. & HUSON, A. 1989. A model study of muscle forces and joint-force direction in normal and dysplastic neonatal hips. *J Biomech,* 22**,** 873-84.

STANSFIELD, B. W., HILLMAN, S. J., HAZLEWOOD, M. E., LAWSON, A. M., MANN, A. M., LOUDON, I. R. & ROBB, J. E. 2003. Normalisation of gait data in children. *Gait and Posture,* 17**,** 81-87.

STANSFIELD, B. W., HILLMAN, S. J., HAZLEWOOD, M. E. & ROBB, J. E. 2006. Regression analysis of gait parameters with speed in normal children walking at self-selected speeds. *Gait and Posture,* 23**,** 288-294.

STEVENS, S. S., BEAUPRE, G. S. & CARTER, D. R. 1999. Computer model of endochondral growth and ossification in long bones: biological and mechanobiological influences. *J Orthop Res,* 17**,** 646-53.

STOKES, I. A. 2002. Mechanical effects on skeletal growth. *J Musculoskelet Neuronal Interact,* 2**,** 277-80.

SUTHERLAND, D. 1997. The development of mature gait. *Gait and Posture,* 6**,** 163-170.

SUTHERLAND, D., PIKE, L., KAUFMAN, K., MOWERY, C., KAPLAN, G. & ROMANUS, B. 1994. Hip function and gait in patients treated for bladder exstrophy. *Journal of Pediatric Orthopaedics,* 14**,** 709-714.

SUTHERLAND, D. H., OLSHEN, R., COOPER, L. & WOO, S. L. Y. 1980. The development of mature gait. *Journal of Bone and Joint Surgery - Series A,* 62**,** 336-353.

SVERDLOVA, N. S. & WITZEL, U. 2010. Principles of determination and verification of muscle forces in the human musculoskeletal system: Muscle forces to minimise bending stress. *J Biomech,* 43**,** 387-96.

TADDEI, F., CRISTOFOLINI, L., MARTELLI, S., GILL, H. S. & VICECONTI, M. 2006. Subject-specific finite element models of long bones: An in vitro evaluation of the overall accuracy. *J Biomech,* 39**,** 2457-67.

TANCK, E., HOMMINGA, J., VAN LENTHE, G. H. & HUISKES, R. 2001. Increase in bone volume fraction precedes architectural adaptation in growing bone. *Bone,* 28**,** 650-4.

TARDIEU, C. 1998. Short adolescence in early hominids: Infantile and adolescent growth of the human femur. *American Journal of Physical Anthropology,* 107**,** 163-178.

TARDIEU, C. & DAMSIN, J. P. 1997. Evolution of the angle of obliquity of the femoral diaphysis during growth--correlations. *Surg Radiol Anat,* 19**,** 91-7.

TARDIEU, C., GLARD, Y., GARRON, E., BOULAY, C., JOUVE, J. L., DUTOUR, O., BOETSCH, G. & BOLLINI, G. 2006. Relationship between formation of the femoral bicondylar angle and trochlear shape: Independence of diaphyseal and epiphyseal growth. *American Journal of Physical Anthropology,* 130**,** 491-500.

TARDIEU, C. & TRINKAUS, E. 1994. Early ontogeny of the human femoral bicondylar angle. *Am J Phys Anthropol,* 95**,** 183-95.

TAYLOR, M. E., TANNER, K. E., FREEMAN, M. A. & YETTRAM, A. L. 1996. Stress and strain distribution within the intact femur: compression or bending? *Med Eng Phys,* 18**,** 122-31.

THELEN, E. 1979. Rhythmical stereotypies in normal human infants. *Animal Behaviour,* 27**,** 699-715.

THELEN, E., FISHER, D. M. & RIDLEY-JOHNSON, R. 1984. The relationship between physical growth and a newborn reflex. *Infant Behavior and Development,* 7**,** 479-493.

TOWNSLEY, W. 1948. The influence of mechanical factors on the development and structure of bone. *Am J Phys Anthropol,* 6**,** 25-45.

TRUETA, J. 1957. The normal vascular anatomy of the human femoral head during growth. *J Bone Joint Surg Br,* 39-B**,** 358-94.

TRUETA, J. & HARRISON, M. H. 1953. The normal vascular anatomy of the femoral head in adult man. *J Bone Joint Surg Br,* 35-B**,** 442-61.

UPADHYAY, S. S., BURWELL, R. G., MOULTON, A., SMALL, P. G. & WALLACE, W. A. 1990. Femoral anteversion in healthy children. Application of a new method using ultrasound. *J Anat,* 169**,** 49-61.

VAN RIETBERGEN, B., HUISKES, R., ECKSTEIN, F. & RUEGSEGGER, P. 2003. Trabecular bone tissue strains in the healthy and osteoporotic human femur. *J Bone Miner Res,* 18**,** 1781-8.

VICECONTI, M., ANSALONI, M., BALEANI, M. & TONI, A. 2003. The muscle standardised femur. *J Biomech,* 36**,** 145-6.

VICECONTI, M., CASALI, M., MASSARI, B., CRISTOFOLINI, L., BASSINI, S. & TONI, A. 1996. The 'standardized femur program' proposal for a reference geometry to be used for the creation of finite element models of the femur. *Journal of biomechanics,* 29**,** 1241.

WAGNER, D. W., DIVRINGI, K., OZCAN, C., GRUJICIC, M., PANDURANGAN, B. & GRUJICIC, A. 2010. Combined musculoskeletal dynamics/structural finite element analysis of femur physiological loads during walking. *Multidiscipline Modeling in Materials and Structures,* 6**,** 417-437.

WINTER, D.A., 2005. *Biomechanics and Motor Control of Human Movement 3rd edition*. New Jersey: Wiley and Sons.

WINTER, D. A., PATLA, A. E. & FRANK, J. S. 1990. Assessment of balance control in humans. *Medical Progress through Technology,* 16**,** 31-51.

WOLFF, J., 1892. *The Law of Bone Remodelling*. (Das Gesetz der Transformation der Knochen.) Springer, Berlin.

WONG, M. & CARTER, D. R. 1988. Mechanical stress and morphogenetic endochondral ossification of the sternum. *J Bone Joint Surg Am,* 70**,** 992-1000.

WONG, M. & CARTER, D. R. 1990. A theoretical model of endochondral ossification and bone architectural construction in long bone ontogeny. *Anatomy and Embryology,* 181**,** 523-532.

YOSHIHASHI, A. K., DRAKE, A. J., 3RD & SHAKIR, K. M. 1998. Ward's triangle bone mineral density determined by dual-energy x-ray absorptiometry is a sensitive indicator of osteoporosis. *Endocr Pract,* 4**,** 69-72.

ZAJAC, F. E. 1989. Muscle and tendon: properties, models, scaling, and application to biomechanics and motor control. *Critical Reviews in Biomedical Engineering,* 17**,** 359-411.

ZAJAC, F. E., NEPTUNE, R. R. & KAUTZ, S. A. 2002. Biomechanics and muscle coordination of human walking: Part I: Introduction to concepts, power transfer, dynamics and simulations. *Gait and Posture,* 16**,** 215-232.

ZAJAC, F. E., NEPTUNE, R. R. & KAUTZ, S. A. 2003. Biomechanics and muscle coordination of human walking: Part II: Lessons from dynamical simulations and clinical implications. *Gait and Posture,* 17**,** 1-17.

ZATSIORSKY, V. M., IOC MEDICAL COMMISSION. & INTERNATIONAL FEDERATION OF SPORTS MEDICINE. 2000. *Biomechanics in sport : performance enhancement and injury prevention,* Oxford UK ; Malden, MA, USA, Blackwell Science.

ZHANG, Q., CHEN, W., LIU, H. J., LI, Z. Y., SONG, Z. H., PAN, J. S. & ZHANG, Y. Z. 2009. The role of the calcar femorale in stress distribution in the proximal femur. *Orthop Surg,* 1**,** 311-6.

APPENDIX I

Table A-E detail muscles which articulate the human femur and the muscle properties used in AnyBody musculoskeletal modelling system (PCSA, Prox- proximal, Dist- distal, Ant- anterior, Pos- posterior, Lat-lateral, Med- medial, Mid-mid point). Horsman *et al*, (2007)

Primary action	**Muscle**	**Origin**	**Insertion**	**PCSA (cm^2) ***	**Muscle Length* (cm)**	**Tendon Length* (cm)**
Hip abductor	Gluteus minimus	External surface of ilium between inferior and anterior gluteal lines	Linear facet on the antero-lateral aspect of greater trochanter	Lat-10.0 Mid-8.1 Med-7.4	2.8 3.4 3.7	7.3 7.3 7.3
Hip abductor	Gluteus medius	External surface of ilium between anterior and posterior gluteal lines	Elongate facet on the lateral surface of the greater trochanter.	Ant- 37.9 Post- 60.8	3.8 4.5	0 3.0
Hip abductor and lateral rotator	Piriforms	Anterior surface of sacrum between anterior sacral foramina.	Medial side of superior border of greater trochanter of femur.	8.1	3.9	1.6
Hip abductor and lateral rotator	Obturator internus	Anterolateral wall of true pelvis; deep surface of obturator membrane and surrounding bone	Medial side of greater trochanter of femur	25.4	2.1	8.2

Table A Muscle actions, muscle fibre and tendon length, origin, insertions, PCSA, and length which articulate the femur in an adult.

Hip abductor and lateral rotator	Gemellus superior	External surface of the ischial spine	Along the length of superior surface of the obturator internus tendon and into the medial side of greater trochanter of femur with obturator internus tendon	4.1	3.4	0
Hip abductor and lateral rotator	Gemellus inferior	Upper aspect of ischial tuberosity	Along the length of inferior surface of the obturator internus tendon and into the medial side of greater trochanter of femur with obturator internus tendon	4.1	3.4	0
Hip adductor	Adductor brevis	External surface of body of pubis and inferior pubic ramus	Posterior surface of proximal femur, and upper one-third of linea aspera	Prox- 3.8 Mid- 3.5 Dist- 3.2	9.5 10.4 11.2	0 0 0
Hip adductor and knee flexor	Gracillis	A line on the external surfaces of the body of the pubis, the inferior pubic ramus, and the ramus of the ischium	Medial surface of the proximal shaft of the tibia	4.9	18.1	14.0

Table B Muscle actions, muscle fibre and tendon length, origin, insertions, PCSA, and length which articulate the femur in an adult.

Hip adductor and lateral rotator	Obturator externus	External surface of obturator membrane and adjacent bone	Trochanteric fossa	Inf-5.5 Sup-24.6	6.9 2.8	3.5 3.0
Hip adductor and medial rotator	Adductor magnus	Adductor part- ischiopubic ramus Hamstring part- adductor tubercle and supracondylar line	Posterior surface of proximal femur, linea aspera, medial supracondylar line	Prox-26.5 Mid-22.1 Dist-5.0	10.8 10.4 10.7	4.2 0 0
Hip adductor and medial rotator	Adductor longus	External surface of body of pubis	Linea aspera on middle third of shaft of femur	15.1	10.6	0
Hip extensor	Gluteus maximus	Fascia covering gluteus medius, external surface of ilium behind posterior gluteal line, fascia of erector spinae, dorsal surface of lower sacrum, lateral margin of the coccyx, external surface of sacrotuberous ligament.	Posterior aspect of iliotibial tract of fascia lata and gluteal tuberosity of proximal femur	Sup- 49.7 Inf- 22.5	12.0 15.1	0 0
Hip flexor	Psoas major	Posterior abdominal wall	Lesser trochanter of femur	19.5	9.9	11.3

Table C Muscle actions, muscle fibre and tendon length, origin, insertions, PCSA, and length which articulate the femur in an adult.

Hip flexor	Iliacus	Posterior abdominal wall (iliac fossa)	Lesser trochanter of femur	Lat-6.6 Mid-13.0 Med-7.6	10.3 5.2 8.9	11.3 11.3 15.5
Hip flexor and knee extensor	Rectus femoris	Straight head originates from the anterior inferior iliac spine; reflected head originates from the ilium just superior to the acetabulum	Quadriceps femoris tendon	28.9	7.8	9.6
Hip Flexor and knee flexor	Satorius	Anterior superior iliac spine	Anterior surface of tibia just inferolateral to tibial tuberosity	5.9	34.7	7.9
Hip flexor and adductor	Pectineus	Pectineal line and adjacent bone of the pelvis	Oblique line extending from base of lesser trochanter to linea aspera on posterior surface of proximal femur	6.8	11.5	0
Knee extensor	Vastus medialis	Femur- medial part of intertrochanteric line, pectineal line, medial lip of the linea aspera, medial supracondylar line	Quadriceps femoris tendon and medial border of patella	Inf-9.8 Mid-23.2 Sup-26.9	7.6 7.6 8.3	9.6 9.6 9.6

Table D. Muscle actions, muscle fibre and tendon length, origin, insertions, PCSA, and length which articulate the femur in an adult.

Knee extensor	Vastus intermedius	Femur- upper two-thirds of anterior and lateral surfaces	Quadriceps femoris tendon and lateral border of patella	38.1	7.7	12.6
Knee extensor	Vastus lateralis	Femur- lateral part of the intertrochanteric line, margin of greater trochanter, lateral margin of the greater tuberosity, lateral lip of the linea aspera.	Quadriceps femoris tendon	Inf- 10.7 Sup- 59.0	4.2 9.1	9.6 9.6
Knee flexor and hip extensor and medial rotator	Semitendinosus	Inferomedial part of upper area of ischial tuberosity	Medial surface of proximal tibia	14.7	14.2	23.7
Knee flexor and hip extensor and medial rotator	Semimembranosus	Superolateral impression on the ischial tuberosity	Groove adjacent bone on medial and posterior surface of medial tibial condyle	17.1	8.1	15.7
Knee flexor, hip extensor and lateral rotator	Bicep femoris	Long head- inferomedial part of the upper area of the ischial tuberosity; short head- lateral lip of linea aspera	Head of fibula	27.2 11.8	8.5 9.1	13.0 3.1
Lateral rotator	Quadratus femoris	Lateral aspect of the ischium just anterior to the ischial tuberosity	Quadrate tubercle on the intertrochanteric crest of the proximal femur	14.6	3.4	0

Table E Muscle actions, muscle fibre and tendon length, origin, insertions, PCSA, and length which articulate the femur in an adult.

APPENDIX II

Reference	Constitutive Model	Components	Properties (Young's modulus/ Poisson's ratio)	Element and Node Number
ADULT				
Polgar et al (2003)	Homogenous, isotropic linear elastic	Cortical Trabecular	17GPa/0.33 1500MPa/0.33	7 942 nodes 36135 elements
Phillips (2009)	Four noded linear tetrahedral	Cortical Trabecular	18GPa/0.3 1000MPa/0.2	286,070 elements 172,749 elements
Jonkers (2008)	Four Node Tetrahedral	Cortical Trabecular	17GPa 570MPa	95,000- 115,000 elements
Speirs et al (2007)	Second order Tetrahedral	Cortical Trabecular	17GPa/0.3 1GPa/0.3	4mm elements
Bessho et al (2007)	Tetrahedral Linear 3 mm	Cortical Trabecular	20GPa/0.4	5291 nodes 95,238 elements
Wagner *et al*, (2010)	4-node tetrahedral, linear	Cortical Trabecular Intramedullar	1850-16737MPa/0.3 77-1835MPa/0.3 20MPa/0.3	88891 elements 18497 elements

JUVENILE				
Shefelbine and Carter (2004)	Hexahedral, Linear isotropic	Newly mineralised bone Cartilage	500MPa/0.2 2MPa/0.49	17000 elements
Carter and Wong (1998)	Conventional linear elastic quadrilateral elements	Newly mineralised bone Cartilage	500MPa/0.2 2.04MPa/0.47	956 elements
Ribble *et al* (2003)	8-node isoperimetric hexahedral elements	Cortical Trabecular Cartilage	11500MPa/0.3 345MPa/0.3 375MPa/0.3	8800 elements 5000 elements
Carriero *et al*, (2010	Linear isotropic, hexahedral elements	Cortical Trabecular Cartilage Intramedullar	20GPa/0.3 600MPa/0.3 5MPa/0.3 1MPa/.49	10500 elements

Table F Properties of finite element models of the femur in the literature. Showing element type, mesh density, material properties for adult and juvenile models.

APPENDIX III

TWO DIMENSIONAL MODELLING TO PREDICT OSSIFICATION IN THE JUVENILE FEMUR

INTRODUCTION

This work began before the procurement of the full scans from Laboratoire d'Anatomie Comparée of the Muséum National d'Histoire Naturelle of Paris. Once the full models were obtained these became a priority and this section of work became obsolete in completing the aims of the thesis therefore it is incomplete and thus in the Appendix. However this work developed some good areas of research and will have a place in future work.

The femora specimens that were procured from the Scheuer collection, University of Dundee were dry specimens, and therefore lacked the cartilage that is present during juvenile femora. Due to this lack of cartilage on the femora specimens the importance of the missing cartilage, during FEA, needs to be assessed. This would have informed the future work in this thesis of whether a FEA of the femur can be produced with an estimated amount of cartilage placed on the femur. Previous work has used computer simulation to predict ossification and bone growth, this work will be discussed to gain an understanding of the considerations needed when undertaking this work.

The development of the juvenile femur is well documented (Trueta, 1954; Osborne, 1980) however it is not fully understood. Mechanical influences are believed to play a large role in the remodelling of the adult femur, and are assumed to play a greater role for the juvenile skeleton (Carpenter and Carter 2008). Understanding growth in the juvenile skeleton can help increase the understanding and treatment of abnormal growth in children. The role of mechanical influence on juvenile bone development has only been examined in a cursory manner when compared to studies on the adult skeleton. There are two methods of ossification in long bones, intramembranous and endochondral. They play significantly different roles in the growth of the femur; intramembranous ossification is the process responsible for bones growing in length at the diaphysis and endochondral ossification is responsible for the growth of long bone at the epiphyses regions. The analysis of bone growth as previously discussed showed

that the adult femur has been associated with the mechanical strains that are evident under loading. One area of research which has developed this factor further is the computer simulation of bone growth. Computer simulations can be used to study events that may occur gradually *in vivo* but can be simulated over a much shorter time period and enabling the identification of key stages and important factors influencing development. This of course is subject to the degree of accuracy to which a computer model can represent an *in vivo* environment. Numerous studies have focused on the mechanobiological effect on femoral growth.

Carter and Wong (1988a; b) studied the role of stresses in prenatal and postnatal skeletal development using a 2D model. The study revealed that when high octahedral and compressive stresses are present the growth of bone was inhibited, whilst high shear and tensile stresses promoted bone growth. Subsequently, Carter and Wong (1988b) produced a computer simulation of bone growth using FEA, and attempted to predict the normal ossification of the femur through the use of the rules which follow the observations from the previous studies (Figure A).

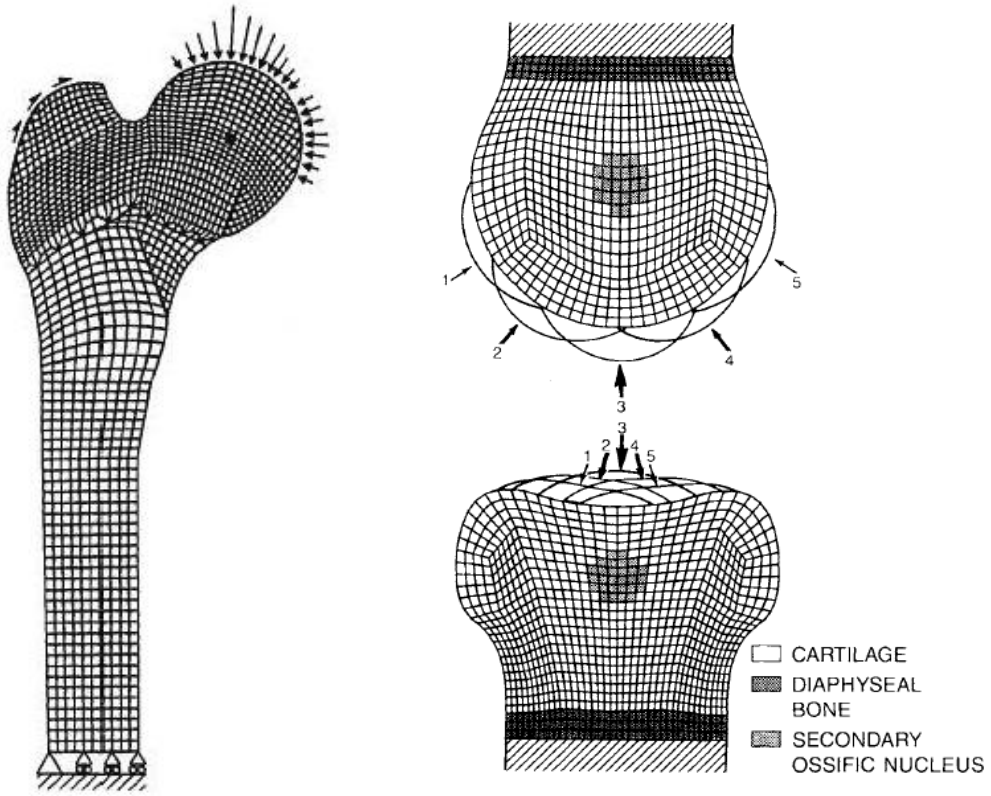

Figure A Finite element model of the proximal femur Carter and Wong, 1987; Finite element meshes of the convex and concave chondroepiphyes showing loading conditions and progression of ossification (Carter and Wong, 1988).

The next stage was to create a more complex model (Wong and Carter, 1990) which predicted the growth rate over time and produced a more accurate prediction of the growth *in vivo.* This model has since been used in many mechanobiological studies but to study different areas other than the endochondral growth (Shefelbine et al, 2002b; 2004), and therefore this initial model needs to be discussed to understand the findings of these further studies. The aim of the research was to model the endochondral ossification observed in long bones. A 2D model representing the shape of an adult femur was developed. The model was loaded with a hip pressure orientated at three different angles and a pressure on the greater trochanter was also applied. This study achieved a number of skeletal morphogenesis developments through computational modelling. These were the primary centre of ossification, the medullary canal, the growth plate and also the secondary ossification centre. Wong and Carter, (1990) used these previous results to build a stress based algorithm which was said to represent the rules of construction which guide the limb ontogeny. The study successfully predicted a process similar to that of the ossification seen in long bones. Using the growth algorithm, the areas of localised cyclic shear stresses formed mineralised bone, and over time the growth front was increased followed by a centre of ossification being produced. Stevens *et al,* (1999) furthered this work by developing the growth rate of the model with mechanical and biological factors being necessary for the model.

Subsequent studies (Shefelbine *et al,* 2002b) have since developed and manipulated the model by adjusting the growth rate and other values to fit different areas of bone development that are to be studied, but the initial model is still used in the more recent studies. Researchers have used 2D computer modelling to study shear stresses at the growth plate of a developing juvenile femur and hypothesised what should be expected in terms of growth according to the stresses (Ribble *et al,* 2001). A variety of load cases were used to represent typical activities of three ages (birth; 2 years old; 8 years old), Figure B. A muscle model described in Miller *et al,* (1999) was used to calculate the loading.

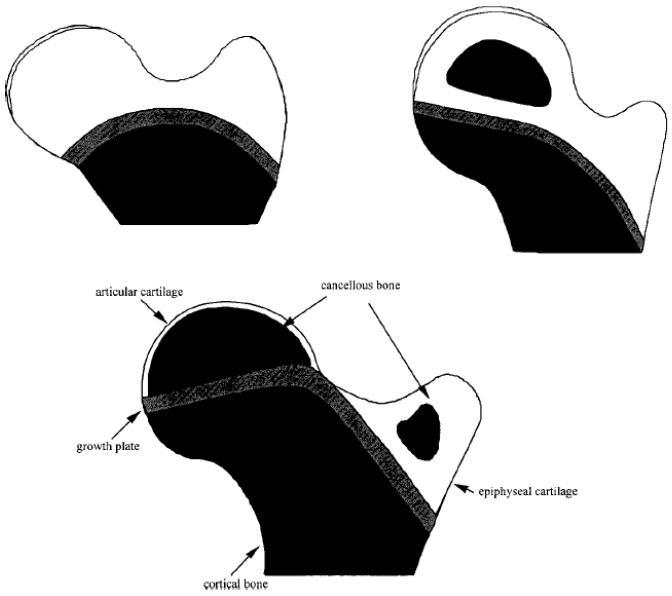

Figure B. Schematics of the internal architecture of the proximal femur models at birth, 2 years and 8 years (Ribble *et al,* 2001).

A FEM produced significant shear stresses laterally within the growth plate coinciding with the development of the neck shaft angle. This was particularly evident in the birth model during lying and kicking and preparing to walk, with the shear stress results being very similar. However, it is surprising that the results did not vary more due to the presumed increase in joint contact force because of the increased body weight during the preparatory condition before walking. Hence questions arise about the model loading. The results in this study are totally dependent on the assumed and combined muscle activity and force, whereas more realistic results would be provided using true representations of muscle forces from musculoskeletal models, individual muscles and motion capture data. As this initial work was in 2D, more complex 3D models have since been developed, these 3D models added multiple adaptive iterations to the FEA (Shefelbine *et al,* 2002; Shefelbine and Carter 2004a; b) utilising the important initial work produced by Carter and Wong (1988). In this work a number of distinctive femoral developments have been assessed using computer simulations normally comparing normal growth against abnormal growth such as CP and hip dysplasia (DDH). These developments include the changes in the femoral growth front (Shefelbine and Carter, 2004a; Carriero *et al,* 2011) and femoral anteversion (Shefelbine and Carter, 2004b). Hip dysplasia is characterised by ligament laxity which can cause a dislocated femoral head. Prior to Shefelbine's work it was quite accepted amongst practitioners that it was mechanical influence that affected growth in

development dysplasia of the hip, and the study produced proof of this concept. The growth front was shown to develop at a greater rate on the medial side of the growth plate as seen in the development of DDH. This was due to the different hip pressure angles which were represented during the loading conditions. The findings of this and the other mechanobiology studies can help to develop the understanding of how loading can affect growth during development. A recent study performed by Carriero *et al,* (2011) modelled abnormal hip contact forces and muscular loading, as seen in children who suffer with CP, can affect the development of the growth plate. Normal loading and loading typical of CP sufferers was applied to a normal femur model, representing a 7 year old. The same method of growth was used as developed in previous studies (Carter and Wong, 1988; Shefelbine *et al,* 2002) The growth plate showed that during the CP loading cases there was a smaller load magnitude in the superior-inferior and anterior-posterior component, which would result in a lower neck shaft angle and femoral anteversion, both of which are observed in CP. As in previous work showing the effects of DDH, the abnormal loading of CP can also develop an altered loading in the growth plate. These studies have shown how mechanobiological simulation can help to increase the understanding of abnormal growth. The method has also been used to provide information about the changes seen in between species. Shefelbine *et al,* (2002) used the growth model to calculate the changes in bicondylar angle of the femur. This was done by changing the symmetry of loading on the distal condyles to coincide with the variations seen in gait characteristics from the different species studied, extending to modern humans, chimpanzees and australopithecines (pre Homo species). The asymmetrical loading conditions caused the model to grow with a changed BA. The use of a mechanobiological approach in the understanding development of bipedalism shows the wide variety of applications that it has to offer.

This research has contributed to a greater understanding of the effect of mechanical influence during normal growth, and also during growth where abnormal loading is evident. However one crucial part of the theory which may be subject to criticism is the main determinant rule used for bone growth calculation. Whether the femur as a structure is under predominantly compressive forces has been under discussion in the literature for many years. Therefore if the bone is under compression as an adult then this may be the case in the juvenile femur. Thus the rule that bone is formed under tensile stress and inhibited from compressive stresses may not be correct under these considerations. Further discussion of these considerations can be seen in Chapter 2.1.6.

The aim of this work was to inform future work in this thesis of whether a FEA of the femur can be produced with an estimated amount of cartilage placed on the femur. Further still this this work would develop an understanding of the relationship between the mechanical influence and the ossification of the juvenile femur under a compressive state.

METHOD

MODEL 1

A 2D finite element model was developed to represent the proximal femur of a 4 month old *in utero* foetus. A 4.6month *in utero* dry femoral specimen was supplied from the Scheuer collection at the University of Dundee, this was then CT scanned at a resolution of 0.0574mm x 0.0574mm x 0.0574mm and a 3D model was built. The 2D model was constructed using a single slice from the micro CT scan (of the dry bone) and was overlaid in GIMP (Mattis and Kimball, 2003), an image manipulation program, with a radiograph of a femur of the same gestational age that included the cartilage and the growth plate (Figure C).

Figure C The prenatal femur specimen scanned (left) and a cross section through an intact femur (Osborne, 1980) (right) showing bony shaft and cartilaginous epiphyses.

Once the image was generated in GIMP (Figure 2) the JPEG was then input to software (DXA to FEM Converter 2, Sisias *et* al, 2001) so that a meshed model was created and the different materials could be identified.

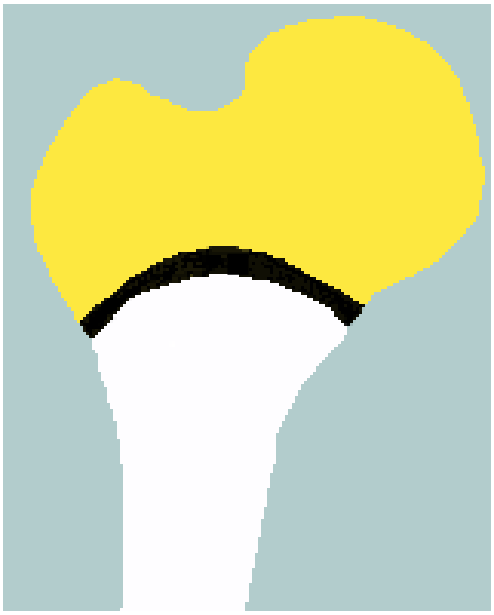

Figure D JPEG of the proximal femur created in GIMP identifying three materials, bone (white), growth plate (black) and cartilage (yellow)

The model (Figure E) was meshed using PLANE183 elements, and had a total of 2460 elements. Of these, 1647 were assigned a material property of 108MPa (v = 0.34) representing cartilage, 99 assigned property of 134 (v = 0.3) representing the growth plate and finally a material property of 11500MPa (v = 0.3) representing juvenile cortical bone was assigned to 714 elements. All materials were idealised to isotropic linear elastic behaviour. The material properties of the shaft did not influence the stresses that were observed in the femoral head during testing the model therefore modelling cortical rather than trabecular was assumed to be more appropriate and would be consistent with the modelling of older ages later in this work.

2.1.1.1 Loading

Due to the simplification of the femoral structure, it is difficult to replicate the prenatal loading conditions that are observed *in vivo*, although position of the hip has been documented (Spoor, 1989) and therefore the direction of the force can be accurately modelled. The force of the muscle load was calculated as a consequence of the hip force

which was calculated as 3.1 times bodyweight (Heimkes, 1993). The ossification is sensitive to the radial degree around the head at which the hip pressure is applied, for this purpose a 120 degree pressure was applied. This pressure was observed *in vivo* by Professor Ulrich Witzel as most optimal to produce the correct positioning of the main concentration of stress to represent where a primary ossification centre would occur.

Due to this simplicity of the model, only the hip force and two muscular forces were applied. The secondary force was calculated from the primary resultant force through vector mechanics to achieve a model that is under compression and the resultant force is through the middle of the shaft (Figure E). The two muscular were then calculated from this second resultant force (Equation A). The two muscular forces were the gluteus medius and the vastus lateralis, Heimkes (1993) named this the vastogluteal sling because of direction that the muscles cause resultant forces to act. Although this was introduced to show how the direction and magnitude of Pauwels resultant hip force influences the neck shaft angle. This can further be explored to see how it influences the ossification of the proximal epiphyses of the femur, this be seen in the current model.

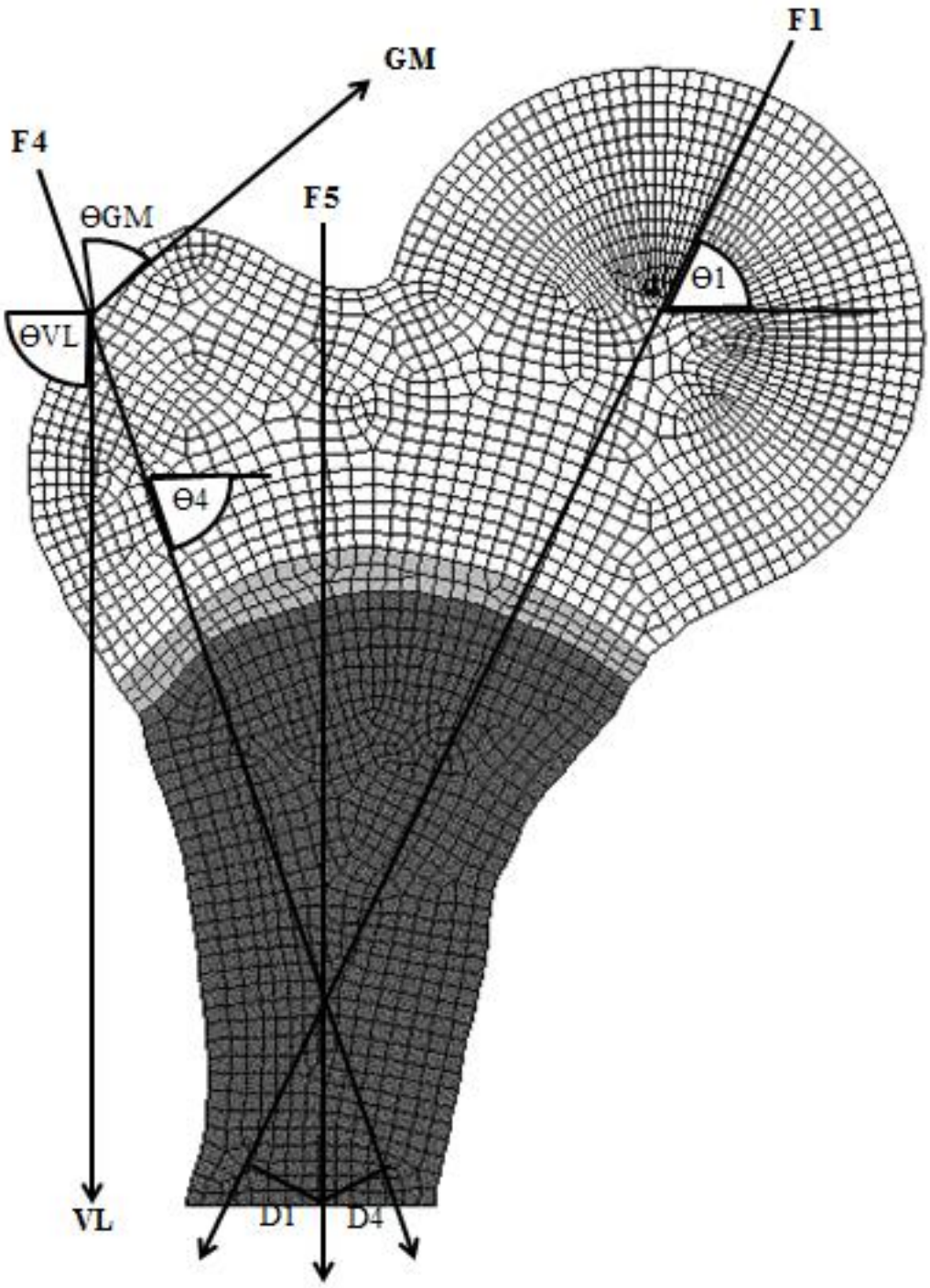

Figure E. 2D model of 4.6month old femur showing loading regime; Light to dark shade, respectively represent cartilage, growth plate and bone.

The secondary force (F4), angle of the force and the location where the force is applied can be calculated through the following, when F1, Θ1 and D1 are known -

F4+F1=F5

F4 cosΘ4 = F1 cosΘ1

D1 x F1 = D4 x D1

When the angle of the muscles (gluteus medius, GM, and vastus lateralis, VL) are known (physiological angles) it is possible to calculate the forces of VL and GM from hip force through the following equation

X= F4 sinΘ4 = Fgm cosΘgm + Fvl cosΘvl

Y= F4sinΘ4 = Fgm cosΘgm + Fvl cosΘvl

Equation A Calculating the muscle forces from the secondary resultant force.

Table G shows the values which were used in the initial model for Equation A

Equation Derivatives	Value
F1	530
FGM	116
FVL	1063.3
F4	1015.1
D1	1.3
D2	0.68
Θ1	69
ΘGM	85
ΘVL	57
Θ4	79.2

Table G Values of forces angles and distance required to calculate the forces for gluteus medius and vastus lateralis.

The muscular loading was applied to 9 nodes so that it was distributed evenly and representing the distribution of the muscles at their origin and insertion points. The

angles of the muscles were applied as observation made in illustrations and diagrams which were found to be a similar angle to that described in Heimkes *et al* (1993).

RESULTS

SIMULATION OF THE SECONDARY OSSIFCATION CENTRE

Initial stress plots reveal when the hip pressure is applied at the correct position that a high compressive level of stress appears at the position where an ossification centre would be expected, regardless of if a muscle force is present. Although without the hip pressure and just the muscle force present, the area of concentrated stress indicating a secondary ossification site is not present. It is worth noting that the stress in the shaft of the femur is not relevant to the age of the specimen as it would already be completely ossified. Once the model achieved a loading which was considered correct, with muscle and hip loading applied, and one which caused concentrations of stress at the areas which would be seen to ossify *in vivo* the area of highest compressive stress was assigned a bone material property as shown in Figure F

.

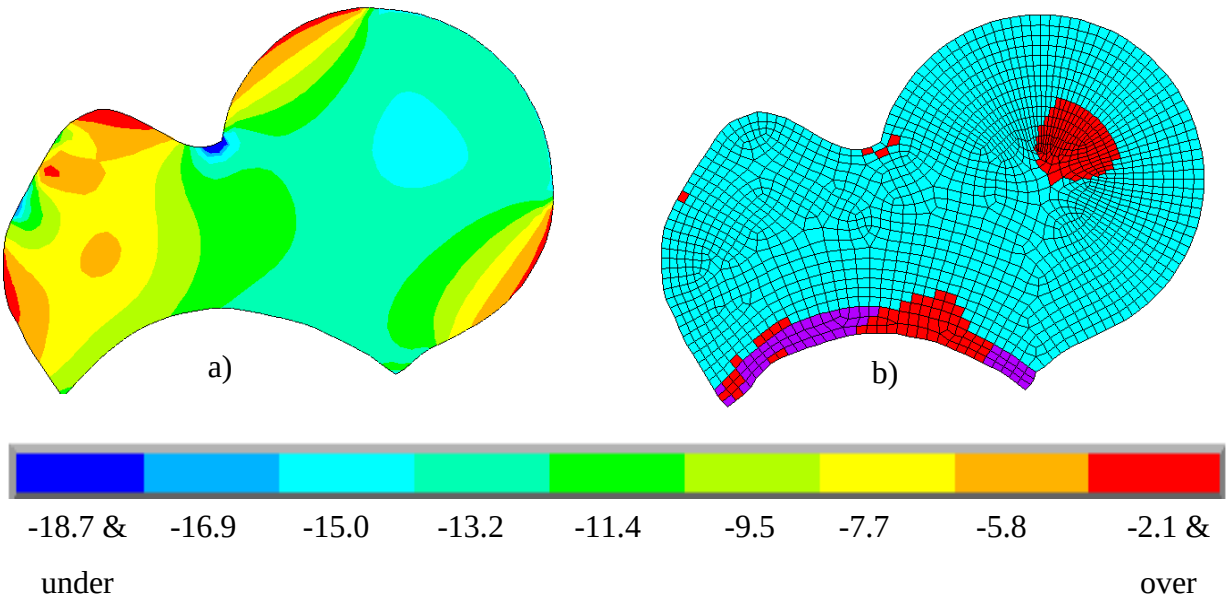

Figure F. Minimum stress analysis of the prenatal femur showing a high compressive area in the region of the secondary ossification site a) peak stress was then assigned a different material property to simulate ossification b).

When hip pressure and muscle activity ratio is constant, this location of secondary ossification stays same position (Figure Ha). The secondary centre of concentrated stress occurs at a greater level of compression when there is an increase in muscle force and when there is very low muscle force there is no secondary ossification evident (Figure G). The increase in muscle force shows an increase in compressive stress produced at the secondary ossification site of 170% rising from -1.9Pa at 10% to -5.3Pa at 70% muscle activity which then converges at 80% muscle activity to 6.0MPa.

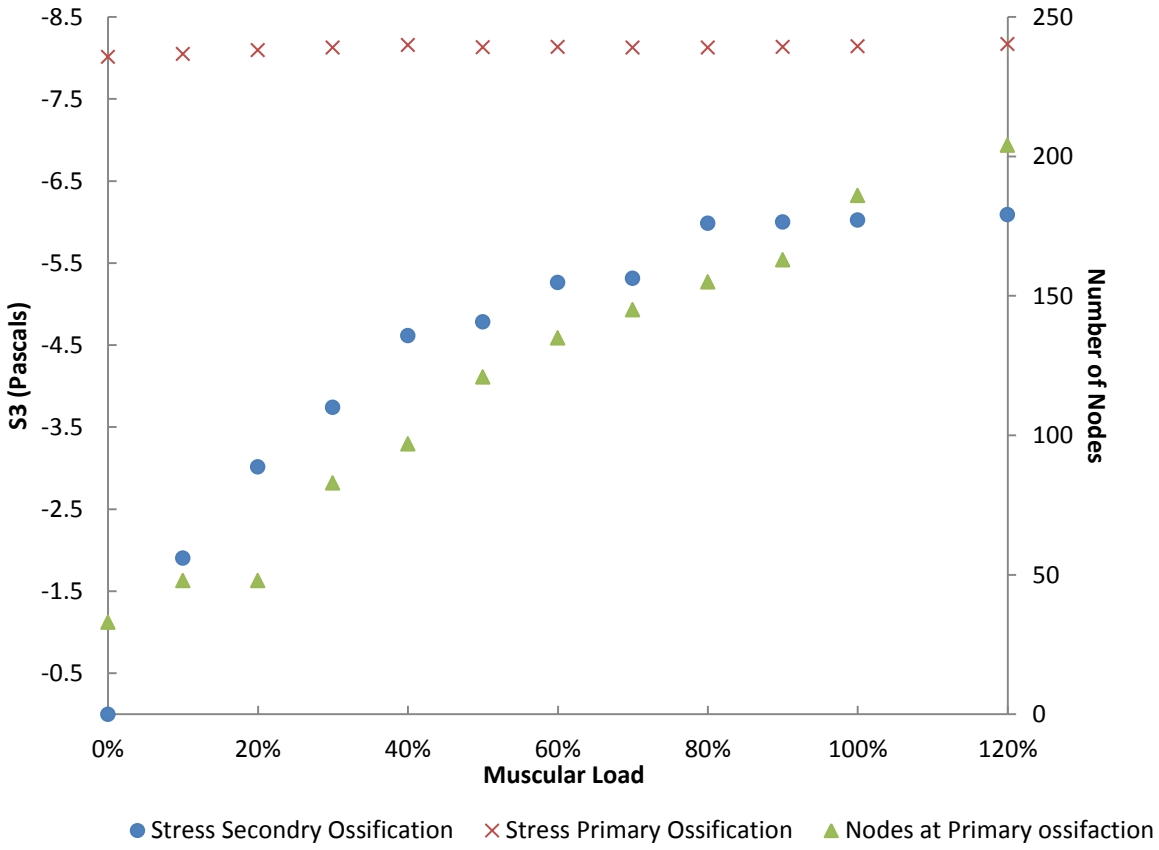

Figure G. Effect of an increased muscle load on the primary and secondary ossification. Nodes at the primary ossification site show the size increase in the size of the ossification area.

The relationship between JCF and the muscle force is clearly seen in Figure G. As the ratio between the forces is increased linearly the concentration of the stress is geometrically in the same position although the stress level is increased, as would be expected. However when the only the muscle force is increased, also vice versa, the positioning of the concentration of stress at the secondary ossification size. (Figure H).

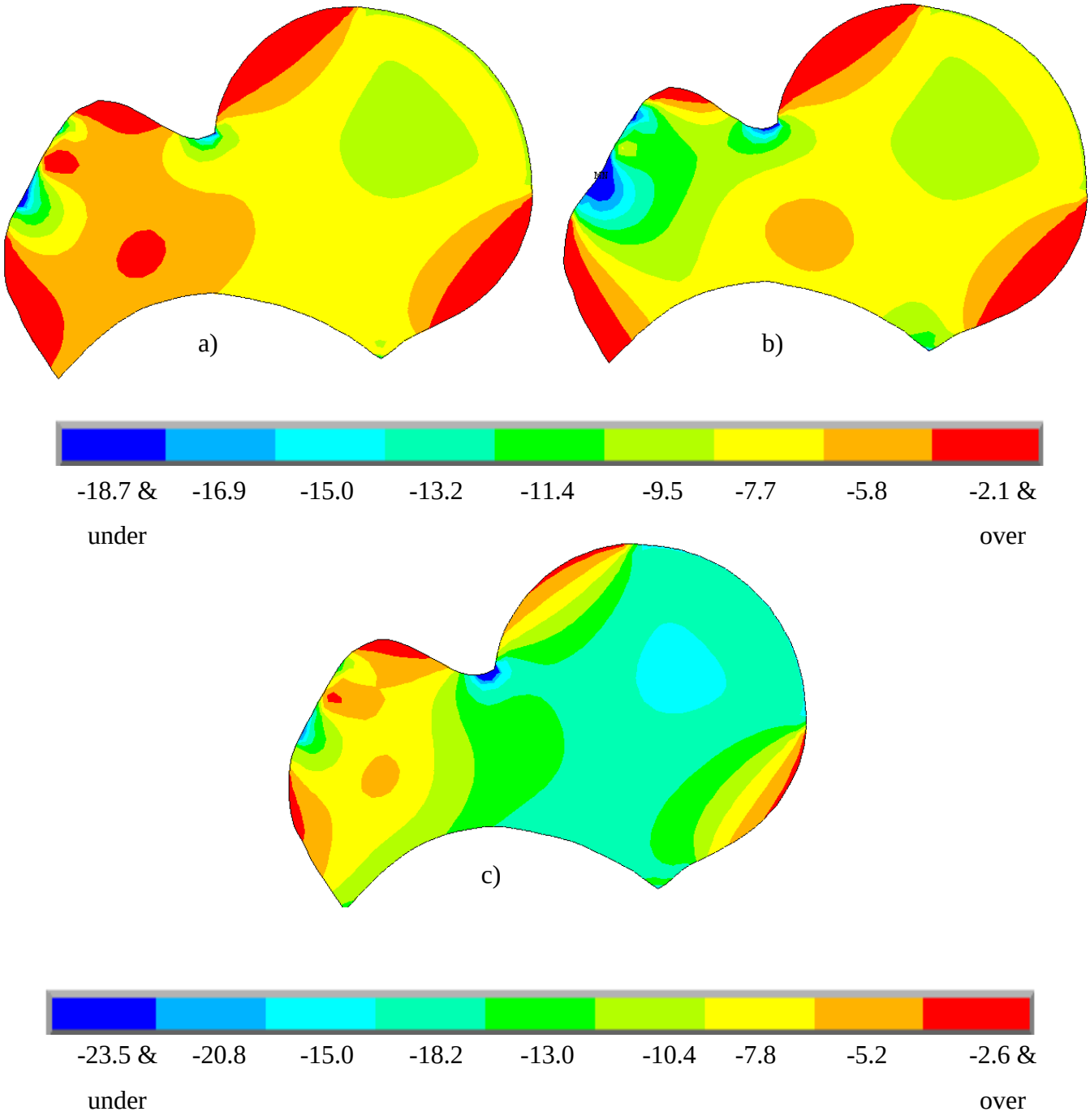

Figure H. Relocation of the concentration of stress when the muscle force to hip force ratio changes (hip force: muscle force) a) ratio1:1; b) ratio 1:2, c) ratio 2:1.

Examining the effect of muscle and hip force on stress concentration it is evident that when no muscle force is present the primary ossification still occurs. However, when no hip pressure is applied i.e. (only a muscular force) there are no marked stress concentrations at the femoral head or the greater trochanter (Figure I). This indicated

that primary ossification can occur independent of the muscle force, but will not occur with muscle force only (i.e. independent of hip joint loading).

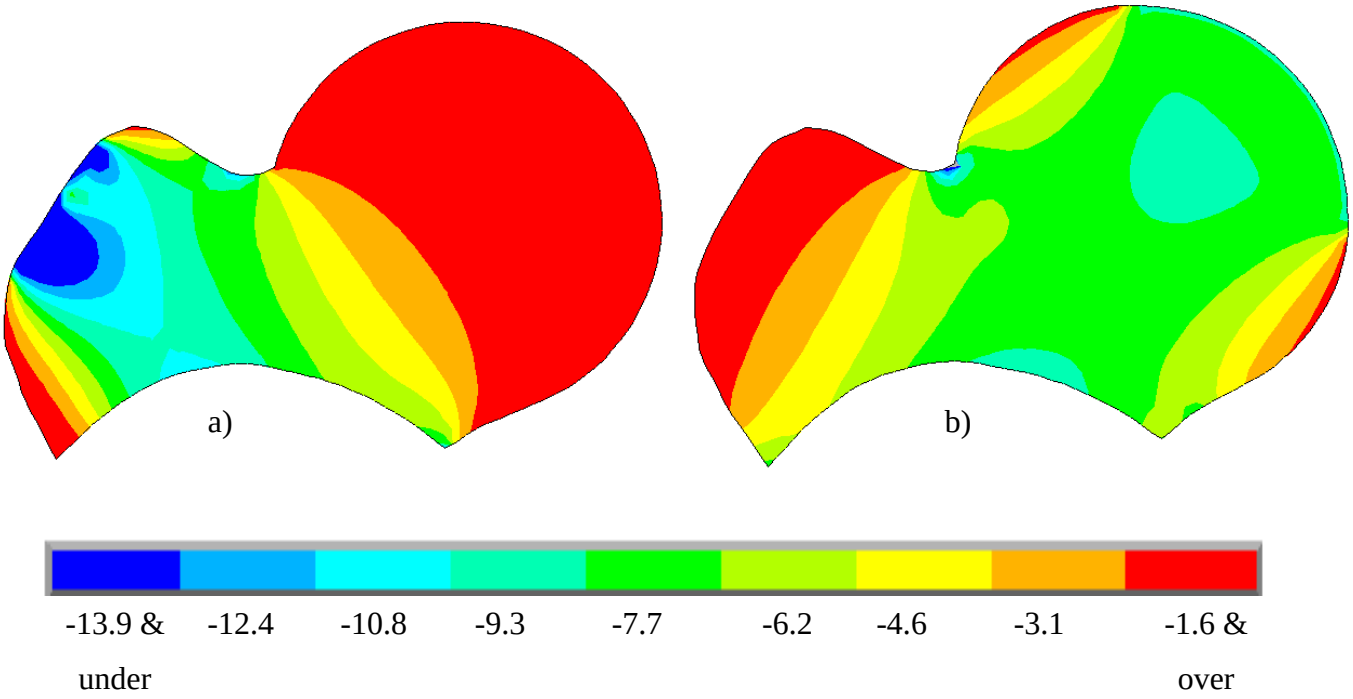

Figure I Stress plots with only muscle forces applied (a) and with only hip pressure (b).

MODEL 2

The second model of the simulation was created in the same manner as the initial model. The aim was to idealise the shape of the 2 year old femur so that the secondary ossification centre could be explored with greater accuracy.

This model was built from a radiograph from Trueta (1954) it is representative of a 2 year old Figure J. A radiograph in the sagittal plane was idealised into a two dimensional model for FEA. The main difference between the geometry of this model and the previous is the extension of the femoral neck and the prominently developed femoral head ossification centre.

The model (Figure J) was meshed using PLANE183 elements, and had a total of 4010 elements. 1429 were assigned a material property of 108Mpa (v = 0.34) representing cartilage and a material property of 11500MPa (v = 0.3) representing juvenile cortical bone was assigned to the remaining 2581 elements.

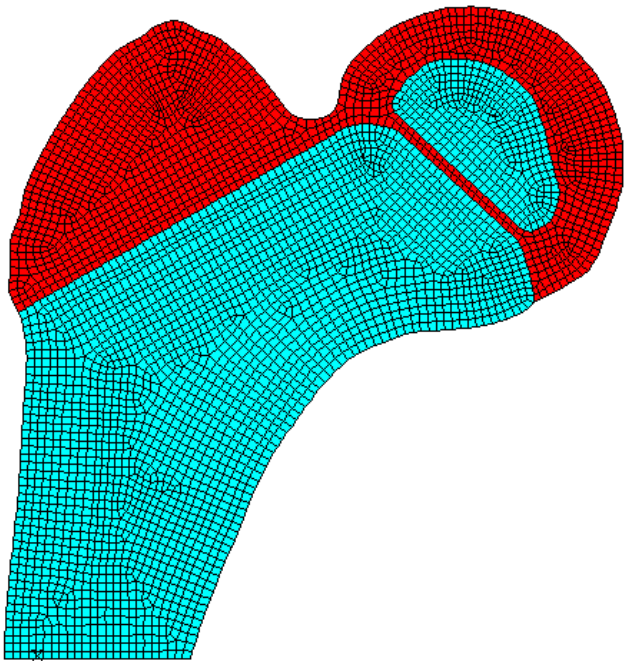

Figure J. 2 year old 2D meshed finite element model of the proximal femur, blue showing bone and red showing the cartilage.

2.1.1.2 Loading

A change in the loading for this model was needed so that the increased activity of a normal 2 year old child is accounted for. Therefore the loading showed an increase hip load due to an increased BW. The hip pressure was increased from 7.38kg to 40.3kg and the muscle forces were increased accordingly. The muscle force was changed accordingly for the resultant force to remain in a central position.

SIMULATIONS OF SECONDARY OSSIFCATIONS

These results are not complete and require more work but due to time restrictions and a full area of research in this work is beyond the scope of the thesis.

Preliminary results did discover some interesting possibilities about the change in the way that the femur develops the more developed it becomes. The previous models

showed the relationship between the secondary ossification centre requiring the hip and muscles to produce the loading required to create the concentration of stress required for ossification whereas the primary ossification only needs the hip force to appear. In older aged model (Figure K) the secondary ossification centre appears without the hip force and only requires the force from the muscles. Suggesting the initial ossification of the secondary ossification is not driven by the hip force as was seen in the previous model. It could also be said that Showing the increased need for the muscle to be active to obtain normal growth at later stages of development.

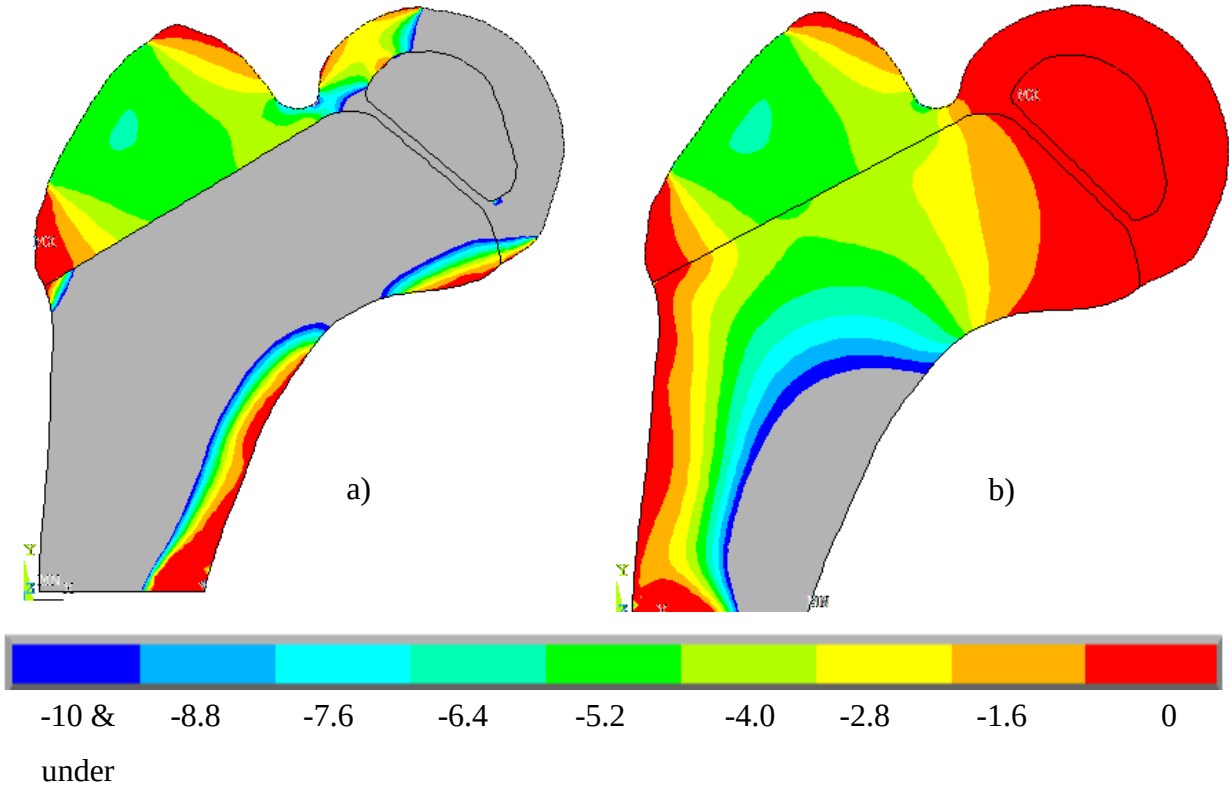

Figure K. The 2 year old model with all forces applied, hip and muscle forces (a) and when only the muscles forces are applied (b).

DISCUSSION

The development of the juvenile has been observed in the past but little work has try to model and understand its development and growth in accordance to the loading changes associated with the change in locomotion and gait. The rate at which the ossification occurs the femoral head has been observed in many radiographic studies (Trueta, 1957; Osborne, 1980, Gardner and Gray, 1970) yet the true significance of why the ossifications occur at the stages at which they do has not been justly examined.

This work remains in progress but the initial results have been promising and work will continue. Two findings in this study emphasise the relationship of the developing gait and juvenile femur. Firstly, regardless of whether there is a muscle force present when the hip pressure is applied there is a high concentration of compressive stress in the expected region of an ossification centre. An increase in muscle force does not affect the primary ossification stress level but intensifies the volume of the area covered by the ossification which is apparent *in vivo* (Figure G). Studying the ossification growth using the radiographs in the study by Osborne (1980) (Figure L) there is an enlargement of the primary ossification site and a progression of growth front towards the hip prior to any visible evidence of a secondary ossification. But during this time there is an increase in activity from the muscles which would help to enlarge the ossification centre (Figure G). This increase in size from the ossification centre is a direct response to the increase in muscle activity of the gluteus medius and the vastus lateralis (Sutherland *et al*, 1980).

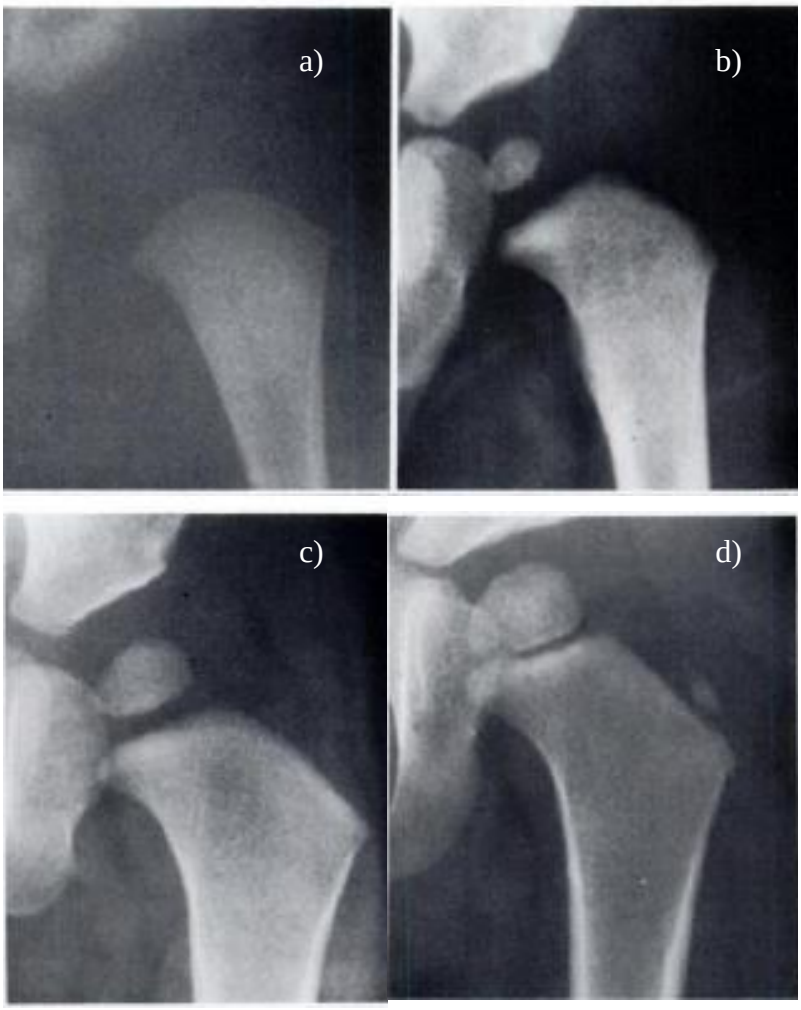

Figure L. Reproduced from Osborne 1980, X-rays showing the development of the femoral ossification centre for a 6 day old (a), 8 month old (b), 13 month old (c) and 2 year old (d) for use in comparison against the models produced.

A second result can help to explore the correlation with the results of the computer model and gait development further. What would be questionable in this study would be the lack of relationship between the suggested increase in muscle activity at 9 months and the time between a secondary ossification centre appearing, even though there is evidence of the concentration of stress present. Figure I explores the ratio relationship between the muscle force and the hip force effects on the location of the secondary ossification site. When the ratio between the muscle force and hip force changes the concentration of stress at what would be the secondary ossification site moves. This could be related to erratic and random movements seen in early developments until a sense of organisation in movement is seen. Therefore until equilibrium between the forces ratio is reached (i.e. walking) for a considerable amount of time then the

movement of the concentration of stress may not be constant enough to produce ossification. Thelen (1979) observed this behaviour in 2-12 month olds and described 47 recurring movement patterns, 18 of which were primarily lower limb movements. Comparing this to what movements are considered to be everyday activities in 2 year old children which are walking, running (Ribble *et al*, 2001) and then again in adults, walking, running, jumping, sit to stand, sitting and stair walking. There are significantly less and therefore more constant and consistent movements the more mature a person gets. Explaining the often well organised bone structure that is seen (Osborne, 1980). Further still heel-toe walking is not evident until 2 years which can be seen as a first indicator of mature gait. Additionally muscle forces (Ribble et al 2001) and activity (Sutherland et al 1980) in the gluteus medius was estimated to increase in force by up to 380% from the actions studied in an infant to those seen in a 2 year old. At this point the muscle activity reaches a high enough level of both intensity and organisation to ossify the stress concentrated site, after already increasing the size of the primary ossification site.

Wong and Carter (1988) studied the ossification during growth in two simply loaded models. The load was applied similarly to the hip pressure load seen in the present study which caused an ossification centre where the stress is concentrated. Their goal was to achieve a focal point at which high levels of octahedral shear tensile stress. Later work (Shefelbine *et al* 2002, Ribble *et al*, 2001) in a variety of different research have also used this approach when studying the development of bone during growth. Other theories and ways of looking at the stresses observed in bone growth need to be explored. The results of the present study do this by looking at the ossification centre formed under a compressive state as suggested in previous work (Munih *et al*, 1992: Sverdlova and Witzel, 2011). In these works it is suggested that the tensile stresses are compensated for and transferred away from the bone by muscles and tendons, with further support in very recent anatomical investigation (Hammer, 2010). The well accepted ‘Trajectorial theory’ was discussed in which there are two directions of trabecular bone alignment, the vertical trabecular to support the femoral head during compression and the horizontal supposedly to support the femoral head during tension. However during the investigation it was theorised that both directional lines of trabecular are to deal with compression under different everyday activities i.e. vertical trabecular for standing activities and horizontal trabecular for squatting positions. Although this theory would still conform to Wolff’s Law it conflicts with the accepted

trajectorial theory. The results of the current study would suggest such an adaptation. With a primary ossification being formed from the hip pressure under a highly compressive load at a position of being hyper-flexed, (fetal position) similar to a squat position.

The study has shown that using, physiologically correct computer modelling techniques can be used to observe the development of ossification in the juvenile femoral head can be studied and can possible these findings could possibly be applied to further areas of bone growth. The results observed in the present study are similar to that seen *in vivo*. Initially an ossification centre appears in the cartilaginous head of the femur which would be formed through a constant hip pressure being. In the model hip pressure even at a low level results in a concentration of compressive stress at where an ossification centre would be expected to appear *in vivo*. In conclusion the time at a location which these events occur correlate well with the development of gait. At approximately 8 months there is an onset of crawling (Sutherland, 1980) which would increase in the force of the gluteus medius but would not induce a large requirement of the vastus lateralis. This would most likely occur during standing and walking phase, approximately 1 year, as would a greater use of the gluteus medius because of a greater need for hip stability (Soderberg and Dostal, 1978). During walking a greater hip pressure is observed which can help to progress the ossification of the femoral head, and have a subsequent effect on the positioning of the secondary ossification. Previous work has suggested that bone is inhibited under compression and is promoted under tension, whilst the present model shows a model under compression would induce ossification of the bone. In this study however it was deemed important just to focus on the areas where stress would be focused and for future work to be directed at iteratively changing the material of the highly stressed areas to simulate the growth of the juvenile femur.

This work can help to understand underdevelopment or abnormal developments which occur during intramembranous ossification such as. Legg Calve Perthe's Disease (LCPD) where the apophysis can appear abnormally developed on the evidence of this work this could be due to irregular muscle activity during growth. Irregular muscle activity can include muscle anaesthesia, or cerebral palsy.

APPENDIX IV

Details of all specimens provided by Scheuer Collection at the University of Dundee (Table H) and by the Laboratoire d'Anatomie Comparée of the Muséum National d'Histoire Naturelle of Paris (Table I). N.B. there are more specimens detailed in the tables than were used in the research.

Specimen	Age	Entities
SB	4.6 months old *in utero*	Diaphysis
STH SS2	6 months old	Diaphysis
		Proximal and distal epiphyses
P4	1 year old	Diaphysis
		Proximal and distal epiphyses
STH SS1	3 years old	Diaphysis
		Proximal and distal epiphyses
STH B	7 years old	Diaphysis
		Proximal and distal epiphyses
		Great Trochanter

Table H Information of the specimens used to CT scan provided by Scheuer Collection at the University of Dundee.

Specimen	Age	Sex
Fo-Tno	9 months old *in utero*	Female
TaNo	3 years old	Female
FlSa	7 years old	Male

Table I Information of the specimens used to CT scan provided by Laboratoire d'Anatomie Comparée of the Muséum National d'Histoire Naturelle of Paris

APPENDIX V

The predictive musculoskeletal modelling provided large amounts of muscle force data. Table J to Table R shows the muscle force data for 24 muscles at 9 stages of the gait cycle.

2% (N/Kg)	3 yrs	4 yrs	5 yrs	6 yrs	7 yrs	Adult
Vastus Intermedius	0.000	0.000	0.000	0.000	0.000	0.041
Vastus Lateralis	0.000	0.000	0.000	0.000	0.000	0.143
Vastus Medialis	0.000	0.000	0.000	0.000	0.000	0.068
Rectus Femoris	0.000	0.000	0.983*	0.000	0.000	0.000*
Quadratus Femoris	0.072	0.000	0.398	0.102	0.182	0.076
Pectineus	0.036	0.000	0.280	0.141	0.246	0.000
Obturator Internus	0.773	0.346	1.583	1.345	1.528	3.402
Obturator Externus	0.338	0.000	1.564	0.814	0.950	1.531
Gemellus	0.185	0.093	0.370	0.318	0.363	0.803
Adductor Brevis	0.015	0.000	0.404	0.206	0.355	0.000
Adductor Magnus	0.815	0.665	1.573	1.636	2.220	0.000
Adductor Longus	0.053	0.016	0.999	0.504	0.840	0.000
Gracillis	0.196*	0.610	0.289	0.223	0.316	0.000*
Piriforms	0.283	0.185	0.556	0.514	0.559	1.228
Tensor Fascia Lata	0.070	0.000	0.282	0.146	0.077	0.193
Gluteus Maximus	1.810	1.138	1.742	1.698	1.029	3.920
Gluteus Minimus	0.851	0.787	1.043	1.179	1.318	2.864
Gluteus Medius	2.591	3.381	3.788	4.334	4.337	9.760
Iliacus	0.312	0.000	1.015	0.431	0.775	0.000
Satorius	0.487	0.614	1.042	0.737	0.737	1.091
Bicep Femoris	2.977	7.677	1.439	3.680	0.697	4.713
Semimembranosus	1.181	0.580	2.408	2.470	2.597	0.000
Semitendinosus	1.155	2.752	2.516	2.300	2.614	1.593
Psoas Major	0.237	0.395	0.932	0.407	1.103	2.259

Table J Muscle forces for the different age groups for 24 muscles at 2% of the gait cycle. *denotes significance (<0.05).

10% (N/Kg)	3 yrs	4 yrs	5 yrs	6 yrs	7 yrs	Adult
Vastus Intermedius	0.443	0.218	0.222	0.516	0.049	0.740
Vastus Lateralis	1.532	0.750	0.768	1.790	0.169	3.552
Vastus Medialis	0.708	0.344	0.361	0.836	0.080	1.673
Rectus Femoris	0.514	0.000	1.744	0.395	1.203	1.903
Quadratus Femoris	0.115*	0.091	0.522*	0.116*	0.225	0.020*
Pectineus	0.057	0.000	0.229	0.064	0.225	0.000
Obturator Internus	1.390	1.280	2.109	1.231	1.768	5.514
Obturator Externus	0.773	0.340	1.869	0.703	0.851	2.047
Gemellus	0.336	0.299	0.496	0.303	0.421	1.313
Adductor Brevis	0.031	0.000	0.328	0.096	0.330	0.000
Adductor Magnus	0.544	1.288	1.480	1.342	2.103	0.000
Adductor Longus	0.084	0.000	0.796	0.226	0.754	0.000
Gracillis	0.068	0.134	0.233	0.070	0.217	0.000
Piriforms	0.513	0.567	0.799	0.544	0.716	2.161
Tensor Fascia Lata	0.322	0.000	0.520	0.244	0.392	1.238
Gluteus Maximus	2.962	4.120	3.202	2.705	2.613	7.895
Gluteus Minimus	1.407	1.158	1.544	1.184	1.724	5.274
Gluteus Medius	5.091	6.239	6.357	5.385	7.147	20.823
Iliacus	0.361	0.000	0.759	0.187	0.683	0.000
Satorius	0.438	0.141	0.986	0.430	0.623	1.389
Bicep Femoris	2.880	4.677	2.182	2.286	0.954	3.852
Semimembranosus	3.535*	8.129	2.366	1.061*	0.531	0.000*
Semitendinosus	2.906	1.044	2.084	0.647	0.851	0.000
Psoas Major	0.278	0.001	0.720	0.283	1.527	0.136

Table K Muscle forces for the different age groups for 24 muscles at 10% of the gait cycle. *denotes significance (<0.05), + denotes where the significance is to.

30% (N/Kg)	3 yrs	4 yrs	5 yrs	6 yrs	7 yrs	Adult
Vastus Intermedius	0.000	0.000	0.000	0.113	0.000	0.000
Vastus Lateralis	0.000	0.000	0.000	0.392	0.000	0.000
Vastus Medialis	0.000	0.000	0.000	0.184	0.000	0.000
Rectus Femoris	1.249	0.000	0.582	0.576	0.957	1.642
Quadratus Femoris	0.255*	0.000	0.195	0.112	0.110	0.000*
Pectineus	0.181	0.000	0.227	0.104	0.277	0.000
Obturator Internus	1.132	0.523	1.296	0.602	1.322	3.840
Obturator Externus	1.118	0.000	0.628	0.144	0.470	0.620
Gemellus	0.303	0.138	0.314	0.149	0.331	0.945
Adductor Brevis	0.232	0.000	0.325	0.157	0.415	0.000
Adductor Magnus	0.379	1.358	1.834	1.172	2.275	0.000
Adductor Longus	0.645	0.000	0.750	0.373	0.988	0.000
Gracillis	0.256*	0.177*	0.234	0.104	0.295	0.000*+
Piriforms	0.364	0.279	0.547	0.284	0.574	1.610
Tensor Fascia Lata	0.455	0.000	0.327	0.171	0.189	1.231
Gluteus Maximus	0.629	1.246	1.422	1.030	0.242	2.015
Gluteus Minimus	1.767	1.099	1.398	0.837	1.685	4.501
Gluteus Medius	3.970	5.252	5.922	3.744	6.445	16.943*
Iliacus	0.946	0.109	0.727	0.320	1.299	0.416
Satorius	1.078	0.232	0.726	0.265	0.830	1.730
Bicep Femoris	1.077*a	3.385*+b	0.690*b	0.178*ab	0.216*b	0.319*b
Semimembranosus	0.981*+a	0.000*+b	0.011*ab	0.026*a	0.000*ab	0.000*ab
Semitendinosus	0.897	2.059	0.178	0.085	0.323	0.071
Psoas Major	0.527	0.218	1.339	0.752	1.683	1.958

Table L. Muscle forces for the different age groups for 24 muscles at 30% of the gait cycle. * denotes significance (<0.05), + denotes where the significance is to (a or b).

45% (N/Kg)	3 yrs	4 yrs	5 yrs	6 yrs	7 yrs	Adult
Vastus Intermedius	0.000	0.000	0.000	0.000	0.000	0.000
Vastus Lateralis	0.000	0.006	0.000	0.000	0.000	0.000
Vastus Medialis	0.000	0.003	0.000	0.000	0.000	0.000
Rectus Femoris	1.597	0.000*+	1.778*	1.234*	1.595*	3.340*
Quadratus Femoris	0.551	0.338	0.321	0.304	0.174	0.228
Pectineus	0.352	0.161	0.460	0.422	0.519	0.367
Obturator Internus	0.543	1.018	0.800	0.679	1.128	3.725
Obturator Externus	1.713	0.910	0.674	1.145	0.985	1.847
Gemellus	0.273	0.281	0.281	0.285	0.380	1.153
Adductor Brevis	0.463	0.174	0.602	0.524	0.668	0.172
Adductor Magnus	0.144	0.845	1.861	0.887	2.240	0.000
Adductor Longus	1.337	0.606	1.598	1.526	1.848	0.802
Gracillis	0.449	0.295	0.406	0.386	0.439	0.105
Piriforms	0.332	0.453	0.514	0.484	0.680	2.111
Tensor Fascia Lata	0.565	0.020	0.652	0.784	0.799	2.308
Gluteus Maximus	0.006	0.353	0.099	0.000	0.000	0.000
Gluteus Minimus	2.287	2.210	2.144	2.252	2.679	7.101
Gluteus Medius	4.106	6.966	6.008	4.987	7.032	21.022
Iliacus	1.794	1.112	2.023	2.091	2.447	3.820
Satorius	1.388	0.854	1.321	1.556	1.521	3.689
Bicep Femoris	0.476	1.575*+a	0.316*a	0.375	0.157*+ab	0.752*b
Semimembranosus	1.261	0.000	0.000	0.557	0.524	3.344
Semitendinosus	1.278	2.624	0.000	0.566	0.671	1.676
Psoas Major	0.766	0.951	2.138	1.807	3.424	11.689

Table M Muscle forces for the different age groups for 24 muscles at 45% of the gait cycle. *denotes significance (<0.05), + denotes where the significance is to (a or b).

52% (N/Kg)	3 yrs	4 yrs	5 yrs	6 yrs	7 yrs	Adult
Vastus Intermedius	0.000	0.000	0.000	0.000	0.000	0.000
Vastus Lateralis	0.000	0.000	0.000	0.000	0.000	0.003
Vastus Medialis	0.000	0.000	0.000	0.000	0.000	0.001
Rectus Femoris	1.305	0.869	2.646	2.880	3.040	6.696
Quadratus Femoris	0.617	0.179	0.562	0.553	0.356	0.096
Pectineus	0.382	0.089	0.488	0.538	0.481	0.276
Obturator Internus	0.506	0.436	1.318	0.579	1.060	2.205
Obturator Externus	1.868	0.494	1.402	1.992	1.475	0.839
Gemellus	0.271	0.130	0.427	0.378	0.383	0.747
Adductor Brevis	0.533	0.106	0.648	0.706	0.635	0.150
Adductor Magnus	0.239	0.179	1.161	1.152	0.992	0.000
Adductor Longus	1.521	0.346	1.760	2.011	1.747	0.706
Gracillis	0.534*	0.088*	0.511*	0.614*	0.485*	0.030*+
Piriforms	0.319	0.207	0.718	0.591	0.649	1.391
Tensor Fascia Lata	0.463	0.303	0.650	0.971	0.801	1.815
Gluteus Maximus	0.000	0.135*+	0.000	0.000	0.000*	0.000*
Gluteus Minimus	2.086	1.012	2.656	2.694	2.465	5.044
Gluteus Medius	4.307	2.460	5.709	6.516	5.804	14.420
Iliacus	1.893	0.538*+	2.160	2.637*	2.314	2.749*
Satorius	1.526	0.475	1.689	1.986	1.693	2.653
Bicep Femoris	0.612	0.491	0.561	0.641	0.472	0.462
Semimembranosus	1.942	0.000	0.571	1.015	1.619	3.728
Semitendinosus	1.869	2.644	0.632	0.977	1.581	1.774
Psoas Major	0.831*	2.756	2.240	2.210*	3.168	8.136*+

Table N. Muscle forces for the different age groups for 24 muscles at 52% of the gait cycle. *denotes significance (<0.05), + denotes where the significance is to.

63% (N/Kg)	3 yrs	4 yrs	5 yrs	6 yrs	7 yrs	Adult
Vastus Intermedius	0.069	0.222	0.021	0.028	0.016	0.135
Vastus Lateralis	0.239	0.891	0.000*	0.008	0.001	0.630*
Vastus Medialis	0.109	0.404*	0.000*+	0.003	0.000	0.289*
Rectus Femoris	1.970	0.000	2.767	3.282	3.614	4.355
Quadratus Femoris	0.775*	0.000*+	0.680*	0.517*	0.572*	0.035*
Pectineus	0.418	0.003	0.407	0.311	0.411	0.149
Obturator Internus	1.451*	0.000*+	2.785*	1.493*	1.544*	1.515*
Obturator Externus	2.253	0.000	2.244	1.669	1.871	0.598
Gemellus	0.430	0.000	0.702	0.393	0.416	0.414
Adductor Brevis	0.572	0.006	0.380	0.444	0.501	0.023
Adductor Magnus	0.257	0.678	0.911	1.785	1.023	0.000
Adductor Longus	1.646	0.017	1.285	1.167	1.427	0.127
Gracillis	0.612*ab	0.002*+a	0.566*ab	0.378*ab	0.407*ab	0.000*+ba
Piriforms	0.563	0.000	1.059	0.641	0.613	0.621
Tensor Fascia Lata	0.791	0.000	1.223	0.804	0.858	0.935
Gluteus Maximus	0.009	0.168	0.213	0.210	0.000	0.000
Gluteus Minimus	2.449	0.077	3.348	2.110	2.134	2.397
Gluteus Medius	4.390	0.842	6.521	6.815	2.962	4.955
Iliacus	1.929*	0.062*+	2.169*	1.659*	1.902*	1.242*
Satorius	2.001*	0.000*+	2.561*	1.555*	1.836*	1.345*
Bicep Femoris	0.903	0.464	1.998*	0.509*	0.592*	0.013*+
Semimembranosus	2.143	0.000	1.479	0.413	0.179	0.996
Semitendinosus	1.379	1.140	1.590	0.119	0.498	0.335
Psoas Major	0.615	0.028	2.223	1.122	1.949	3.480

Table O. Muscle forces for the different age groups for 24 muscles at 63% of the gait cycle. *denotes significance (<0.05), + denotes where the significance is to (a or b).

70% (N/Kg)	3 yrs	4 yrs	5 yrs	6 yrs	7 yrs	Adult
Vastus Intermedius	0.2543	0.5061	0.7081	0.9584	0.8547	0.5992
Vastus Lateralis	0.8738	2.0074	2.2885	3.3844	3.2343	2.7059
Vastus Medialis	0.3976	0.9224	1.0440	1.5443	1.4815	1.2363
Rectus Femoris	2.5064	0.1655	3.4245	3.1929	3.8289	2.4486
Quadratus Femoris	0.3151	0.0000	0.3633	0.2708	0.4679	0.0251
Pectineus	0.1571*	0.0000	0.1928*	0.2264*	0.1975*	0.0000*+
Obturator Internus	0.8103	0.0086*	1.2927*	1.0067	1.0991	1.6575
Obturator Externus	1.0016	0.0000	1.3374	0.8504	1.3171	0.6971
Gemellus	0.2160	0.0119	0.3149	0.2820	0.3167	0.4048
Adductor Brevis	0.1774*	0.0000	0.2338	0.3249	0.2197	0.0000*
Adductor Magnus	0.2079	0.5896	0.7134	1.6469	0.9169	0.0000
Adductor Longus	0.5586*	0.0000	0.6144	0.8171	0.5966	0.0000*
Gracillis	0.1125*	0.0000	0.1651	0.2284	0.1357	0.0000*
Piriforms	0.2674	0.0712	0.4640	0.4415	0.4027	0.6264
Tensor Fascia Lata	0.5094	0.0000	0.5986	0.4842	0.4511	0.6552
Gluteus Maximus	0.2245	0.9187	0.5964	0.7431	0.1097	0.1527
Gluteus Minimus	0.9895	0.2595	1.3506	1.4435	1.1814	1.8992
Gluteus Medius	2.3322	1.8700	2.9851	5.3459	2.7327	5.1759
Iliacus	0.7495	0.0000	1.0142	0.9234	0.9466	0.4924
Satorius	0.8137	0.0000	1.0621	0.7202	0.8399	0.9093
Bicep Femoris	0.1869	0.5771	0.1364	0.0976	0.0274	0.0000
Semimembranosus	0.5365	0.0000	0.2753	0.0000	0.0000	0.5503
Semitendinosus	0.0999	1.0599	0.1560	0.0000	0.3036	0.1975
Psoas Major	0.3602	0.2603	1.2905	0.5259	1.1956	2.8222

Table P. Muscle forces for the different age groups for 24 muscles at 70% of the gait cycle. *denotes significance (<0.05), + denotes where the significance is to.

85% (N/Kg)	3 yrs	4 yrs	5 yrs	6 yrs	7 yrs	Adult
Vastus Intermedius	1.328	0.000	1.195	1.305	1.483	0.036
Vastus Lateralis	4.560	0.000	4.149	4.560	5.319	0.216
Vastus Medialis	2.077	0.000	1.905	2.085	2.441	0.100
Rectus Femoris	1.912	0.000	1.474	1.587	2.251	1.108
Quadratus Femoris	0.076	0.284	0.319	0.188	0.259	0.111
Pectineus	0.024	0.000	0.093	0.172	0.100	0.000
Obturator Internus	0.522	0.984	1.019	1.354	1.029	3.123
Obturator Externus	0.111	0.512	0.929	0.745	0.916	1.488
Gemellus	0.129	0.216	0.237	0.322	0.242	0.735
Adductor Brevis	0.053	0.000	0.152	0.260	0.149	0.000
Adductor Magnus	1.213	2.878	2.232	1.987	1.732	0.000
Adductor Longus	0.136	0.000	0.387	0.636	0.337	0.000
Gracillis	0.072	0.077	0.101	0.186	0.101	0.000
Piriforms	0.258	0.486	0.448	0.581	0.410	1.170
Tensor Fascia Lata	0.243	0.000	0.135	0.244	0.208	0.725
Gluteus Maximus	1.675	4.517	3.296	2.824	2.505	4.253
Gluteus Minimus	0.689	0.227	0.985	1.469	1.105	2.667
Gluteus Medius	3.773	4.822	5.011	6.447	4.969	9.412
Iliacus	0.113	0.000	0.272	0.555	0.285	0.000
Satorius	0.088	0.000	0.189	0.208	0.361	0.942
Bicep Femoris	1.673	4.835	1.744	0.597	1.284	1.524
Semimembranosus	1.074*	0.000	0.265	0.108	0.144	0.000*
Semitendinosus	1.052	2.797	0.234	0.192	0.230	0.156
Psoas Major	0.378	0.000*+	0.345*	0.532*	1.289*	5.634*

Table Q. Muscle forces for the different age groups for 24 muscles at 85% of the gait cycle. *denotes significance (<0.05), + denotes where the significance is to.

98% (N/Kg)	3 yrs	4 yrs	5 yrs	6 yrs	7 yrs	Adult
Vastus Intermedius	1.213	0.000	2.416	1.591	1.784	0.000
Vastus Lateralis	4.190	0.000	8.362	5.510	6.170	0.000
Vastus Medialis	1.966	0.000	3.944	2.589	2.936	0.000
Rectus Femoris	1.842	0.000	2.778	1.508	2.036	1.242
Quadratus Femoris	0.041	0.037	0.284	0.125	0.103	0.069
Pectineus	0.033	0.000	0.106	0.202	0.105	0.000
Obturator Internus	0.608	0.406	1.832	1.544	1.512	4.842
Obturator Externus	0.163	0.162	1.178	0.626	0.835	1.786
Gemellus	0.180	0.100	0.430	0.379	0.358	1.166
Adductor Brevis	0.007	0.000	0.152	0.298	0.149	0.000
Adductor Magnus	0.421	0.286	1.314	2.084	1.284	0.000
Adductor Longus	0.003	0.000	0.425	0.730	0.403	0.000
Gracillis	0.228	0.570	0.124	0.234	0.130	0.000
Piriforms	0.242	0.175	0.640	0.663	0.560	1.636
Tensor Fascia Lata	0.441	0.000	0.607	0.458	0.325	1.409
Gluteus Maximus	0.871	0.669	1.701	1.920	1.299	2.586
Gluteus Minimus	1.355	0.756	1.988	1.968	2.018	4.278
Gluteus Medius	3.921	2.867	6.940	7.575	6.884	11.622
Iliacus	0.575	0.012	0.477	0.678	0.357	0.000
Satorius	0.855	0.640	0.889	0.678	0.729	2.262
Bicep Femoris	2.708	7.538	1.035	1.065	1.547	0.918
Semimembranosus	1.134*	0.000	0.407	0.604	0.526	0.000*
Semitendinosus	1.157	2.236	0.385	0.614	0.533	0.000
Psoas Major	0.570	0.098	0.327	0.373	1.690	1.915

Table R. Muscle forces for the different age groups for 24 muscles at 98% of the gait cycle. *denotes significance (<0.05), + denotes where the significance is to.

Figure M to Figure T show the muscle forces the 24 muscles for 100% of the gait cycle grouped by actions.

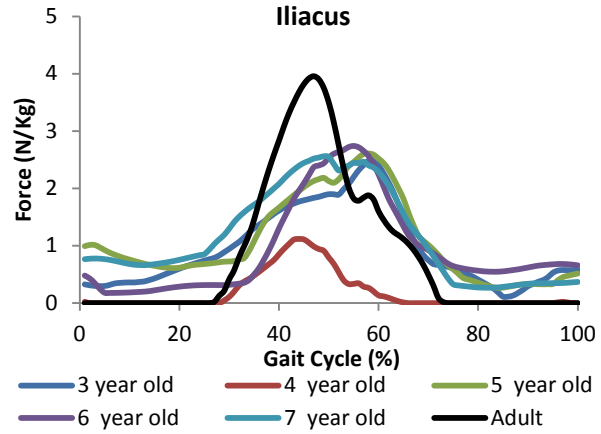

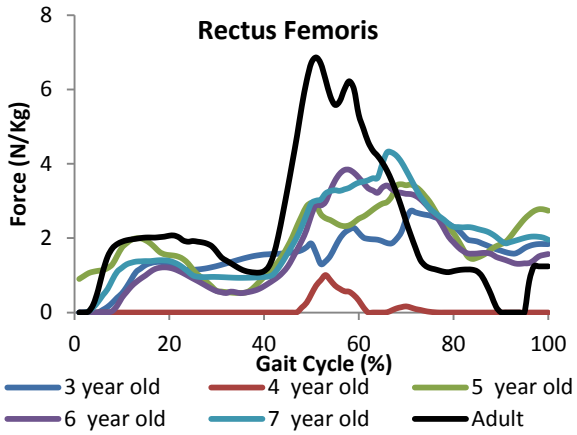

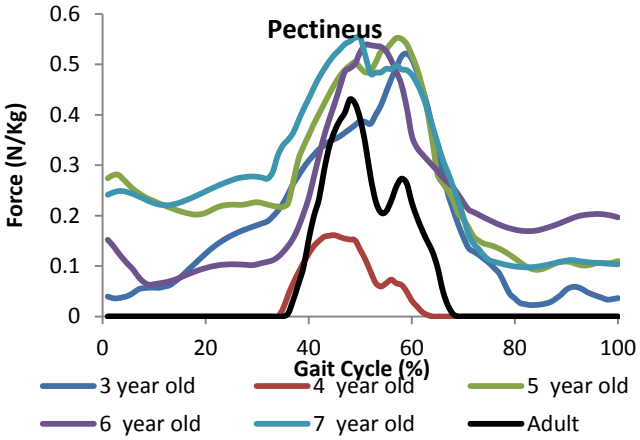

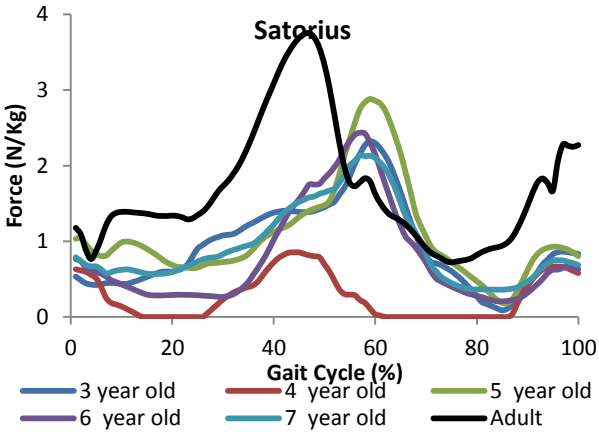

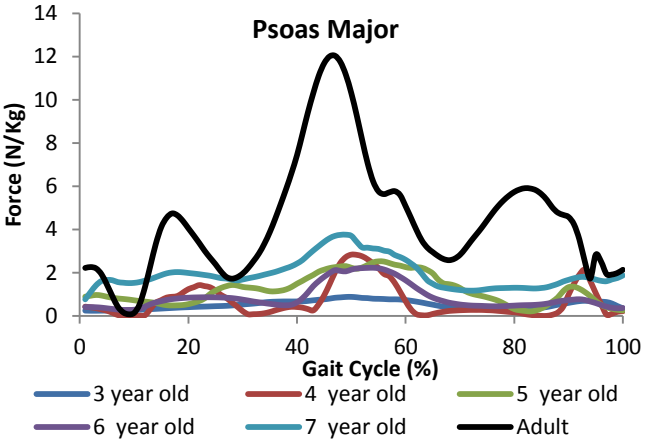

Figure M Hip flexor muscle activity during 100% gait cycle for children and adult subjects.

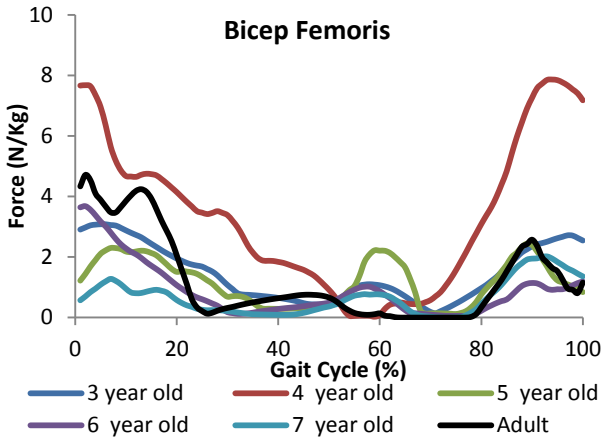

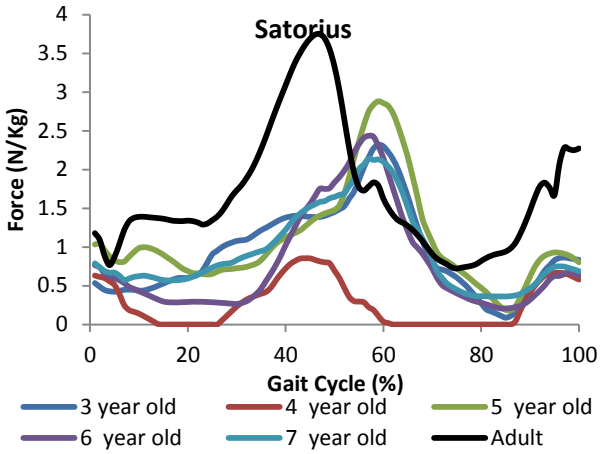

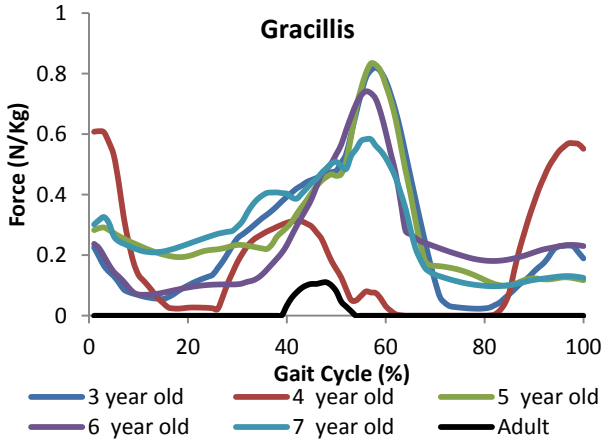

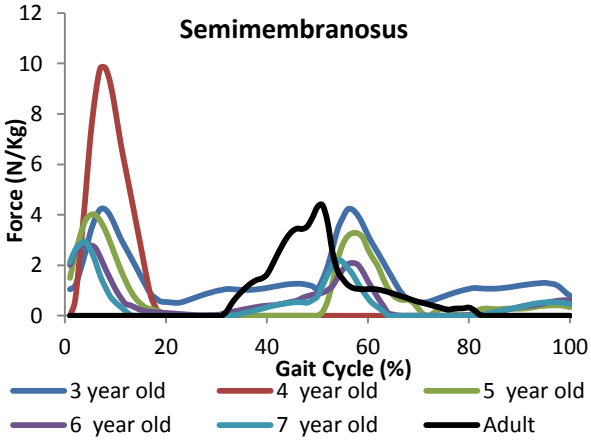

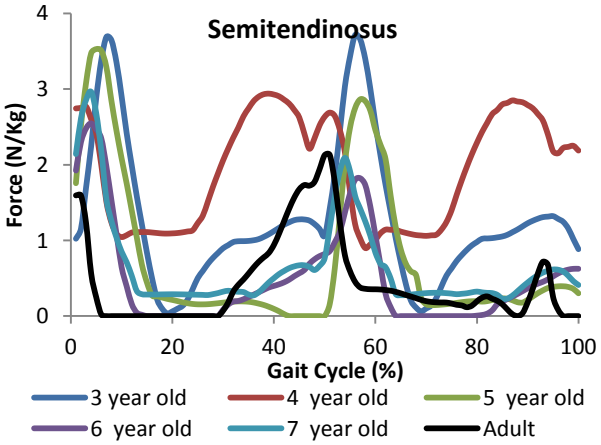

Figure N Knee flexor muscle activity during 100% gait cycle for children and adult subjects.

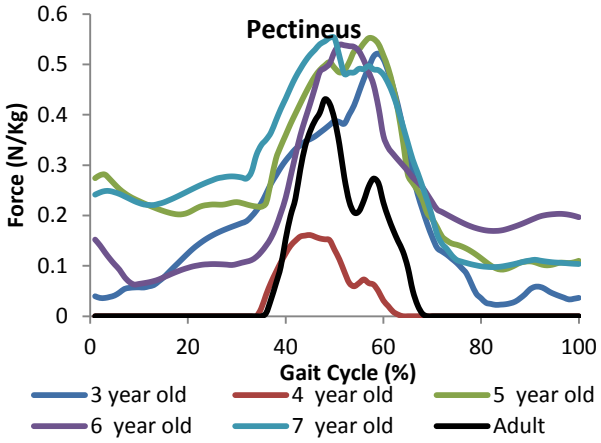

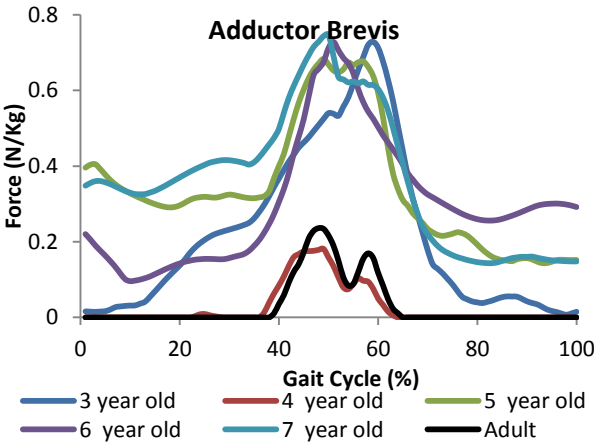

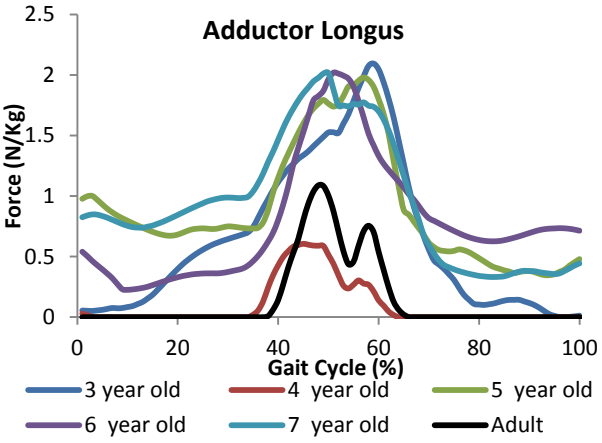

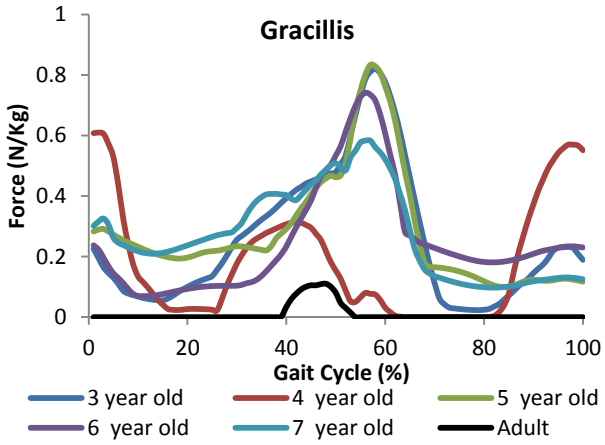

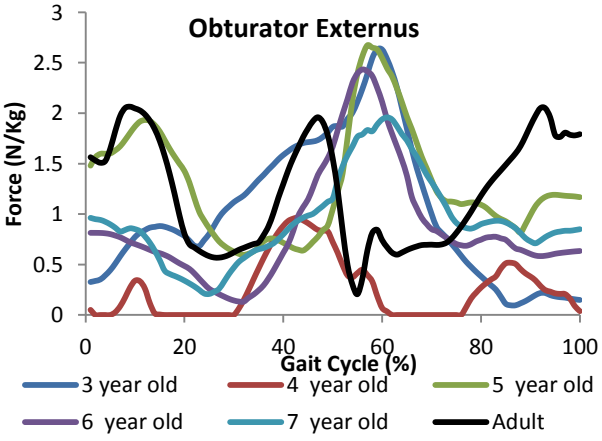

Figure O Hip adductor muscle activity during 100% gait cycle for children and adult subjects.

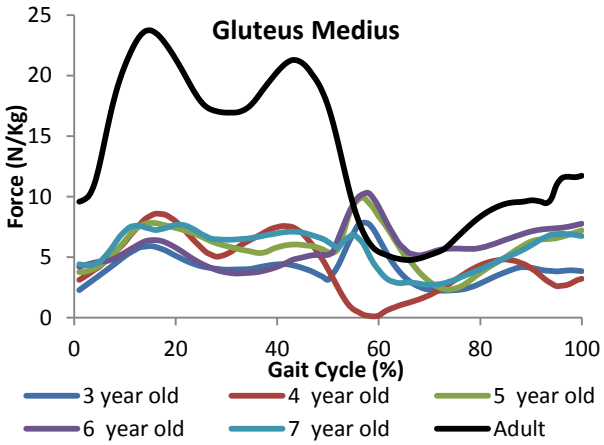

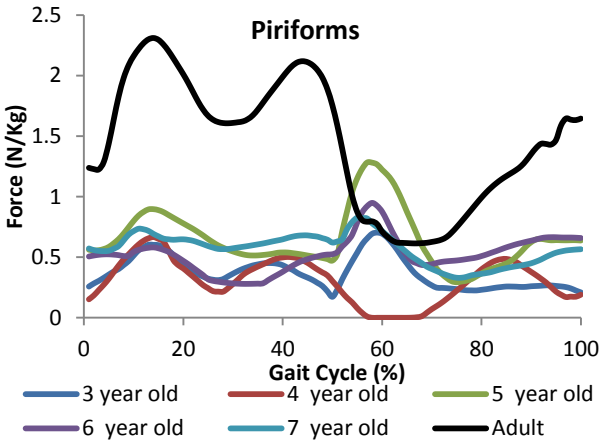

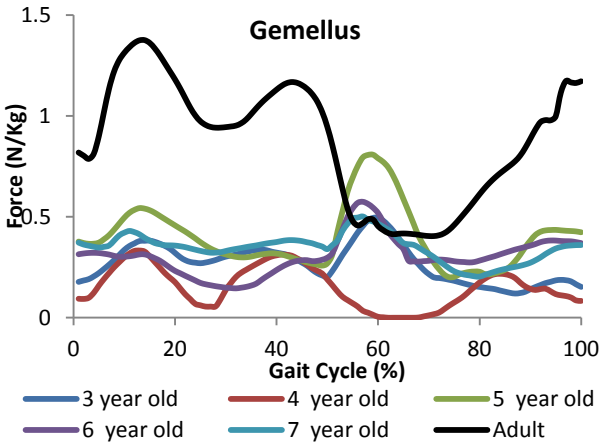

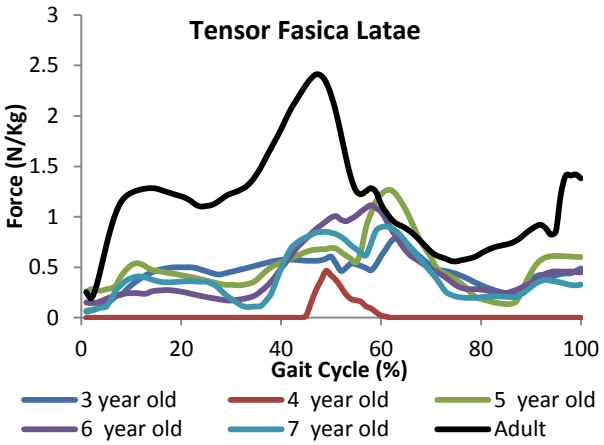

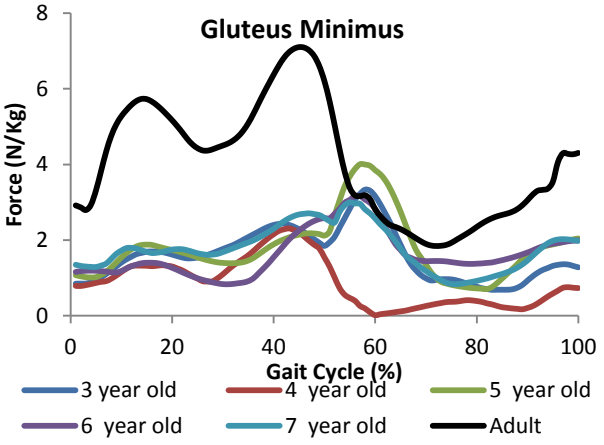

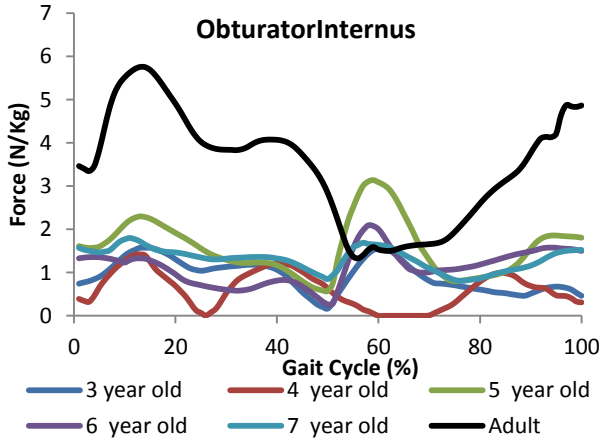

Figure P Hip abductor muscle activity during 100% gait cycle for children and adult subjects.

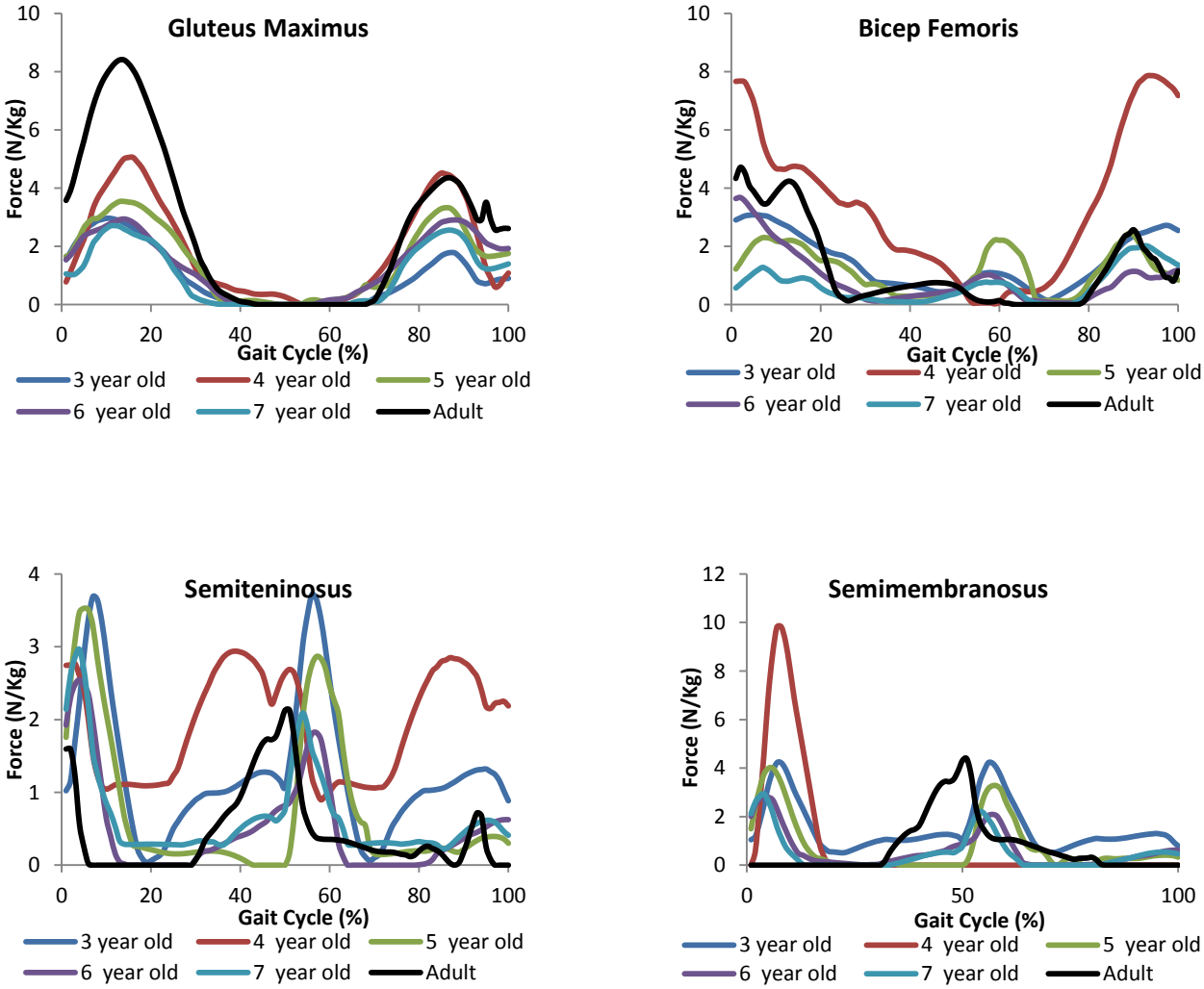

Figure Q Knee flexor muscle activity during 100% gait cycle for children and adult subjects.

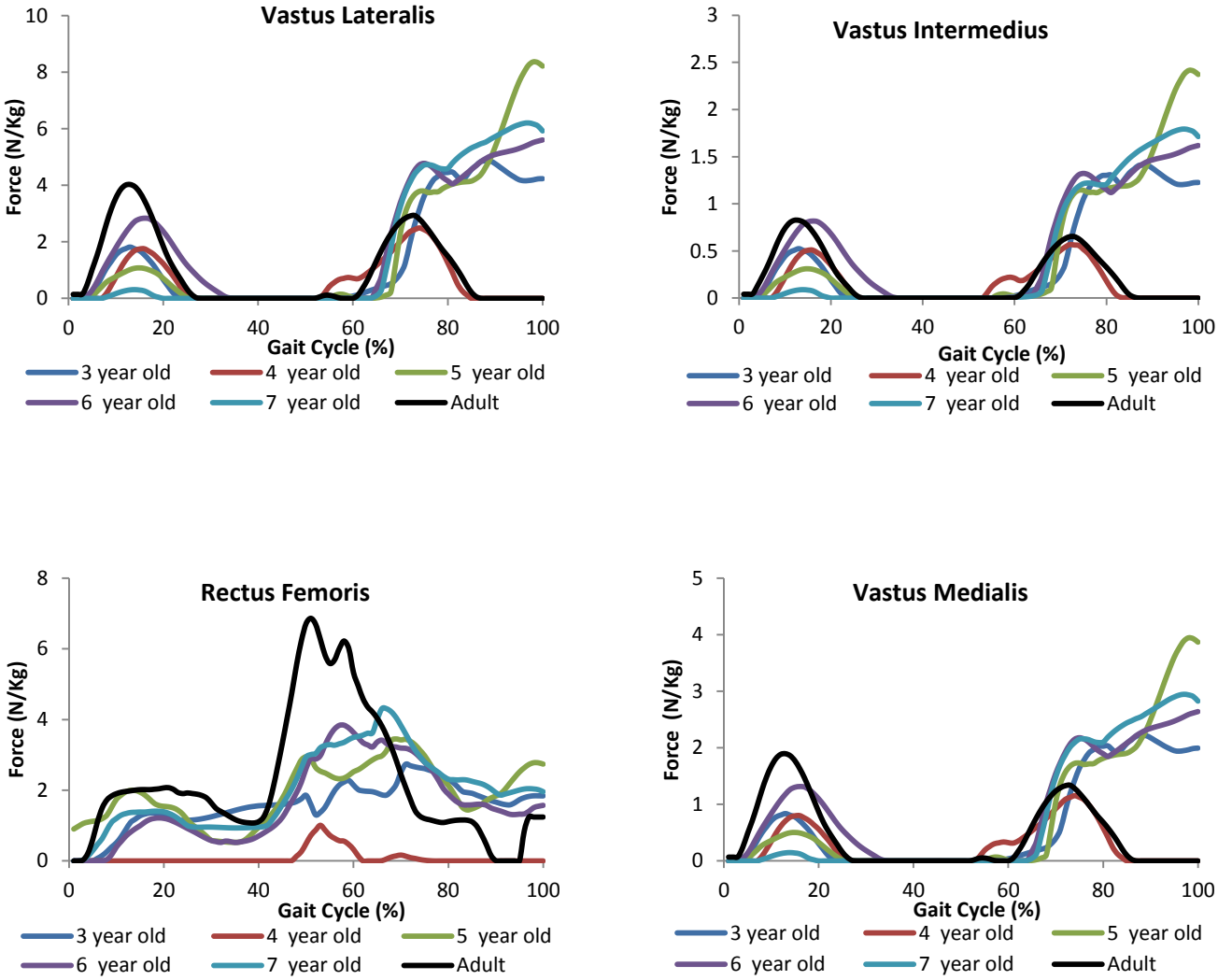

Figure R Knee extensor muscle activity during 100% gait cycle for children and adult subjects.

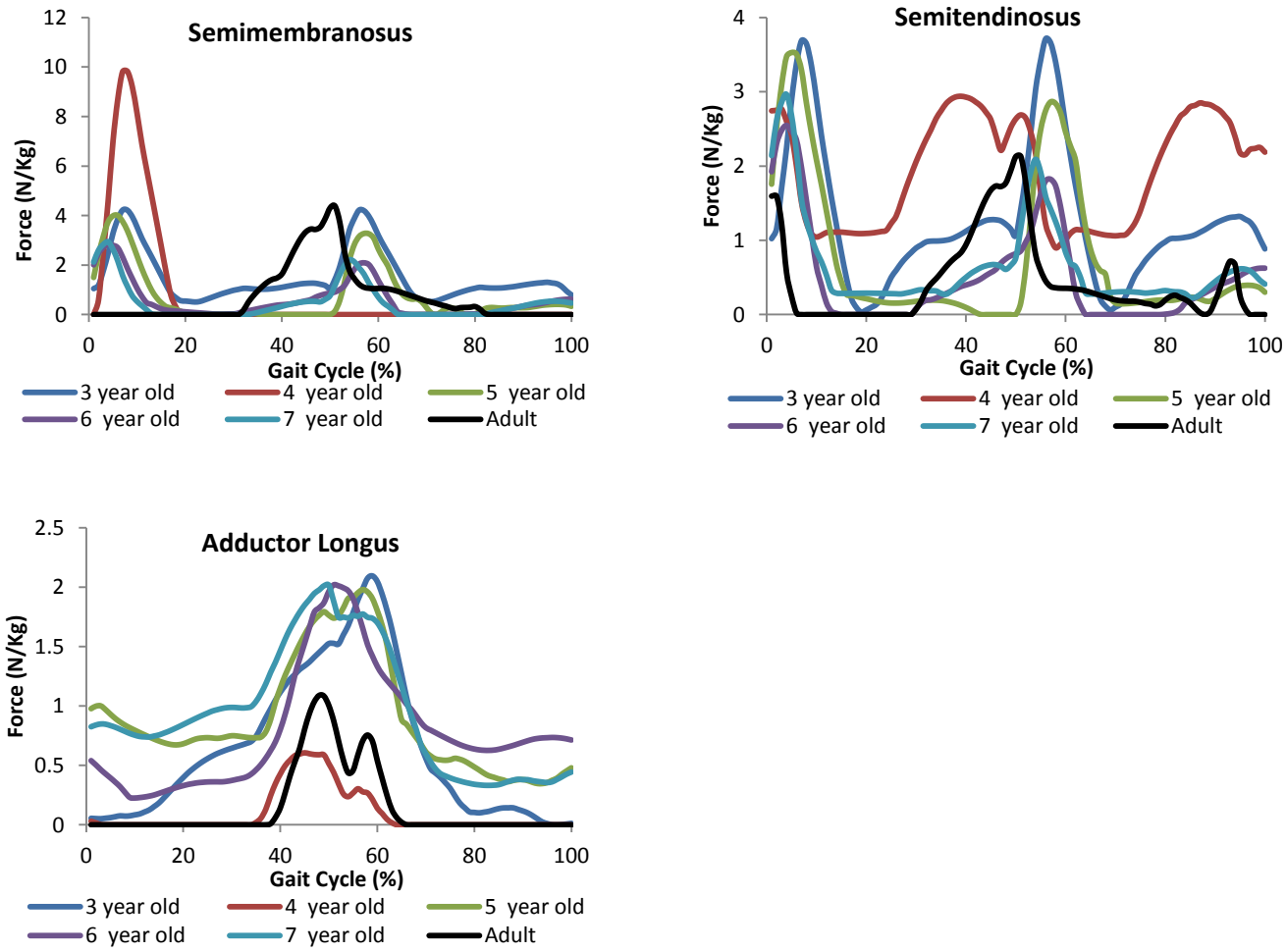

Figure S Internal rotator muscle activity during 100% gait cycle for children and adult subjects.

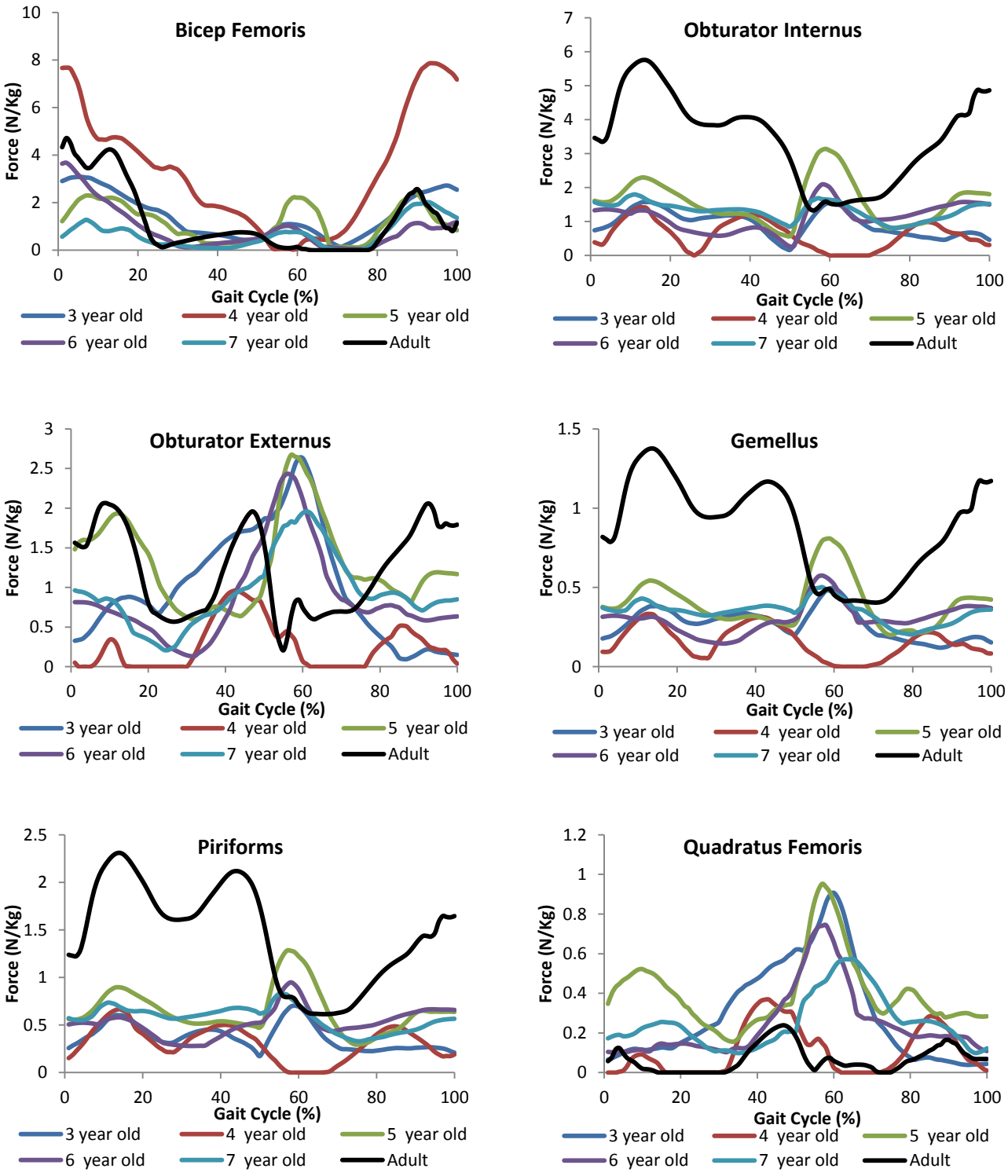

Figure T Hip extensor muscle activity during 100% gait cycle for children and adult subjects

APPENDIX VI

To determine if the models analysed throughout this study have a sufficient mesh density, a convergence test was performed for each model on varied meshes, ranging from ~54000 to ~1million elements. The various mesh sizes can be seen in Table S.

Models	Element Number					
3 year old	60000	150000	200000	440000	700000	1000000
7 year old	54000	134000	228000	540000	1000000	
Adult	62000	112000	190000	490000	600000	1100000

Table S details of the number of elements used in each model during the convergence tests.

Material properties defined during the convergence were the same used as detailed in Chapter 7. A simplistic loading regime was defined for each mesh, the same loading regime was used for each model, a load equal to hip force at 20% during the gait, as calculated from the musculoskeletal modelling (Chapter 6). The models were constrained at the most distal nodes of the model in all DOF. The level of convergence was analysed through inter mesh comparison of nodal von Mises stresses at specific locations.

3 YEAR OLD

The 3 year old model consisted of 4-noded shell elements representing cortical bone and cartilage indicates the position of the nodes which were chosen for analysis. These nodes were chosen as they represented areas of interest during the FEA (Figure U).

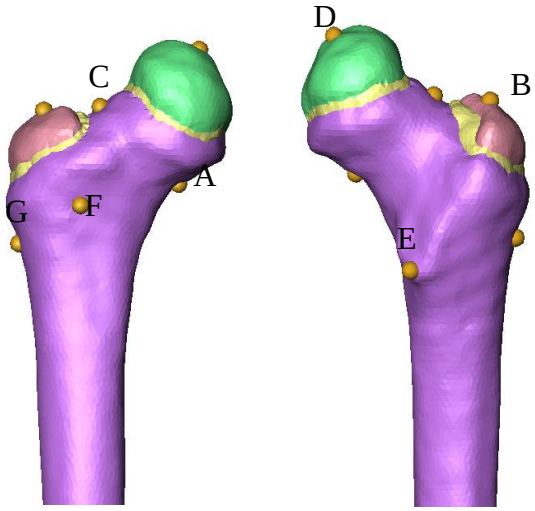

Figure U Posterior and anterior of the 3 year old femur identifying the seven nodes chosen for analysis in convergence tests.

The convergence tests showed that cortical von Mises stress changed minimally through the increasing number of elements in the model (Figure V). The largest stresses were observed at the node A, located under the femoral neck, with the highest observed stress during the model with 440000 elements. The biggest variation in the stress experienced was in node E, at 60000 elements, stress level of 5.9MPa reducing to 4.1MPa at 700000 elements before increasing again at 1000000 elements to 4.3MPa. This may indicate that convergence had still not been achieved. The least change observed was in node G ranging from 1.8MPa to 2.1MPa. This node was located on the anterior portion of the neck, the regular surface where the node was located may have been the reason for the little variation in stress observed.

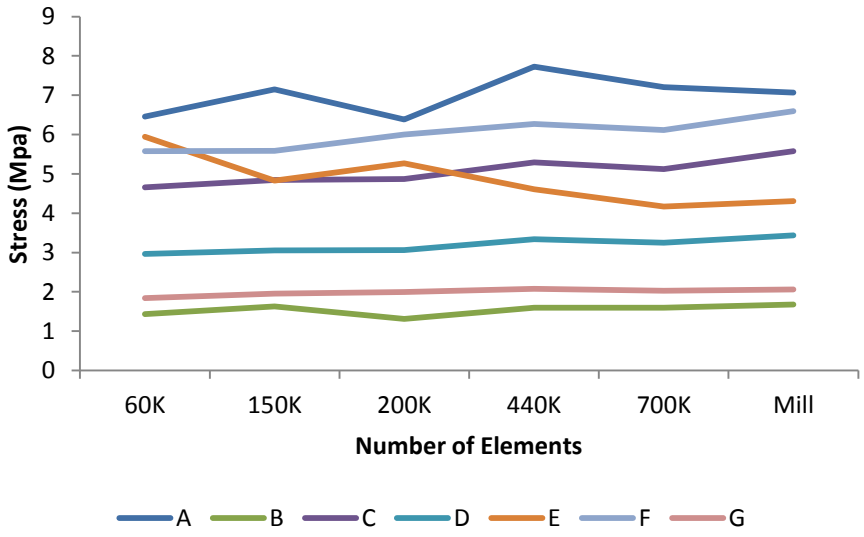

Figure V Shows the stresses observed during the convergence test in the different node locations through the varied meshes.

7 YEAR OLD

As in the 3 year old 4-noded shell elements representing cortical bone and cartilage were chosen for the model. The position of the nodes to be analysed are shown in Figure W.

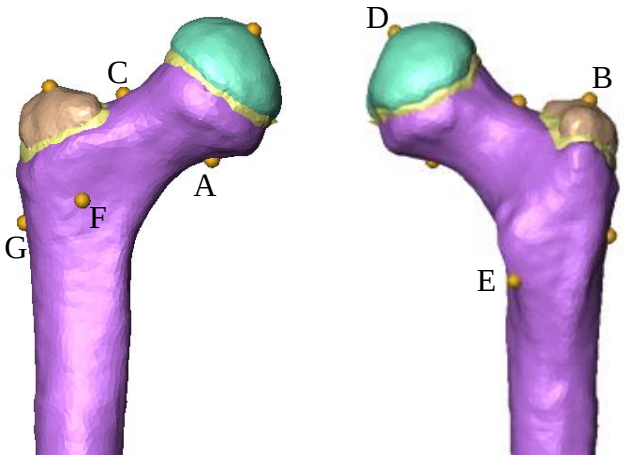

Figure W Posterior and anterior of the 7 year old femur identifying the seven nodes chosen for analysis in convergence tests.

The results of the 7 year old model (Figure X) show very little change between the varied meshes. Node A was the location where the largest stress was observed, the stress was >13MPa larger than any other node location. When the element number reached 228000 there was a small decrease in stress in all locations, except node G. The lowest stress was observed in the greater trochanter, this would be expected due to the loading regime used. Overall in each node location there was very little difference in the stresses observed.

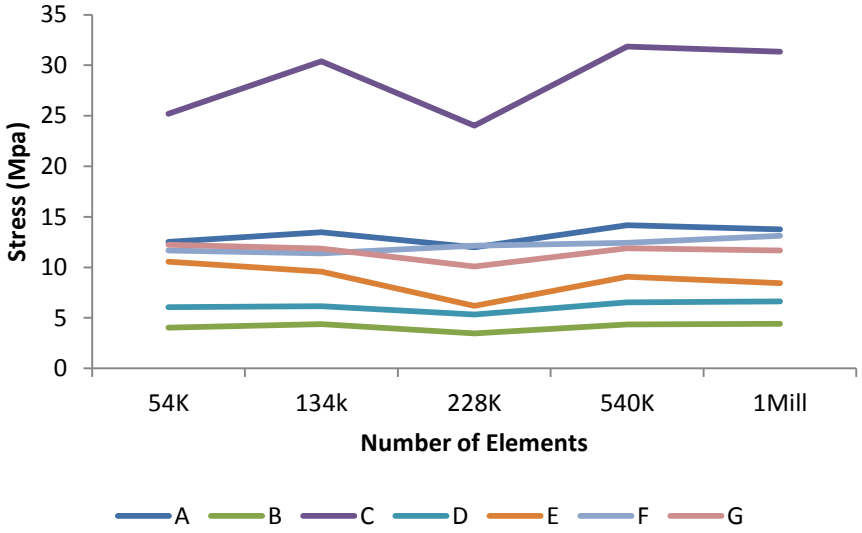

Figure X Shows the stresses observed during the convergence test in the different node locations through the varied meshes.

ADULT

In the adult model 4-noded shell elements representing cortical bone were used to model the femur, the nodal location can be seen in Figure Y.

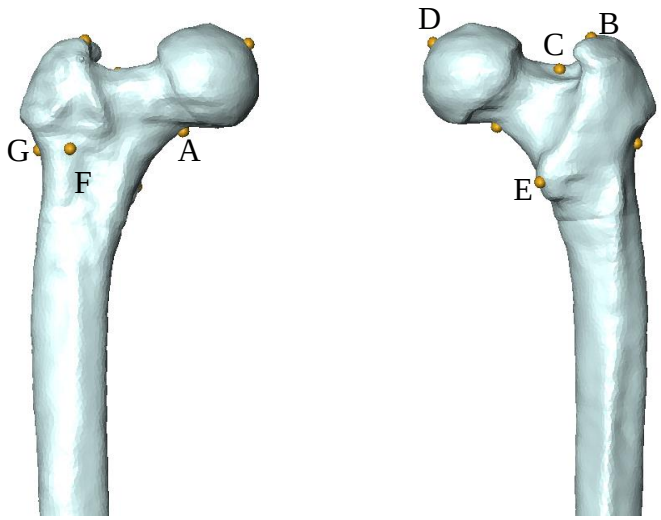

Figure Y Posterior and anterior of the adult femur identifying the seven nodes chosen for analysis in the convergence tests

Similar results were observed in the juvenile femora with node A being the highest stress level, this is due to being in close proximity to where the load was applied. The node (B) applied on the greater trochanter was again showed to have the lowest strain levels not exceeding 3MPa, and showing very little variation between mesh densities. Node E, located on the lesser trochanter, showed a decrease in stress from 8.3MPa to 6.0MPa as the mesh density increased. A problem with the stress variations between the mesh densities may occur when different locations change the order in which they are stressed. An example of this is seen in this model between node F and C, at 112000 elements node F has a lower stress level than node C. However at 190000 elements node C is the higher stressed, during analysis this may change how the results are interpreted. Because the values of these variations are minimal, this may not be too problematic, but if these variations were larger, further convergence tests would be required.

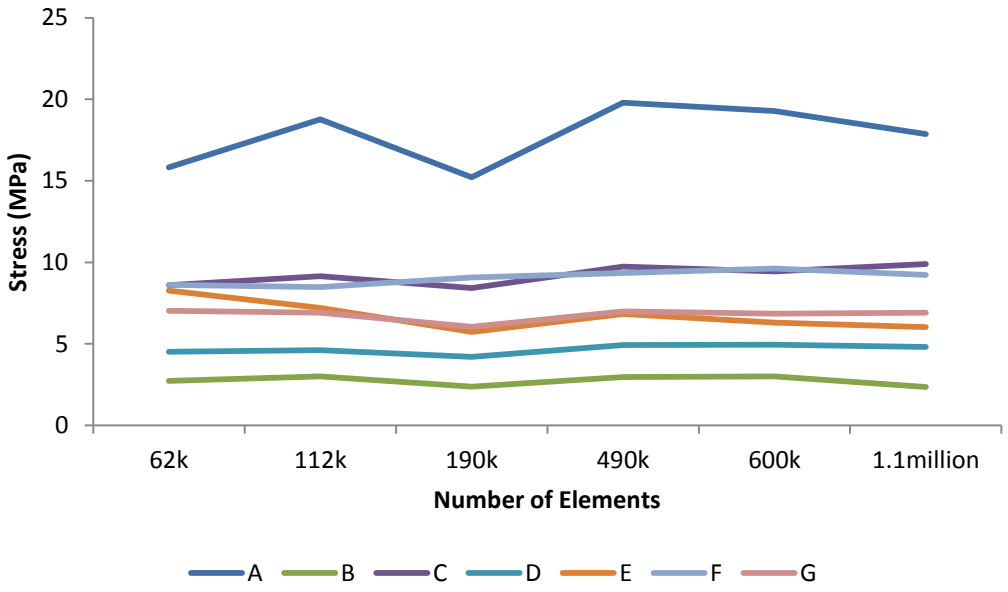

Figure Z Shows the stresses observed during the convergence test in the different node locations through the varied meshes.

CONCLUSION

The convergence testing displayed similar mechanical responses of the femoral models for each age between each mesh density, therefore it is possible that convergence did not occur. There are however more variables to be considered than mesh density, such as computing time and therefore the highest element model was not suitable. However the mesh chosen for use in FEA for each model ~210000 to ~234000 was still higher than that reported in previous literature (Wagner *et al*, 2010). The lack of convergence may be due to a much less dense mesh converging than used in the present study or the simple loading regime used. The loading was much simpler than what would be applied in the FEA, previous research has shown that loading shows little relevance in the results of a convergence test. Ramos and Simoes (2006) compared the results of meshing a model using tetrahedral and hexahedral elements, on both a simplified and a realistic model. Four different models were built, these were a 4 node and a 10 node tetrahedral mesh and an 8-node and a 20-node hexahedral model. In both the simplified loaded model and complex model shows no significant differences in the strain or displacement measurements. This may suggest that as long as the mesh is at a certain level of complexity, any smaller refinements in the meshing may not affect the results of the FEA.

APPENDIX VII

When describing the location of the stress/strains distributions calculated from the FEA. Definitions of the location of the stress/strain distributions are required to explain the results. Figure AA details the definition of the femur showing the anterior, posterior, medial and lateral sides.

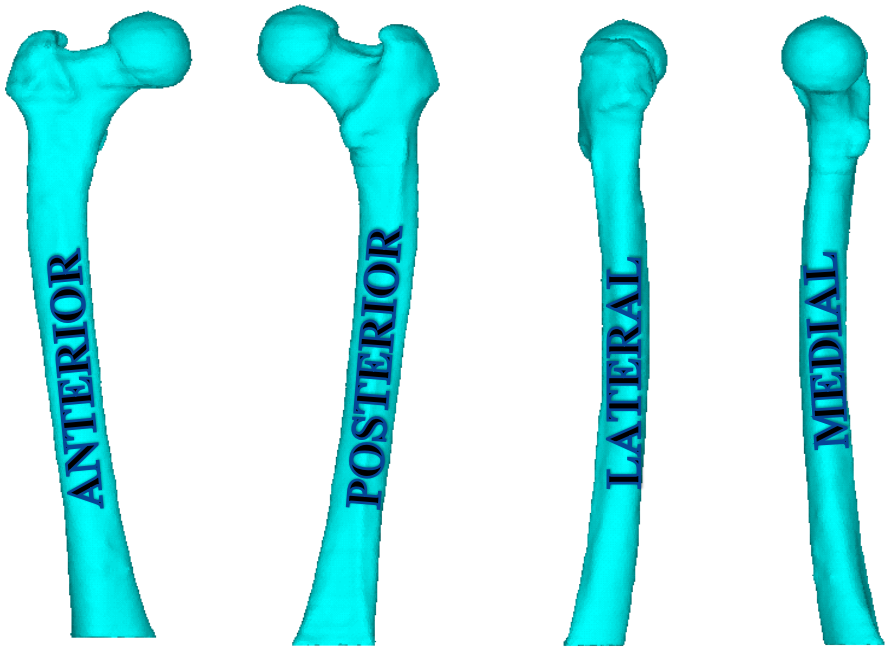

Figure AA Description of the anatomical aspects of an adult femur.

APPENDIX VIII

CONFERENCE PUBLICATION

Lunn, D. E., and Portas, M. (2008) The Effects of a Specific, General and Passive Warm Up on Golf Club Head Speed. *BASES Annual Student Conference*. Bedford, UK.

Lunn, D. E. (2009) Ever Wondered Why and How your Leg Bone Grows? I Have! *Yorkshire and North East Hub Public Engagement Competition.* University of Leeds, Leeds, UK.

Lunn, D. E., Fagan, M. J., Dobson, C. A. (2009) Construction of a Complete Digitised Juvenile Femur for use in Musculoskeletal and Finite Element Models. *IV International Conference on Computational Bioengineering*, Bertinoro, Italy.

Lunn, D. E., Watson, P.J., O'Higgins, P., Fagan, M. J., Dobson, C. A. (2009) New Method using Warped Gait Data to Create Subject Specific Musculoskeletal Models for Cadaveric Bone Samples. *IV International Conference on Computational Bioengineering*, Bertinoro, Italy.

Watson, P.J., **Lunn, D. E**., Alcock, L., Vanicek, N., Dobson, C. A. (2010) The Reliability of Kinetic Data in Musculoskeletal Models during Gait. *The 17th Congress of the European Society of Biomechanics*, Edinburgh, Scotland, UK.

Lunn, D. E., Watson, P.J., Fagan, M. J., Dobson, C. A. (2010) The Reliability of Kinetic and Kinematic Data in Musculoskeletal Models. *Clinical Biosciences Research Day*, Castle Hill Hospital, Cottingham, UK.

Lunn, D, E., Dobson, C. A. (2013) Musculoskeletal Modelling of Childrens Gait. *European Society of Movement in Adults and Children*, Glasgow, UK.